Calculation No: NSTXU-CALC-011-19-00 **Revision No: 0**

PFCs Analysis of the IBDV HHF Tiles

Purpose of Calculation: (Define why the calculation is being performed.)

Calculate the structural response of the Inboard Divertor Vertical High Heat Flux tiles.

Codes and versions: (List all codes, if any, used)

ANSYS v19.1

References (List any source of design information including computer program titles and revision levels.)

1) GENERAL REQUIREMENTS DOCUMENT NSTX-U-RQMT-GRD-001-02
2) NSTX-U SYSTEM REQUIREMENTS DOCUMENT Plasma Facing Components NSTX-U-RQMT-SRD-003-01 July 14, 2018
3) NSTX-U Disruption Analysis Requirements NSTX-U-RQMT-RD-003-02 7/23/18
4) NSTXU Recovery Global Heat Balance Calculations, NSTXU-CALC-10-06-00, by H Zhang

Assumptions (Identify all assumptions made as part of this calculation.)

The tile is assumed to be made of Sigrafine R6510 with a layer of Grafoil between it and the underlying cooling plate. All supports (cooling plate and frame) and hardware (rods & pins) are Inconel 718.

Calculation (Calculation is either documented here or attached)

The ANSYS Workbench version 19.1 is used to analyze the thermal and structural response to the applied preload, heat fluxes and EM loads as specified in SRD. See attached report sections “Method of Analysis” and “Results”

Conclusion (Specify whether or not the purpose of the calculation was accomplished.)

The analysis has shown the tile temperatures are within the allowables but is has identified several areas where high stresses exist. The spherical connection of the pins to the rods show high contact stresses though hand calculations suggest it should be acceptable. It is recommended that the connection be tested to demonstrate acceptable life. Also, the reverse helicity case results in high surface compression for the prescribe 1 MW/m2 for 1 sec. The recommendation is to relax these requirements if possible.

Cognizant Individual (or designee) printed name, signature, and date

Preparer’s printed name, signature and date Andrei Khodak Digitally signed by Andrei Khodak Date: 2018.09.27 15:40:24 -04'00'

I have reviewed this calculation and, to my professional satisfaction, it is properly performed and correct.

Checker’s printed name, signature, and date Art Brooks Digitally signed by Art Brooks Date: 2018.09.27 13:42:29 -04'00'

<u>**N**ational **S**pherical **T**orus e**X**periment - **U**pgrade</u>

NSTX-U

PFCs Analysis of the IBDV HHF Tiles

NSTXU-CALC-011-19_00

September 24, 2018

Prepared By:

Andrei Khodak

Digitally signed by Andrei Khodak
Date: 2018.09.27 15:41:06 -04'00'

Andrei Khodak, Engineering Analyst

Reviewed By:

Art Brooks

Digitally signed by Art Brooks
Date: 2018.09.27 13:42:53 -04'00'

Art Brooks, Engineering Analyst

Reviewed By:

Michael Jaworski

Digitally signed by Michael Jaworski
Date: 2018.09.28 23:34:05 -04'00'

Michael Jaworski, Responsible Engineer

Checks for Calculation No: NSTXU-CALC-011-19 Revision No: 0

PFCs Analysis of the IBDV HHF Tiles

Component was checked against latest design

Yes

All required load cases are included and current

Yes

Discuss method used in the calculation

The use of ANSYS Workbench is considered an acceptable approach to analyzing problems of this type.

Discuss how the calculation was checked (*)

The calculation was checked by

1) comparing the inputs to the models as stated herein with the project requirements
2) comparing results with previous similar analyses of the IBDH

List issue identified and how they were resolved

The analysis has shown the tile temperatures are within the allowables but is has identified several areas where high stresses exist. The spherical connection of the pins to the rods show high contact stresses though hand calculations suggest it should be acceptable. It is recommended that the connection be tested to demonstrate acceptable life. Also, the reverse helicity case results in high surface compression for the prescribe 1 MW/m2 for 1 sec. The recommendation is to relax these requirements if possible.

Checker's name: Art Brooks

Peter H. Titus Digitally signed by Peter H. Titus Date: 2018.09.27 14:50:08 -04'00'

Technical Authority:____(sign and date)

(*) independent calculations can be appended

Minimum Requirements for Checking Calculations

1. Assure that inputs were correctly selected and incorporated into the design.

2. Calculation considers, as appropriate:

   - Performance Requirements (capacity, rating, system output)
   - Design Conditions (pressure, temperature, voltage, etc.)
   - Load Conditions (Electromagnetic (Lorentz Force), seismic, wind, thermal, dynamic)
   - Environmental Conditions (radiation zone, hazardous material, etc.)
   - Material Requirements
   - Structural Requirements (foundations, pipe supports, etc.)
   - Hydraulic Requirements (NPSH, pressure drops, etc.)
   - Chemistry Requirements
   - Electrical Requirements (power source, volts, raceway, and insulation)
   - Equipment Reliability (FMEA)
   - Failure Effects on Surrounding Equipment
   - Tolerance Buildup

3. Assumptions necessary to perform the design activity are adequately described and reasonable.

4. An appropriate calculation method was used.

5. The results are reasonable compared to the inputs.

6. Error bars (range) for inputs used, results / conclusions, assumptions, have been considered and are acceptable.

NOTE: IT IS THE RESPONSIBILITY OF THE CHECKER TO USE METHODS THAT WILL SUBSTANTIATE TO HIS/HER PROFESSIONAL SATISFACTION THAT THE CALCULATION IS CORRECT.

BY SIGNING CALCULATION, CHECKER ACKNOWLEDGES THAT THE CALCULATION HAS BEEN APPROPRIATELY CHECKED AND THAT THE APPLICABLE ITEMS LISTED ABOVE HAVE BEEN INCLUDED AS PART OF THE CHECK.

NSTX-U CALCULATION

Record of Changes

Rev.	8	Description of Changes	Revised by
0	09/21/18	Initial Release	

PFCs Analysis of the IBDV HHF Tiles

Executive Summary

The analysis has shown the tile temperatures are within the allowables but is has identified several areas where high stresses exist. The spherical connection of the pins to the rods show high contact stresses though hand calculations suggest it should be acceptable. It is recommended that the connection be tested to demonstrate acceptable life. Also, the reverse helicity case results in high surface compression for the prescribed 1 MW/m2 for 1 sec.

Introduction

The Inboard Divertor Vertical (IBDV) Tiles are part of the High Heat Flux (HHF) tiles exposed to the highest surface heating from the plasma. As with the other HHF tiles they are both castellated to reduce thermal stresses and fishscaled to eliminate edge heating during normal (forward) helicity operation. They are held in place by Inconel rods at the base of the castellations that are shielded by the tiles from the heat flux carried along magnetic field lines. The rods are held in place by pins that connect to the rods thru a spherical contact which can be engaged by turning the rods, eliminating the need for accessing bolts from the surface of the tile as originally designed.

The IBDV tiles have a number of variations in the design to accommodate diagnostics. The analyses address first the baseline tile without diagnostic cutouts. Rather than analyze all the diagnostic tile s separately a single model was create containing most of the cutouts that exist in the different tiles in one ‘super tile’. This includes cutouts for a mirnov coil, langmuir probes and thermocouples. A separate model was still required for the line of sight tile due to the presence of the large view port.

Assumptions

The tile is assumed to be made of Sigrafine R6510 with a layer of Grafoil between it and the underlying cooling plate. All supports (cooling plate and frame) and hardware (rods & pins) are Inconel 718.

Method of Analysis

The ANSYS Workbench version 19.1 is used to analyze the thermal and structural response to the applied preload, heat fluxes and EM loads as specified in Ref 1. Note the EM loads are calculated using field data (B and dB/dt) from Ref 2 which in turn was developed from Ref 1.

Several Heating scenarios are given in the requirements and are repeated below (TBD)

Results - <u>Baseline Tile, Diagnostics Super Tile, Baseline Tile in POCO</u>

Analysis of Inboard Diverter Vertical (IBDV) high heat flux tile

ORNL

The ANSYS Workbench project diagram is shown in Figure 1. It included a static analysis of preload, halo, and eddy current forces without the thermal load. Two thermal loading conditions were applied to the tile. Finally, all loads were combined.

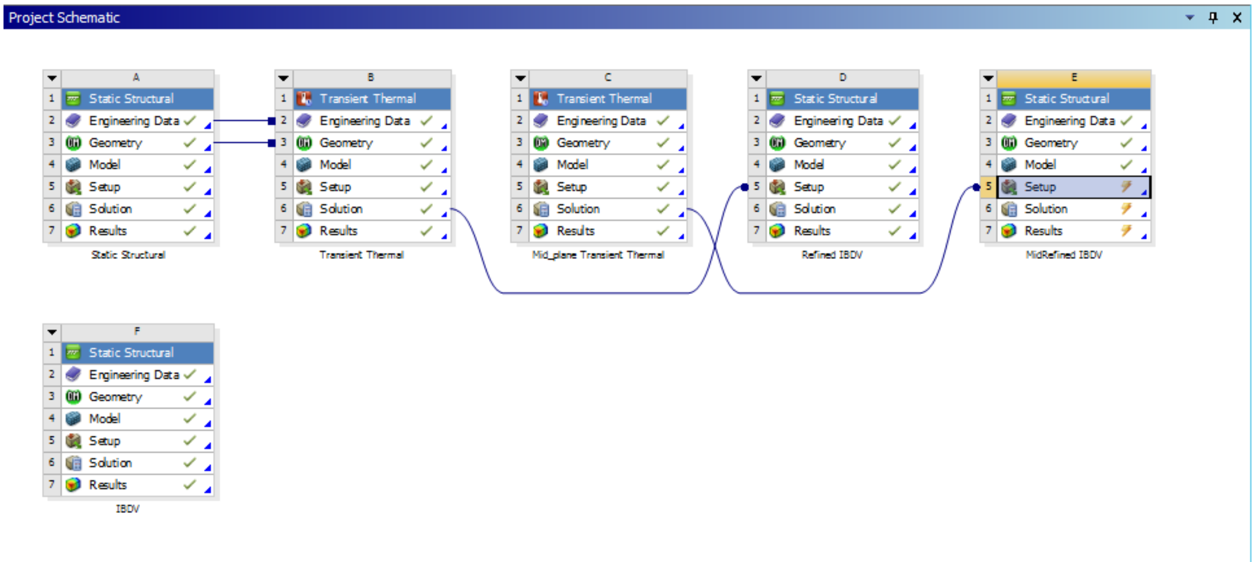

Figure 1: Workbench Schematic of IBDV Analysis.

The components considered in the analysis are listed below in Figure 2 and Figure 3.

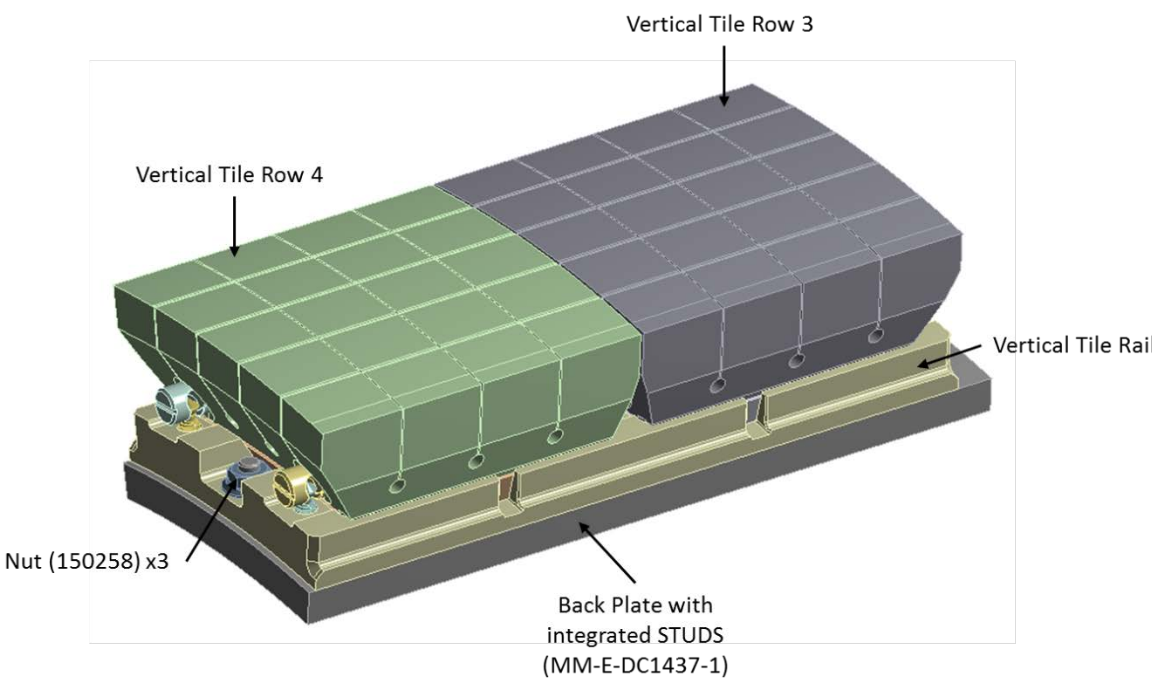

Figure 2: Inboard Diverter Vertical Tile Base Tile Assembly

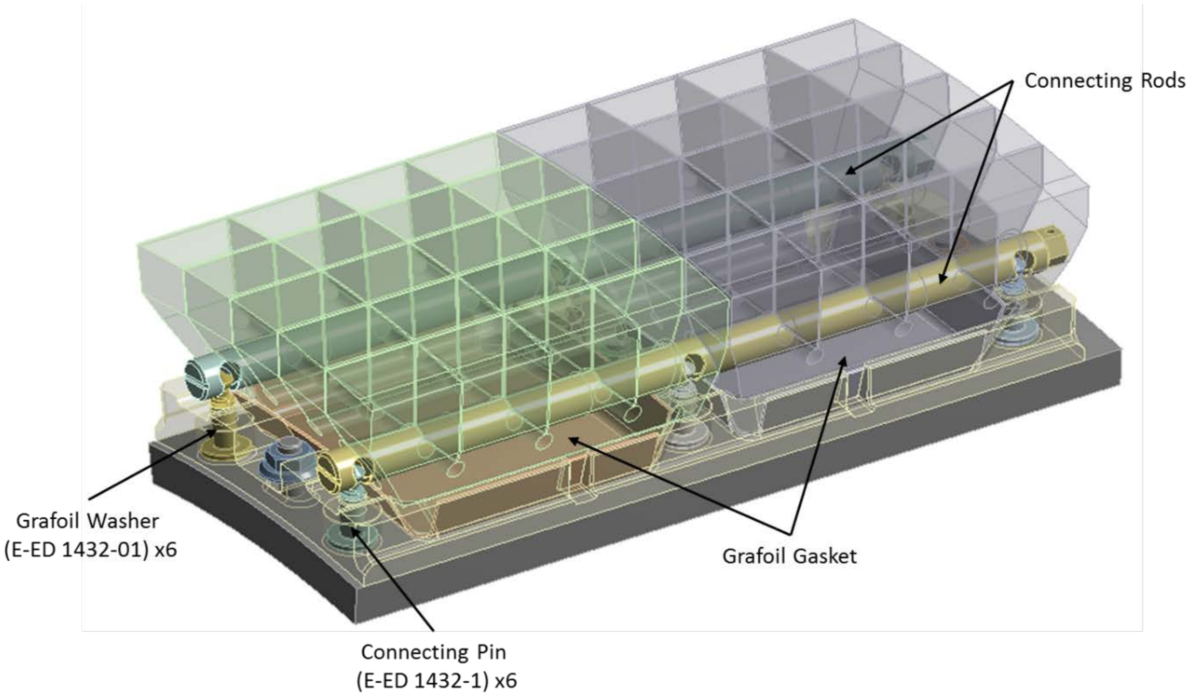

Figure 3: Inboard Diverter Vertical Tile Base Tile Assembly.

The mesh consisted of high order tetrahedrals. The total number of elements and nodes for the whole assembly is 1,494,898 and 2,470,378 respectively. The contact areas between the connecting rods and tiles had a refined mesh. The connecting pin heads also had a refined mesh where they contact the connecting rods. Figure 4 shows the mesh used in the analysis with and without the graphite tile. Figure 5 shows the refined mesh of the tile, connecting rod, and connecting pin contact areas.

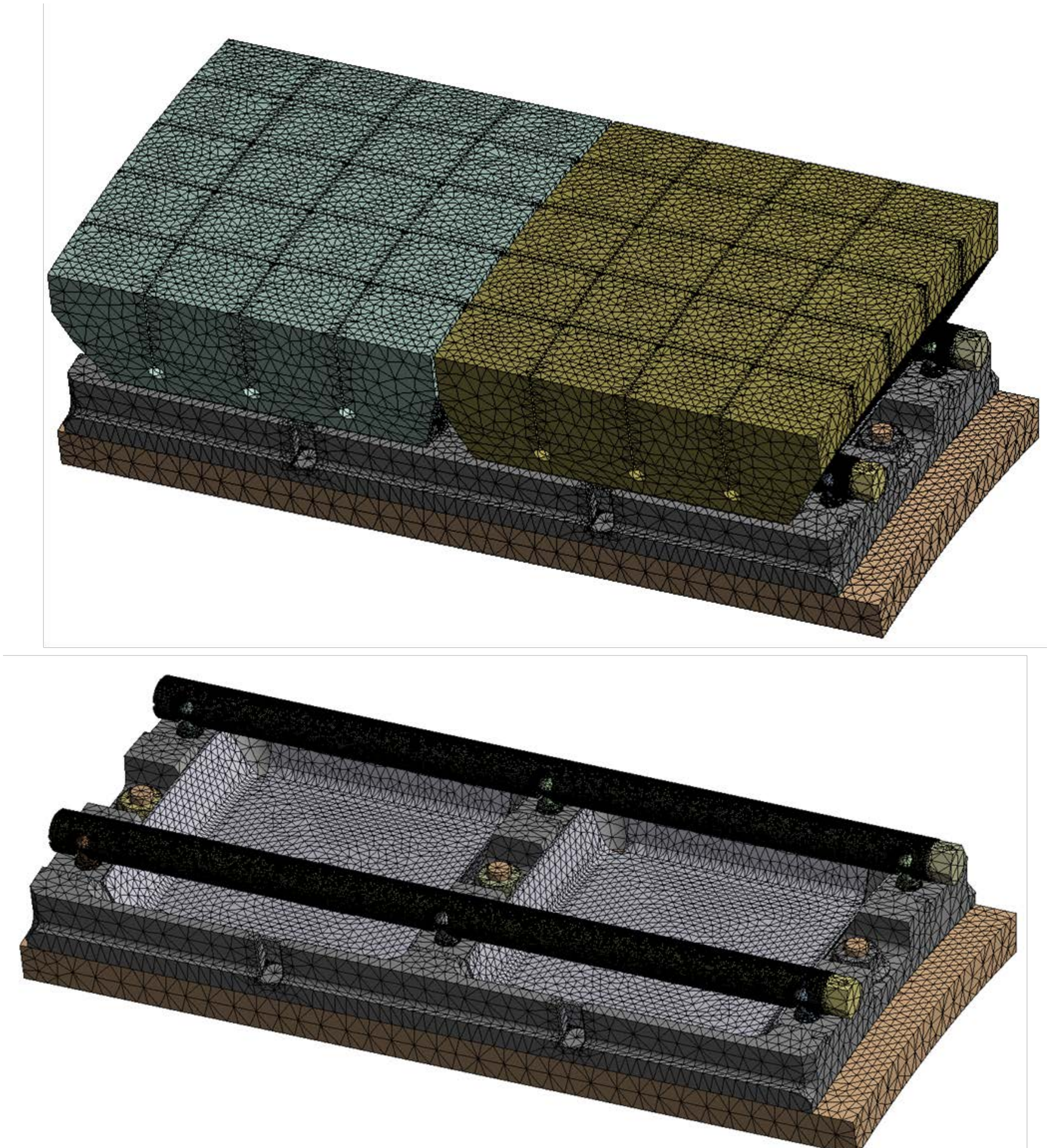

Figure 4: Mesh of the Inboard Diverter Tile Assembly with and without theTiles

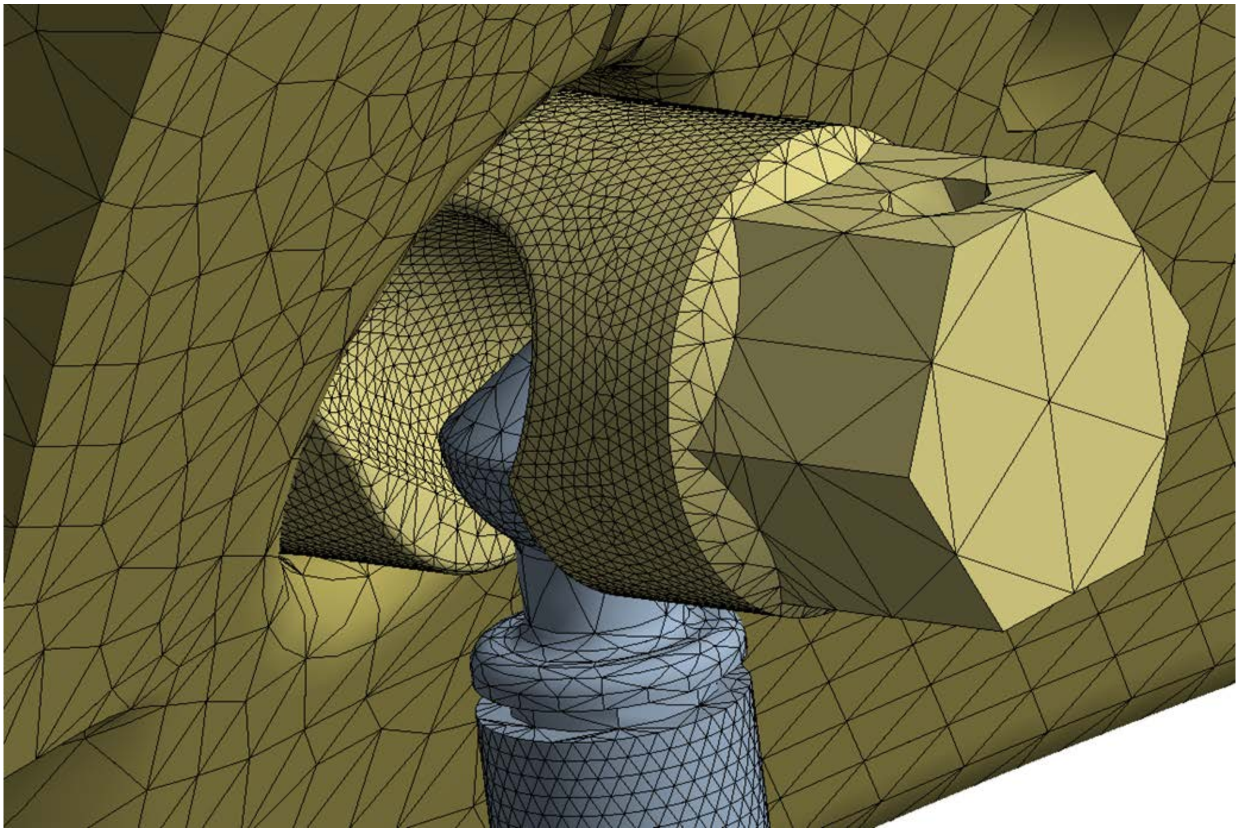

Figure 5: Refined mesh of the connecting rod, connecting pin and tile contact areas.

Table 1 lists each component of the assembly and its material.

Table 1: Components and their materials.

Component	Material
Graphite Tiles (row 3 and row 4)	Graphite SGL R6510
Grafoil Gaskets and Washers	Grafoil
Back Plate with integrated studs	Inconel 718
Vertical Tile Rail	Inconel 718
Connecting rods	Inconel 718
Connecting pins	Inconel 718
Nuts (150258)	Inconel 718

Thermal Analysis

Two transient thermal analyses were performed for case 1 and one for case 3 with an initial ambient temperature of 192.36 ^{o}C for a 5s heat flux pulse mapped over two specified areas of the tile. Both heat flux values for case 1 were 6.77 MW/m^2, over an extent of 0.11m. The peak heat flux started at 6.77 MW/m^2 and tapered linearly down to a heat flux of 0 over 0.11 m. This was followed by a 115 s cooldown period. Case 3 had a uniform heat flux of 57.29 MW/m^2 applied to specific areas on both tiles for 1 second followed by a 124 s cooldown. The heat flux for case 3 is only applied to a small area on the upper side of the castellations. Helium cooling using 25 C helium in the baseplate was assumed with a convective heat transfer coefficient of 300 W/m^{2}K. Radiation was included for the top tile surface only, since all other have no open view factor. The emissivity was 0.7 and the reference background temperature was 103.42 ^{o}C. The starting assembly temperature was assumed to be 192.36 ^{o}C. The first heat flux profile for case 1 is shown in Figure 6. The second heat flux profile for case 1 is shown in Figure 7. The heat flux profile for case 3 is shown in Figure 8. The radiation and convective surfaces are shown in Figure 9. Contact thermal conductance between all parts was 1000 W/m^{2}C.

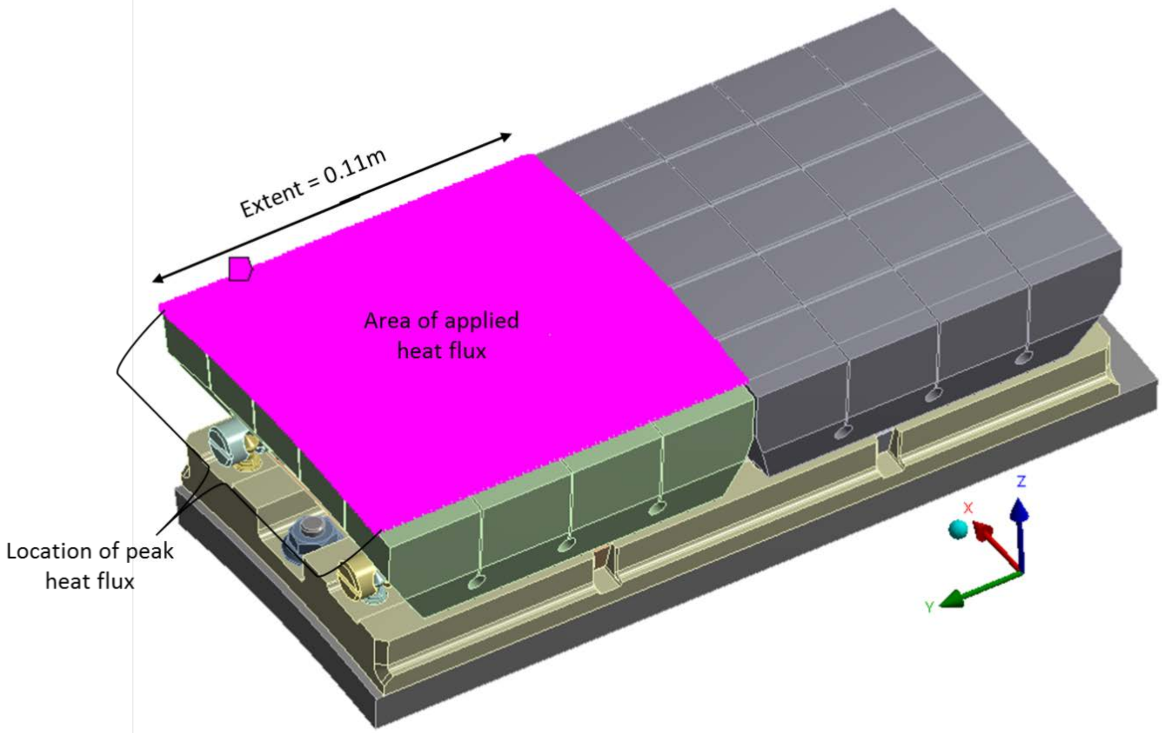

Figure 6: Case 1 heat flux profile 1

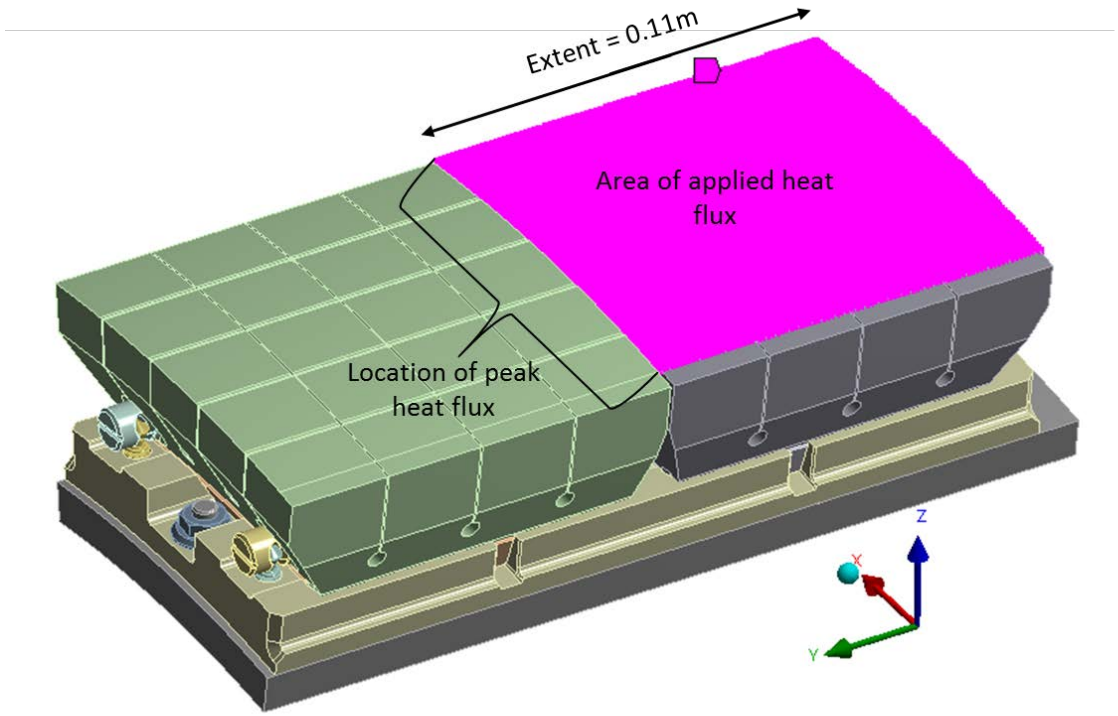

Figure 7: Case 1 heat flux profile 2

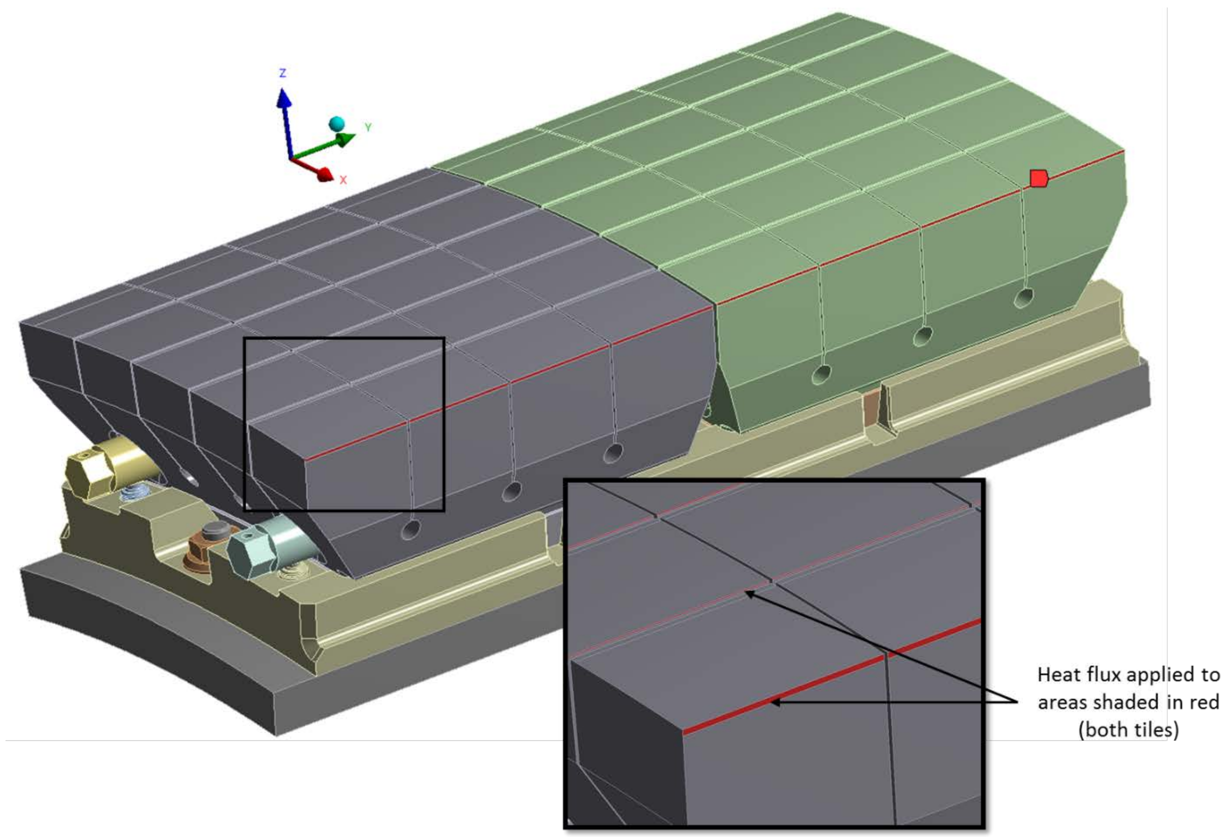

Figure 8: Case 3 heat flux profile

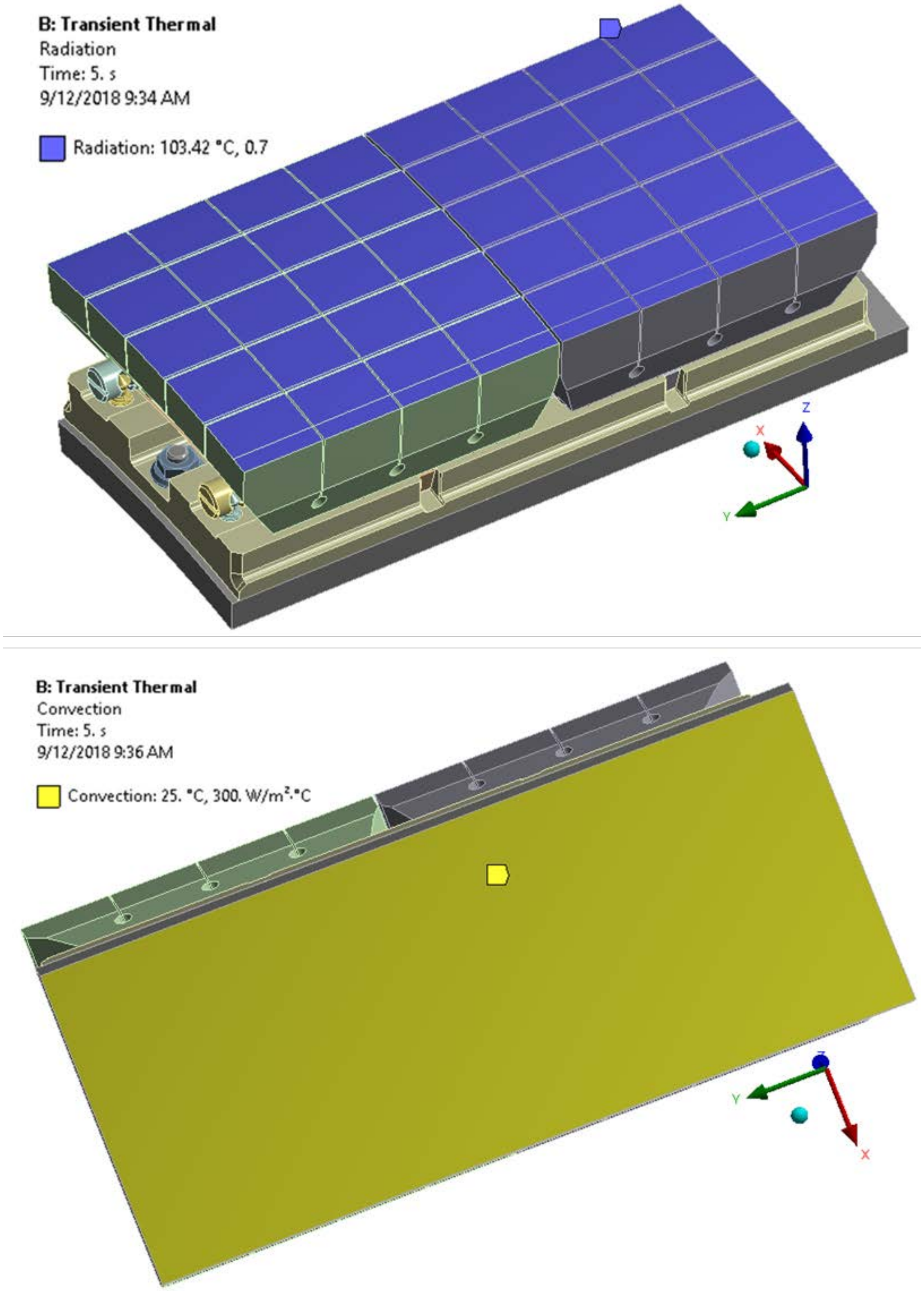

Figure 9: Radiation (top) and Convection (bottom) surfaces.

The peak temperature in the assembly was 1436 °C in the graphite tile for heat flux case 1 profile 1. Figure 10 shows the temperature contour plot of the tile and substructure after 5 seconds of applied heat flux. Figure 11 shows temperature contour plot of the tiles and substructure after 115 s cooldown. Table 2 lists the peak temperature and corresponding time for each component for heat flux case 1 profile 1.

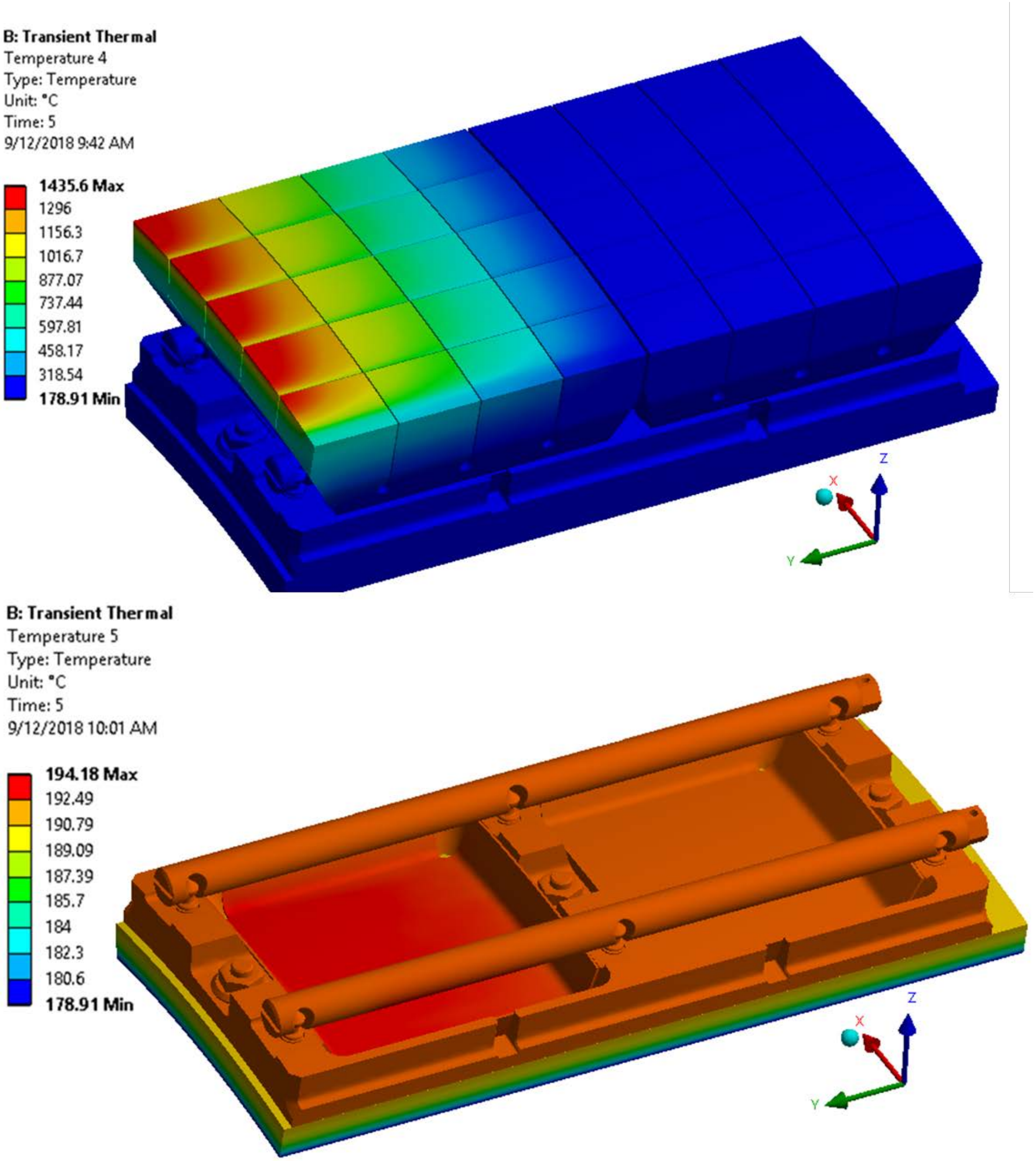

Figure 10: Temperature contour plot of the inboard diverter vertical tiles for heat flux case 1 profile 1 at 5 seconds

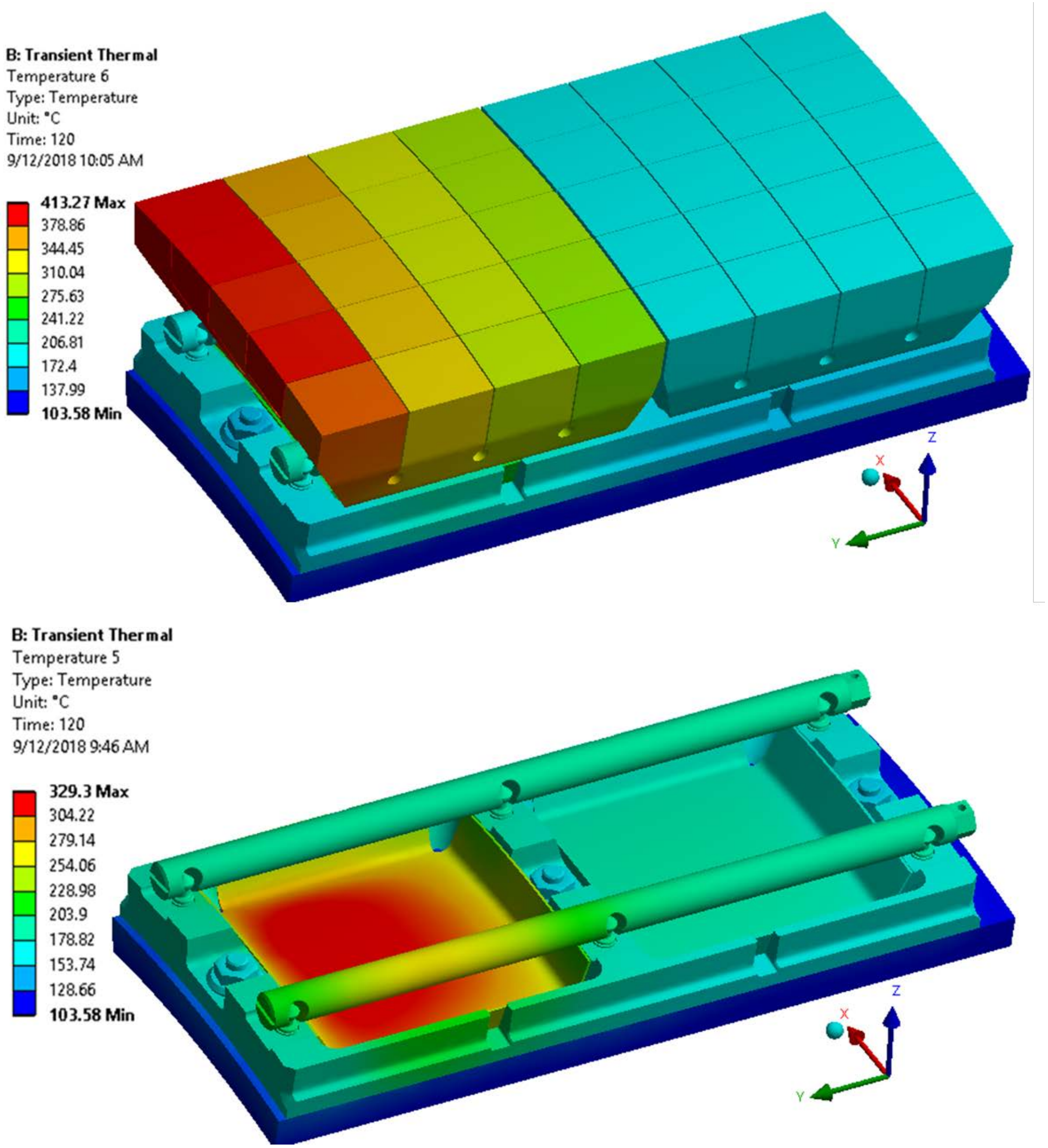

Figure 11: Temperature contour plot of the inboard diverter vertical tiles for heat flux case 1 profile 1 at 120 seconds

Table 2: Peak temperatures for each component for heat flux case 1 profile 1

Component	Peak Temperature (°C)	Time (sec)
Graphite Tiles (row 3 and row 4)	1436	5
Grafoil Gaskets and Washers	335	73
Back Plate with integrated studs	192	0

Vertical Tile Rail	221	114
Connecting rods	279	120
Connecting pins	206	120
Nuts (150258)	192	0

The peak temperature in the assembly was 1427 °C in the graphite tile for heat flux case 1 profile 2. Figure 12 shows the temperature contour plot of the tile and substructure after 5 seconds of applied heat flux. Figure 13 shows temperature contour plot of the tiles and substructure after 115 s cooldown. Table 3 lists the peak temperature and corresponding time for each component for heat flux case 1 profile 2.

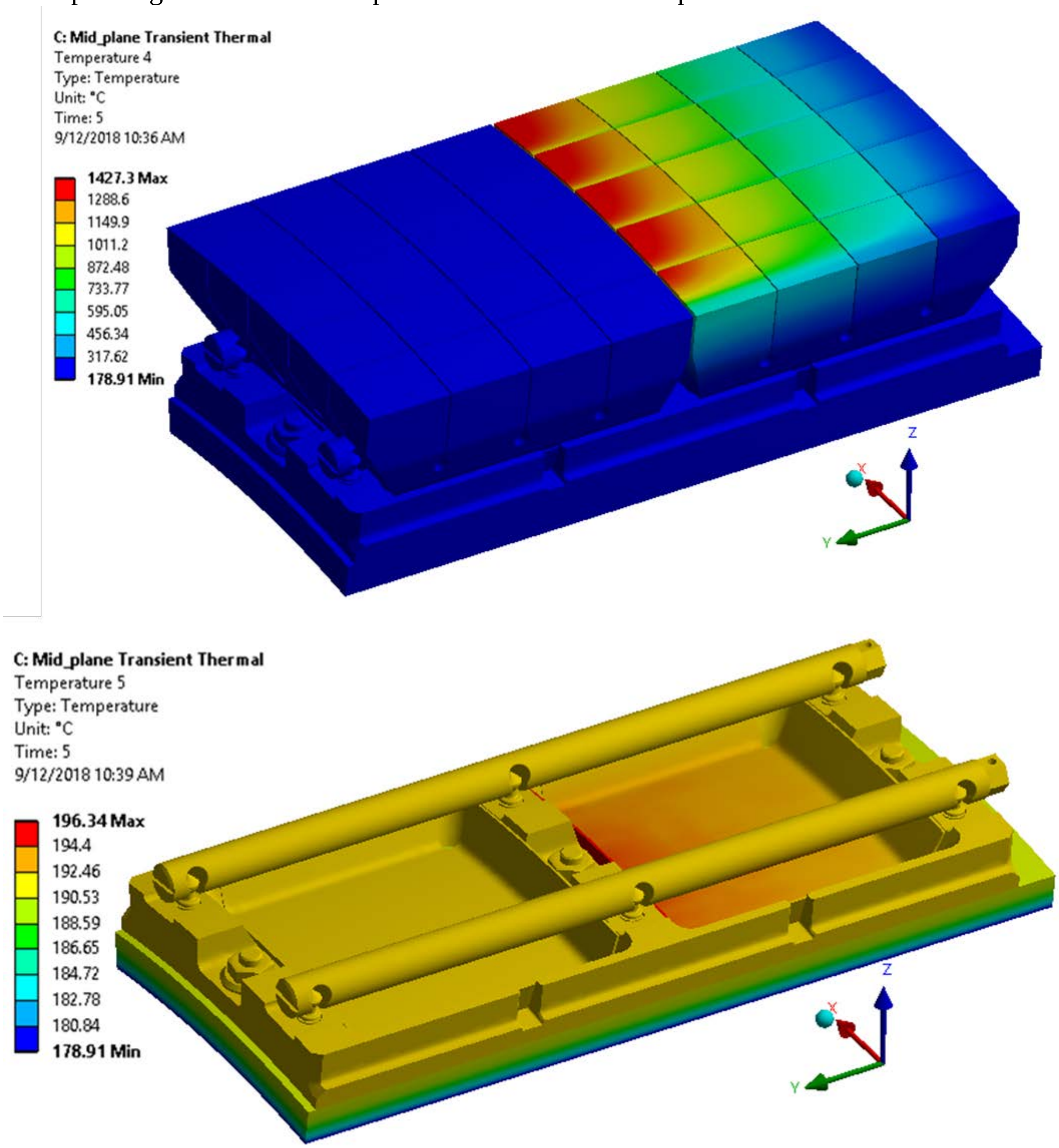

Figure 12: Temperature contour plot of the inboard diverter vertical tiles for heat flux case 1 profile 2 at 5 seconds

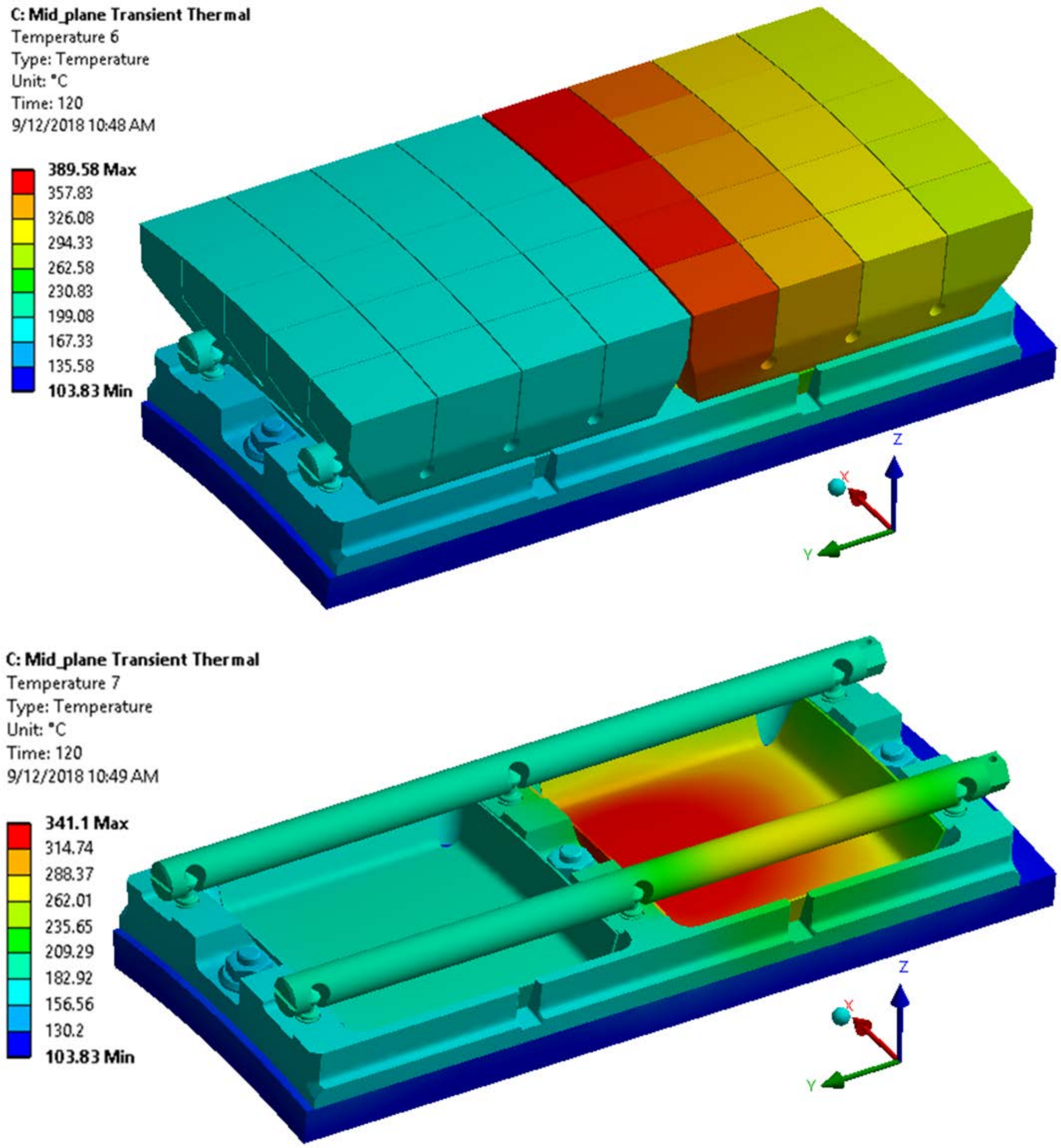

Figure 13: Temperature contour plot of the inboard diverter vertical tiles for heat flux case 1 profile 2 at 120 seconds

Table 3: Peak temperatures for each component for heat flux case 1 profile 2

Component	Peak Temperature (°C)	Time (sec)
Graphite Tiles (row 3 and row 4)	1427	5
Grafoil Gaskets and Washers	353	63
Back Plate with integrated studs	193	5
Vertical Tile Rail	228	120

Connecting rods	283	120
Connecting pins	204	120
Nuts (150258)	193	5

The peak temperature in the assembly was 2206 °C in the graphite tile for heat flux case 3. Figure 14 shows the temperature contour plot of the tile and substructure after 1 seconds of applied heat flux. Figure 15 shows temperature contour plot of the tiles and substructure after 119 s cooldown. Table 4 lists the peak temperature and corresponding time for each component for heat flux case 3.

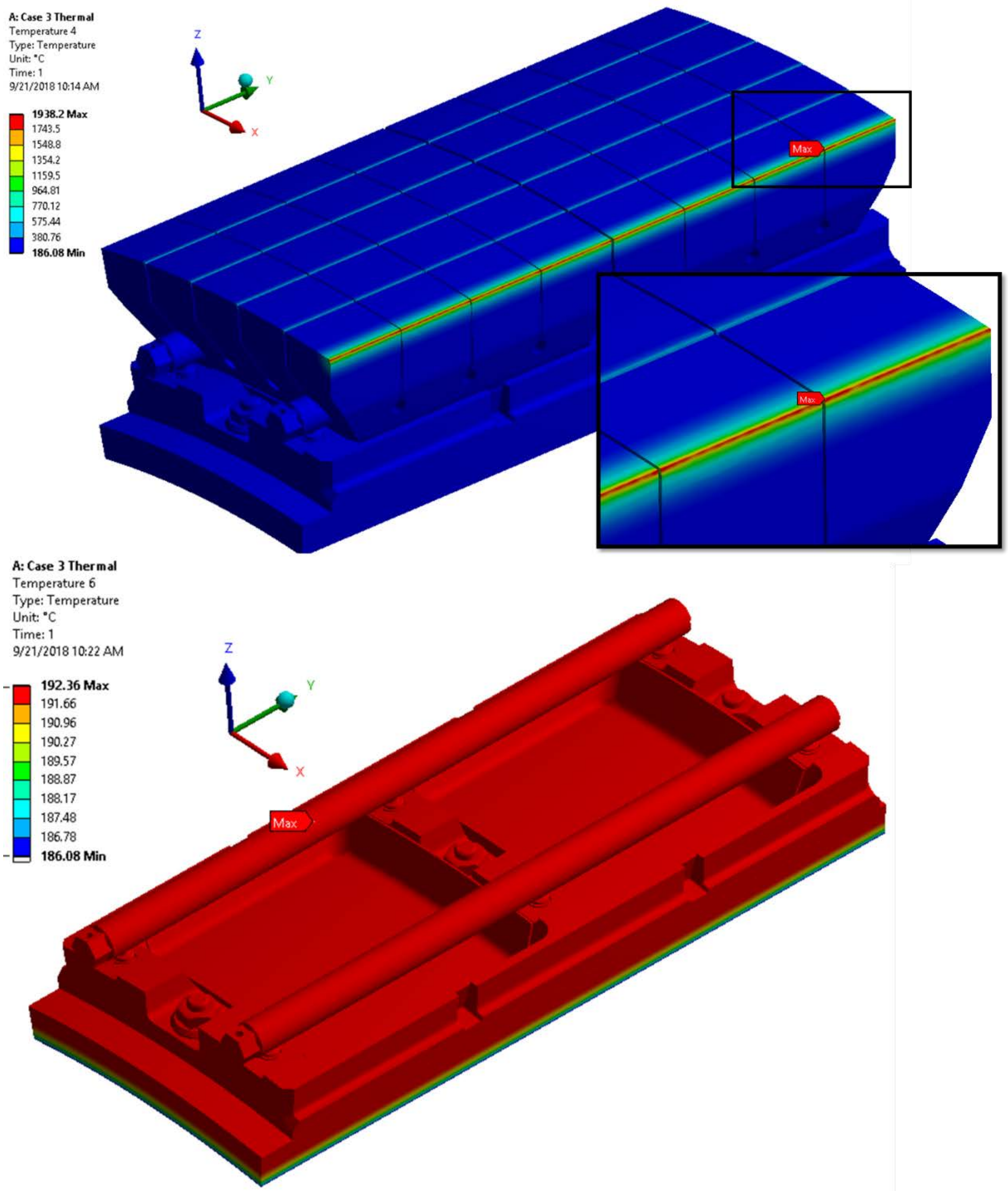

Figure 14: Temperature contour plot of the inboard diverter vertical tiles for heat flux case 3 at 1 seconds

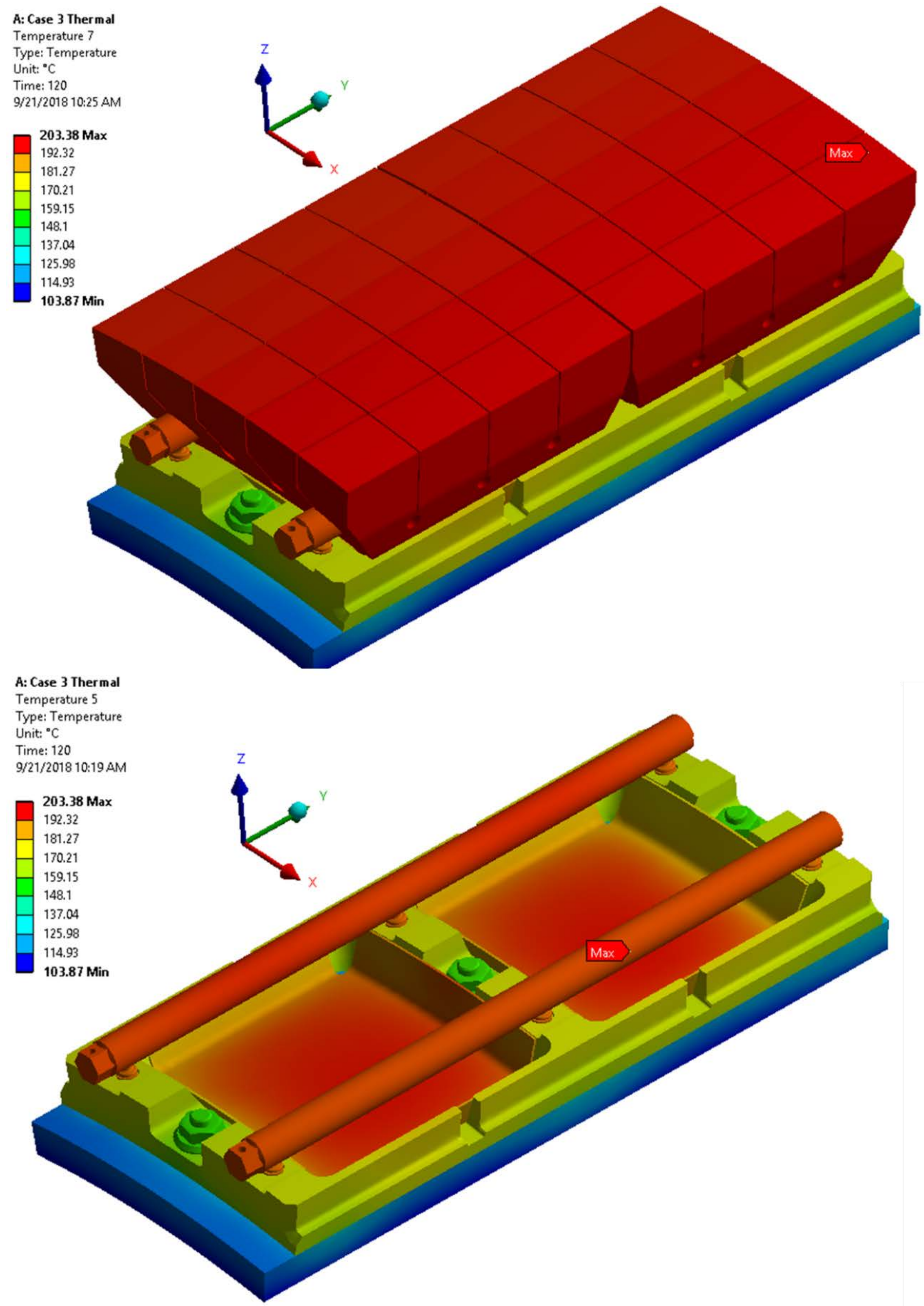

Figure 15: Temperature contour plot of the inboard diverter vertical tiles for heat flux case 3 at 120 seconds

Table 4: Peak temperatures for each component for heat flux case 3

Component	Peak Temperature (°C)	Time (sec)
Graphite Tiles (row 3 and row 4)	1938	1
Grafoil Gaskets and Washers	200	42
Back Plate with integrated studs	192	0
Vertical Tile Rail	193	18
Connecting rods	195	120
Connecting pins	192	0
Nuts (150258)	192	0

Structural-Thermal Analysis

The temperature profiles that resulted from the thermal analysis were imported into a static structure analysis that included bolt preload, eddy current forces, and halo forces. Bolt preload forces of 1000 N were applied to the tree bolts connecting the back plate to the tile rail. Equal and opposite forces were applied to the head of the pins and tile rail. 375 N of force was applied to the 4 outer pins and 750 N of force were applied to the center pins. Figure 16 shows a schematic of the bolt preload and pin loading used for the structural analysis.

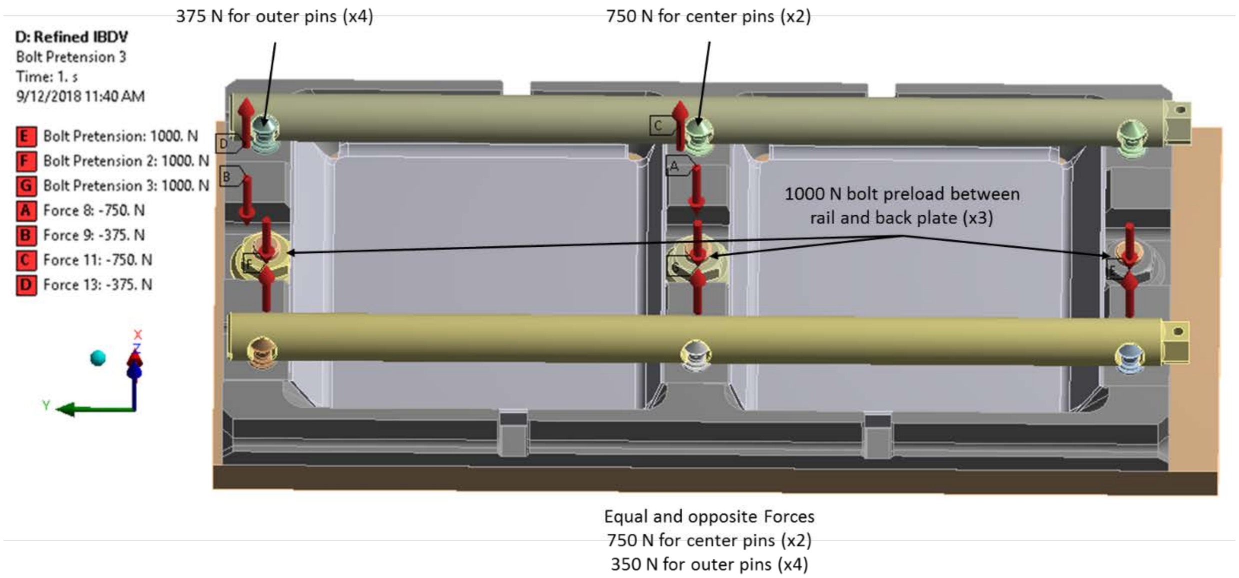

Figure 16: Bolt Preload and pin Loading.

Halo loads were applied to each tile. The row 4 tile halo load was applied in the positive axial and circumferential directions. The row 3 halo load was applied in the negative axial and positive circumferential directions. The loads were divided and applied to each node in each of the tiles. Figure 17 shows direction and magnitudes of the halo loads on the two tiles.

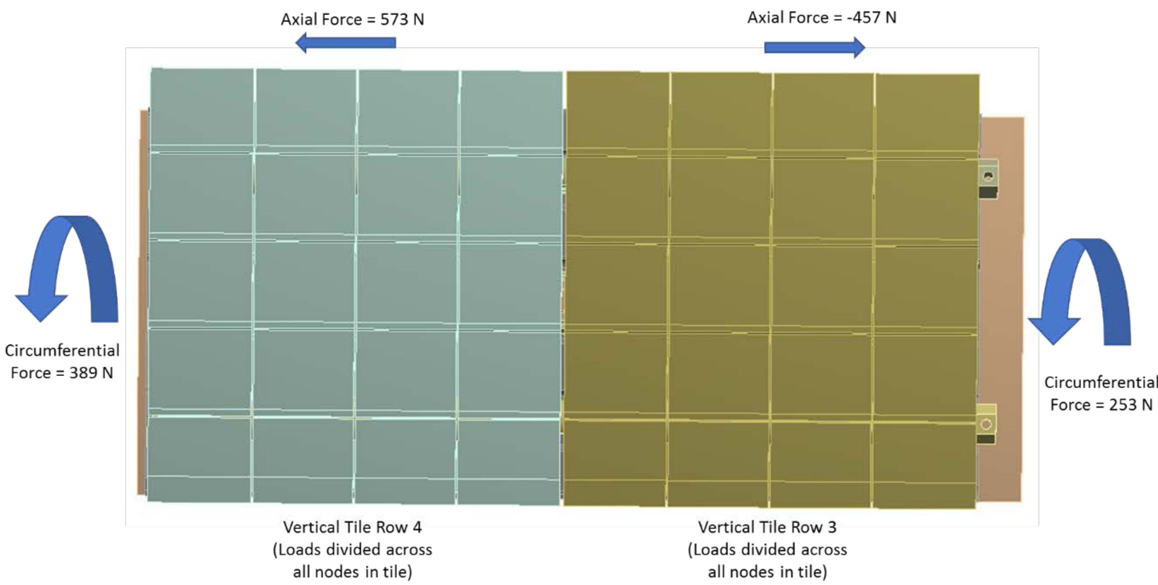

Figure 17: Halo forces applied to all nodes in each of the graphite tiles.

The eddy current loading was applied with equal and opposite loading in the radial direction on the sides of the tile creating moments. Figure 18 shows the surfaces and magnitudes of the eddy current forces applied to the tiles.

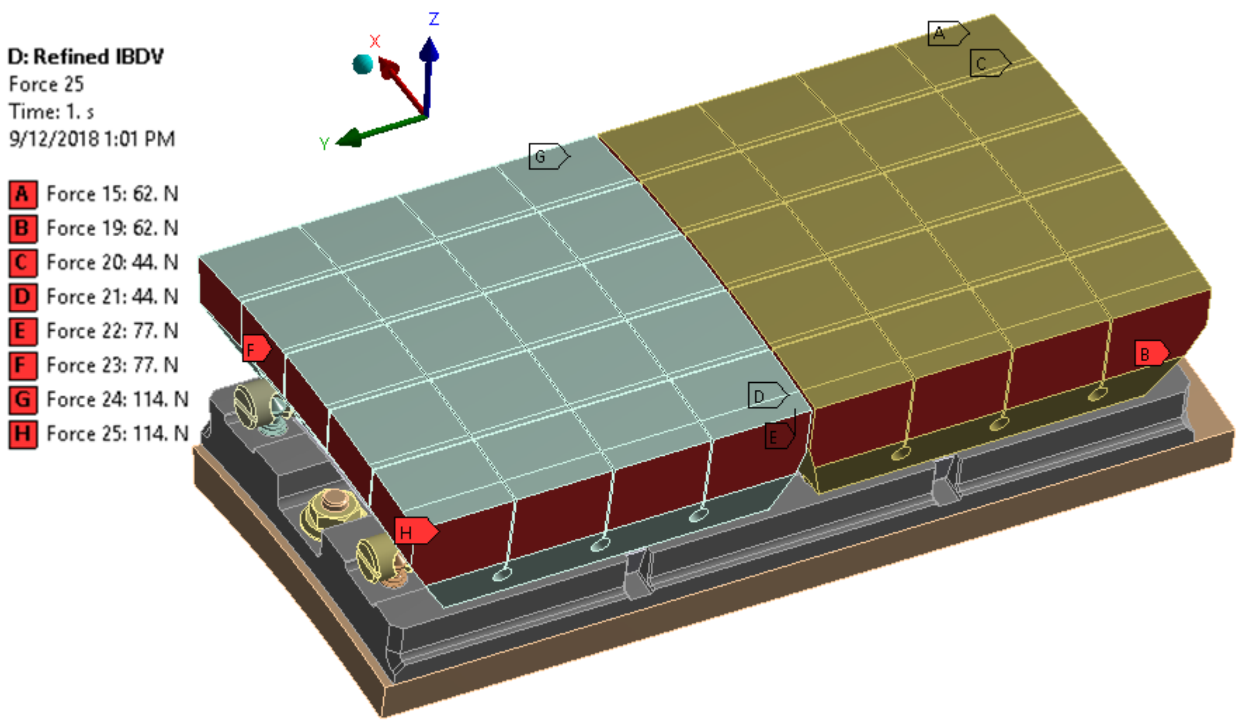

Figure 18 Eddy current loading in IBVD tiles

Fixed displacements were applied to the back plate and tile rail to constrain the model during the analysis. Circumferentially fixed displacements were placed on the sides of the back plate and tile rail. A fixed axial displacement was placed on the back plate

surface on the row 3 tile end of the assembly Figure 19 shows the location of these fixed displacements highlighted in yellow.

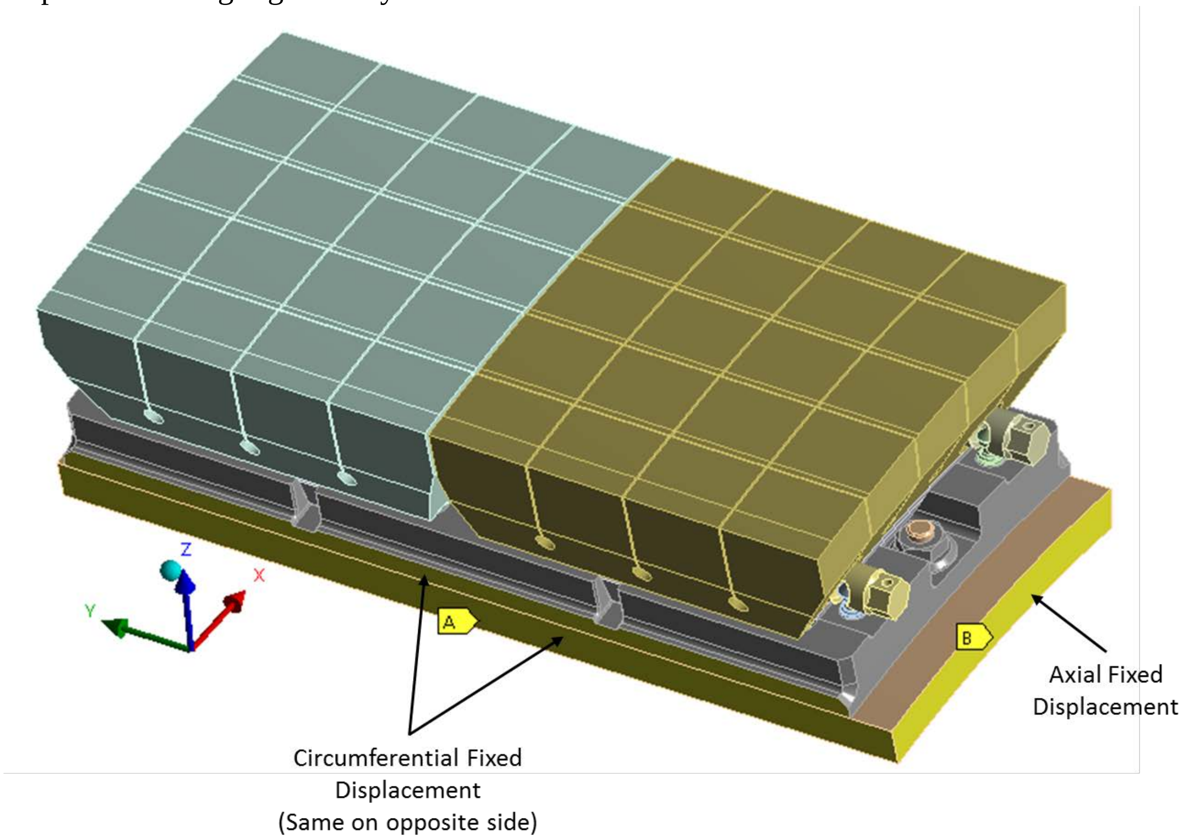

Figure 19: Fixed Displacement locations for IBDV Analysis.

The components of the assembly were connected through various forms of contact. A no separation contact was applied between the grafoil washers and the connecting rod pins as shown in Figure 20. Frictional contact with a coefficient of 0.3 was added between the nuts and tile rail connecting it to the back plate. Figure 21 shows the location of contact between the nuts and tile rail. Finally, the remaining contact between the components was assumed to be frictional with a coefficient of 0.1. This contact is between the following:

1) Tiles and gasket grafoil.
2) Tiles and connecting rods.
3) Connecting rod pins to connecting rods.
4) Tile rail and gasket grafoil.
5) Tile rail and back plate.

Figure 22 shows the locations of the remaining contact in the assembly.

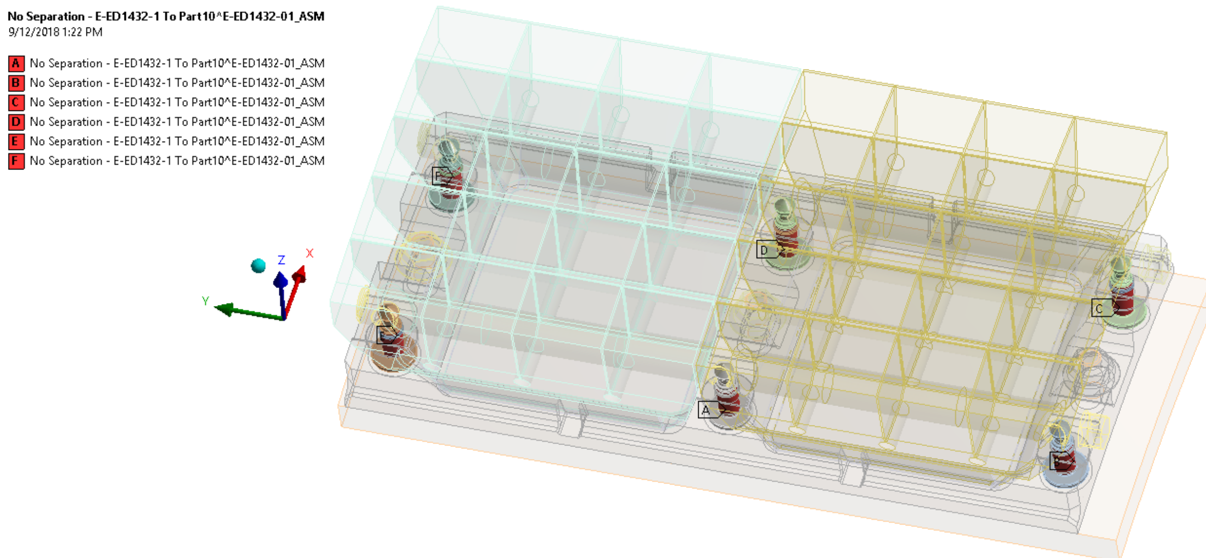

Figure 20: No separation contact between grafoil washers and connecting rod pins.

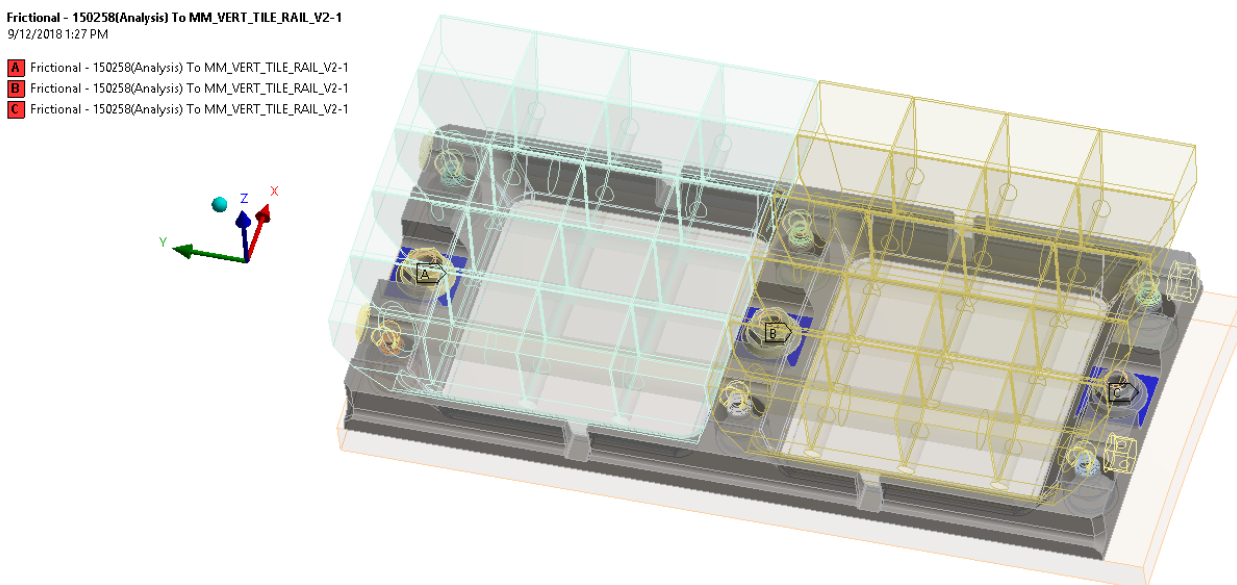

Figure 21: Frictional contact between the nuts and tile rail.

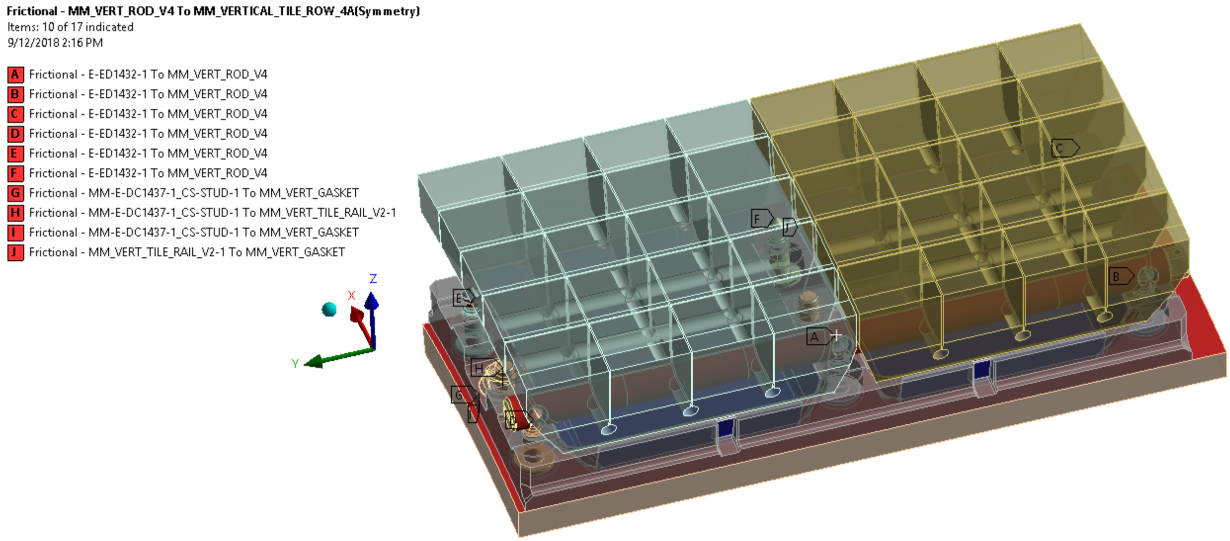

Figure 22: Frictional contact between the graphite tiles and support structure.

Results

The preload, eddy current, and halo loads were combined with the resulting temperature distribution load from the thermal analysis. Note that eddy current and halo loads will be referred to as EM loads. The temperature profile at 5 seconds for each heat flux profile in case 1 was incorporated into a static structural analysis with preload and EM loads. The temperature profile at 5 seconds for load case 3 was incorporated into a static structural model with the preload and EM loads. Finally, the temperature profile that had the highest substructure temperatures at the end of the 115 second cool down was case 1 profile 2. The temperature profile for this case was incorporated with the preload and EM loads. The results from the static analyses for all these heat flux profiles are presented below.

Case 1, Profile 1 and 2 at 5s

Both heat flux case profile 1 and 2 at 5s were compared with each other. The results below represent the worst case between the two profiles. The deformation contour plots in the radial, circumferential, and axial directions of the assembly as a result of the loads is shown in Figure 34, Figure 35, and Figure 36.

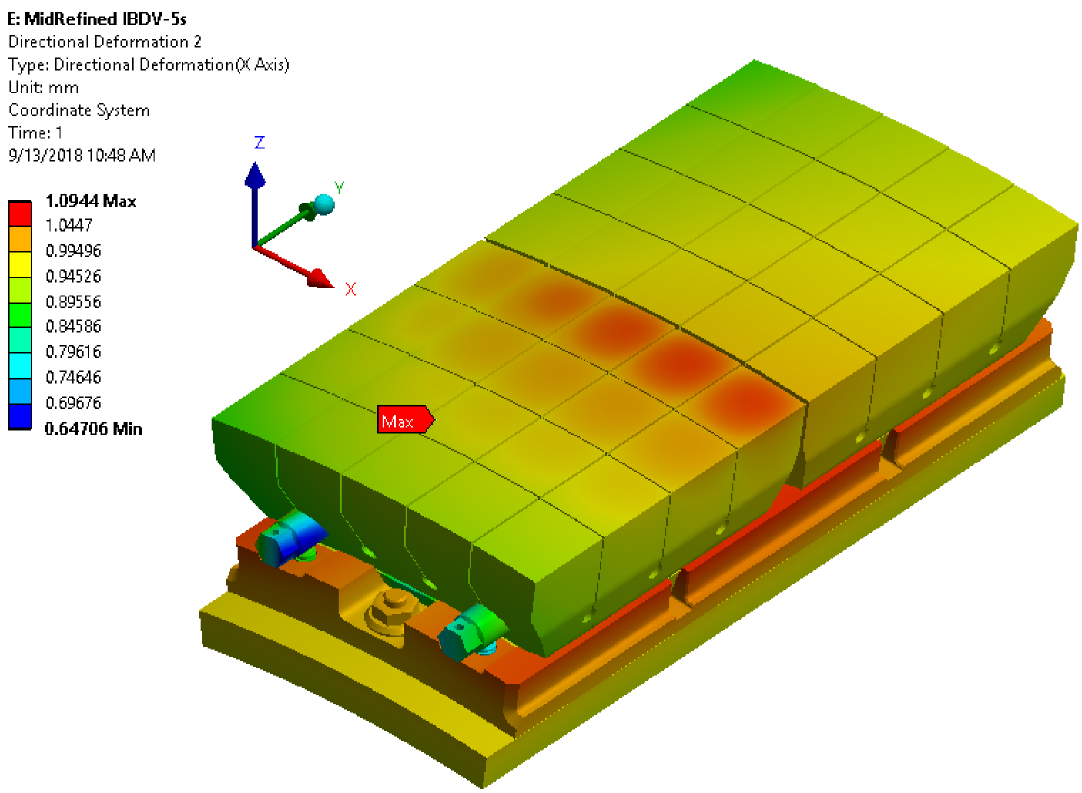

Figure 23: Radial deformation for case 1, profile 2 at 5 seconds.

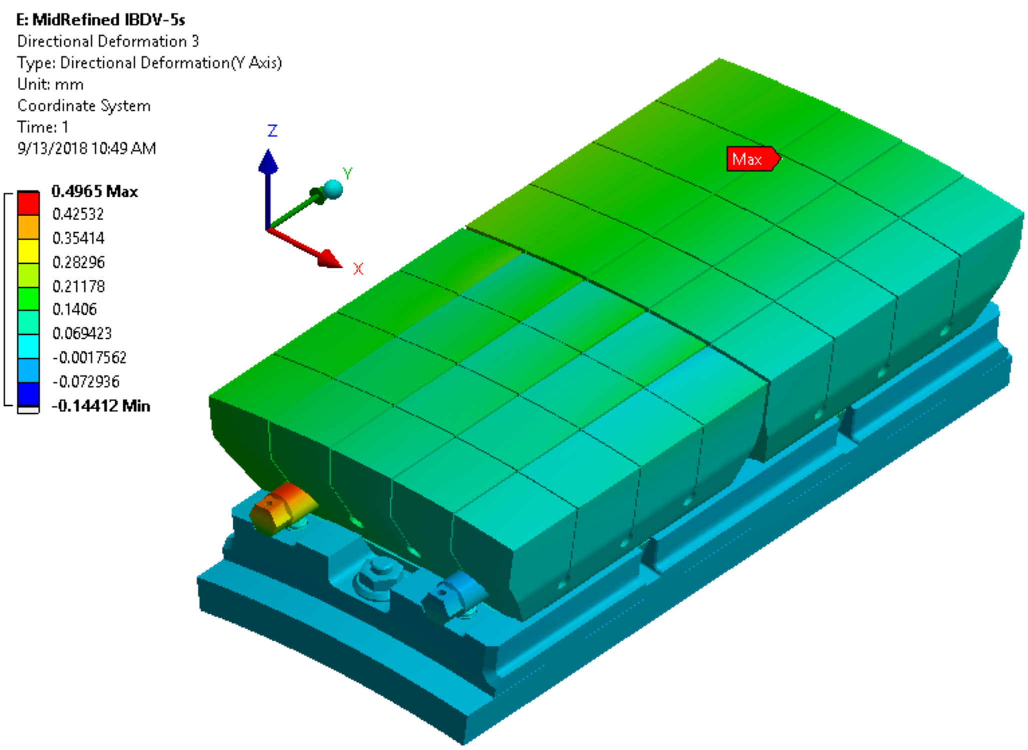

Figure 24: Circumferential deformation for case 1, profile 2 at 5 seconds.

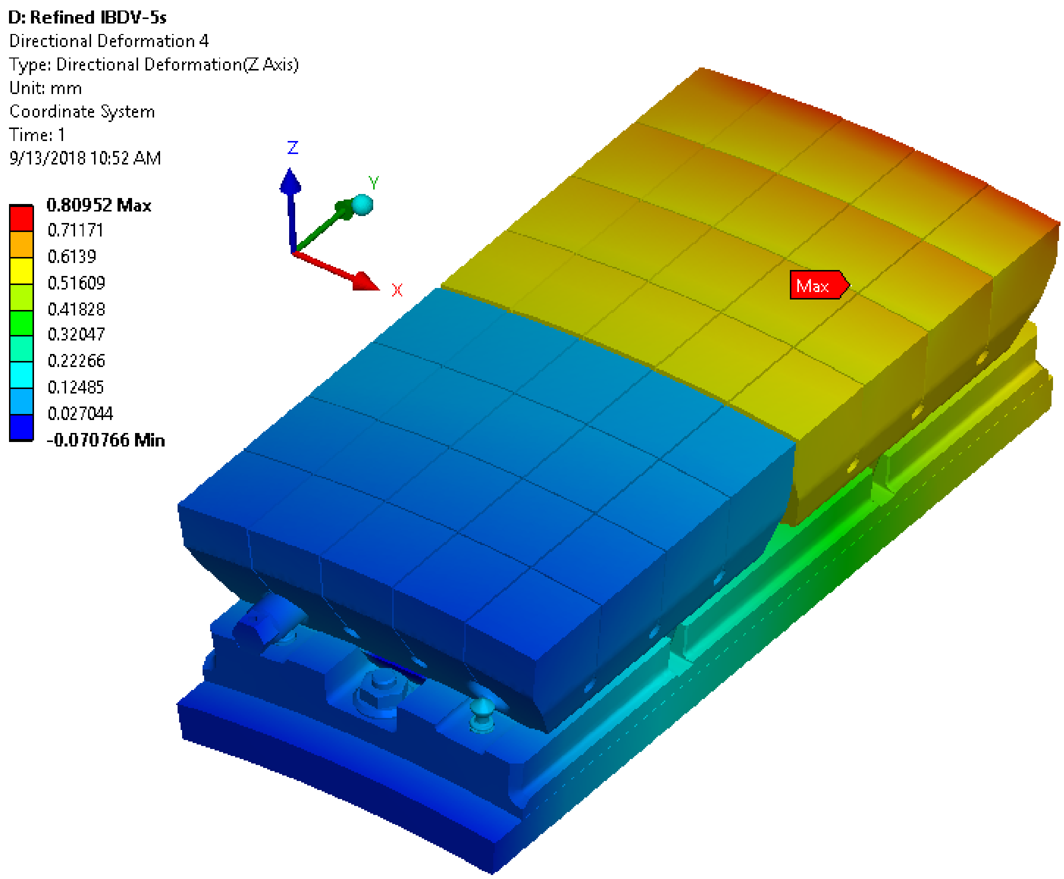

Figure 25: Axial deformation for case 1, profile 1 at 5 seconds.

The following results are for case 1, profile 1 at 5 seconds. Table 5 and Table 6 list the peak maximum and minimum principal stress and the corresponding allowable in the components made of graphite tiles and grafoil gaskets. Table 7 lists the peak equivalent stresses in the Inconel 718 components.

Table 5: Maximum Principal Stress of tiles and grafoil gaskets for case 1, profile 1 at 5 seconds

Component	Peak Stress (MPa)	Allowable (MPa)	Loads
Graphite Tiles row 3	10.37	19	BPL+Halo+Eddy
Graphite Tiles row 4	10.56	19	BPL+Halo+Eddy
Grafoil Gasket	0.91	25	BPL+Halo+Eddy

Table 6: Minimum Principal Stress of tiles grafoil gaskets for case 1, profile 1 at 5 seconds

Component	Peak Stress (MPa)	Allowable (MPa)	Loads
Graphite Tiles row 3	-33.91	-65	BPL+Halo+Eddy
Graphite Tiles row 4	-37.18	-65	BPL+Halo+Eddy
Grafoil Gasket	-1.91	-55	BPL+Halo+Eddy

Table 7: Equivalent Stress in Inconel 718 components for case 1, profile 1 at 5 seconds

Component	Peak Stress (MPa)	Allowable (MPa)	Loads
Back Plate with integrated studs	65.38	276	BPL+Halo+Eddy
Vertical Tile Rail	79.51	276	BPL+Halo+Eddy
Connecting rods	691	276	BPL+Halo+Eddy
Connecting pins	308	276	BPL+Halo+Eddy
Nuts (150258)	65.38	276	BPL+Halo+Eddy

The following results are for case 1, profile 2 at 5 seconds. Table 8 and Table 9 list the peak maximum and minimum principal stress and the corresponding allowable in the components made of graphite tiles and grafoil gaskets. Table 10 lists the peak equivalent stresses in the Inconel 718 components.

Table 8: Maximum Principal Stress of tiles and grafoil gaskets for case 1, profile 2 at 5 seconds

Component	Peak Stress (MPa)	Allowable (MPa)	Loads
Graphite Tiles row 3	10.95	19	BPL+Halo+Eddy
Graphite Tiles row 4	11.47	19	BPL+Halo+Eddy
Grafoil Gasket	0.86	25	BPL+Halo+Eddy

Table 9: Minimum Principal Stress of tiles grafoil gaskets for case 1, profile 2 at 5 seconds

Component	Peak Stress (MPa)	Allowable (MPa)	Loads
Graphite Tiles row 3	-33.72	-65	BPL+Halo+Eddy
Graphite Tiles row 4	-37.10	-65	BPL+Halo+Eddy
Grafoil Gasket	-1.79	-55	BPL+Halo+Eddy

Table 10: Equivalent Stress in Inconel 718 components for case 1, profile 2 at 5 seconds

Component	Peak Stress (MPa)	Allowable (MPa)	Loads
Back Plate with integrated studs	65.31	276	BPL+Halo+Eddy
Vertical Tile Rail	79.13	276	BPL+Halo+Eddy
Connecting rods	681	276	BPL+Halo+Eddy
Connecting pins	306	276	BPL+Halo+Eddy
Nuts (150258)	65.31	276	BPL+Halo+Eddy

Both graphite tiles and the grafoil gaskets resulted in stresses below their allowable values. Figure 26 shows the minimum stress contour plot of the graphite tiles. Figure 27 shows the minimum stress contour plot of the grafoil gaskets.

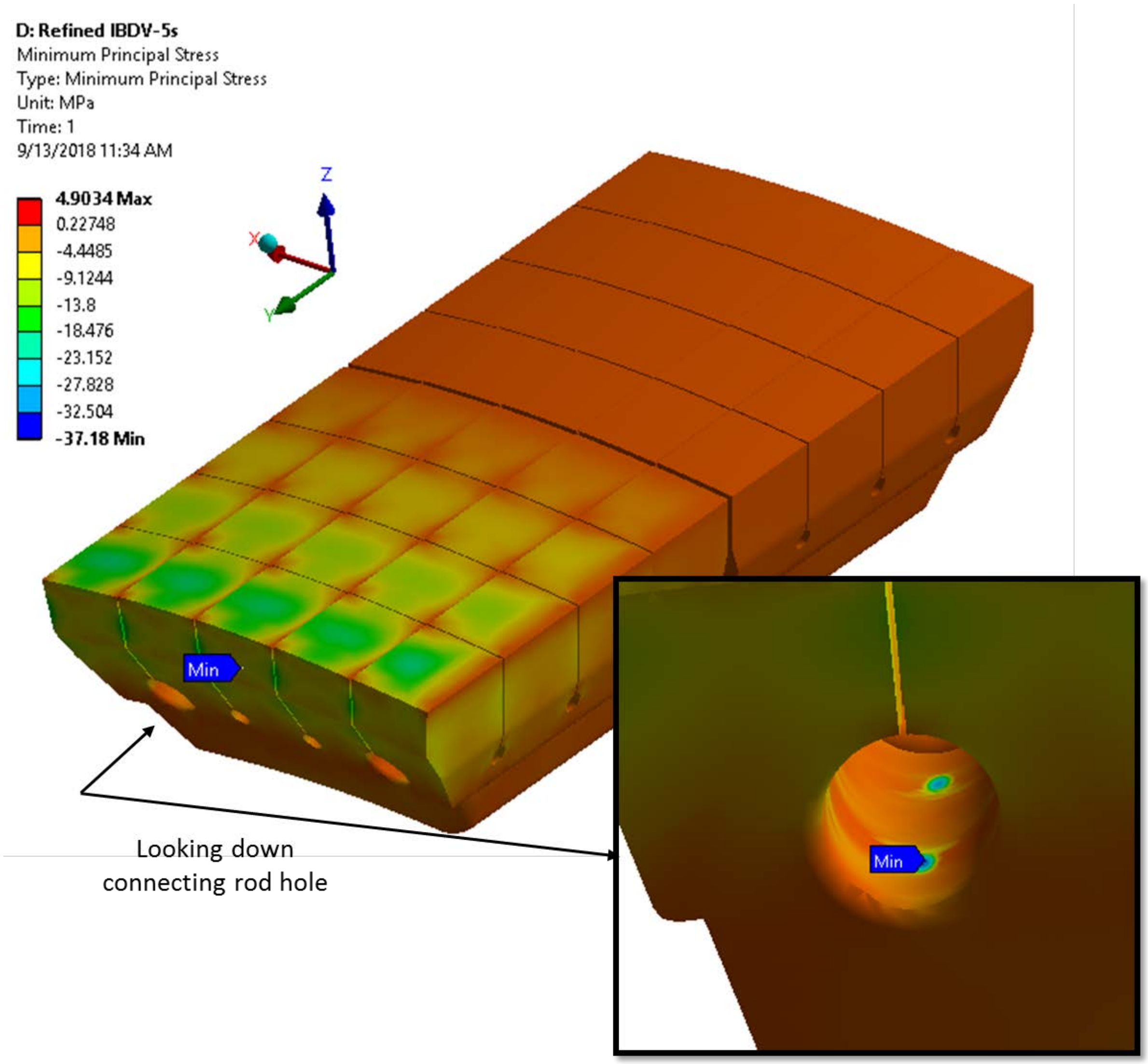

Figure 26: Minimum principal stresses in graphite tiles for case 1, profile 1 at 5 seconds.

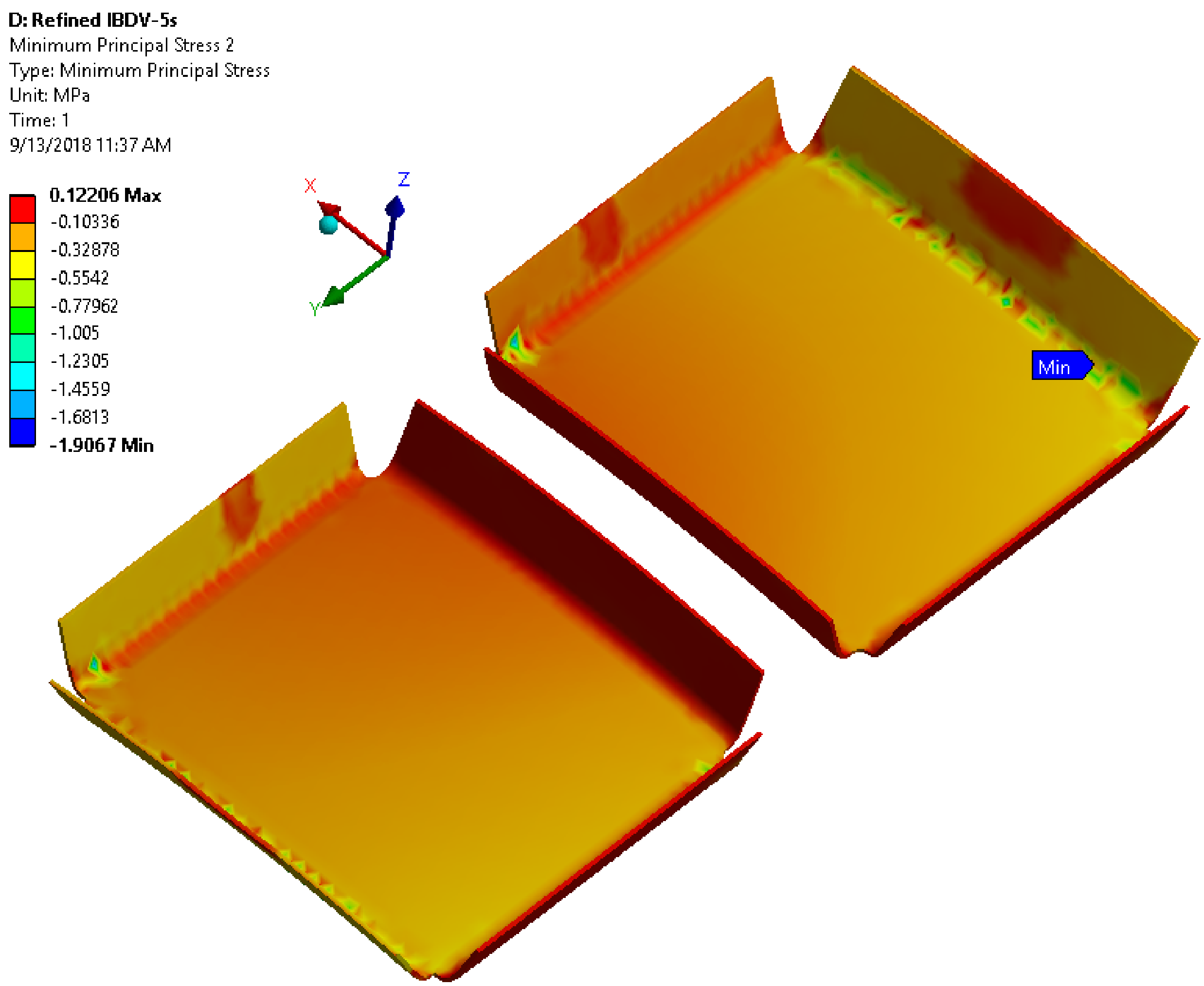

Figure 27: Minimum principal stresses in the grafoil gaskets for case 1, profile 1 at 5 seconds.

Figure 28 and Figure 29 shows the equivalent stress contour plot of all of the Inconel 718 components for both profiles of case 1. Several Inconel 718 components exceeded their allowable values. Figure 30 shows the equivalent stress contour plot of the back plate and nuts. Figure 31 shows the equivalent stress contour plot of the tile rail. The peak stress in these components was below the allowable. The connecting rod pins had localized areas of high stress as shown in Figure 32. These components are likely okay. However, the high stresses in the connecting rods may be cause for concern. Not only are they high, but the high stress extends across several elements. Figure 33 shows the stresses in the connecting rods. It may be possible to reduce the stress in the connecting rods by reducing the preload in the center pins from 750 N to 375 N.

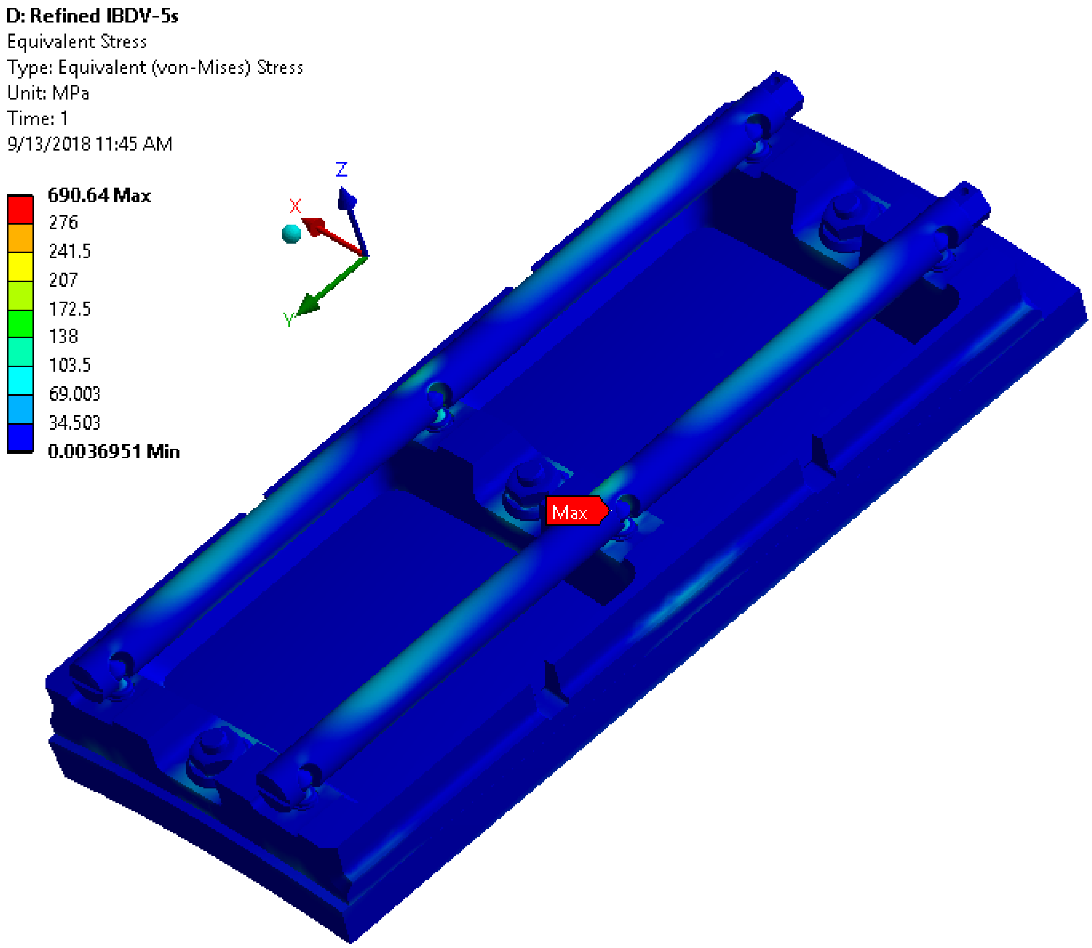

Figure 28: Equivalent stress contour plot of Inconel 718 components for case 1, profile 1 at 5 seconds.

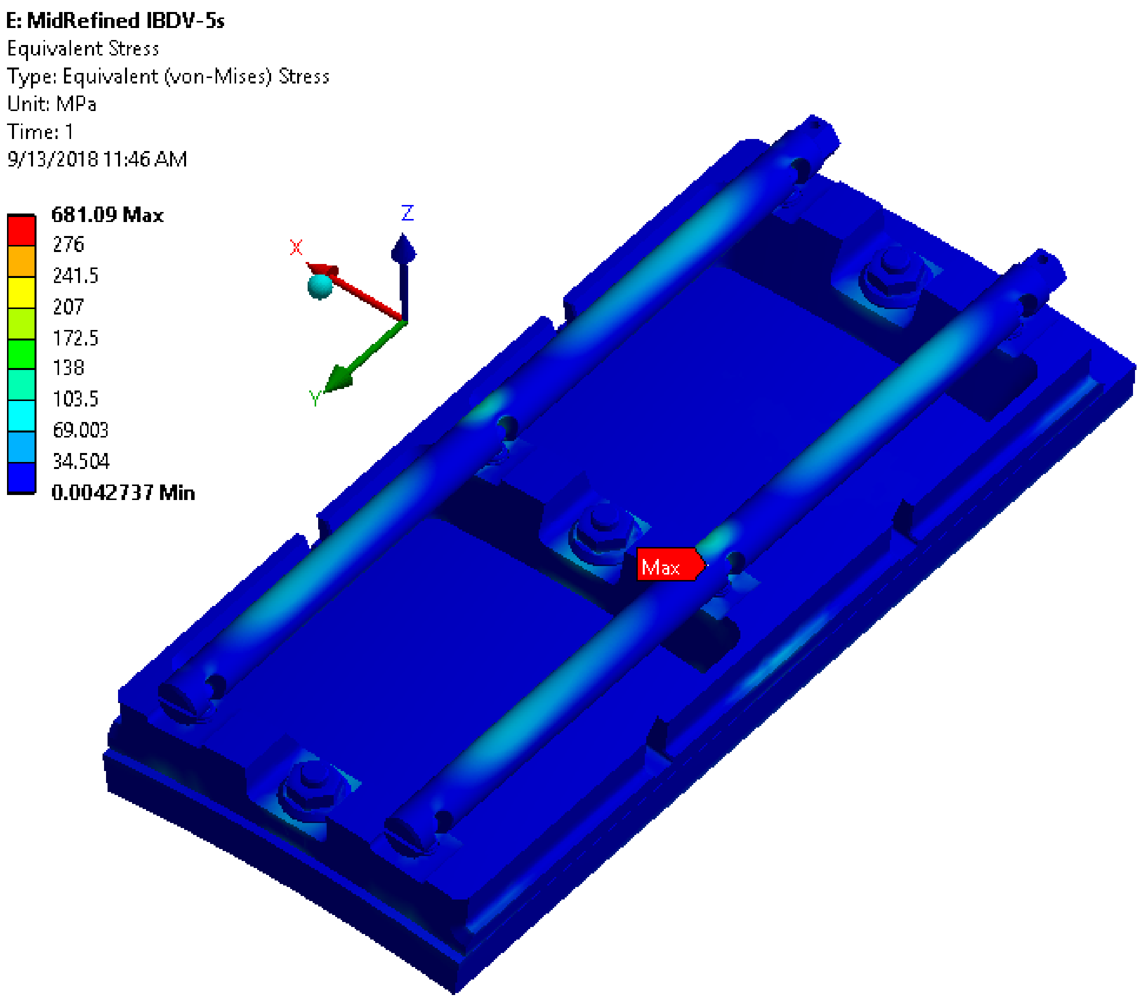

Figure 29: Equivalent stress contour plot of Inconel 718 components for case 1, profile 2 at 5 seconds.

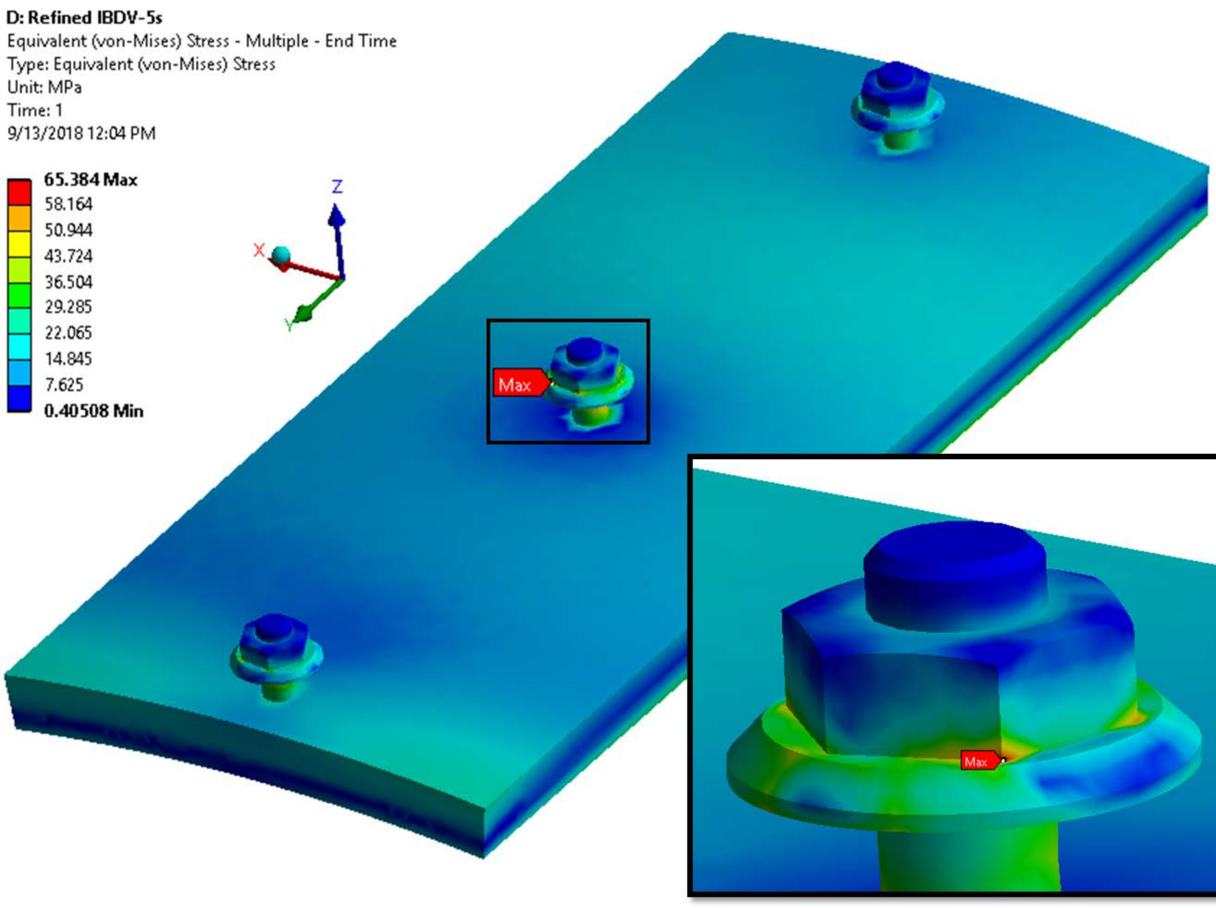

Figure 30: Back plate and nuts equivalent stress contour plot for case 1, profile 1 at 5 seconds.

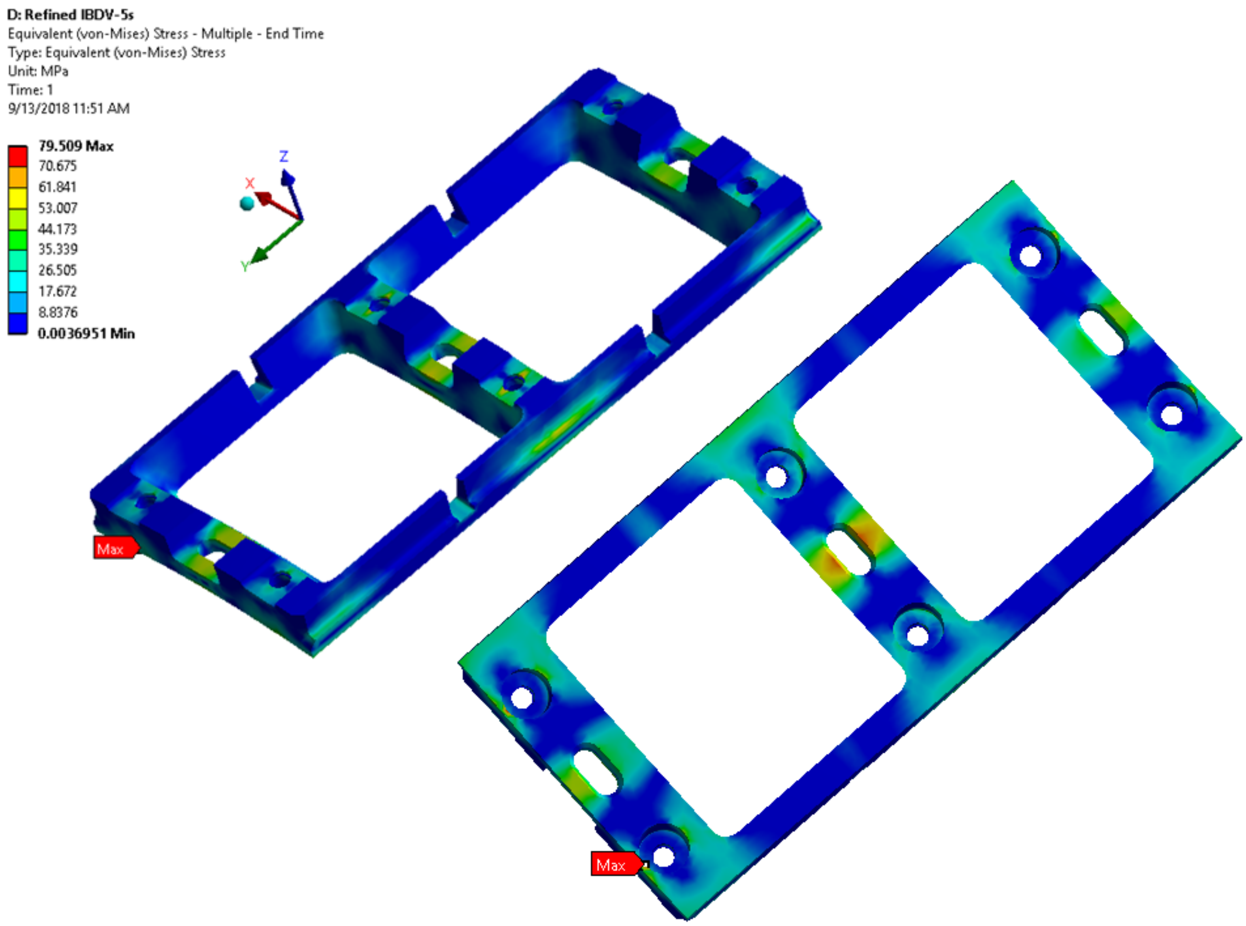

Figure 31: Tile rail equivalent stress for case 1, profile 1 at 5 seconds.

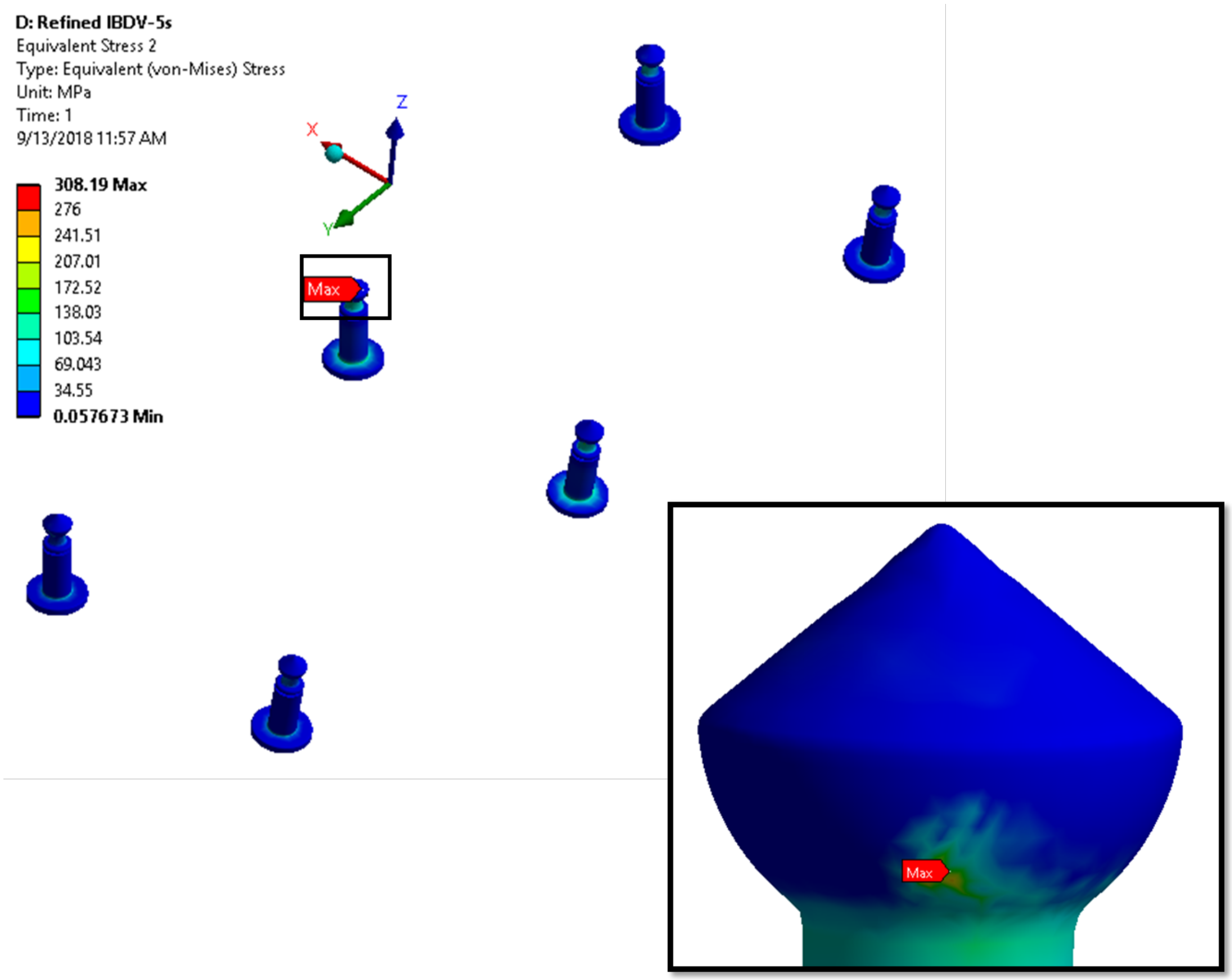

Figure 32: Connecting rod pin equivalent stress contour plot for case 1, profile 1 at 5 seconds.

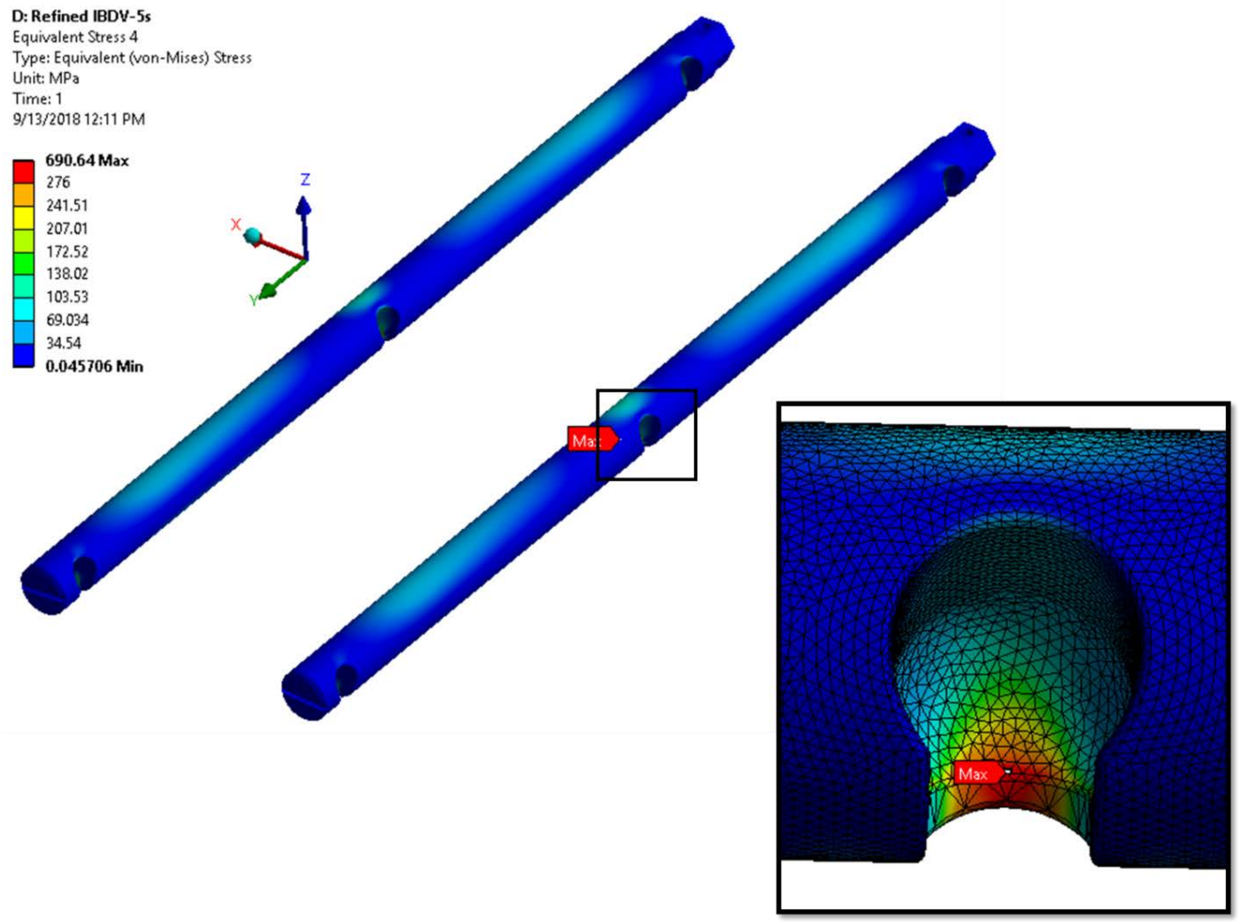

Figure 33: Equivalent stress plot of the connection rods for case 1, profile 1 at 5 seconds.

Case 1, Profile 2 at 120 seconds

The deformation contour plots in the radial, circumferential, and axial directions of the assembly as a result of the loads is shown in Figure 34, Figure 35, and Figure 36.

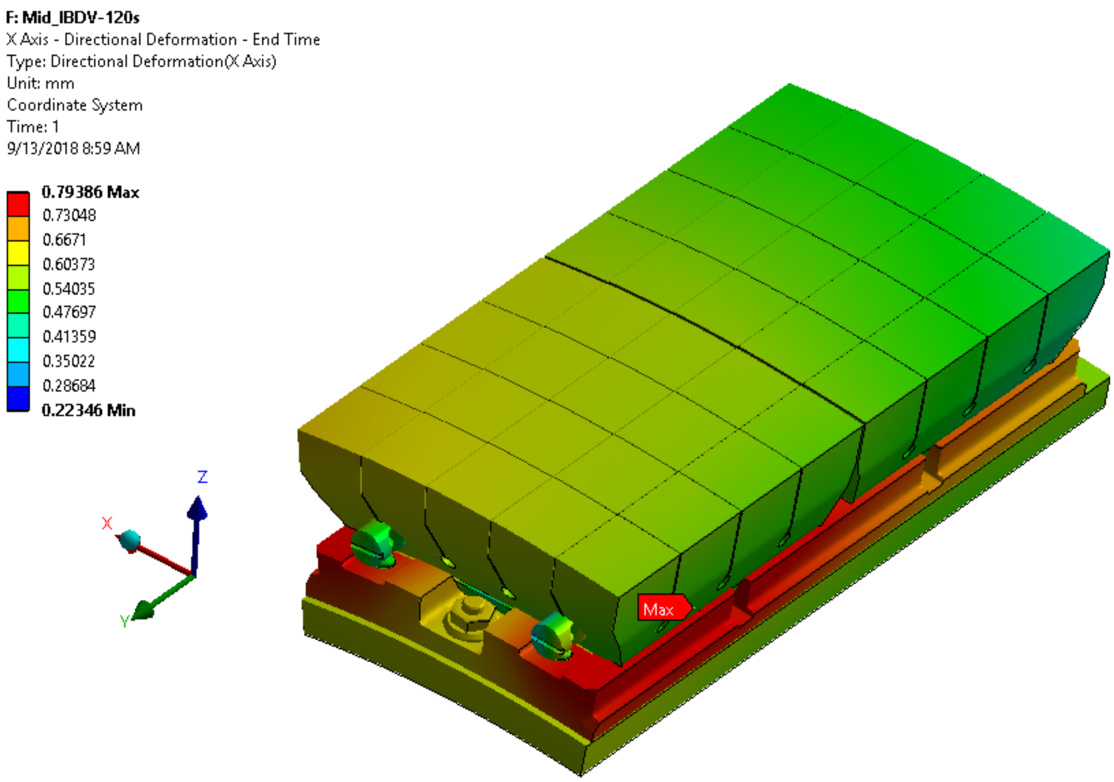

Figure 34: Radial deformation for case 1, profile 2 at 120 seconds.

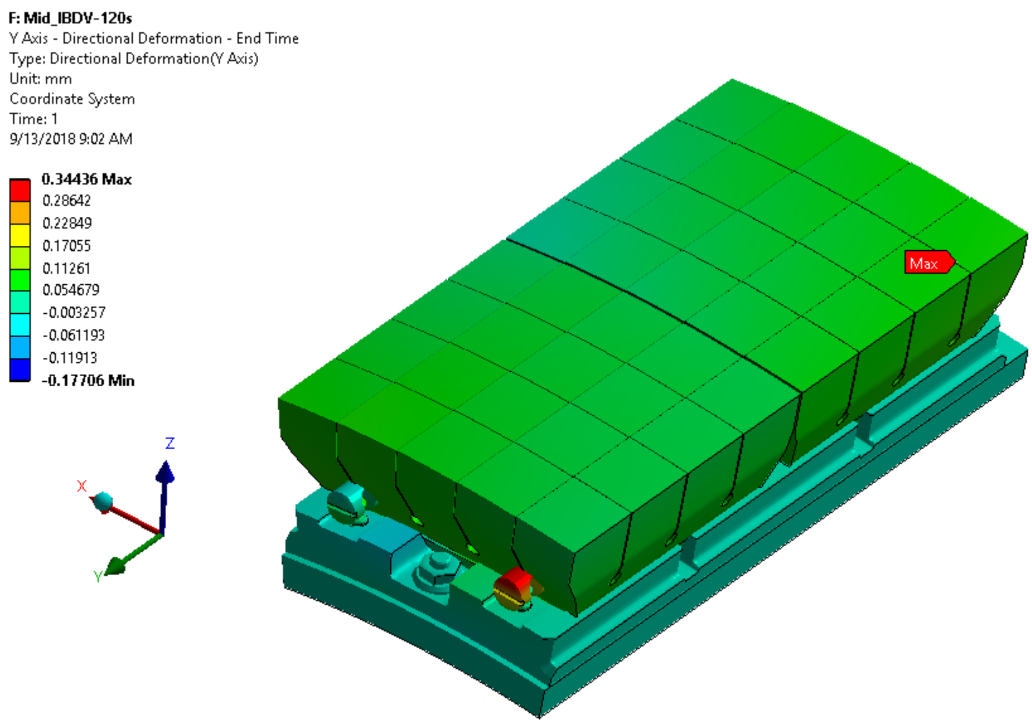

Figure 35: Circumferential deformation for case 1, profile 2 at 120 seconds.

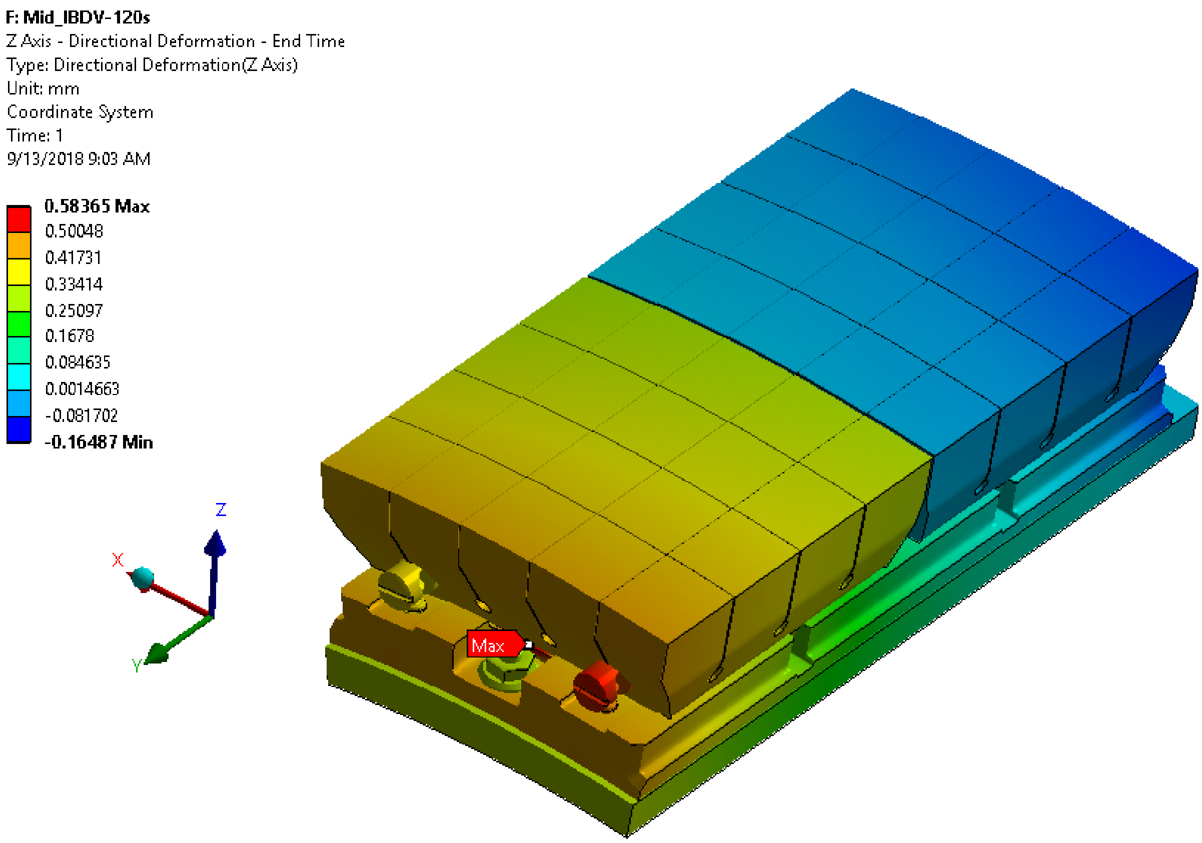

Figure 36: Axial deformation for case 1, profile 2 at 120 seconds.

All results presented in the tables below are from case 1, profile 2 at 120 second. Table 11 and Table 12 list the peak maximum and minimum principal stress and the corresponding allowable in the components made of graphite tiles and grafoil gaskets. Table 13 lists the peak equivalent stresses in the Inconel 718 components.

Table 11: Maximum Principal Stress of tiles and grafoil gaskets

Component	Peak Stress (MPa)	Allowable (MPa)	Loads
Graphite Tiles row 3	9.82	19	BPL+Halo+Eddy
Graphite Tiles row 4	9.73	19	BPL+Halo+Eddy
Grafoil Gasket	0.87	25	BPL+Halo+Eddy

Table 12: Minimum Principal Stress of tiles grafoil gaskets

Component	Peak Stress (MPa)	Allowable (MPa)	Loads
Graphite Tiles row 3	-34.06	-65	BPL+Halo+Eddy
Graphite Tiles row 4	-37.94	-65	BPL+Halo+Eddy
Grafoil Gasket	-2.18	-55	BPL+Halo+Eddy

Table 13: Equivalent Stress in Inconel 718 components

Component	Peak Stress (MPa)	Allowable (MPa)	Loads
Back Plate with integrated studs	225	276	BPL+Halo+Eddy
Vertical Tile Rail	574	276	BPL+Halo+Eddy
Connecting rods	673	276	BPL+Halo+Eddy
Connecting pins	316	276	BPL+Halo+Eddy
Nuts (150258)	225	276	BPL+Halo+Eddy

Both graphite tiles and the grafoil gaskets resulted in stresses below their allowable values. Figure 37 shows the minimum stress contour plot of the graphite tiles. Figure 38 shows the minimum stress contour plot of the grafoil gaskets.

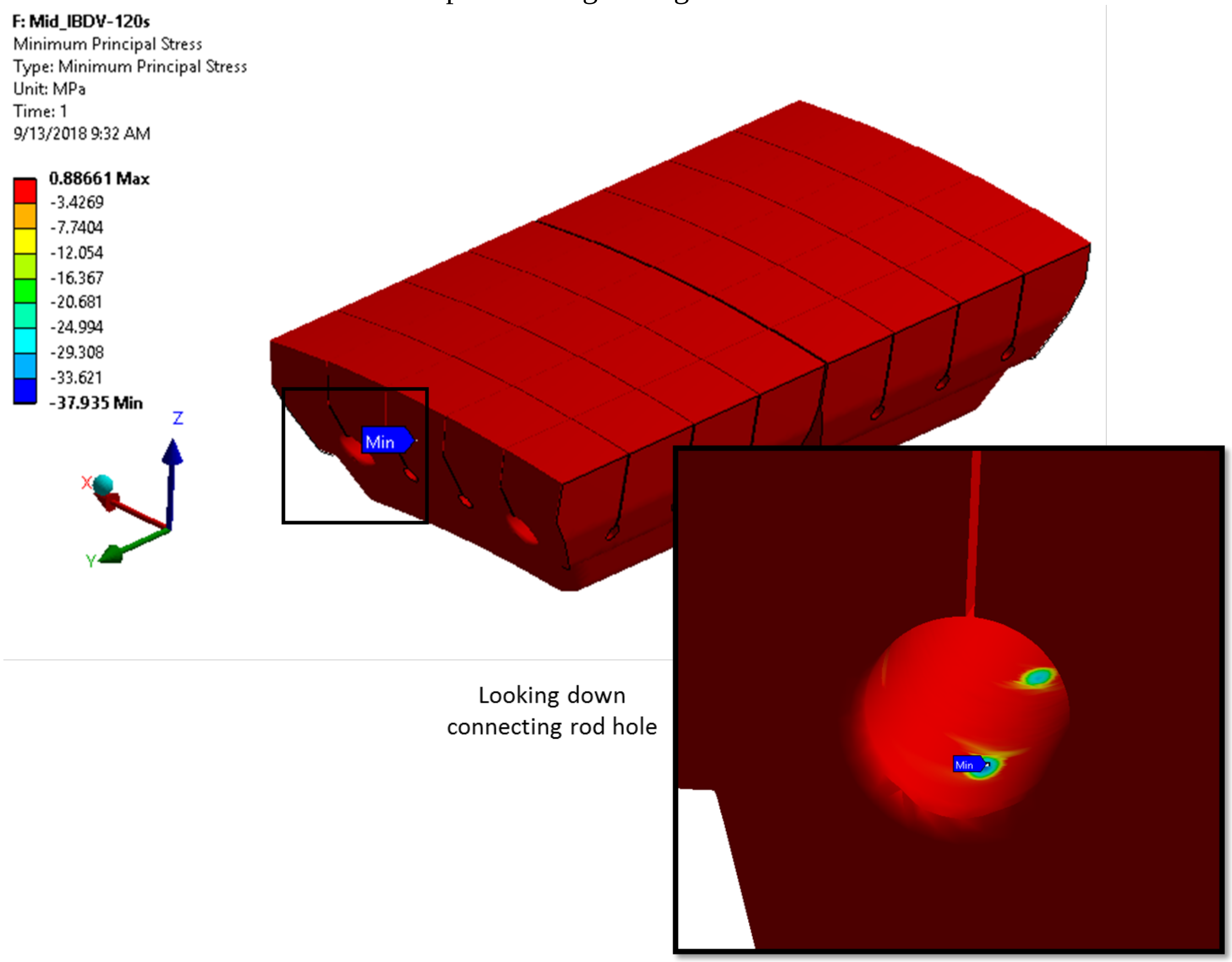

Figure 37: Minimum principal stresses in graphite tiles for case 1, profile 2 at 120 seconds.

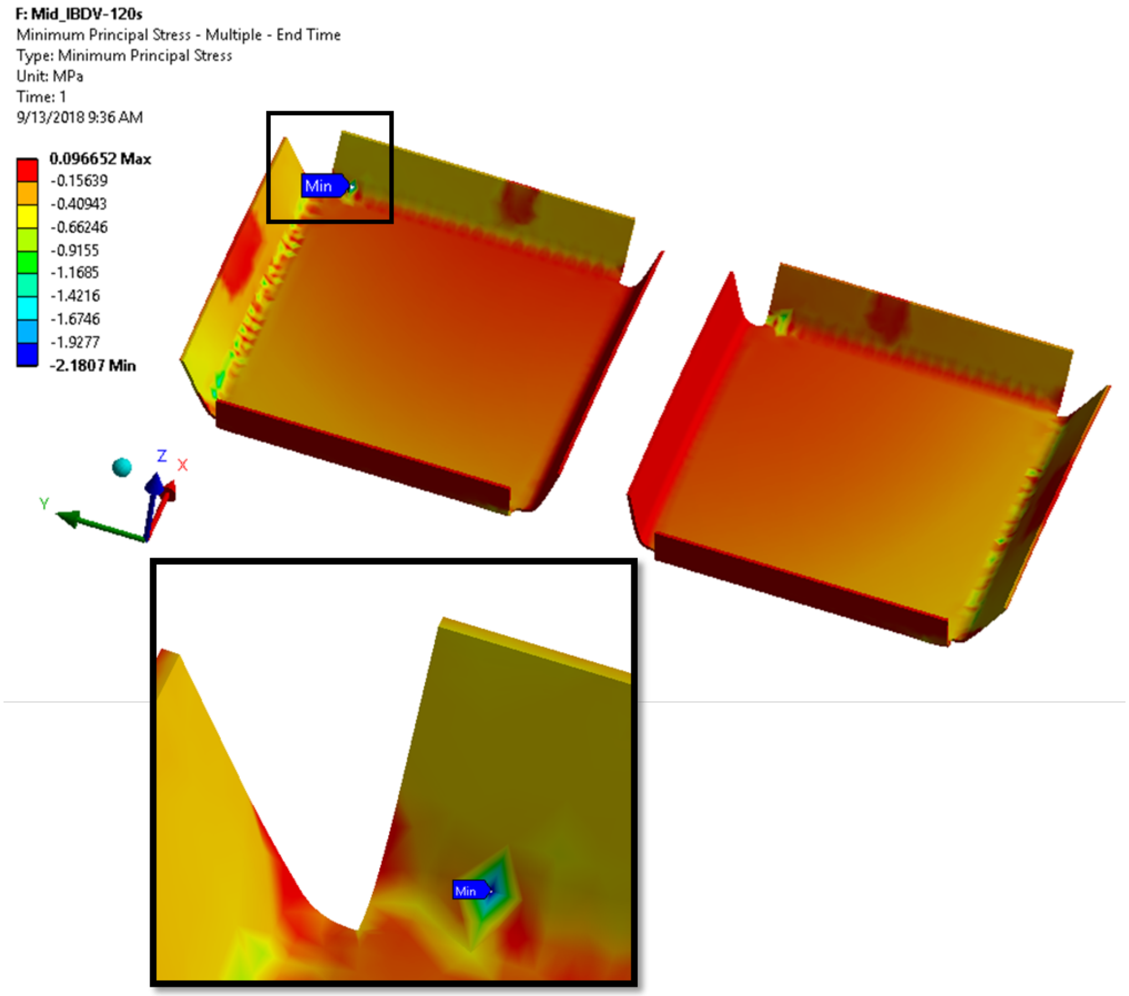

Figure 38: Minimum principal stresses in the grafoil gaskets for case 1, profile 2 at 120 seconds.

Figure 39 shows the equivalent stress contour plot of all of the Inconel 718 components. Several Inconel 718 components exceeded their allowable values. Figure 40 shows the equivalent stress contour plot of the back plate and nuts. The peak stress in these components was below the allowable. The connecting rod pins had localized areas of high stress as shown in Figure 41. These components are likely okay. However, the high stresses in the connecting rods and tile rail may be cause for concern. Not only are they high, but the high stress extends across several elements. Figure 42 shows the stresses in the tile rail. Figure 43 shows the stresses in the connecting rods. It may be possible to reduce the stress in the connecting rods and rail by reducing the preload in the center pins from 750 N to 375 N. Also reducing the preload in the bolts connecting the back plate to the rail will also reduce stress.

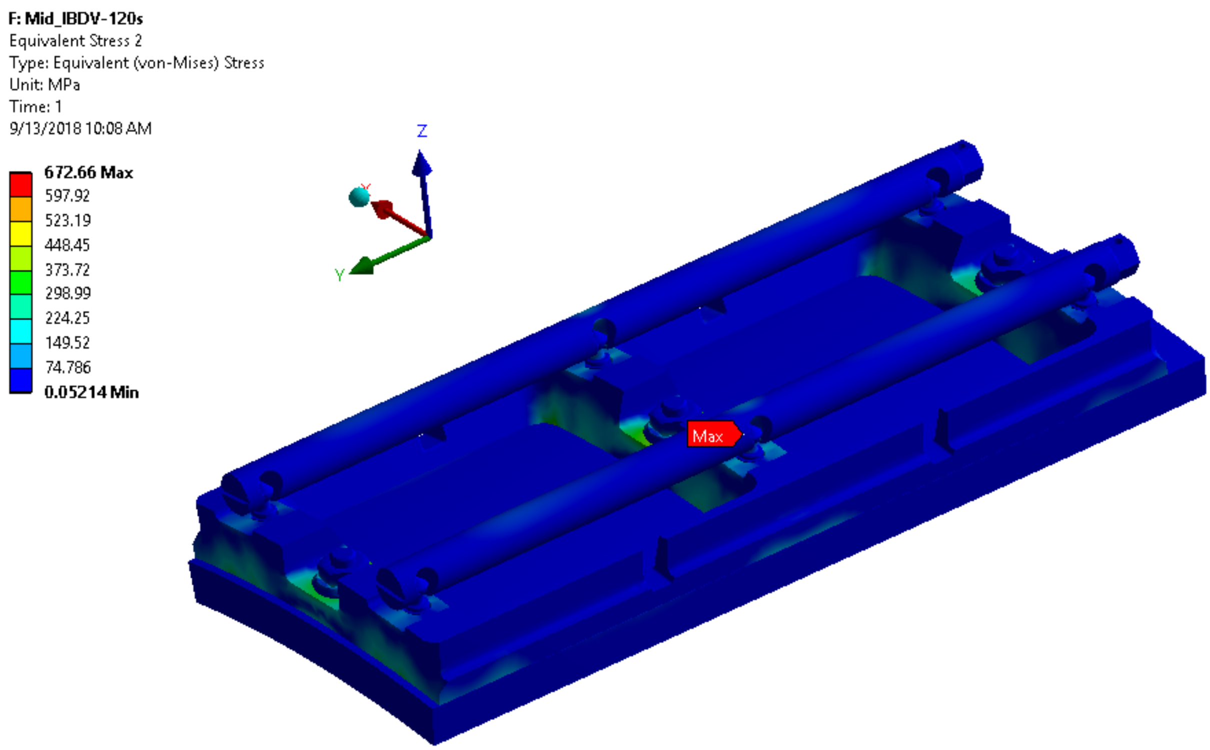

Figure 39: Equivalent stress contour plot of Inconel 718 components for case 1, profile 2 at 120 seconds.

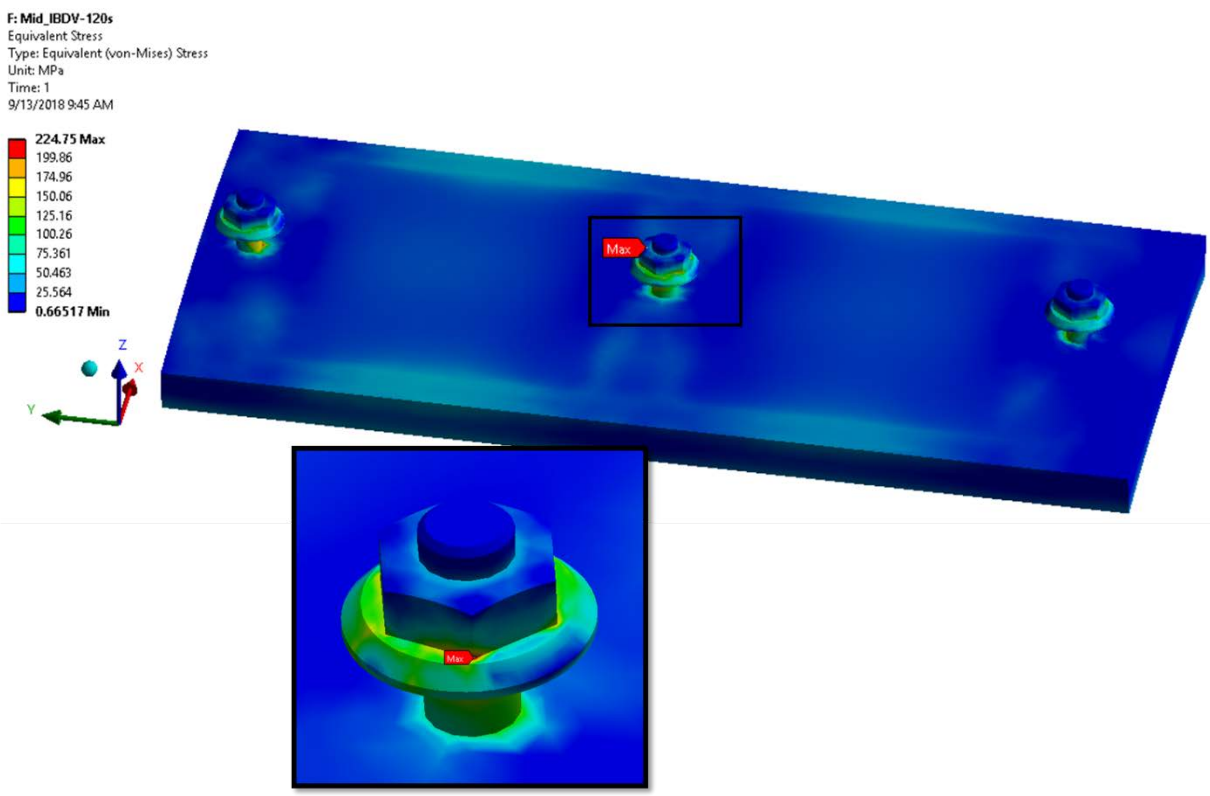

Figure 40: Back plate and nuts equivalent stress contour plot for case 1, profile 2 at 120 seconds.

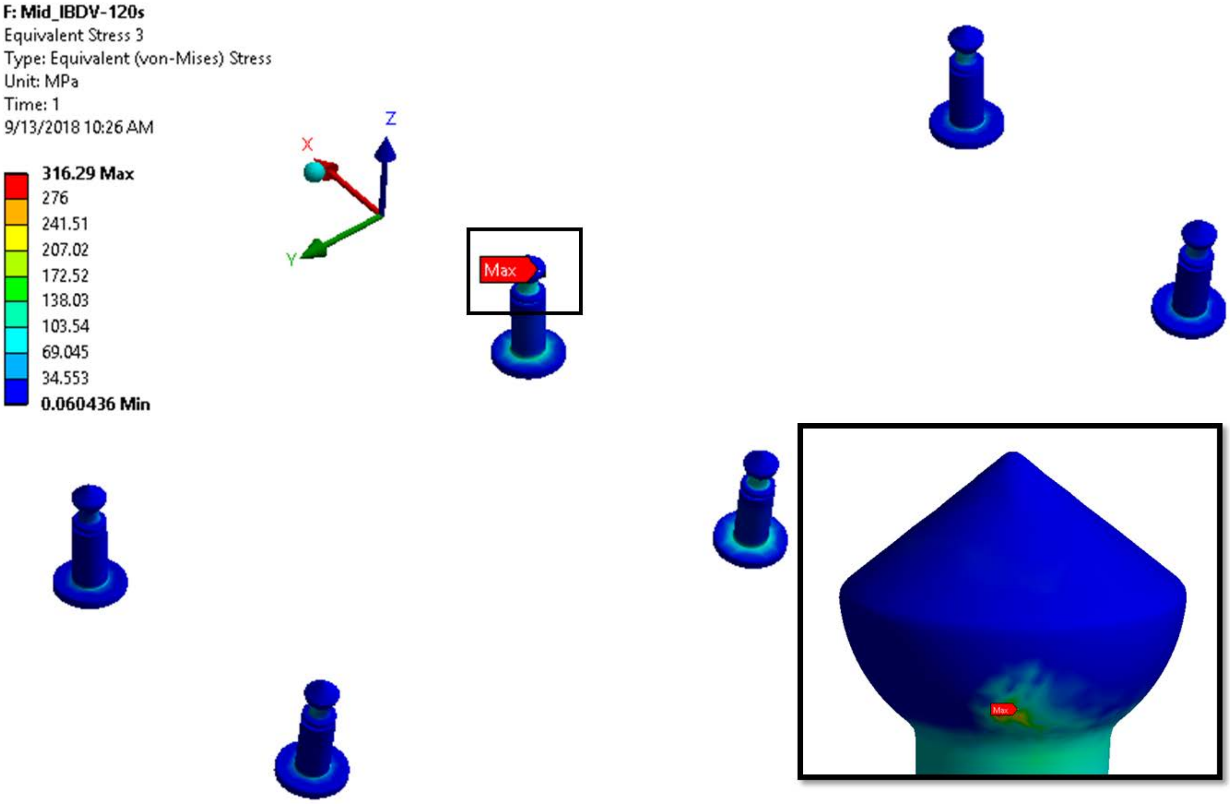

Figure 41: Connecting rod pin equivalent stress contour plot for case 1, profile 2 at 120 seconds.

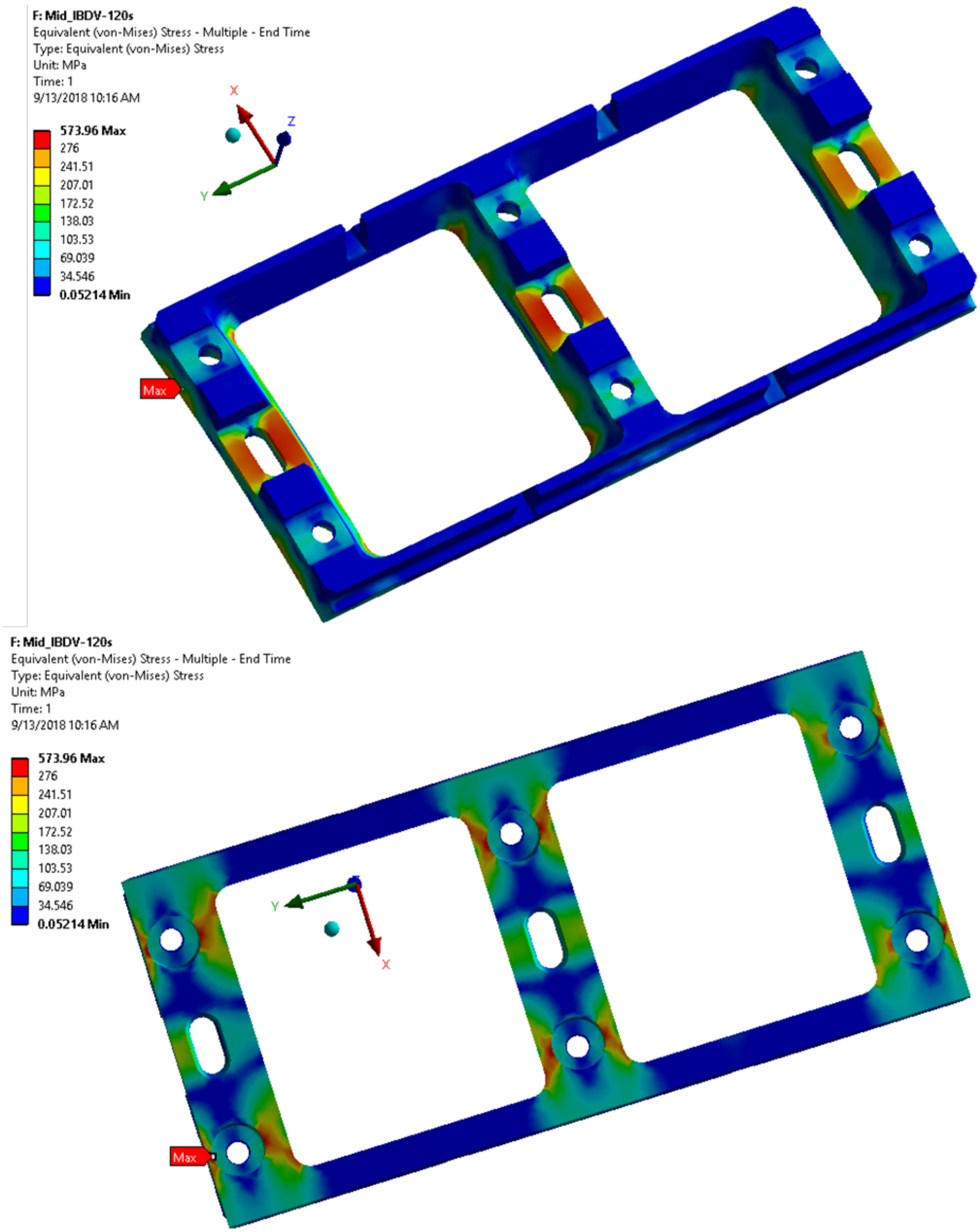

Figure 42: Tile rail equivalent stress for case 1, profile 2 at 120 seconds.

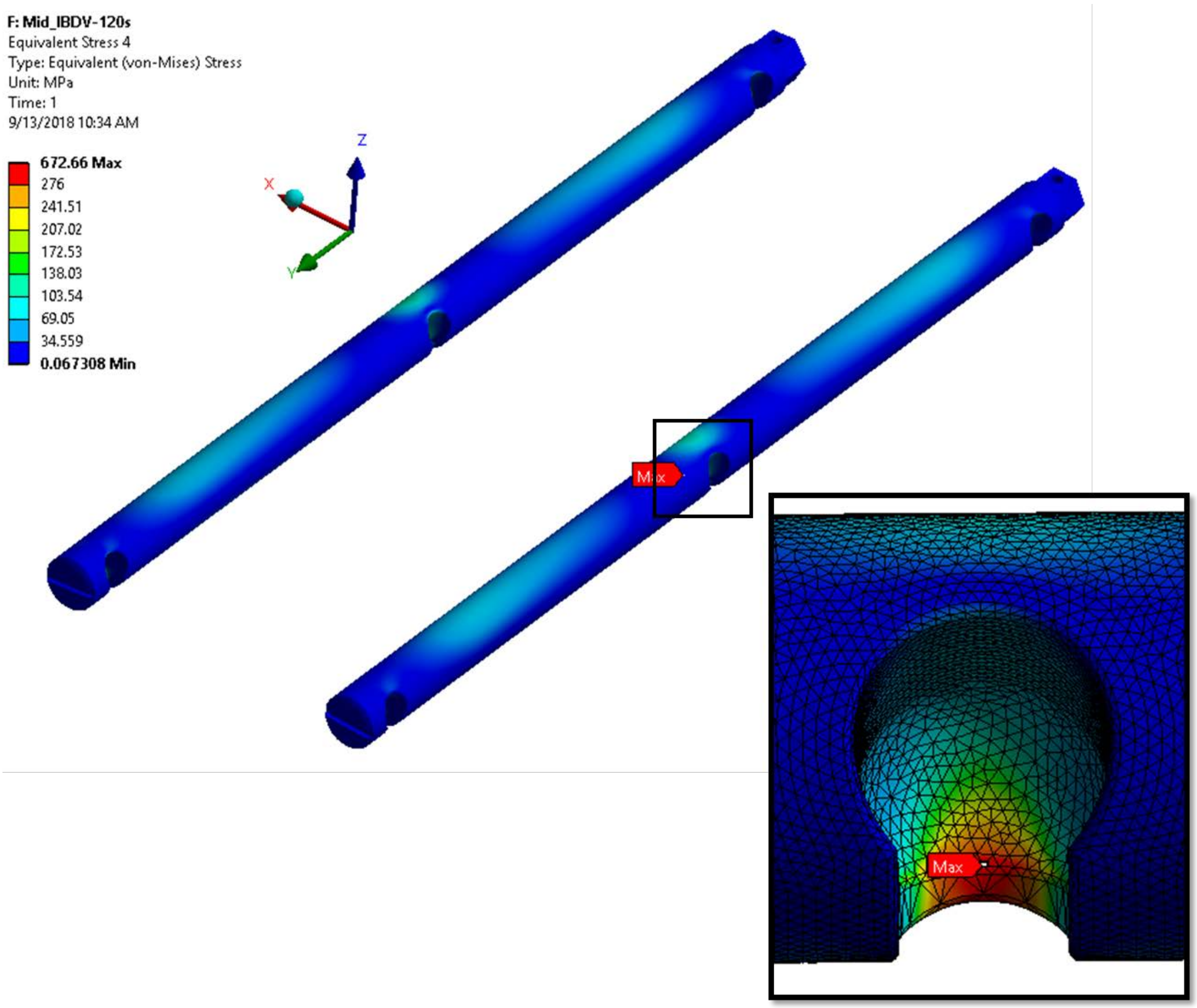

Figure 43: Equivalent stress plot of the connection rods for case 1, profile 2 at 120 seconds.

Case 3 at 1 second

The deformation contour plots in the radial, circumferential, and axial directions of the assembly as a result of the loads is shown in Figure 34, Figure 35, and Figure 36.

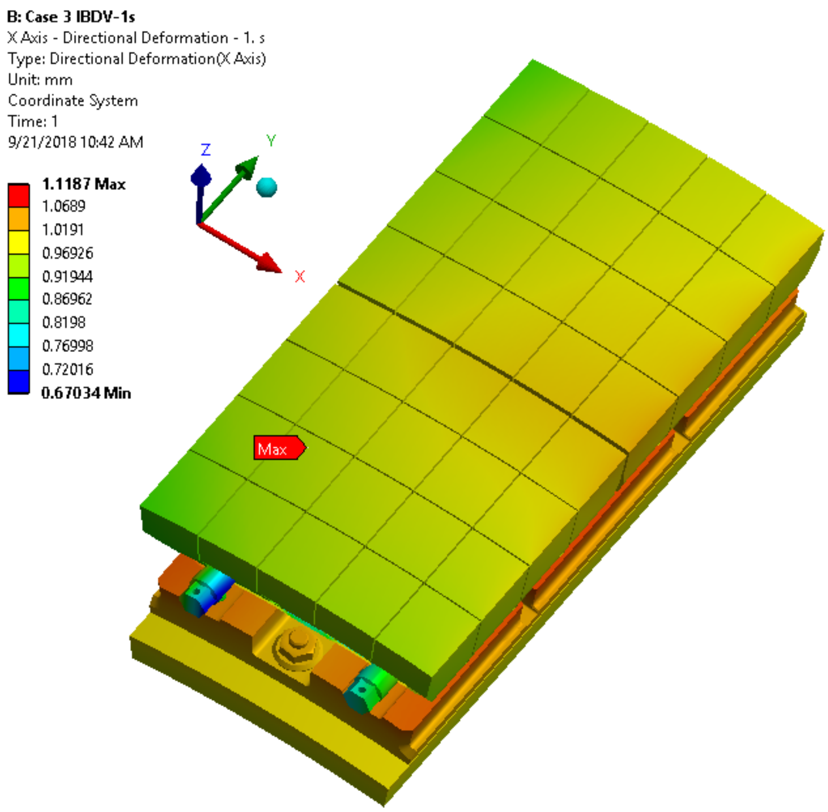

Figure 44: Radial deformation for case 3 at 1 second.

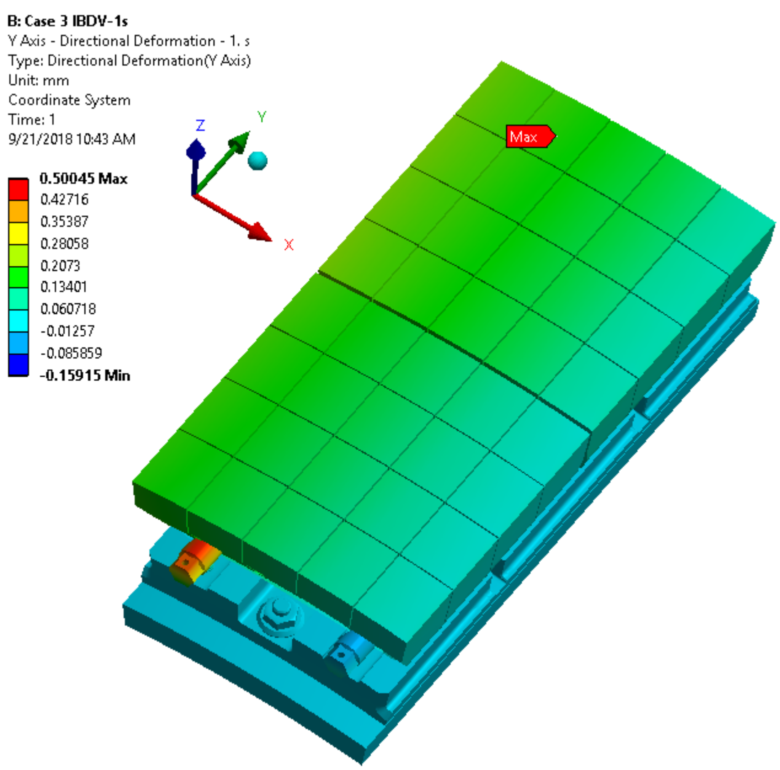

Figure 45: Circumferential deformation for case 3 at 1 second.

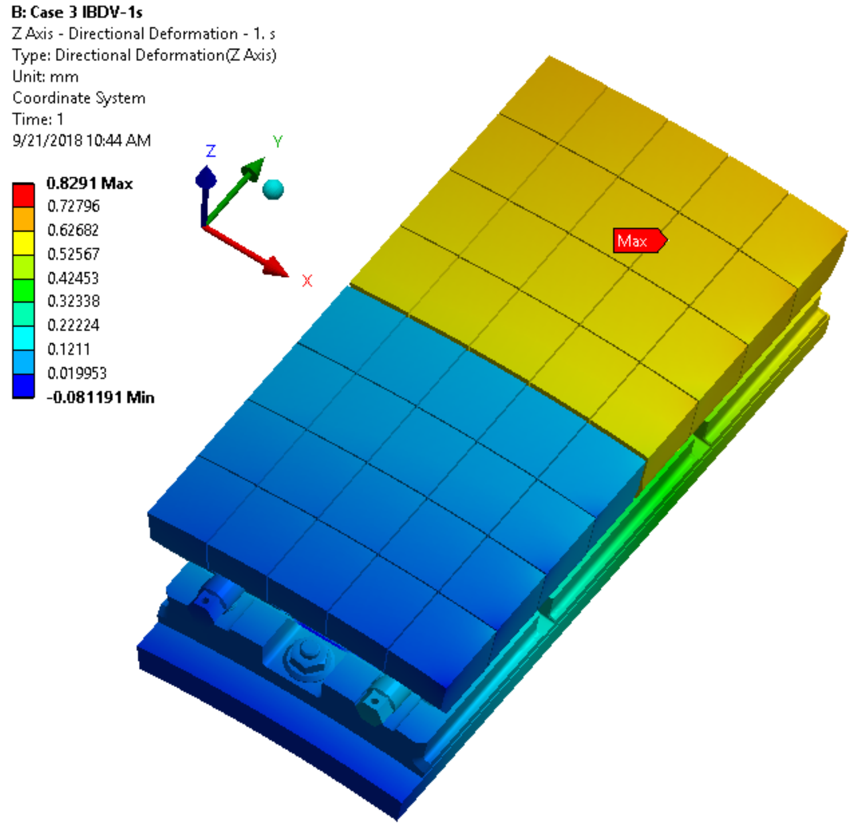

Figure 46: Axial deformation for case 3 at 1 second.

All results presented in the tables below are from case 3 at 1 second. Table 14 and Table 15 list the peak maximum and minimum principal stress and the corresponding allowable in the components made of graphite tiles and grafoil gaskets. Table 16 lists the peak equivalent stresses in the Inconel 718 components.

Table 14: Maximum Principal Stress of tiles and grafoil gaskets

Component	Peak Stress (MPa)	Allowable (MPa)	Loads
Graphite Tiles row 3	14.52	19	BPL+Halo+Eddy
Graphite Tiles row 4	12.81	19	BPL+Halo+Eddy
Grafoil Gasket	0.89	25	BPL+Halo+Eddy

Table 15: Minimum Principal Stress of tiles grafoil gaskets

Component	Peak Stress (MPa)	Allowable (MPa)	Loads
Graphite Tiles row 3	-93.26	-65	BPL+Halo+Eddy
Graphite Tiles row 4	-92.46	-65	BPL+Halo+Eddy
Grafoil Gasket	-2.13	-55	BPL+Halo+Eddy

Table 16: Equivalent Stress in Inconel 718 components

Component	Peak Stress (MPa)	Allowable (MPa)	Loads
Back Plate with integrated studs	54.42	276	BPL+Halo+Eddy
Vertical Tile Rail	64.50	276	BPL+Halo+Eddy
Connecting rods	690	276	BPL+Halo+Eddy
Connecting pins	309	276	BPL+Halo+Eddy
Nuts (150258)	54.41	276	BPL+Halo+Eddy

The grafoil gaskets resulted in stresses below their allowable values. The resulting maximum principal stresses in the tiles were below the allowable. However, the resulting minimum principal stress in the tiles exceeded the allowable. Figure 47 shows the minimum stress contour plot of the graphite tiles. Figure 48 shows the minimum stress contour plot of the grafoil gaskets.

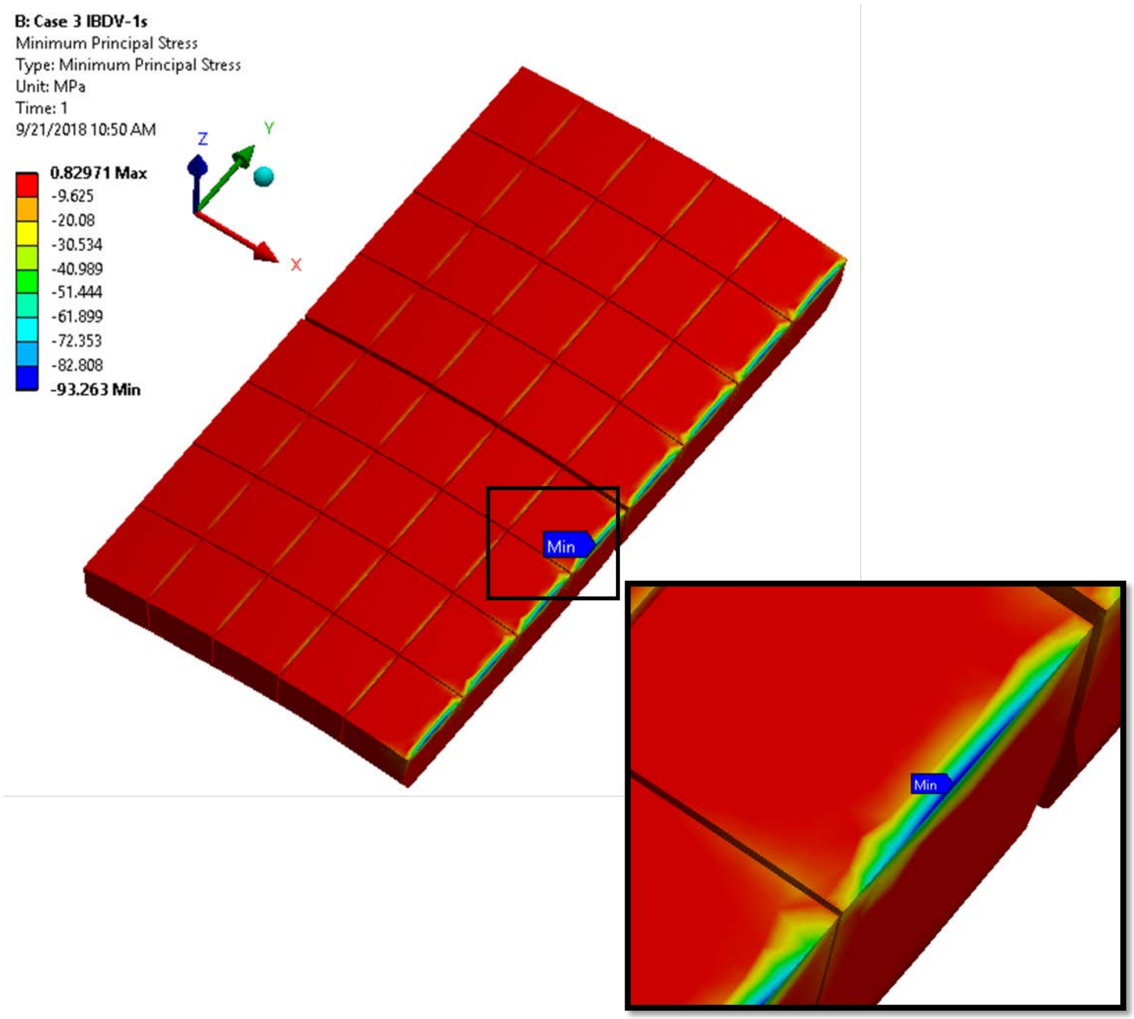

Figure 47: Minimum principal stresses in graphite tiles for case 3 at 1 second.

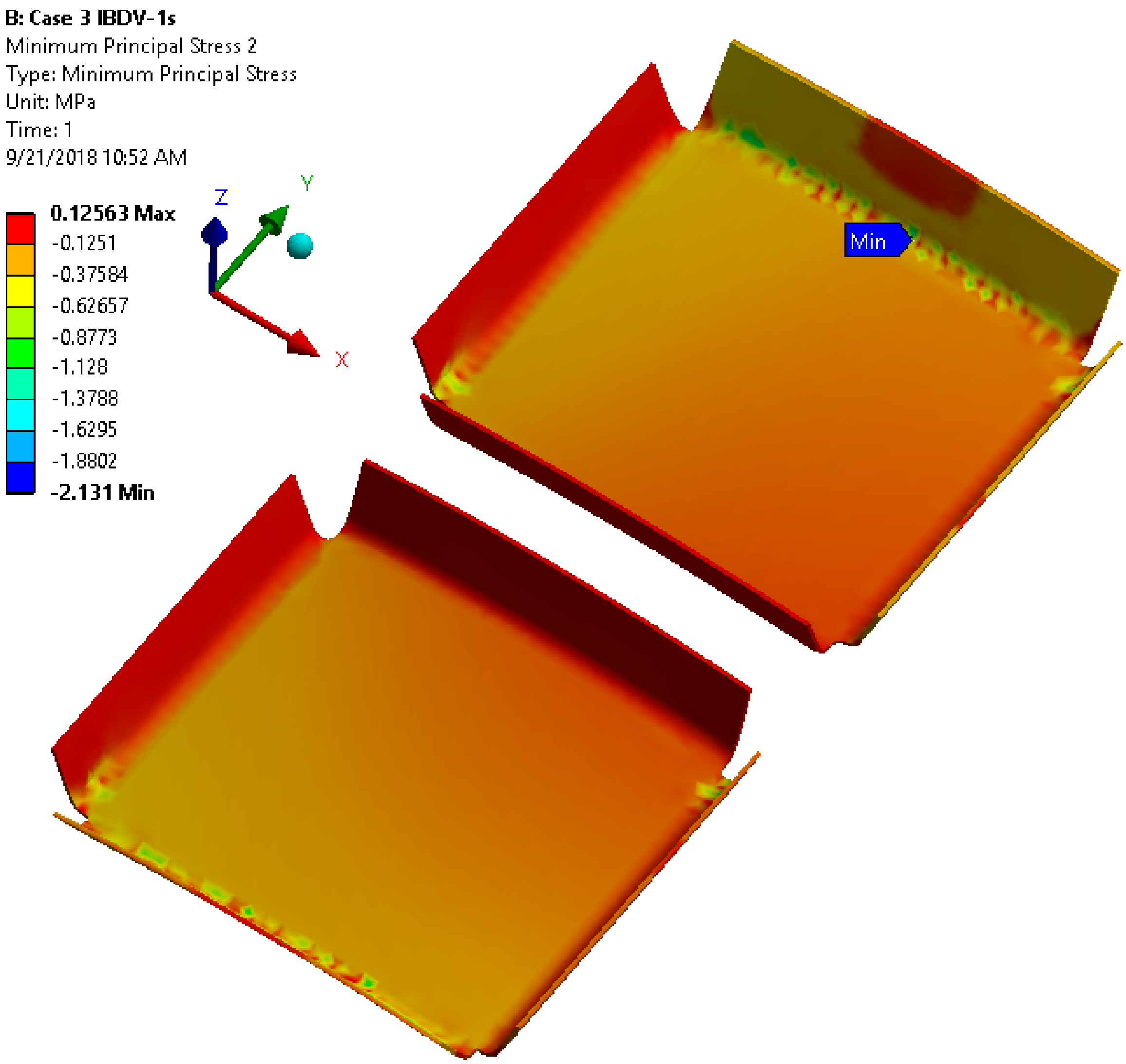

Figure 48: Minimum principal stresses in the grafoil gaskets for case 3 at 1 second.

Figure 49 shows the equivalent stress contour plot of all of the Inconel 718 components. Several Inconel 718 components exceeded their allowable values. Figure 50 shows the equivalent stress contour plot of the back plate and nuts. Figure 51 shows the equivalent stresses in the tile rail. The peak stress in these components was below the allowable. The connecting rod pins had localized areas of high stress as shown in Figure 52. These components are likely okay. However, the high stresses in the connecting rods may be cause for concern. Not only are they high, but the high stress extends across several elements. Figure 53 shows the stresses in the connecting rods. It may be possible to reduce the stress in the connecting rods by reducing the preload in the center pins from 750 N to 375 N.

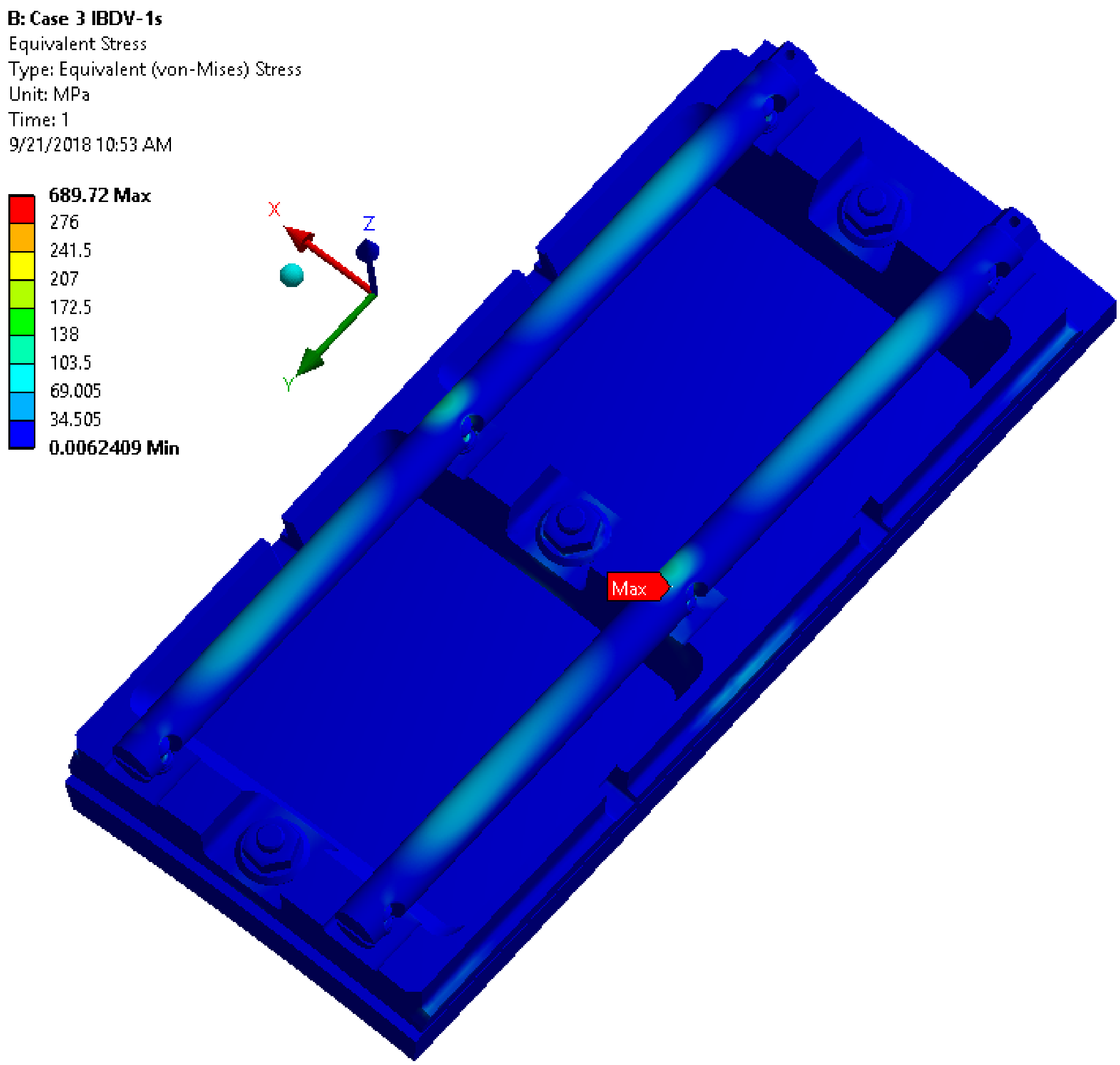

Figure 49: Equivalent stress contour plot of Inconel 718 components for case 3 at 1 second.

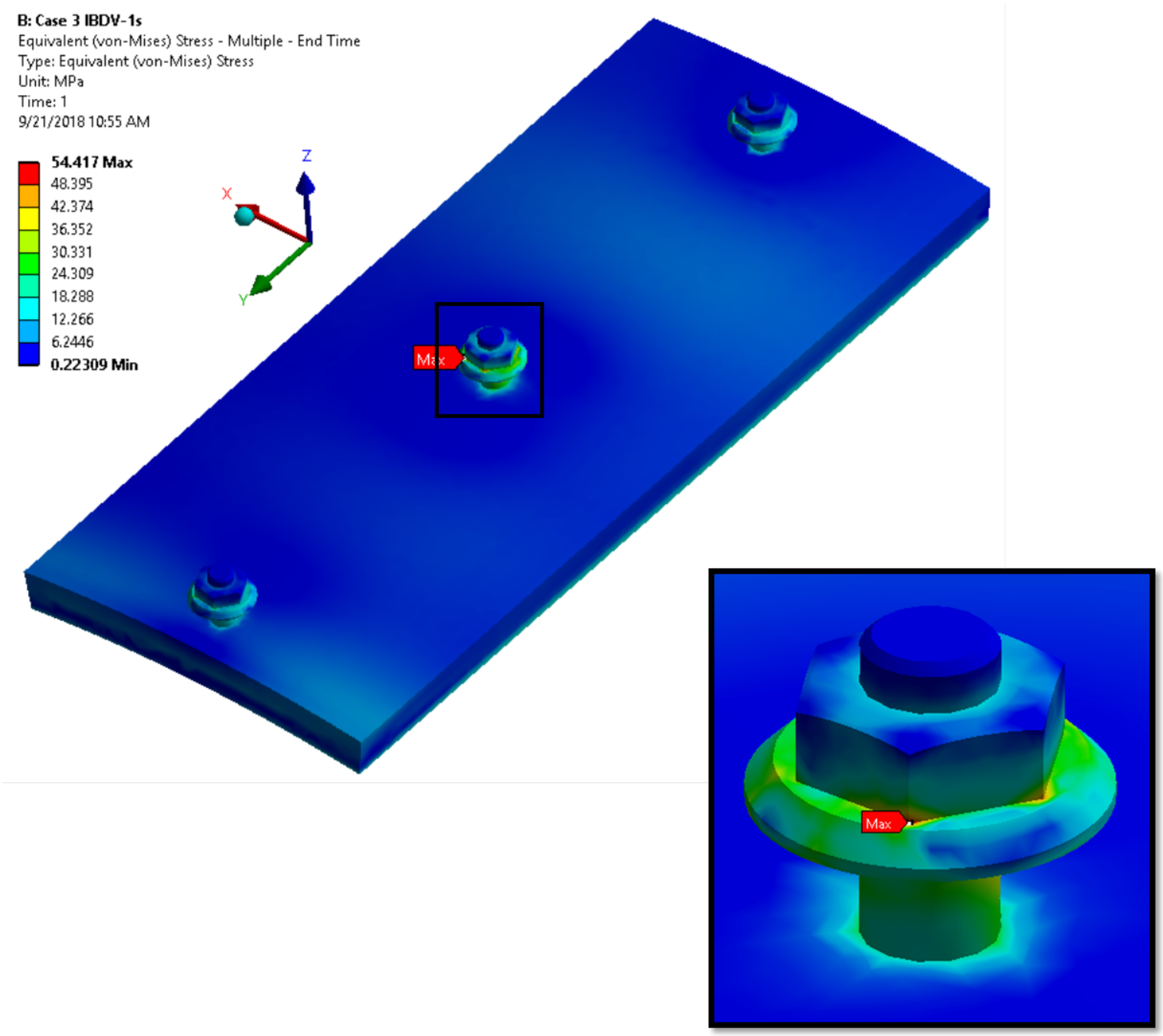

Figure 50: Back plate and nuts equivalent stress contour plot for case 3 at 1 second.

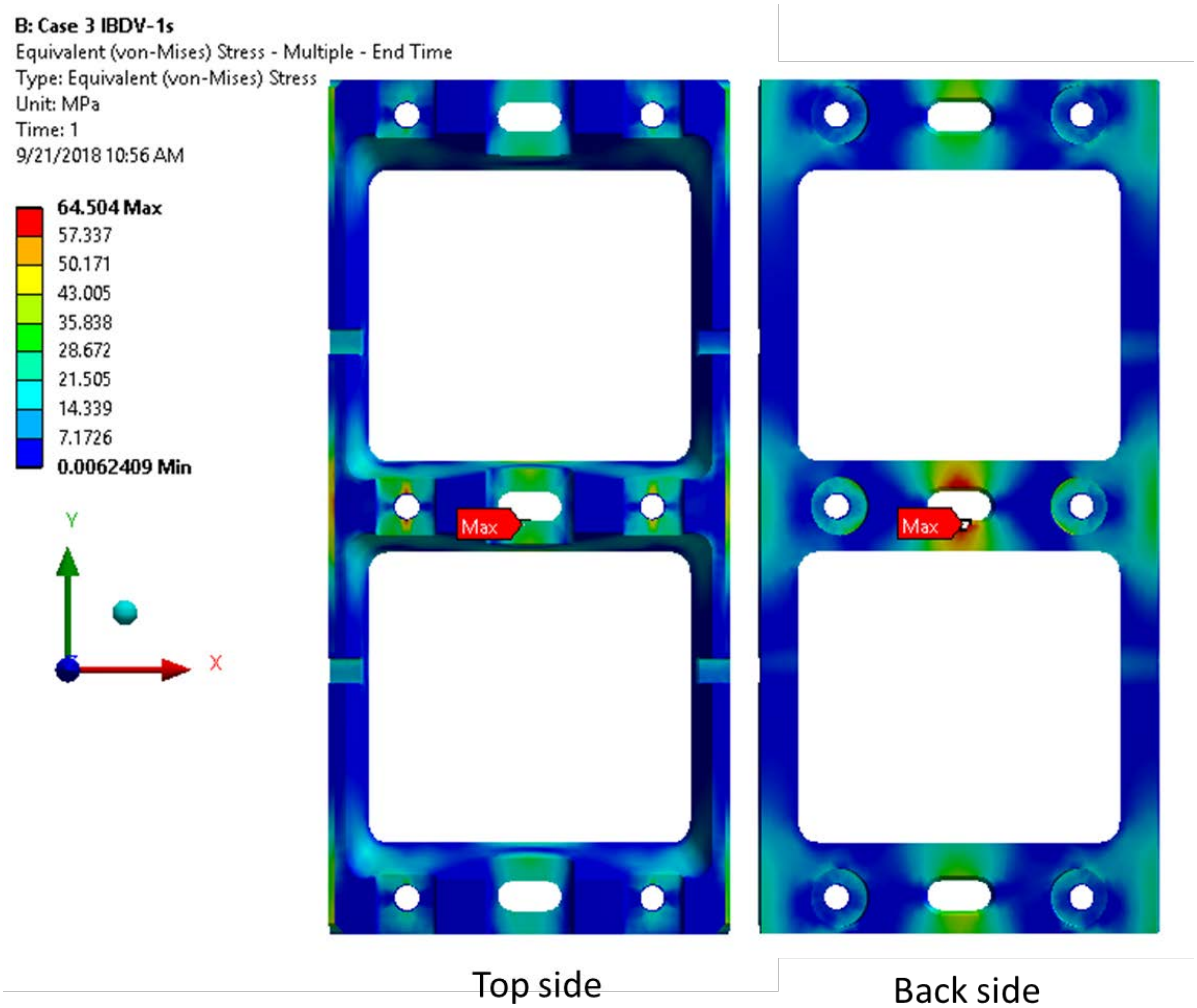

Figure 51: Tile rail equivalent stress for case 3 at 1 second.

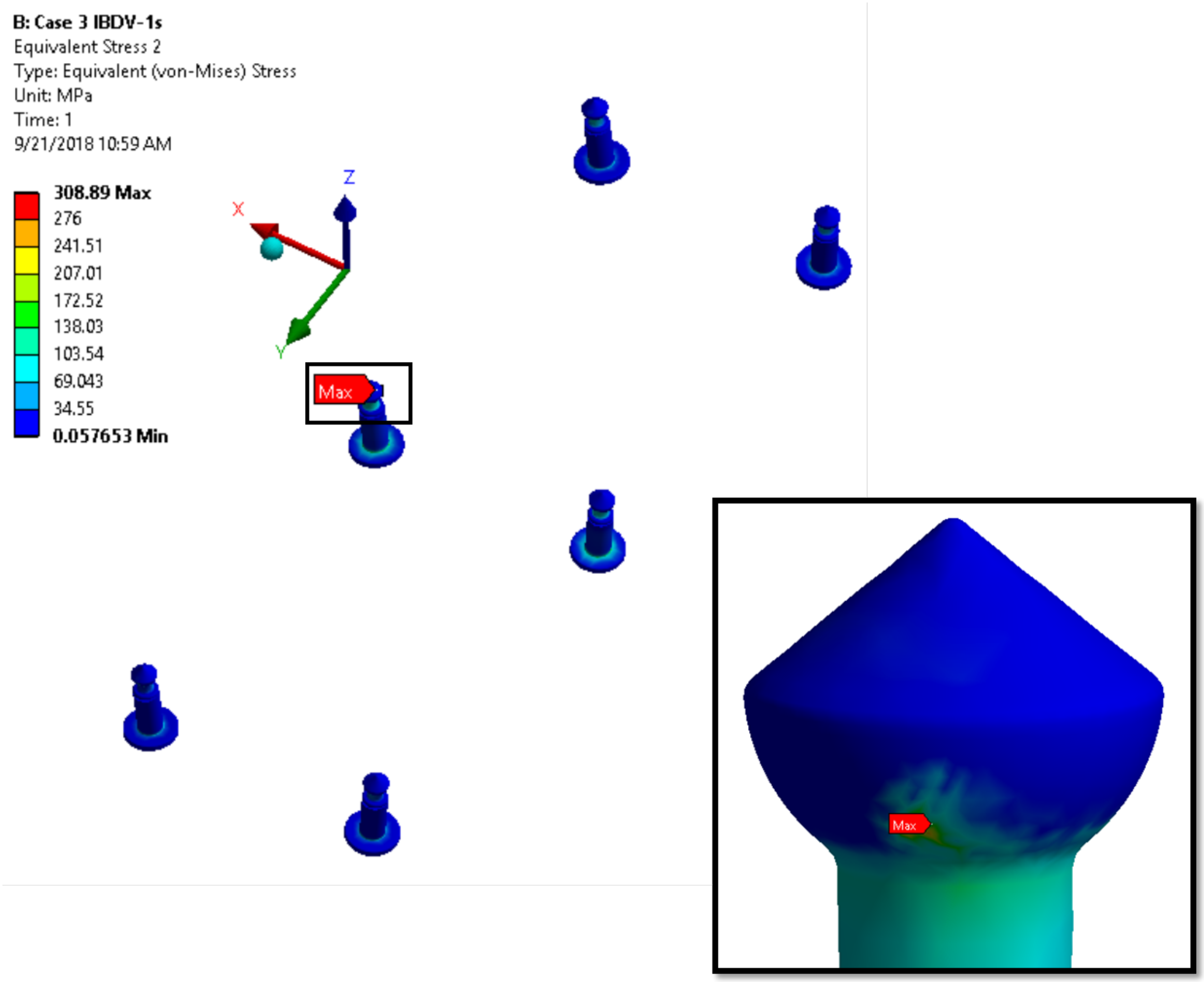

Figure 52: Connecting rod pin equivalent stress contour plot for case 3 at 1 second.

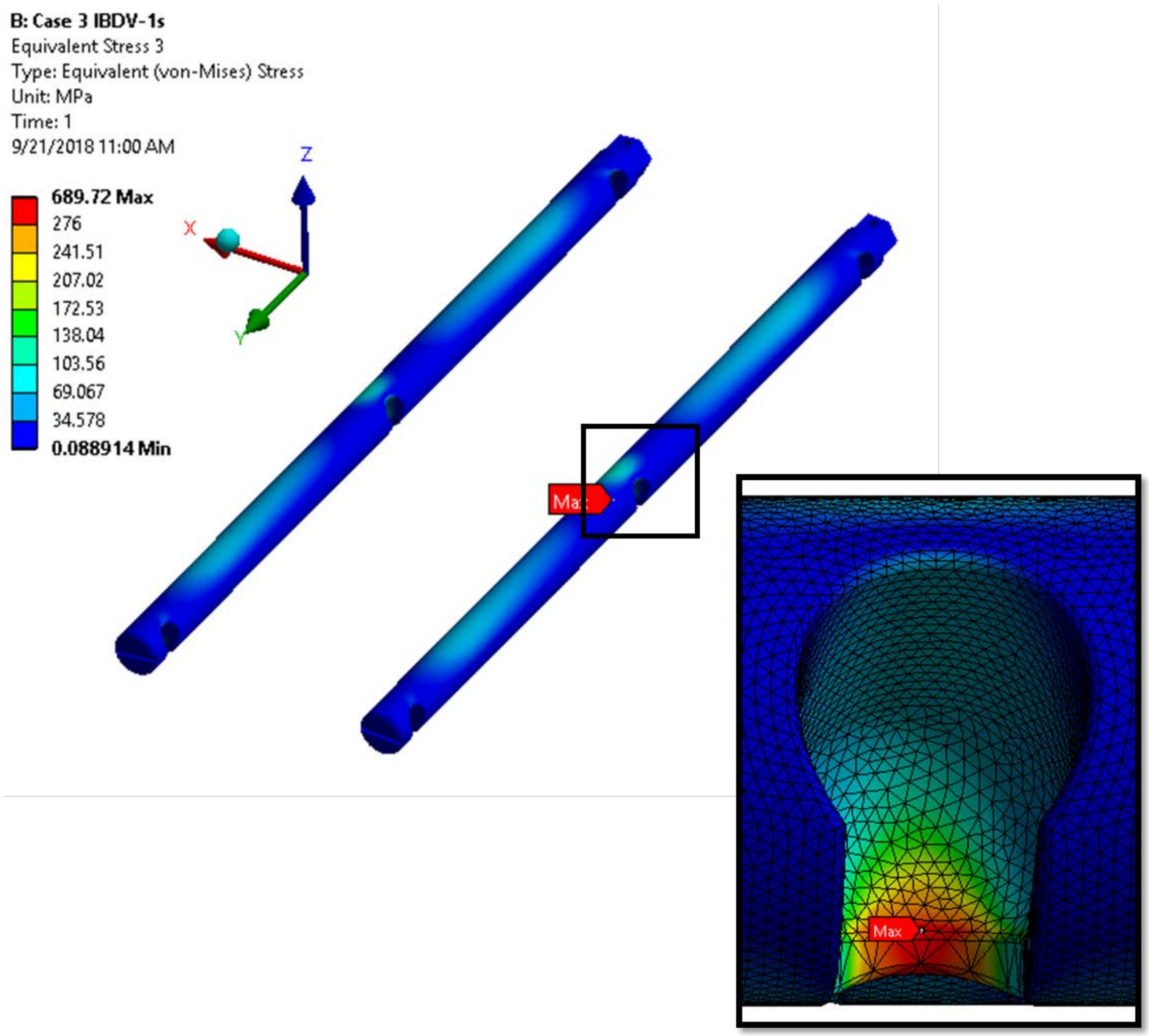

Figure 53: Equivalent stress plot of the connection rods for case 3 at 1 second.

Analysis of Inboard Diverter Vertical (IBDV) high heat flux Super tile

ORNL

The ANSYS Workbench project diagram is shown in Figure 1. It included a static analysis of preload, halo, and eddy current forces without the thermal load. Two thermal loading conditions were applied to the tile. Finally, all loads were combined.

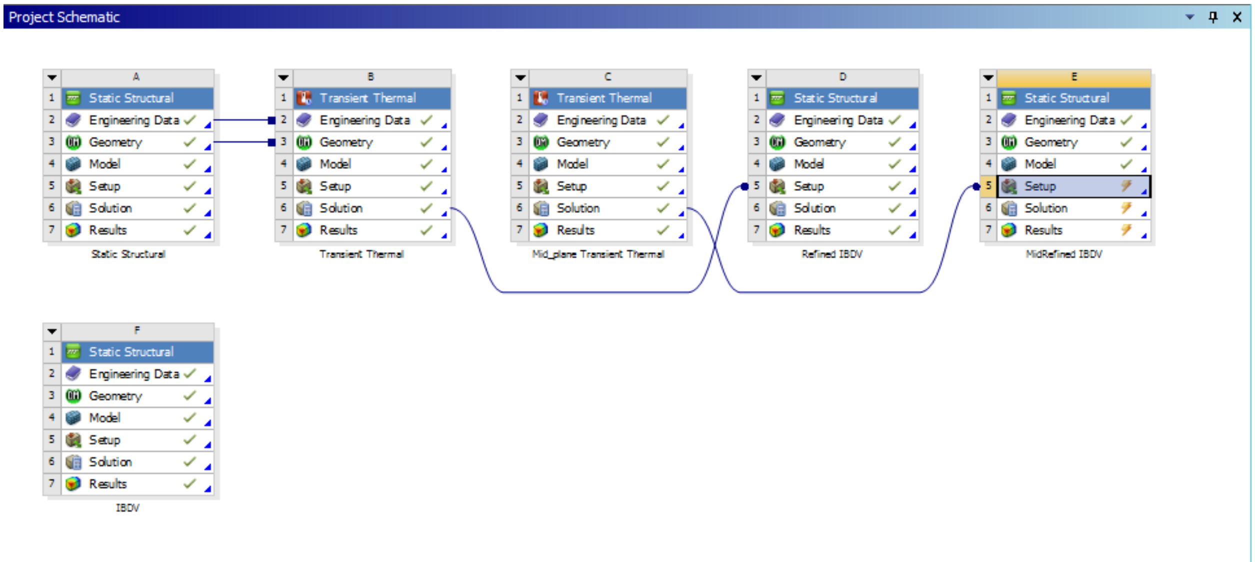

Figure 54: Workbench Schematic of IBDV Analysis.

The components considered in the analysis are listed below in Figure 2 and Figure 3.

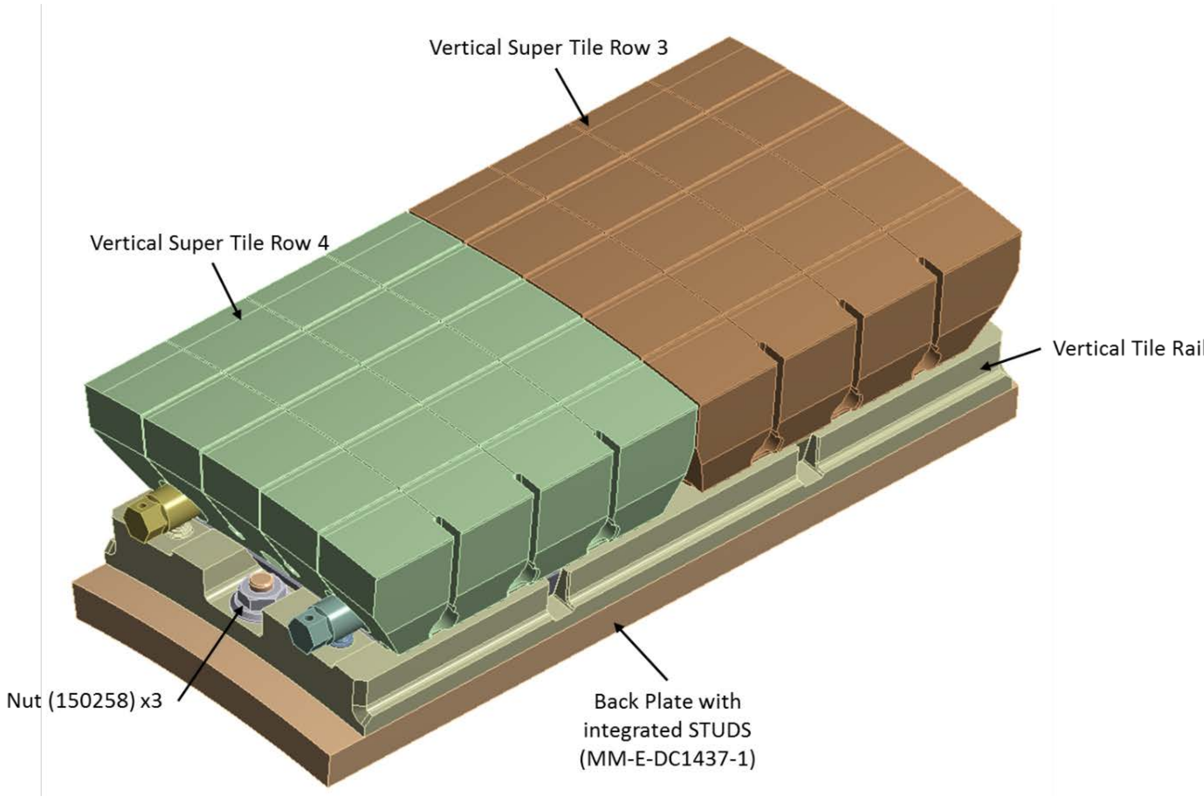

Figure 55: Inboard Diverter Vertical Tile Super Tile Assembly

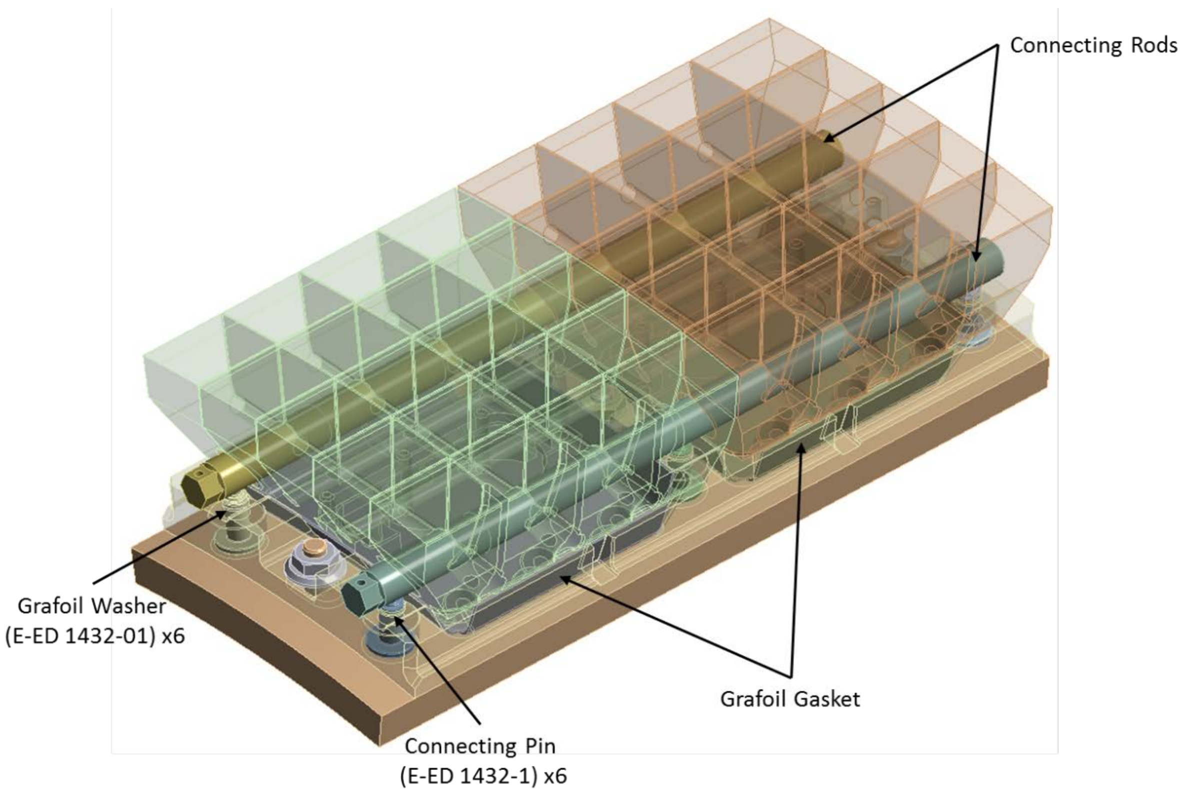

Figure 56: Inboard Diverter Vertical Tile Super Tile Assembly.

The mesh consisted of high order tetrahedrals. The total number of elements and nodes for the whole assembly is 2,384,737 and 3,844,218 respectively. The contact areas between the connecting rods and tiles had a refined mesh. The connecting pin heads also had a refined mesh where they contact the connecting rods. Figure 4 shows the mesh used in the analysis with and without the graphite tile. Figure 5 shows the refined mesh of the tile, connecting rod, and connecting pin contact areas.

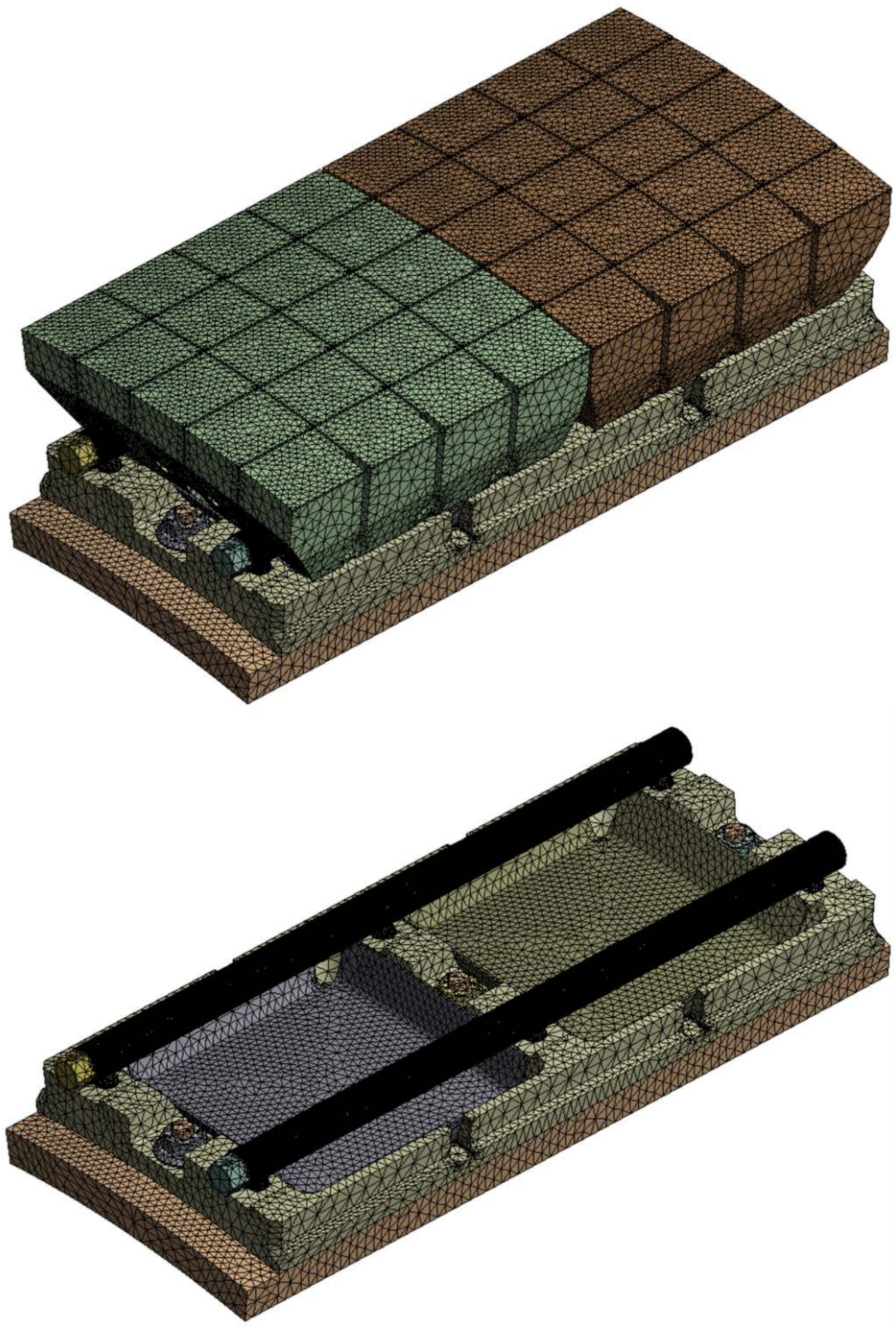

Figure 57: Mesh of the Inboard Diverter Tile Assembly with and without theTiles

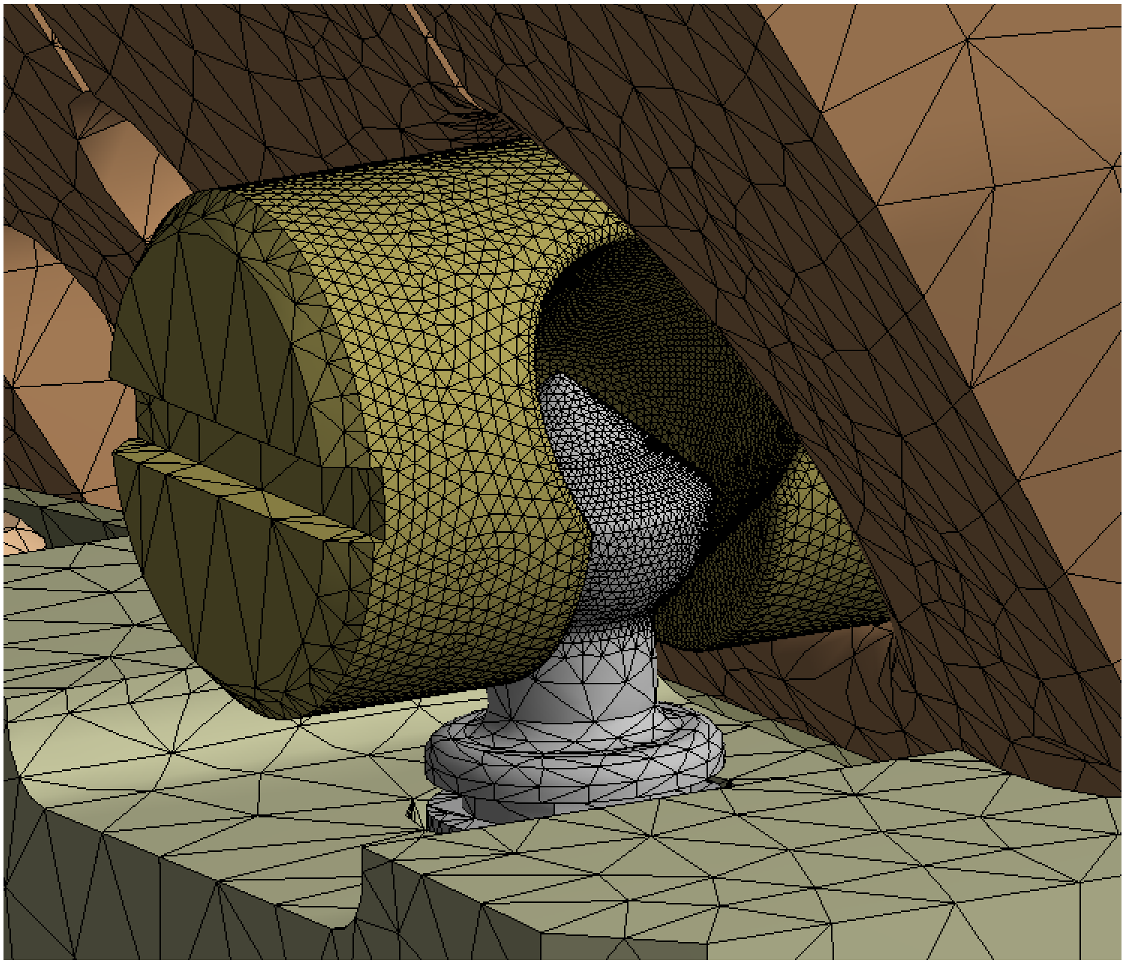

Figure 58: Refined mesh of the connecting rod, connecting pin and tile contact areas.

Table 1 lists each component of the assembly and its material.

Table 17: Components and their materials.

Component	Material
Graphite Tiles (row 3 and row 4)	Graphite SGL R6510
Grafoil Gaskets and Washers	Grafoil
Back Plate with integrated studs	Inconel 718
Vertical Tile Rail	Inconel 718
Connecting rods	Inconel 718
Connecting pins	Inconel 718
Nuts (150258)	Inconel 718

Thermal Analysis

Two transient thermal analyses were performed for case 1 and one for case 3 with an initial ambient temperature of 192.36 ^{o}C for a 5s heat flux pulse mapped over two specified areas of the tile. Both heat flux values for case 1 were 6.77 MW/m^2, over an extent of 0.11m. The peak heat flux started at 6.77 MW/m^2 and tapered linearly down to a heat flux of 0 over 0.11 m. This was followed by a 115 s cooldown period. Case 3 had a uniform heat flux of 57.29 MW/m^2 applied to specific areas on both tiles for 1 second followed by a 124 s cooldown. The heat flux for case 3 is only applied to a small area on the upper side of the castellations. Helium cooling using 25 C helium in the baseplate was assumed with a convective heat transfer coefficient of 300 W/m^{2}K. Radiation was included for the top tile surface only, since all other have no open view factor. The emissivity was 0.7 and the reference background temperature was 103.42 ^{o}C. The starting assembly temperature was assumed to be 192.36 ^{o}C. The first heat flux profile for case 1 is shown in Figure 6. The second heat flux profile for case 1 is shown in Figure 7. The heat flux profile for case 3 is shown in Figure 8. The radiation and convective surfaces are shown in Figure 9. Contact thermal conductance between all parts was 1000 W/m^{2}C.

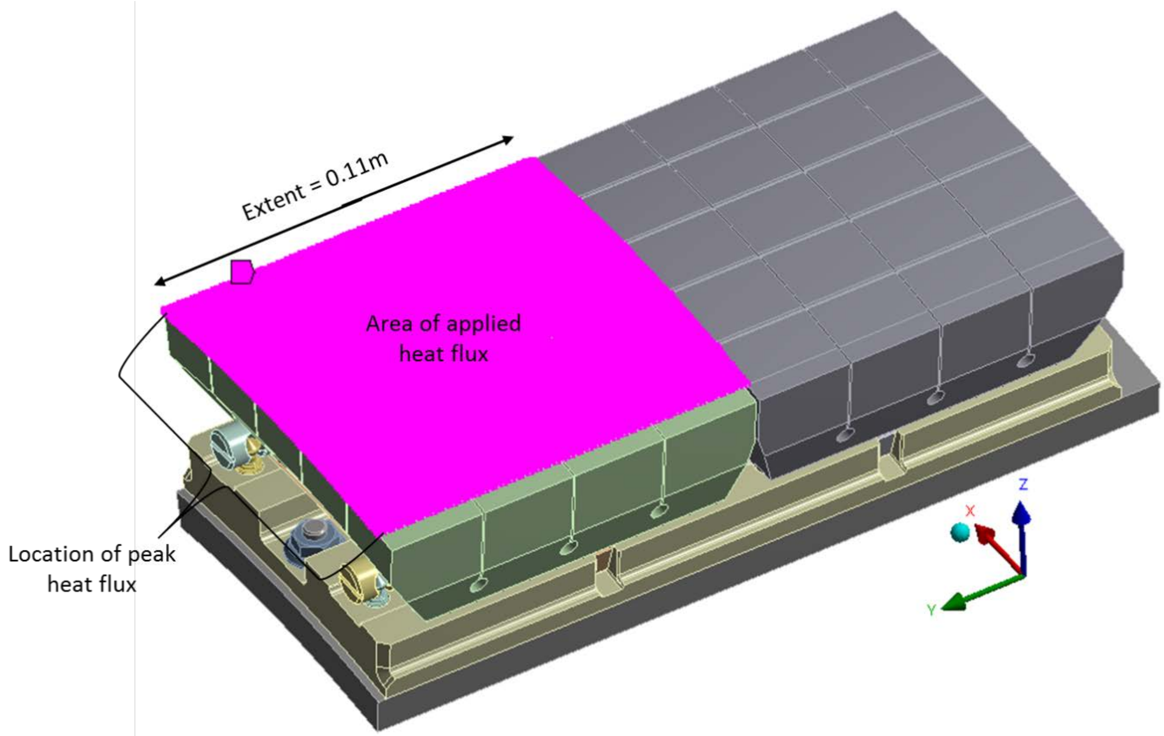

Figure 59: Case 1 heat flux profile 1

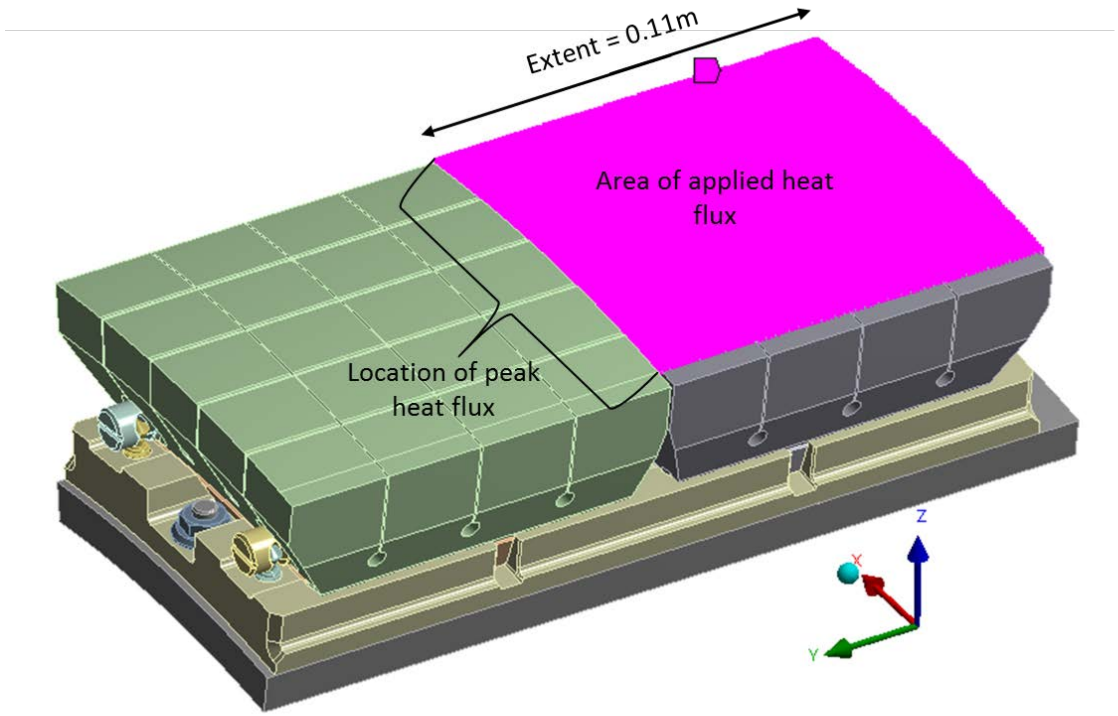

Figure 60: Case 1 heat flux profile 2

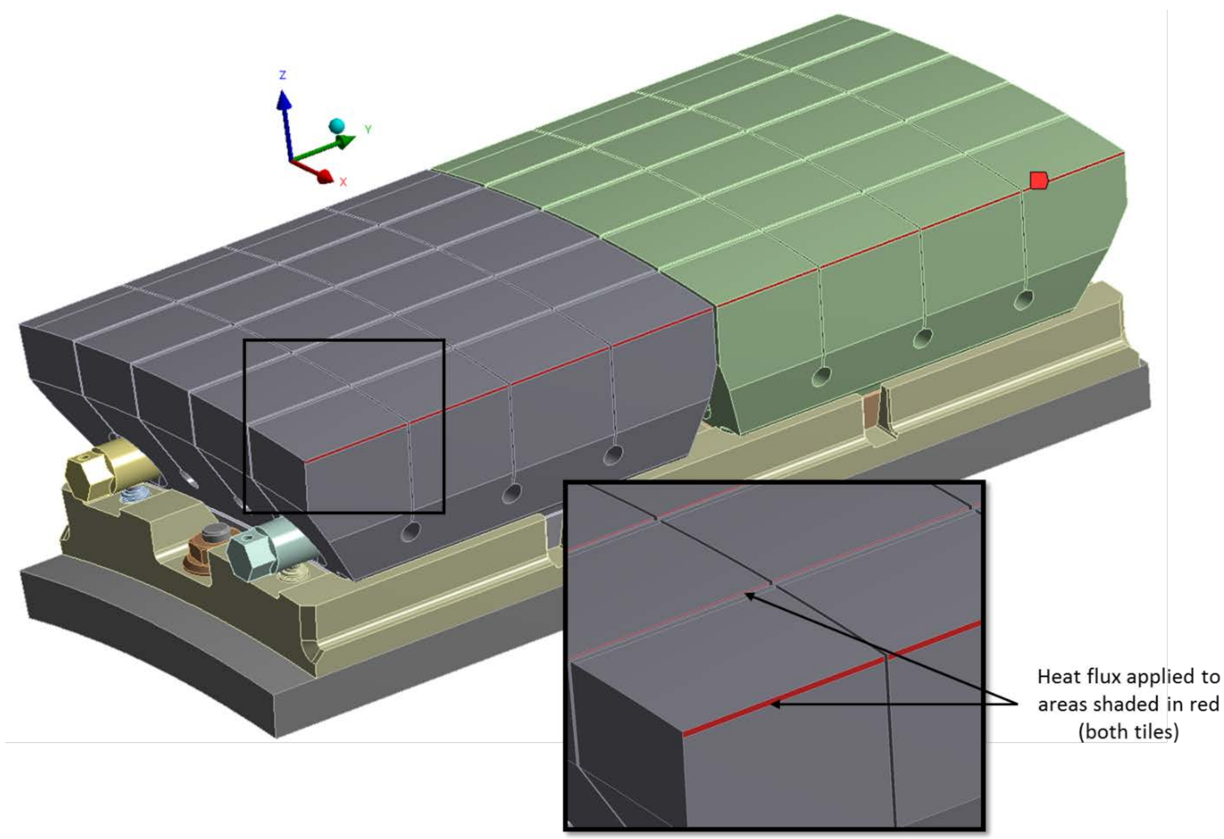

Figure 61: Case 3 heat flux profile

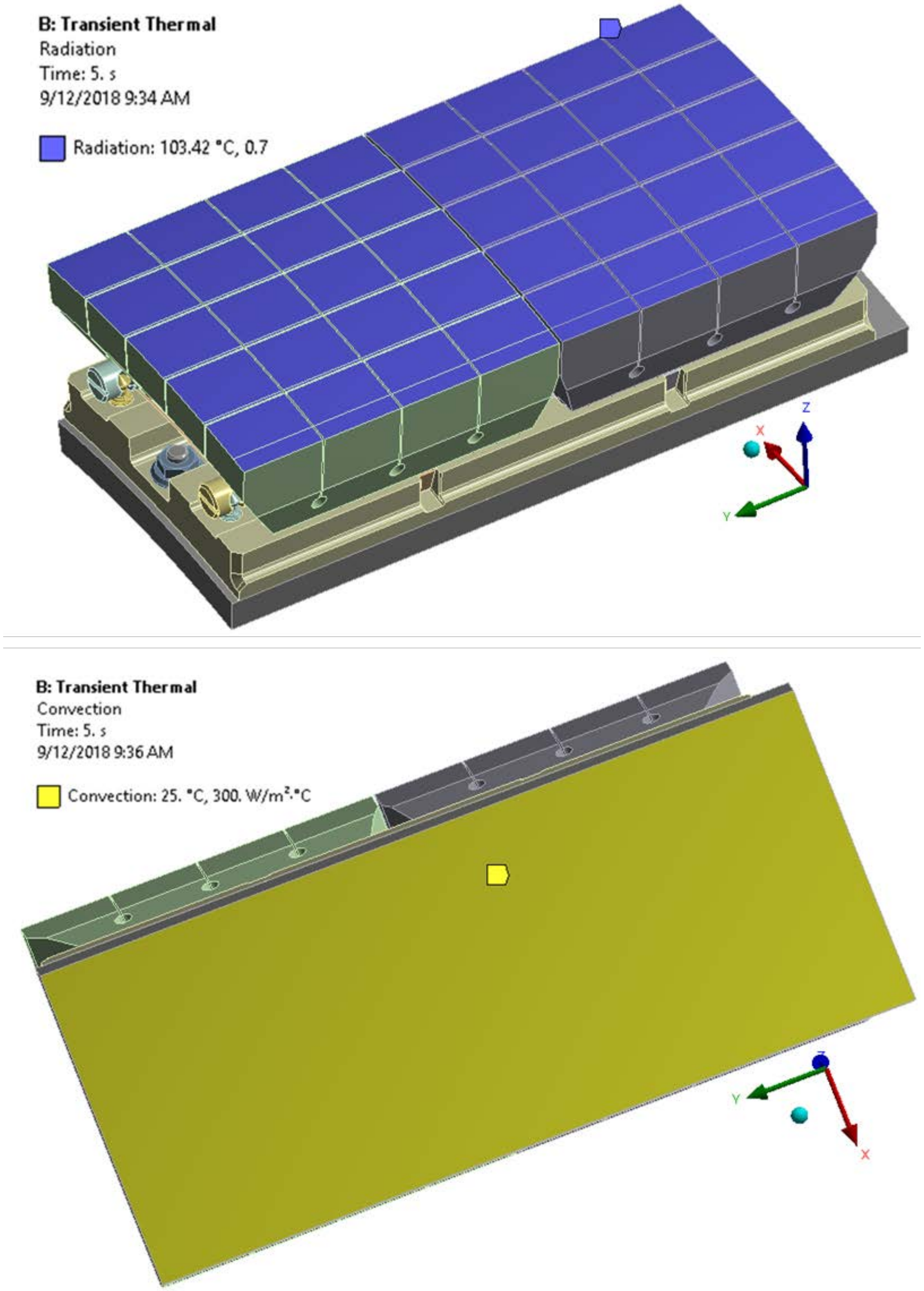

Figure 62: Radiation (top) and Convection (bottom) surfaces.

The peak temperature in the assembly was 1440 °C in the graphite tile for heat flux case 1 profile 1. Figure 10 shows the temperature contour plot of the tile and substructure after 5 seconds of applied heat flux. Figure 11 shows temperature contour plot of the tiles and substructure after 115 s cooldown. Table 2 lists the peak temperature and corresponding time for each component for heat flux case 1 profile 1.

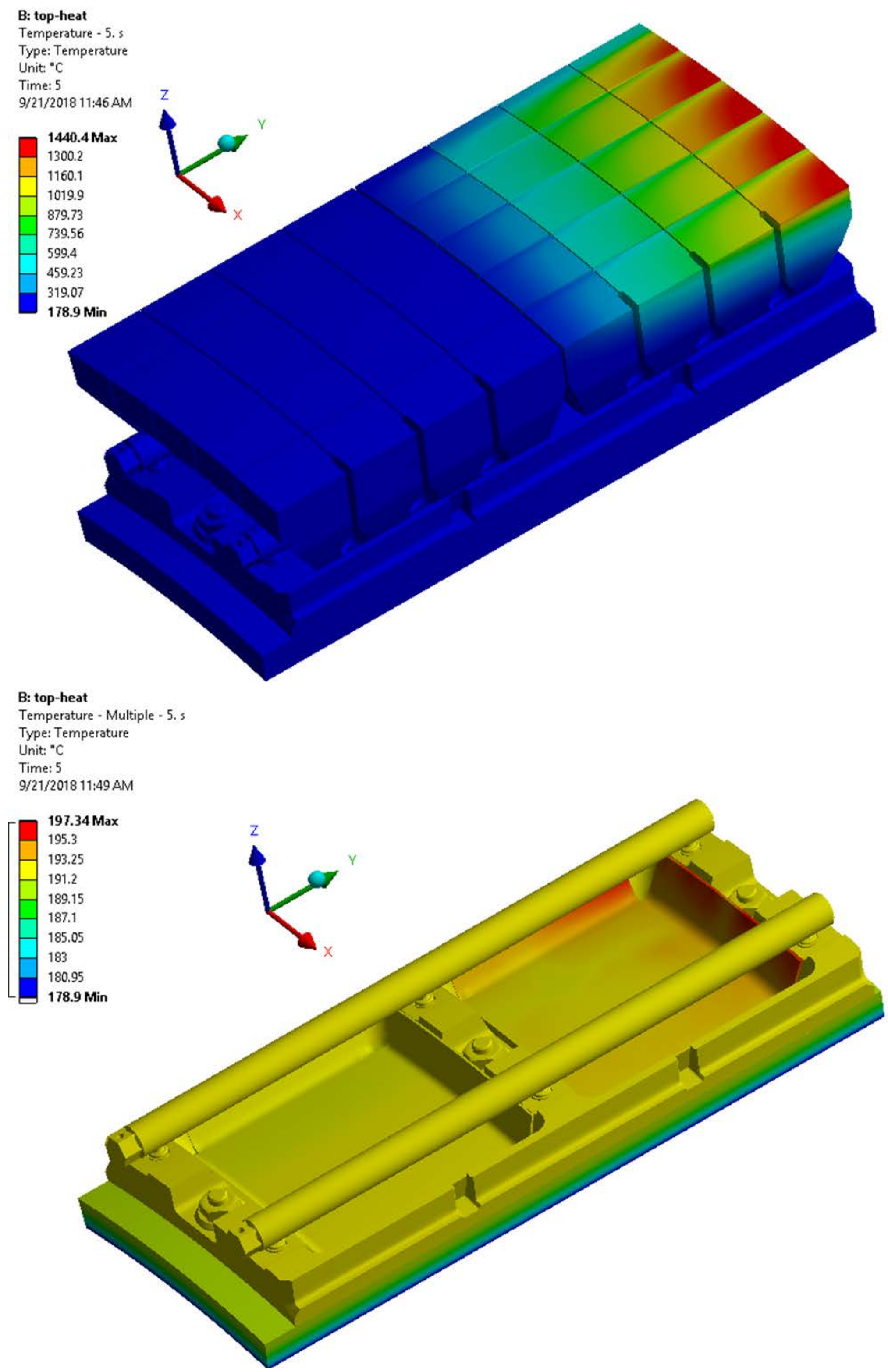

Figure 63: Temperature contour plot of the inboard diverter vertical tiles for heat flux case 1 profile 1 at 5 seconds

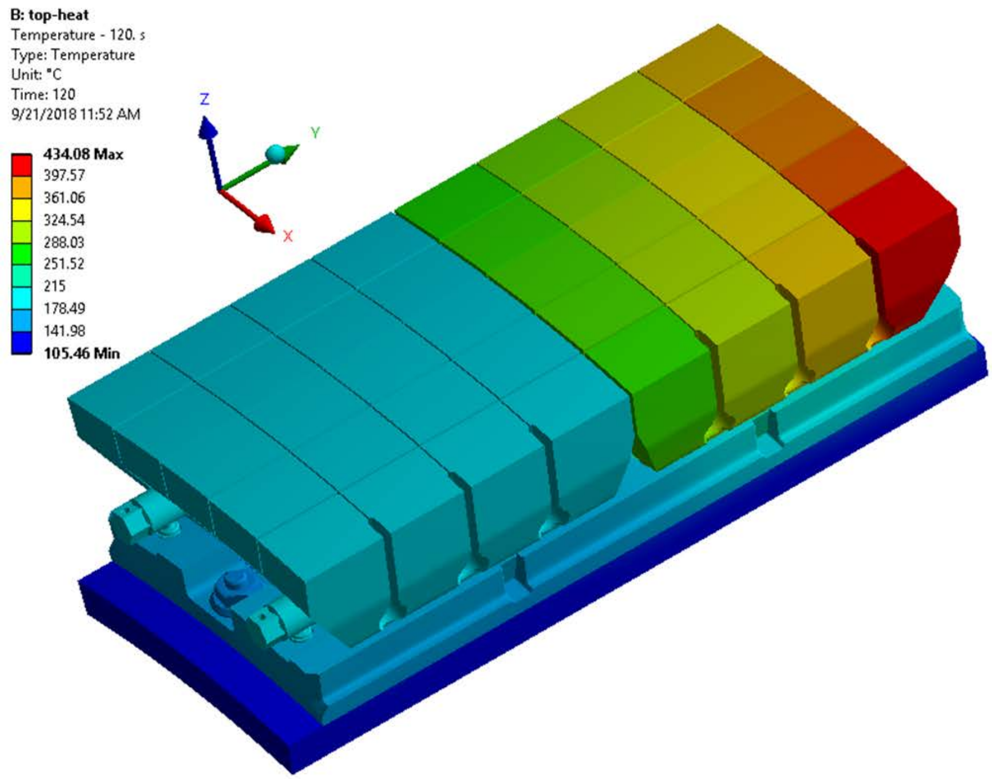

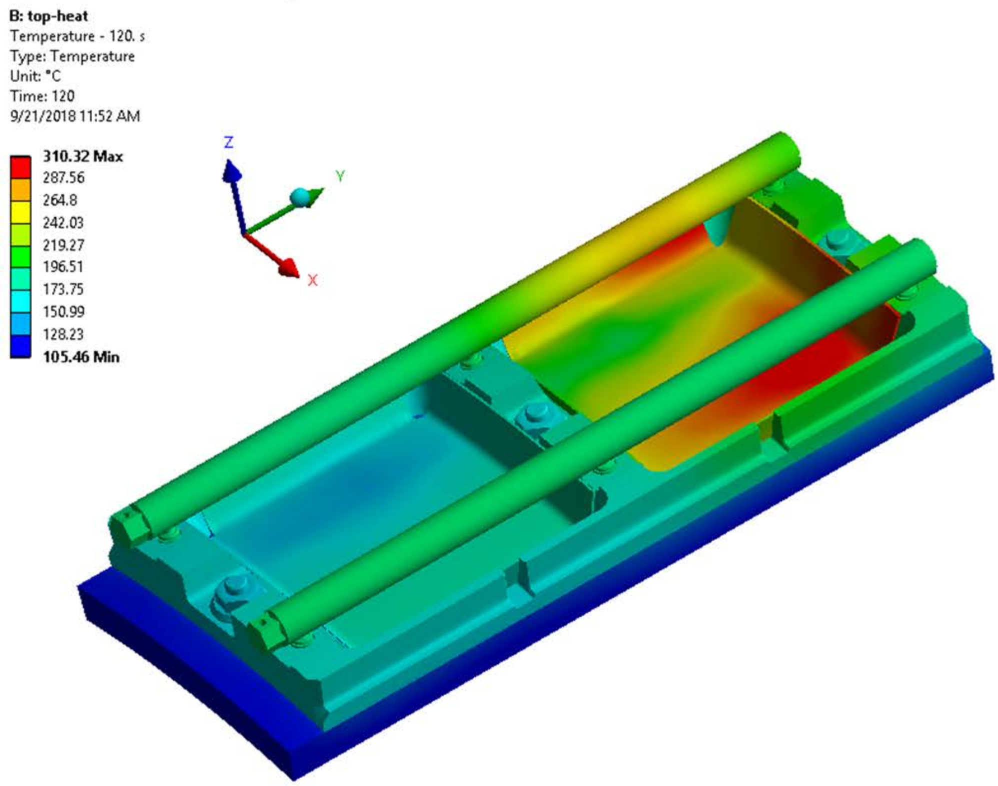

Figure 64: Temperature contour plot of the inboard diverter vertical tiles for heat flux case 1 profile 1 at 120 seconds

Table 18: Peak temperatures for each component for heat flux case 1 profile 1

Component	Peak Temperature (°C)	Time (sec)
Graphite Tiles (row 3 and row 4)	1440	5
Grafoil Gaskets and Washers	327	60
Back Plate with integrated studs	195	49
Vertical Tile Rail	232	83
Connecting rods	270	120
Connecting pins	208	120
Nuts (150258)	195	49

The peak temperature in the assembly was 1431 °C in the graphite tile for heat flux case 1 profile 2. Figure 12 shows the temperature contour plot of the tile and substructure after 5 seconds of applied heat flux. Figure 13 shows temperature contour plot of the tiles and substructure after 115 s cooldown. Table 3 lists the peak temperature and corresponding time for each component for heat flux case 1 profile 2.

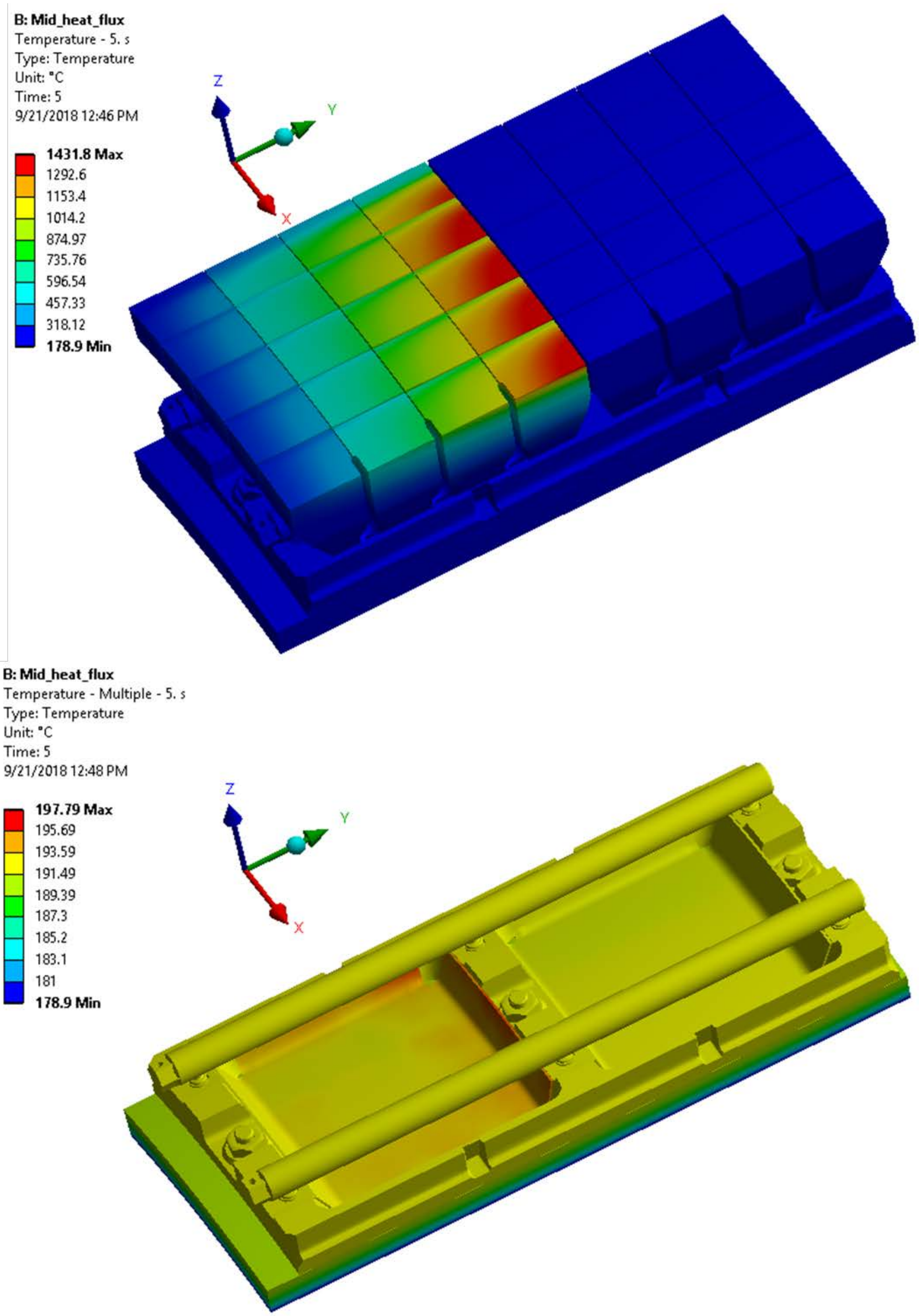

Figure 65: Temperature contour plot of the inboard diverter vertical tiles for heat flux case 1 profile 2 at 5 seconds

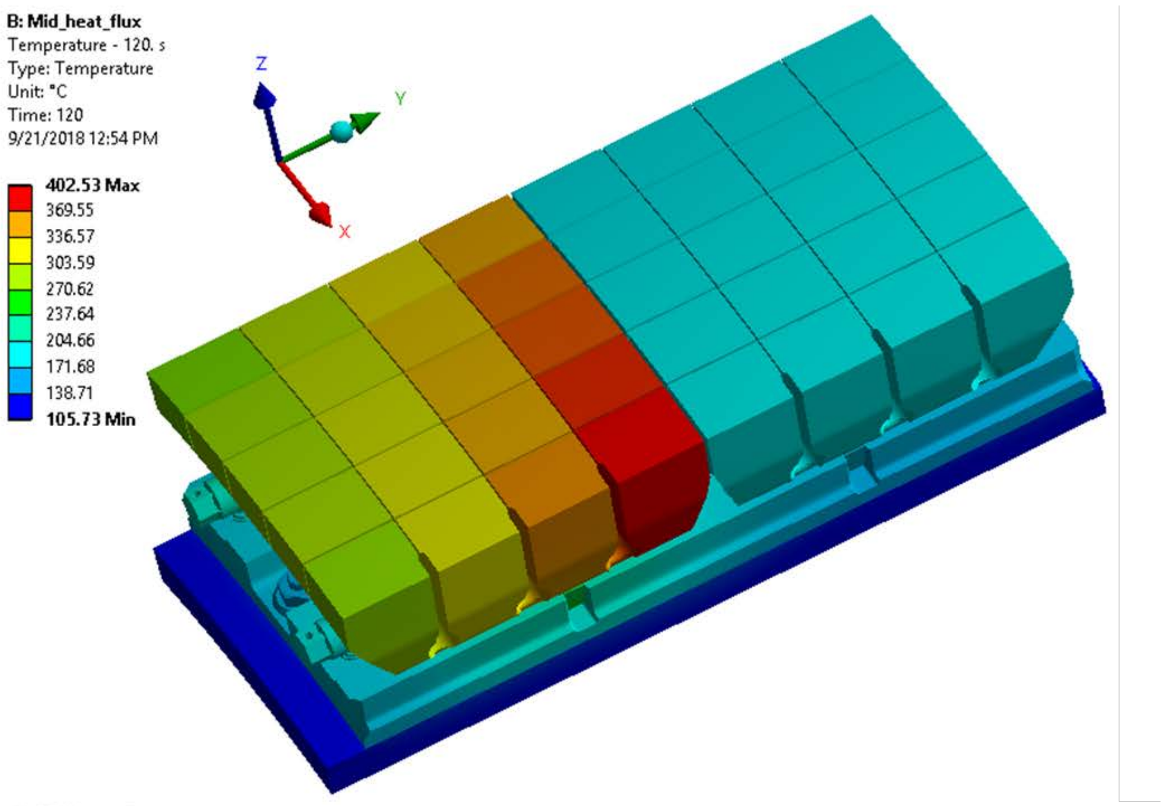

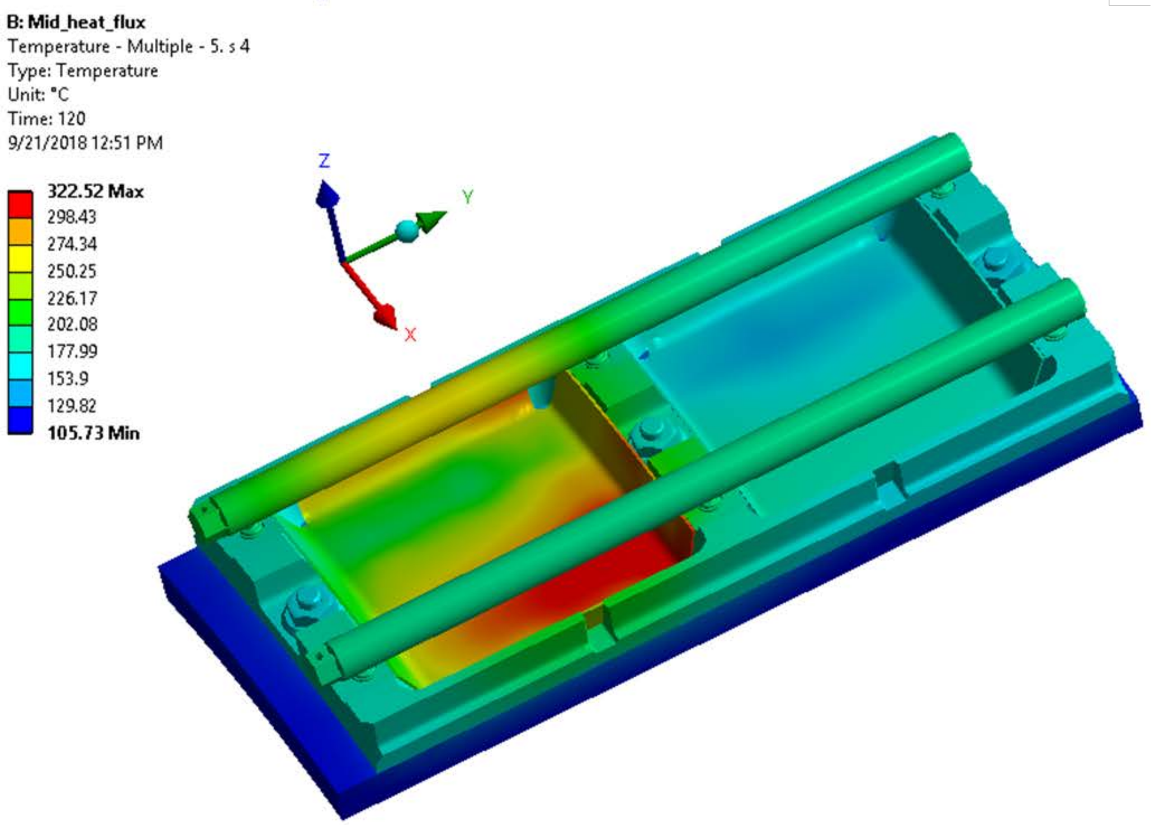

Figure 66: Temperature contour plot of the inboard diverter vertical tiles for heat flux case 1 profile 2 at 120 seconds

Table 19: Peak temperatures for each component for heat flux case 1 profile 2

Component	Peak Temperature (°C)	Time (sec)
Graphite Tiles (row 3 and row 4)	1432	5
Grafoil Gaskets and Washers	338	59
Back Plate with integrated studs	195	48
Vertical Tile Rail	233	71
Connecting rods	275	120
Connecting pins	204	120
Nuts (150258)	195	48

The peak temperature in the assembly was 1897 °C in the graphite tile for heat flux case 3. Figure 14 shows the temperature contour plot of the tile and substructure after 1 seconds of applied heat flux. Figure 15 shows temperature contour plot of the tiles and substructure after 119 s cooldown. Table 4 lists the peak temperature and corresponding time for each component for heat flux case 3.

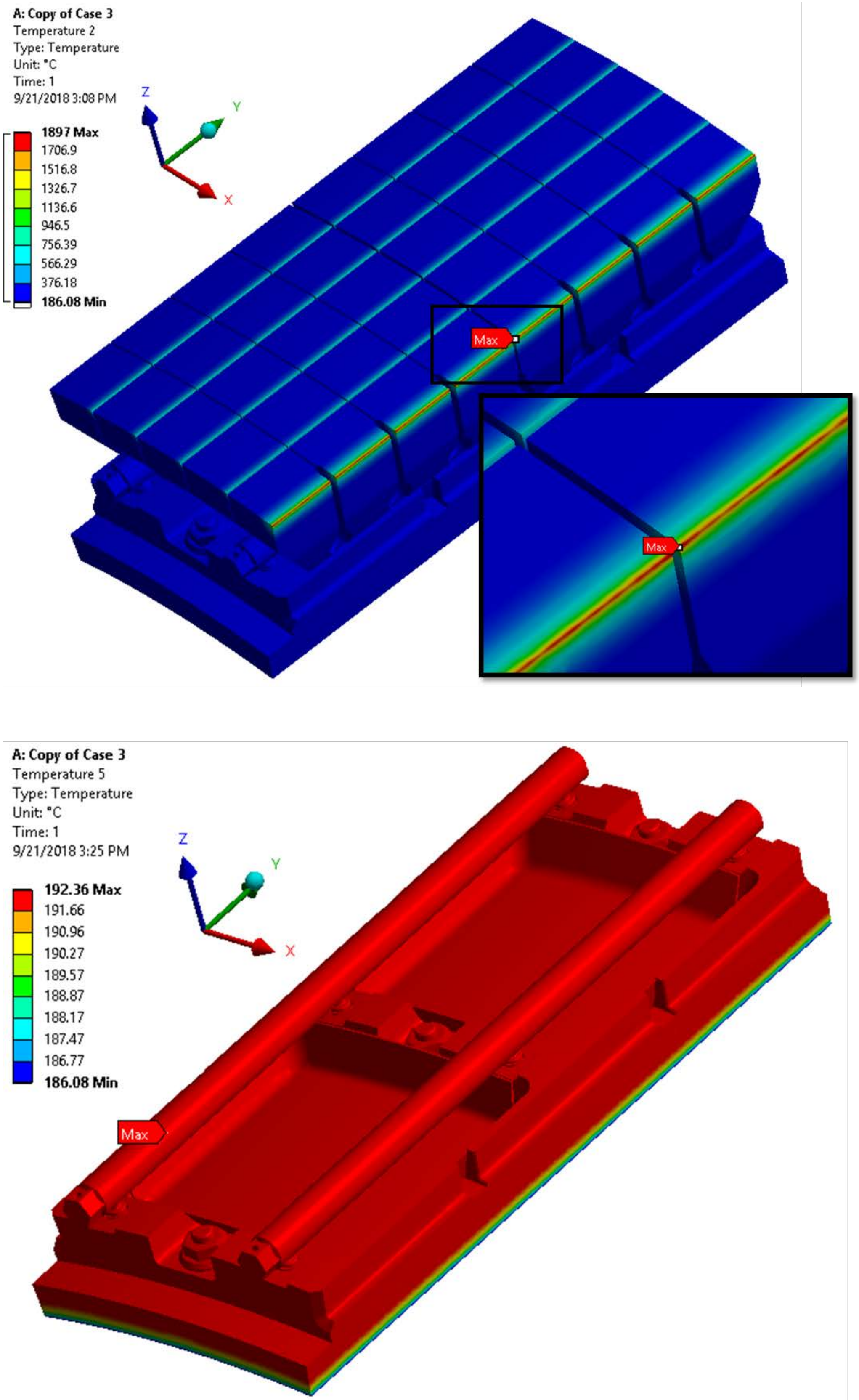

Figure 67: Temperature contour plot of the inboard diverter vertical tiles for heat flux case 3 at 1 seconds

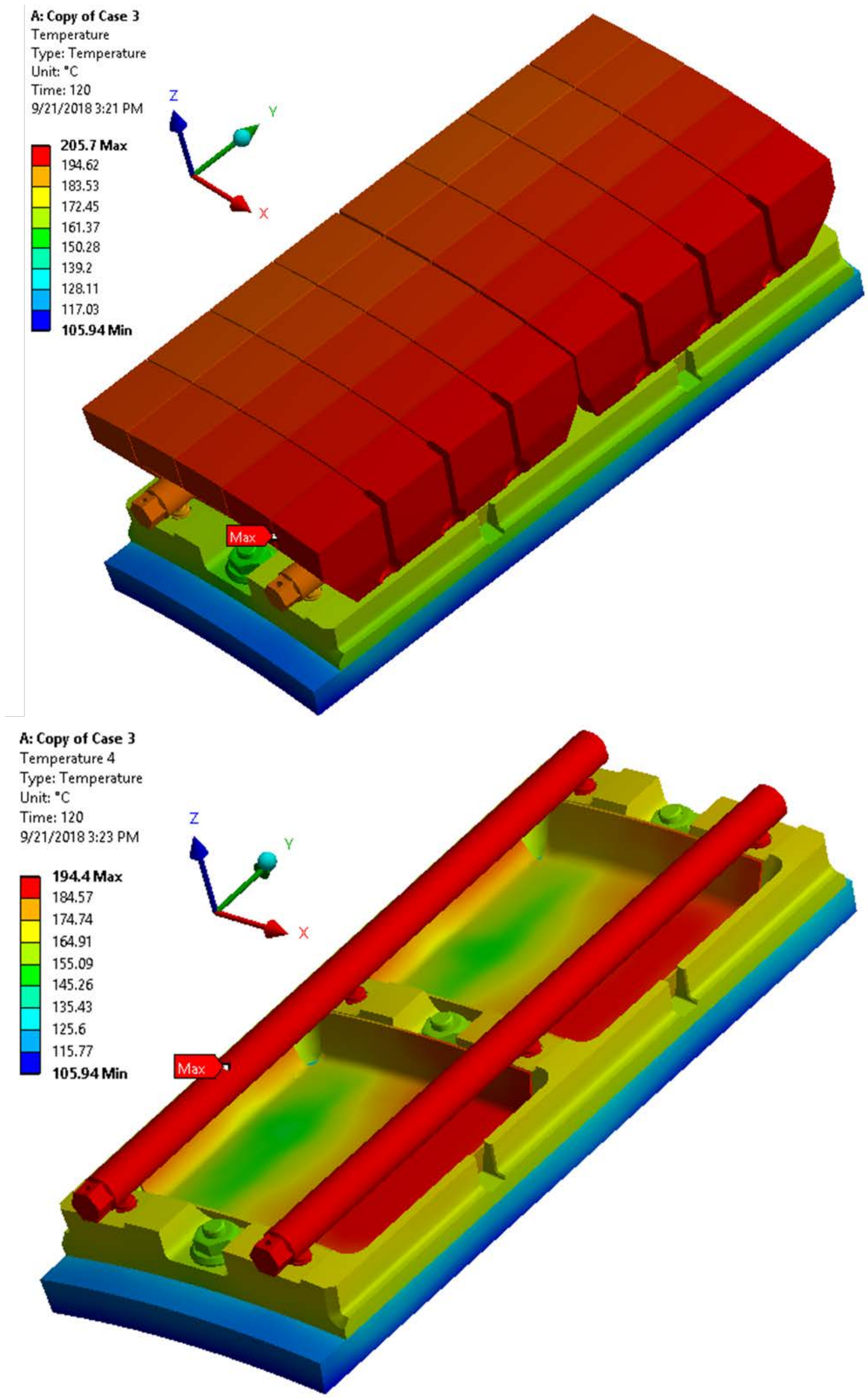

Figure 68: Temperature contour plot of the inboard diverter vertical tiles for heat flux case 3 at 120 seconds

Table 20: Peak temperatures for each component for heat flux case 3

Component	Peak Temperature (°C)	Time (sec)
Graphite Tiles (row 3 and row 4)	1897	1
Grafoil Gaskets and Washers	199	41
Back Plate with integrated studs	192	0
Vertical Tile Rail	192	0
Connecting rods	195	65
Connecting pins	192	0
Nuts (150258)	192	0

Structural-Thermal Analysis

The temperature profiles that resulted from the thermal analysis were imported into a static structure analysis that included bolt preload, eddy current forces, and halo forces. Bolt preload forces of 1000 N were applied to the tree bolts connecting the back plate to the tile rail. Equal and opposite forces were applied to the head of the pins and tile rail. 375 N of force was applied to the 4 outer pins and 750 N of force were applied to the center pins. Figure 16 shows a schematic of the bolt preload and pin loading used for the structural analysis.

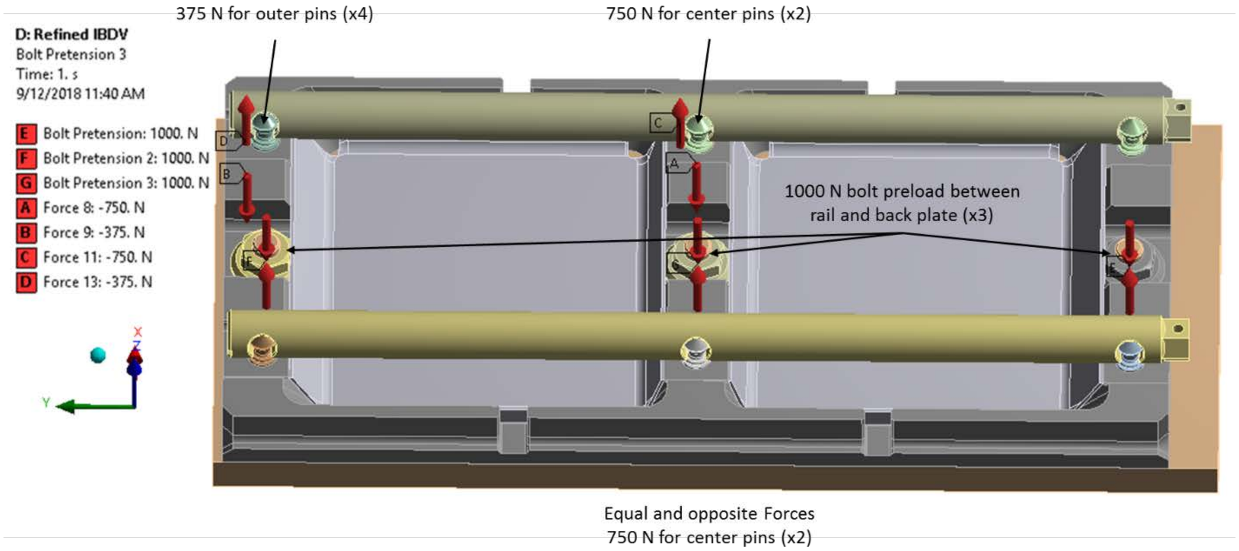

Figure 69: Bolt Preload and pin Loading.

Halo loads were applied to each tile. The row 4 tile halo load was applied in the positive axial and circumferential directions. The row 3 halo load was applied in the negative axial and positive circumferential directions. The loads were divided and applied to each node in each of the tiles. Figure 17 shows direction and magnitudes of the halo loads on the two tiles.

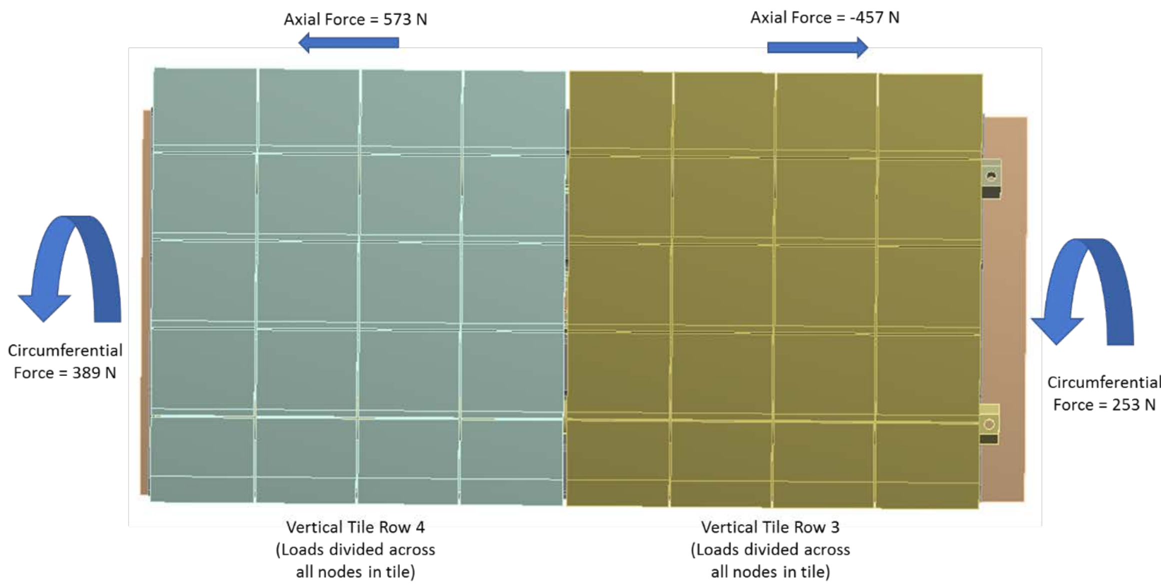

Figure 70: Halo forces applied to all nodes in each of the graphite tiles.

The eddy current loading was applied with equal and opposite loading in the radial direction on the sides of the tile creating moments. Figure 18 shows the surfaces and magnitudes of the eddy current forces applied to the tiles.

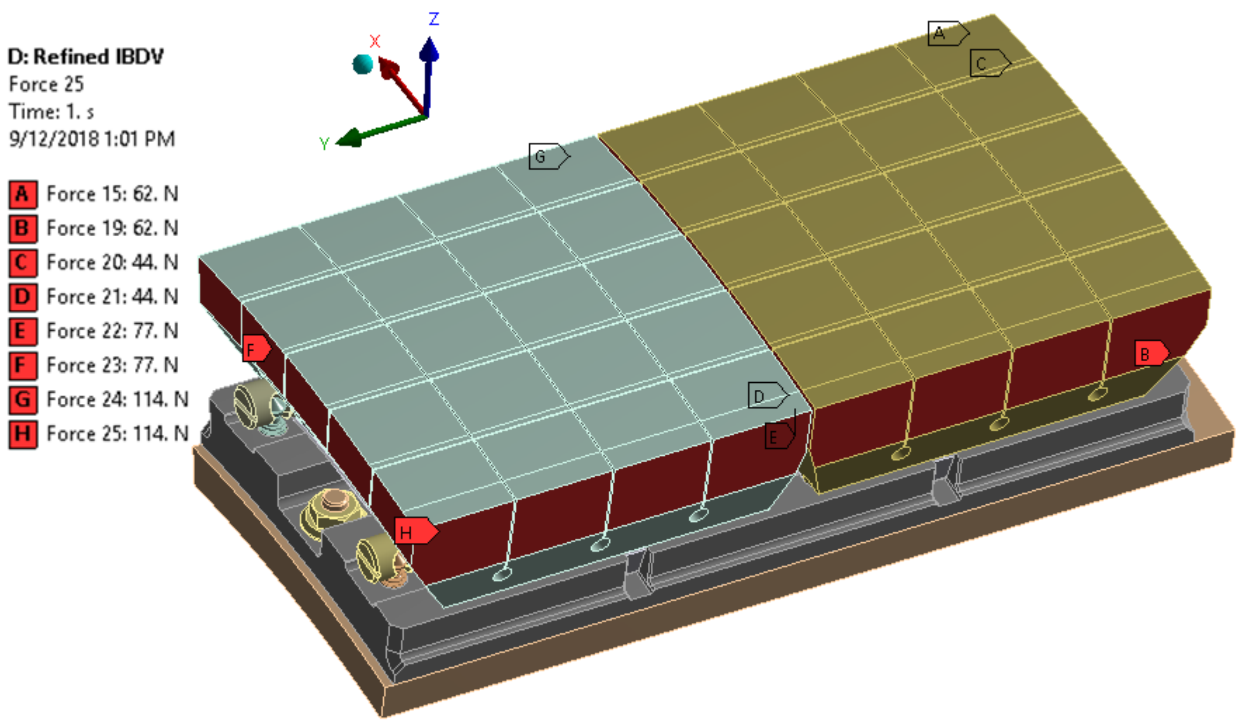

Figure 71 Eddy current loading in IBVD tiles

Fixed displacements were applied to the back plate and tile rail to constrain the model during the analysis. Circumferentially fixed displacements were placed on the sides of the back plate and tile rail. A fixed axial displacement was placed on the back plate

surface on the row 3 tile end of the assembly Figure 19 shows the location of these fixed displacements highlighted in yellow.

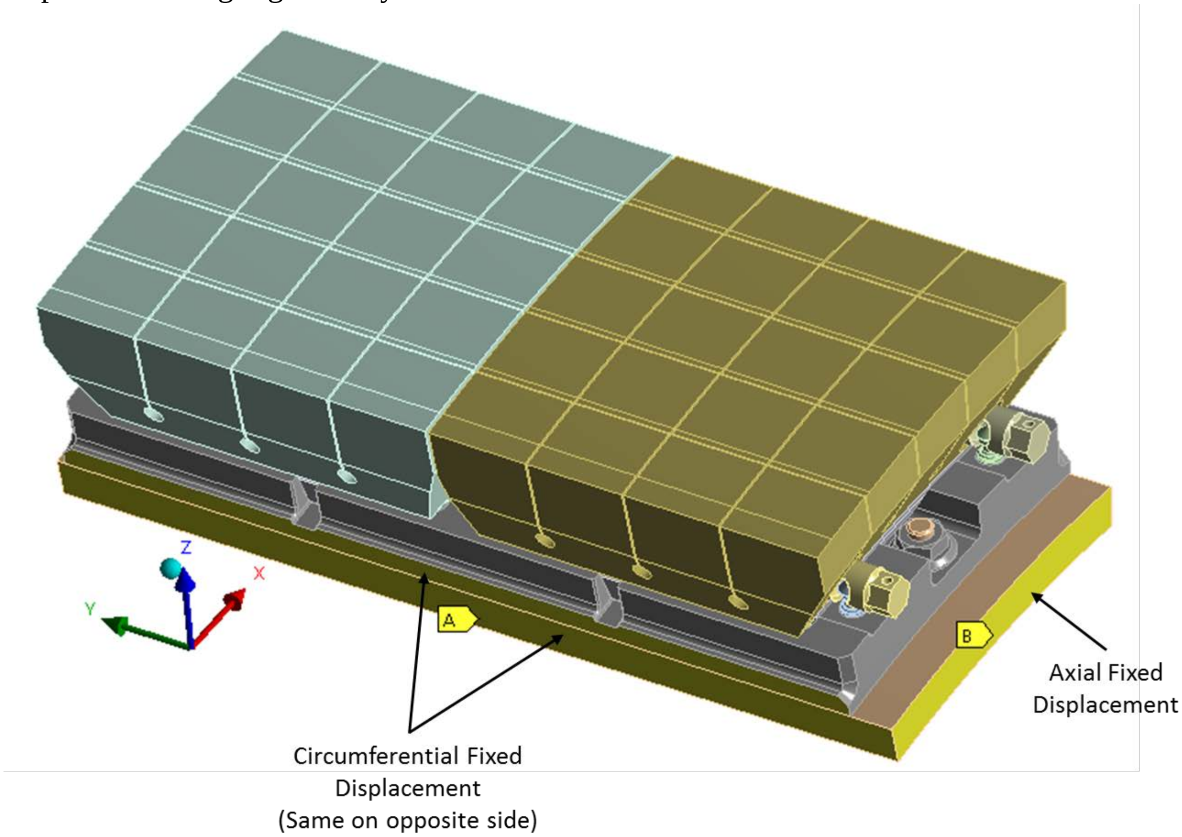

Figure 72: Fixed Displacement locations for IBDV Analysis.

The components of the assembly were connected through various forms of contact. A no separation contact was applied between the grafoil washers and the connecting rod pins as shown in Figure 20. Frictional contact with a coefficient of 0.3 was added between the nuts and tile rail connecting it to the back plate. Figure 21 shows the location of contact between the nuts and tile rail. Finally, the remaining contact between the components was assumed to be frictional with a coefficient of 0.1. This contact is between the following:

1) Tiles and gasket grafoil.
2) Tiles and connecting rods.
3) Connecting rod pins to connecting rods.
4) Tile rail and gasket grafoil.
5) Tile rail and back plate.

Figure 22 shows the locations of the remaining contact in the assembly.

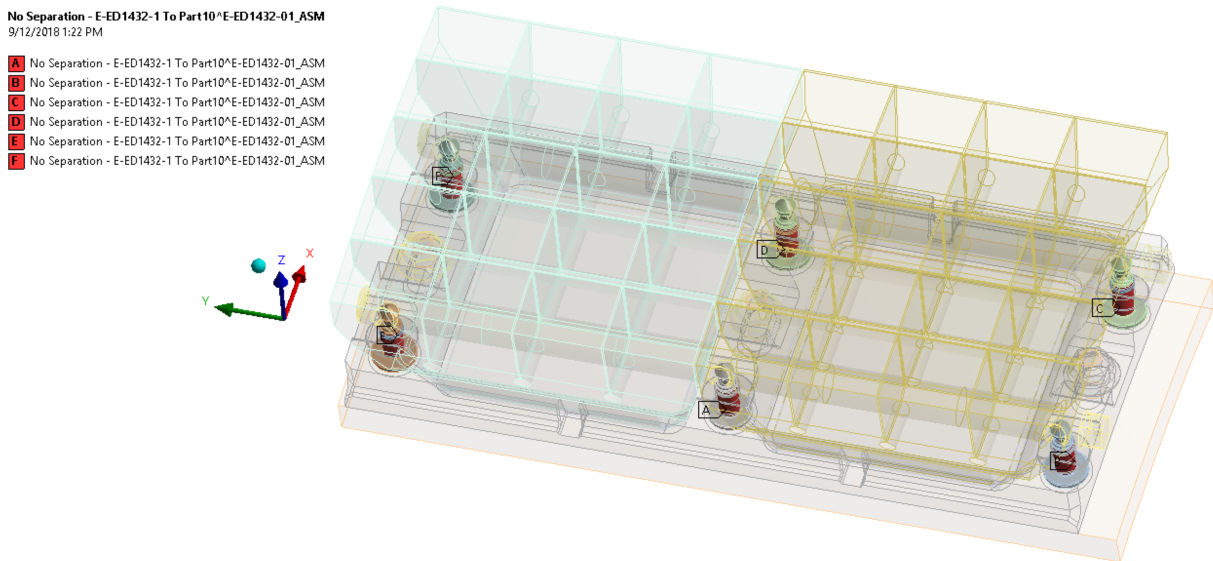

Figure 73: No separation contact between grafoil washers and connecting rod pins.

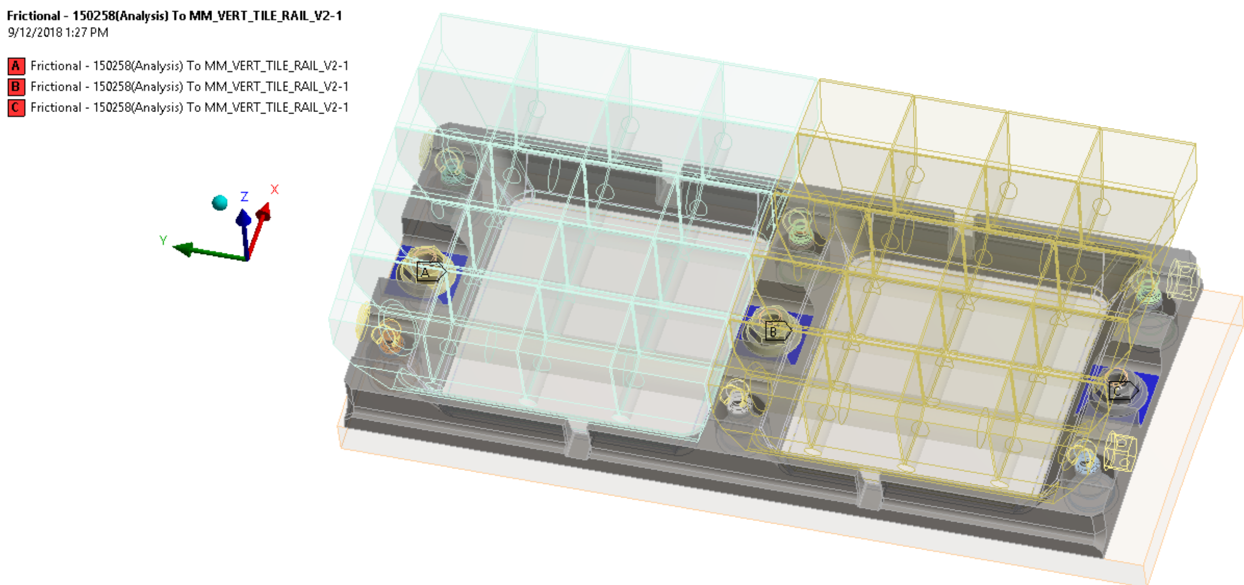

Figure 74: Frictional contact between the nuts and tile rail.

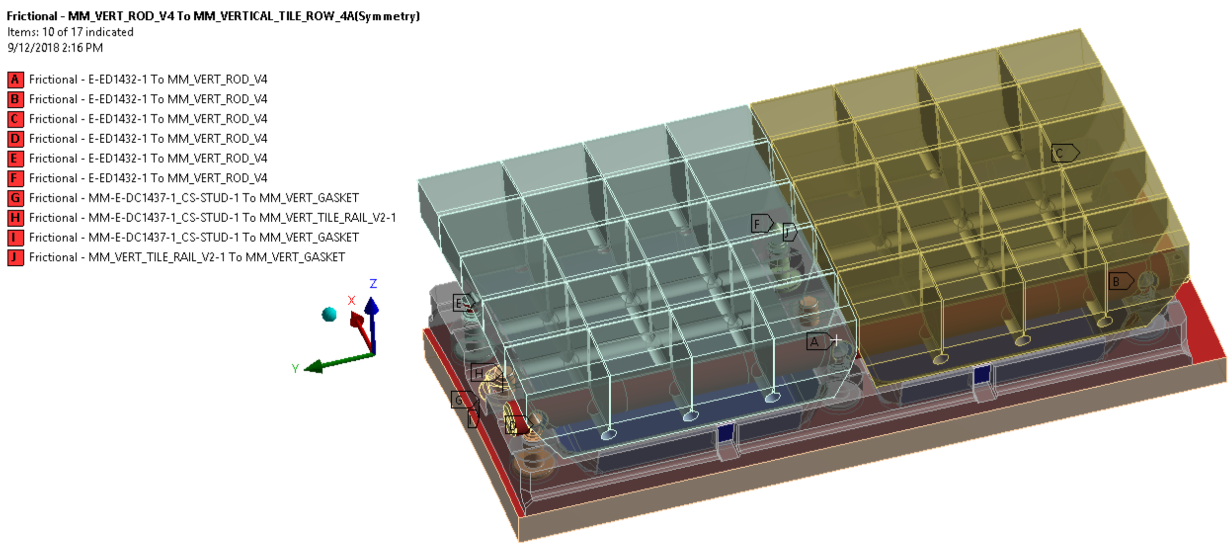

Figure 75: Frictional contact between the graphite tiles and support structure.

Results

The preload, eddy current, and halo loads were combined with the resulting temperature distribution load from the thermal analysis. Note that eddy current and halo loads will be referred to as EM loads. The temperature profile at 5 seconds for each heat flux profile in case 1 was incorporated into a static structural analysis with preload and EM loads. The temperature profile at 5 seconds for load case 3 was incorporated into a static structural model with the preload and EM loads. Finally, the temperature profile that had the highest substructure temperatures at the end of the 115 second cool down was case 1 profile 2. The temperature profile for this case was incorporated with the preload and EM loads. The results from the static analyses for all these heat flux profiles are presented below.

Case 1, Profile 1 and 2 at 5s

Both heat flux case profile 1 and 2 at 5s were compared with each other. The results below represent the worst case between the two profiles. The deformation contour plots in the radial, circumferential, and axial directions of the assembly as a result of the loads is shown in Figure 34, Figure 35, and Figure 36.

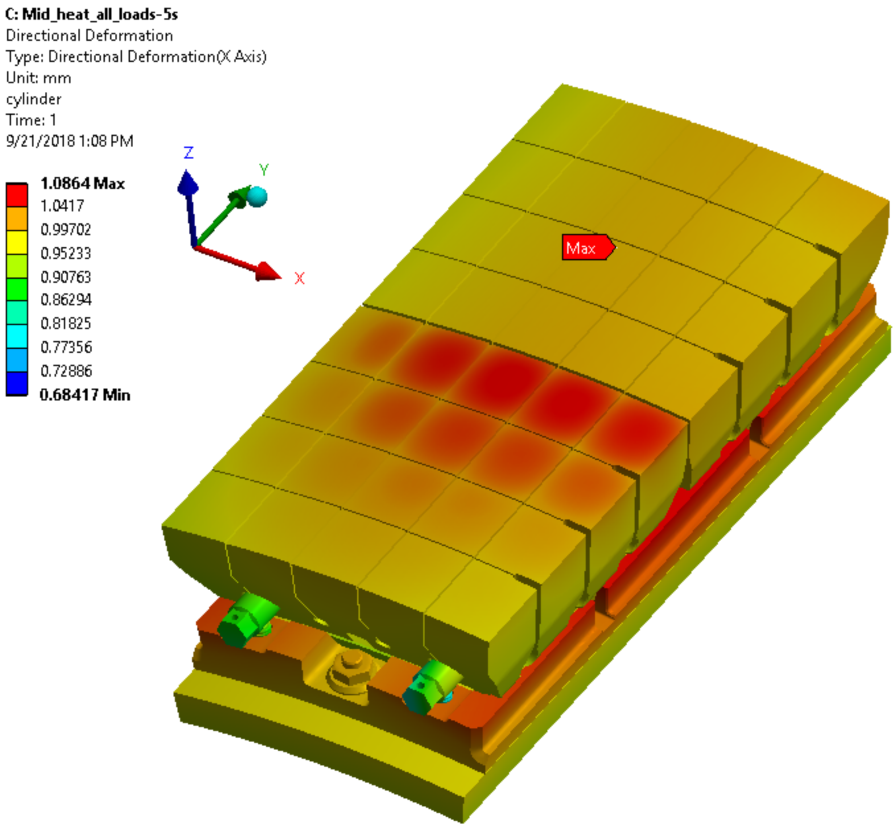

Figure 76: Radial deformation for case 1, profile 2 at 5 seconds.

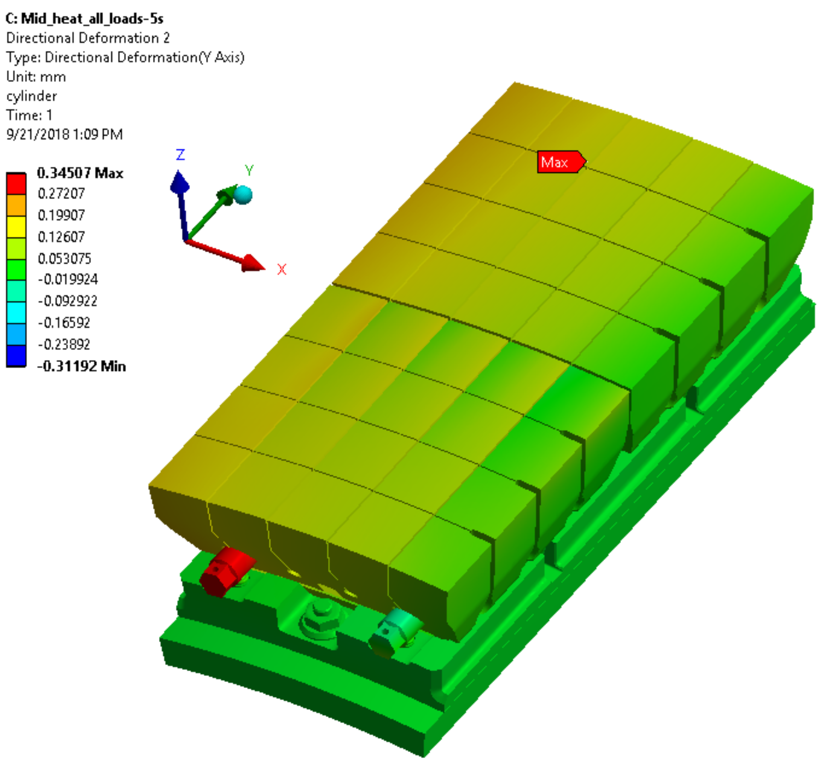

Figure 77: Circumferential deformation for case 1, profile 2 at 5 seconds.

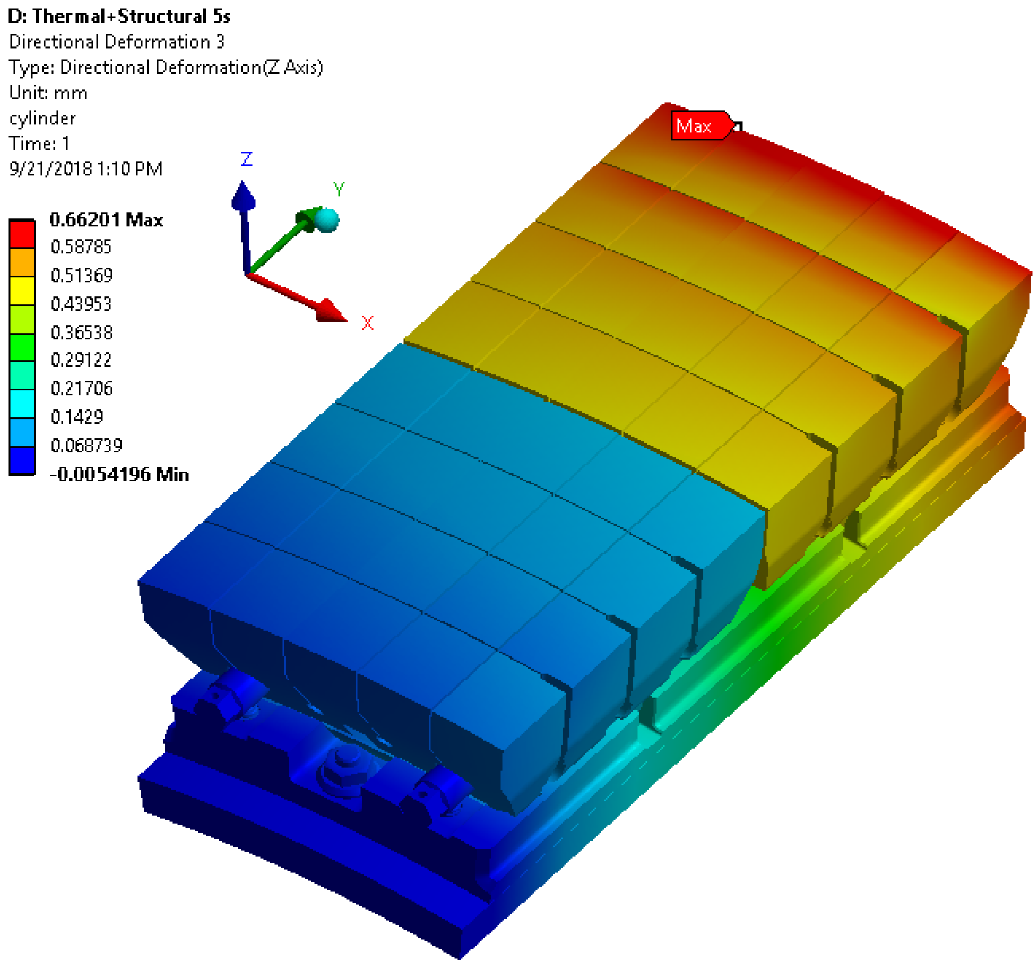

Figure 78: Axial deformation for case 1, profile 1 at 5 seconds.

The following results are for case 1, profile 1 at 5 seconds. Table 5 and Table 6 list the peak maximum and minimum principal stress and the corresponding allowable in the components made of graphite tiles and grafoil gaskets. Table 7 lists the peak equivalent stresses in the Inconel 718 components.

Table 21: Maximum Principal Stress of tiles and grafoil gaskets for case 1, profile 1 at 5 seconds

Component	Peak Stress (MPa)	Allowable (MPa)	Loads
Graphite Tiles row 3	13.26	19	BPL+Halo+Eddy
Graphite Tiles row 4	13.74	19	BPL+Halo+Eddy
Grafoil Gasket	6.55	25	BPL+Halo+Eddy

Table 22: Minimum Principal Stress of tiles grafoil gaskets for case 1, profile 1 at 5 seconds

Component	Peak Stress (MPa)	Allowable (MPa)	Loads
Graphite Tiles row 3	-34.38	-65	BPL+Halo+Eddy
Graphite Tiles row 4	-34.45	-65	BPL+Halo+Eddy
Grafoil Gasket	-9.41	-55	BPL+Halo+Eddy

Table 23: Equivalent Stress in Inconel 718 components for case 1, profile 1 at 5 seconds

Component	Peak Stress (MPa)	Allowable (MPa)	Loads
Back Plate with integrated studs	63.23	717	BPL+Halo+Eddy
Vertical Tile Rail	77.53	717	BPL+Halo+Eddy
Connecting rods	1,732	717	BPL+Halo+Eddy
Connecting pins	1,993	717	BPL+Halo+Eddy
Nuts (150258)	63.23	717	BPL+Halo+Eddy

The following results are for case 1, profile 2 at 5 seconds. Table 8 and Table 9 list the peak maximum and minimum principal stress and the corresponding allowable in the components made of graphite tiles and grafoil gaskets. Table 10 lists the peak equivalent stresses in the Inconel 718 components.

Table 24: Maximum Principal Stress of tiles and grafoil gaskets for case 1, profile 2 at 5 seconds

Component	Peak Stress (MPa)	Allowable (MPa)	Loads
Graphite Tiles row 3	14.10	19	BPL+Halo+Eddy
Graphite Tiles row 4	13.14	19	BPL+Halo+Eddy
Grafoil Gasket	0.86	25	BPL+Halo+Eddy

Table 25: Minimum Principal Stress of tiles grafoil gaskets for case 1, profile 2 at 5 seconds

Component	Peak Stress (MPa)	Allowable (MPa)	Loads
Graphite Tiles row 3	-34.17	-65	BPL+Halo+Eddy
Graphite Tiles row 4	-34.37	-65	BPL+Halo+Eddy
Grafoil Gasket	-1.79	-55	BPL+Halo+Eddy

Table 26: Equivalent Stress in Inconel 718 components for case 1, profile 2 at 5 seconds

Component	Peak Stress (MPa)	Allowable (MPa)	Loads
Back Plate with integrated studs	63.21	717	BPL+Halo+Eddy
Vertical Tile Rail	77.54	717	BPL+Halo+Eddy
Connecting rods	1,727	717	BPL+Halo+Eddy
Connecting pins	1,987	717	BPL+Halo+Eddy
Nuts (150258)	63.21	717	BPL+Halo+Eddy

Both graphite tiles and the grafoil gaskets resulted in stresses below their allowable values. Figure 26 shows the minimum stress contour plot of the graphite tiles. Figure 27 shows the minimum stress contour plot of the grafoil gaskets.

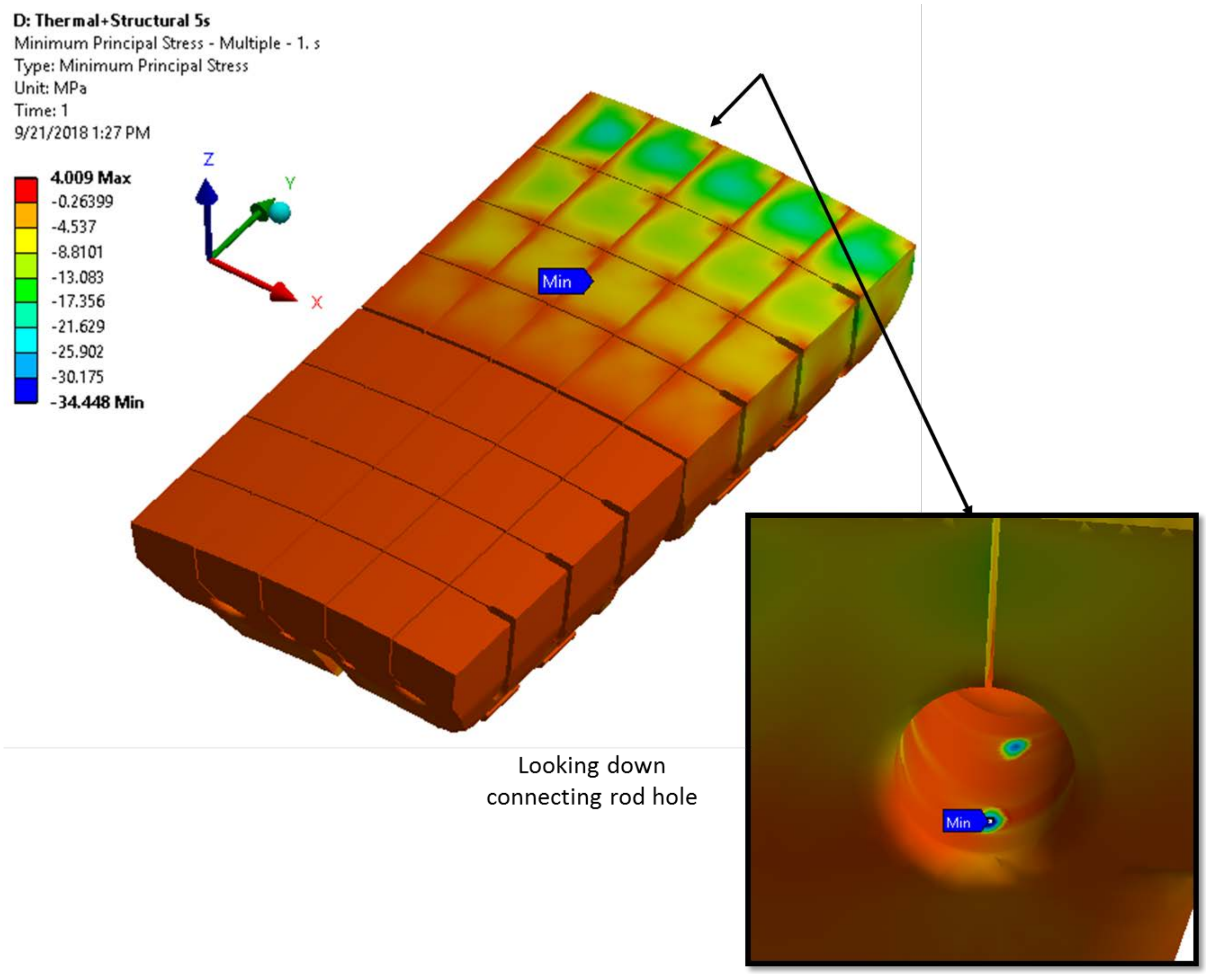

Figure 79: Minimum principal stresses in graphite tiles for case 1, profile 1 at 5 seconds.

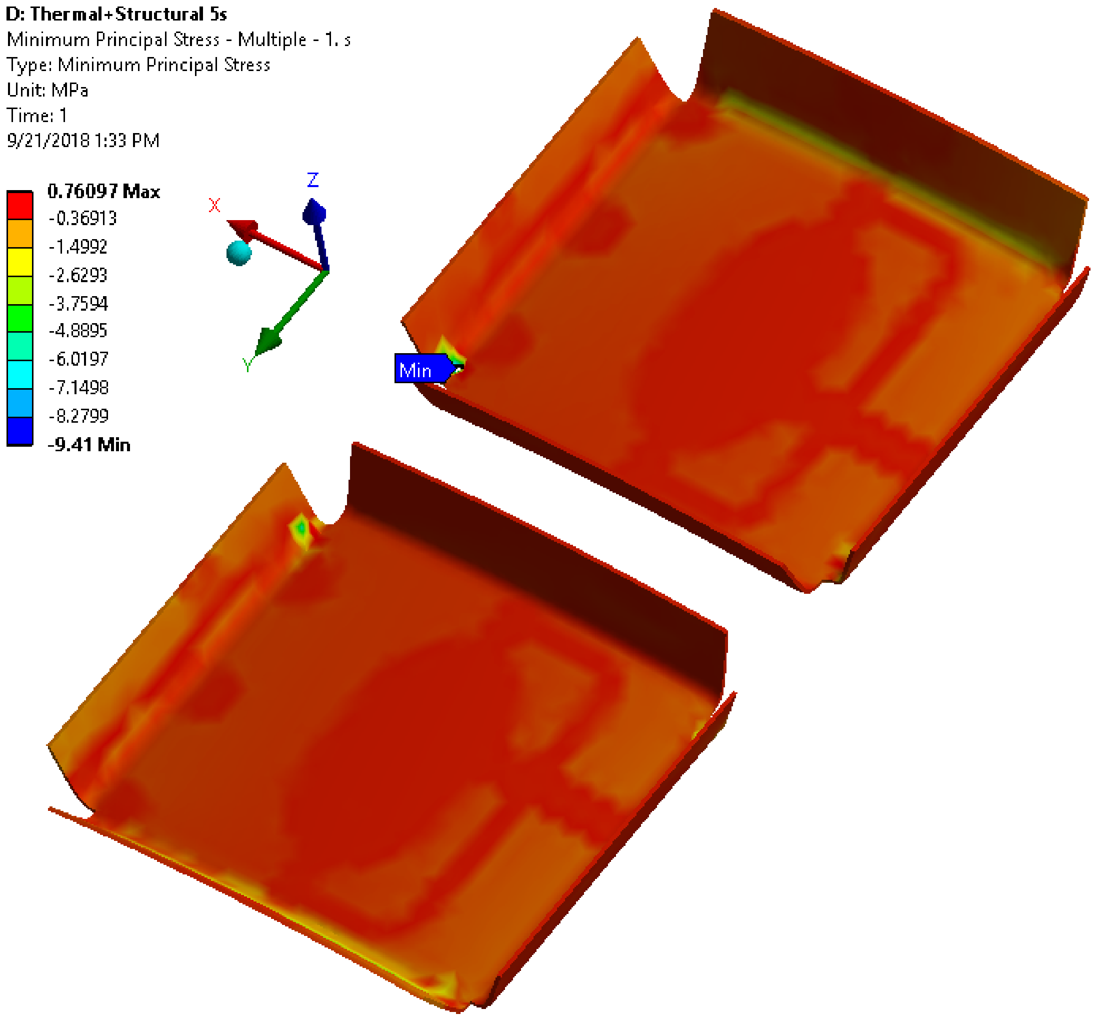

Figure 80: Minimum principal stresses in the grafoil gaskets for case 1, profile 1 at 5 seconds.

Figure 28 and Figure 29 shows the equivalent stress contour plot of all of the Inconel 718 components for both profiles of case 1. Several Inconel 718 components exceeded their allowable values. Figure 30 shows the equivalent stress contour plot of the back plate and nuts. Figure 31 shows the equivalent stress contour plot of the tile rail. The peak stress in these components was below the allowable. The connecting rod pins had and connecting rods had localized areas of high stress as shown in Figure 32. These components are likely okay. Figure 33 shows the stresses in the connecting rods. A sub model of these the connecting pin and rod location was created to address these high stresses.

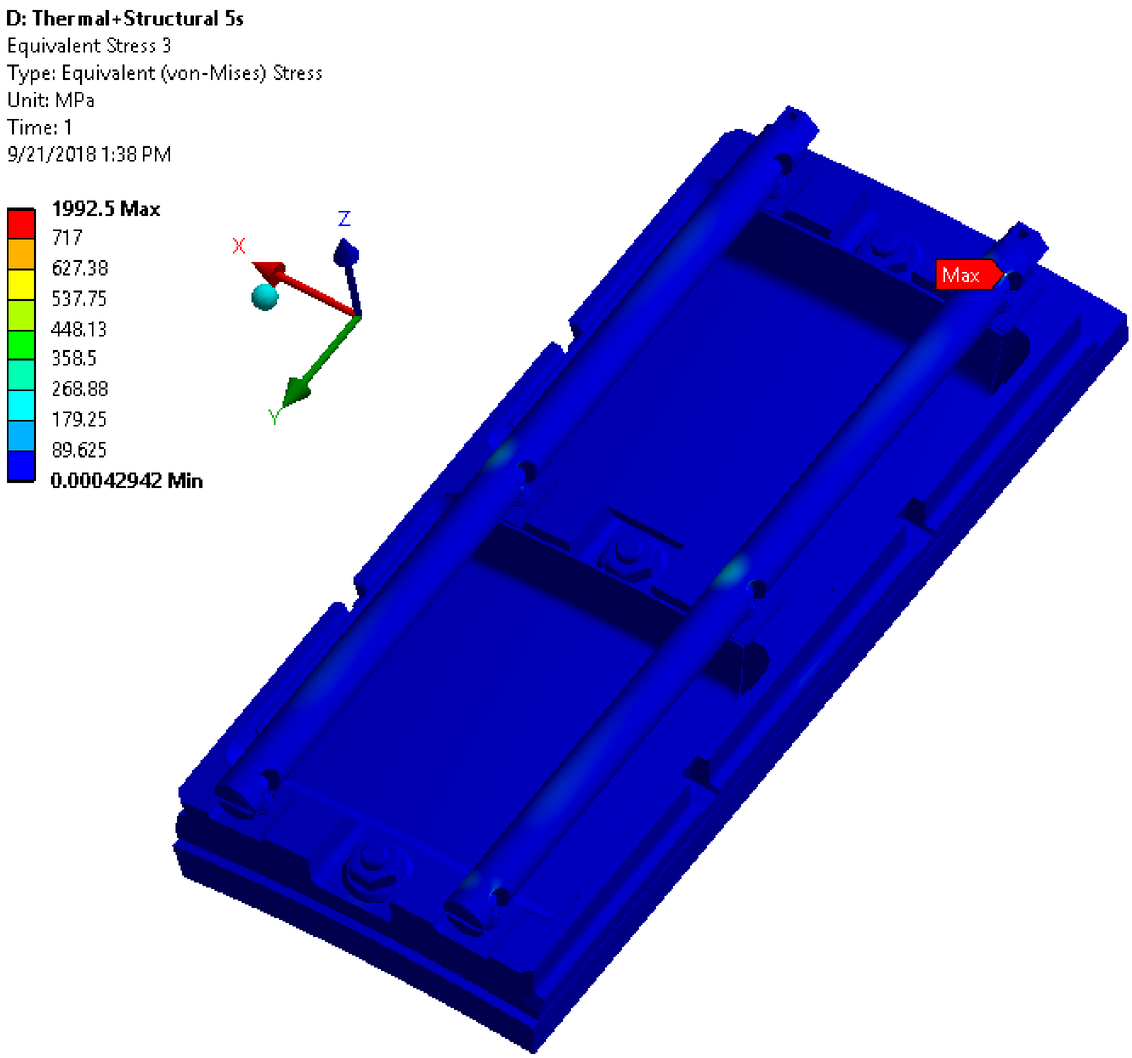

Figure 81: Equivalent stress contour plot of Inconel 718 components for case 1, profile 1 at 5 seconds.

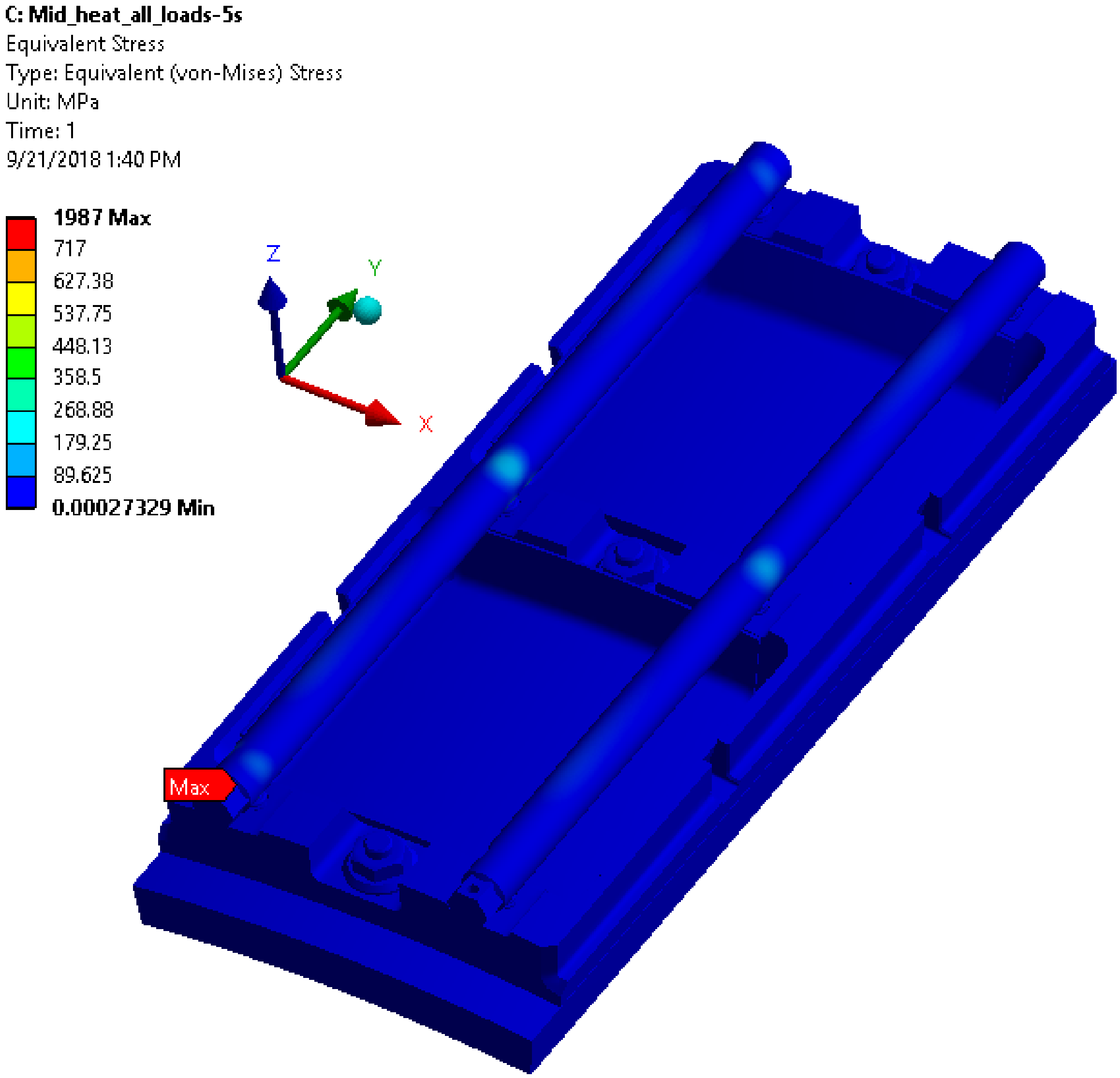

Figure 82: Equivalent stress contour plot of Inconel 718 components for case 1, profile 2 at 5 seconds.

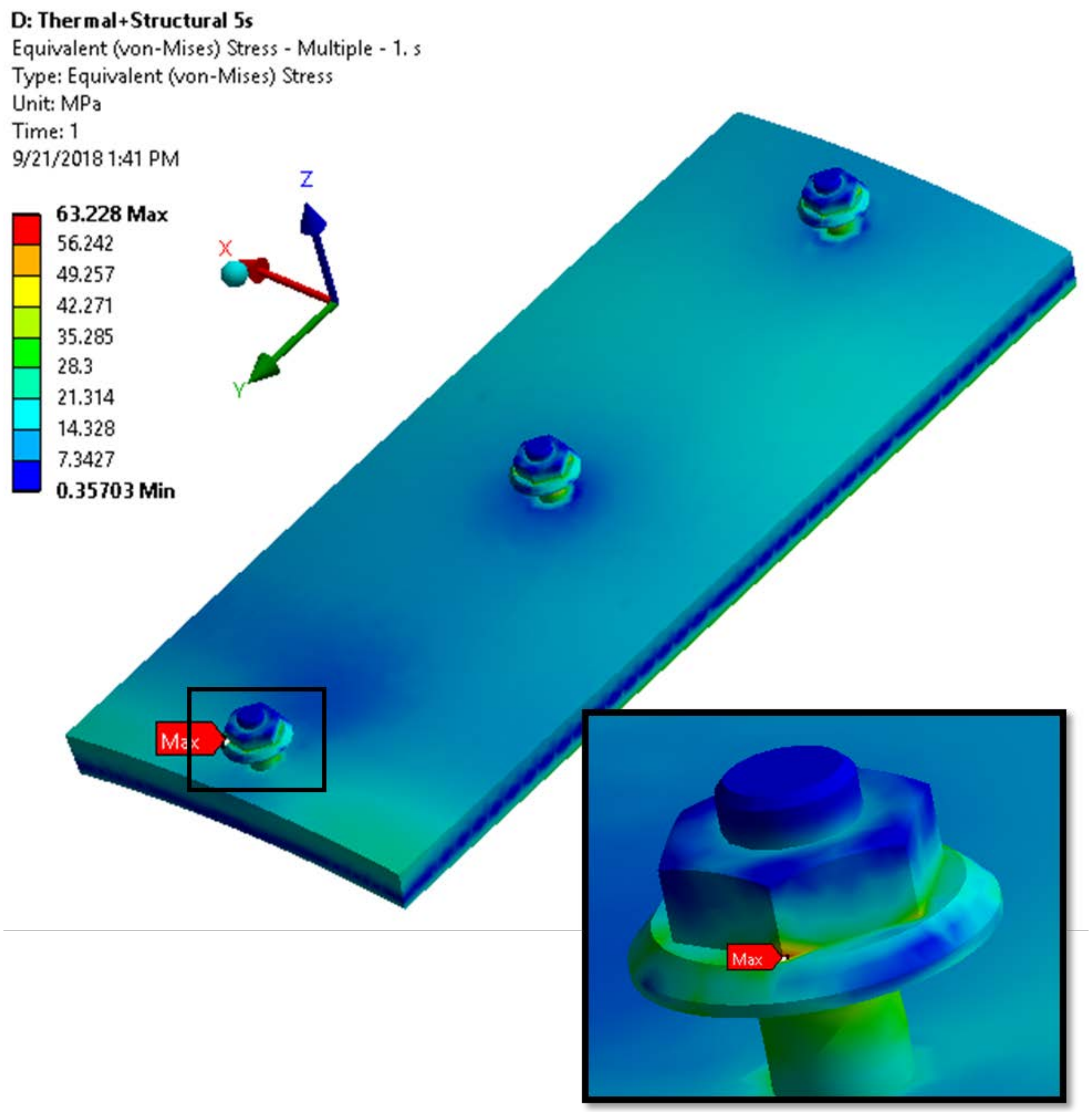

Figure 83: Back plate and nuts equivalent stress contour plot for case 1, profile 1 at 5 seconds.

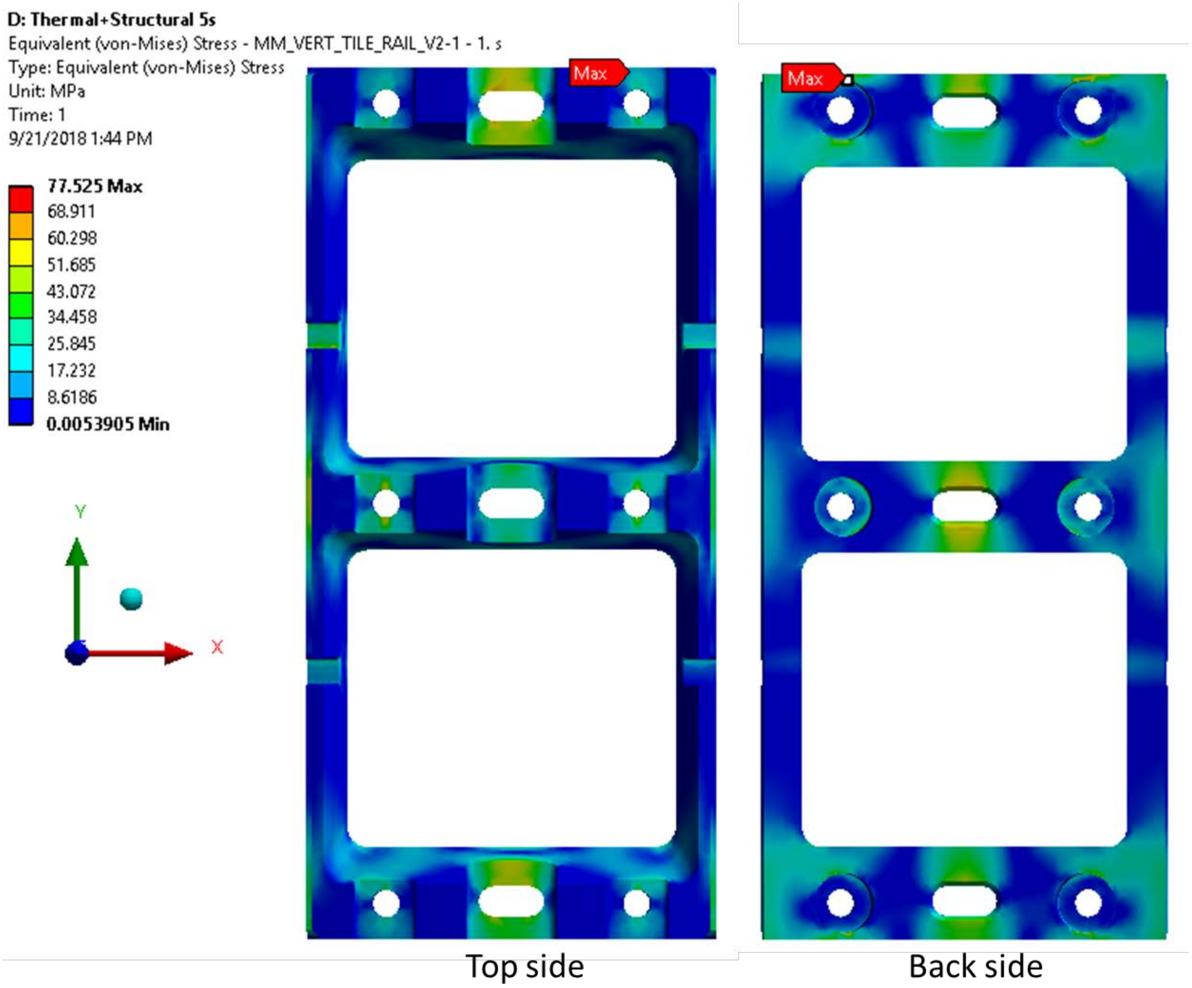

Figure 84: Tile rail equivalent stress for case 1, profile 1 at 5 seconds.

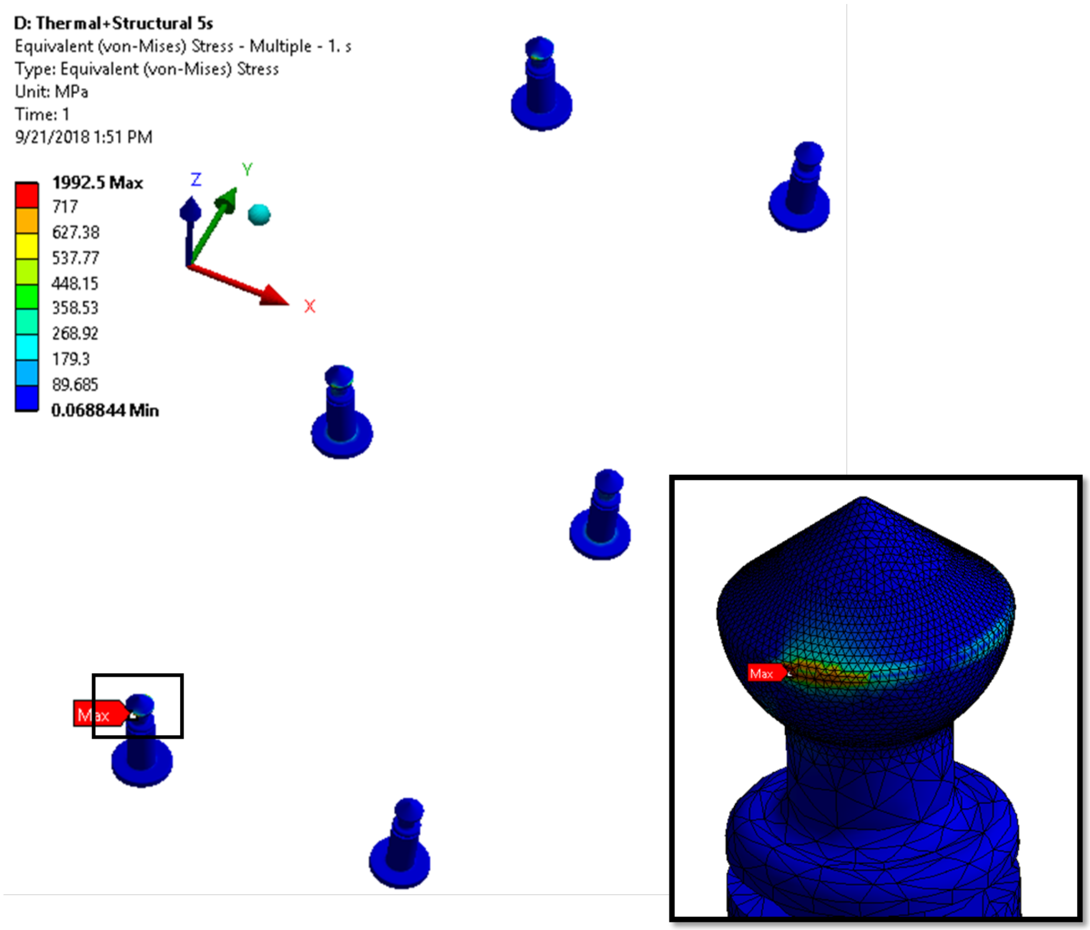

Figure 85: Connecting rod pin equivalent stress contour plot for case 1, profile 1 at 5 seconds.

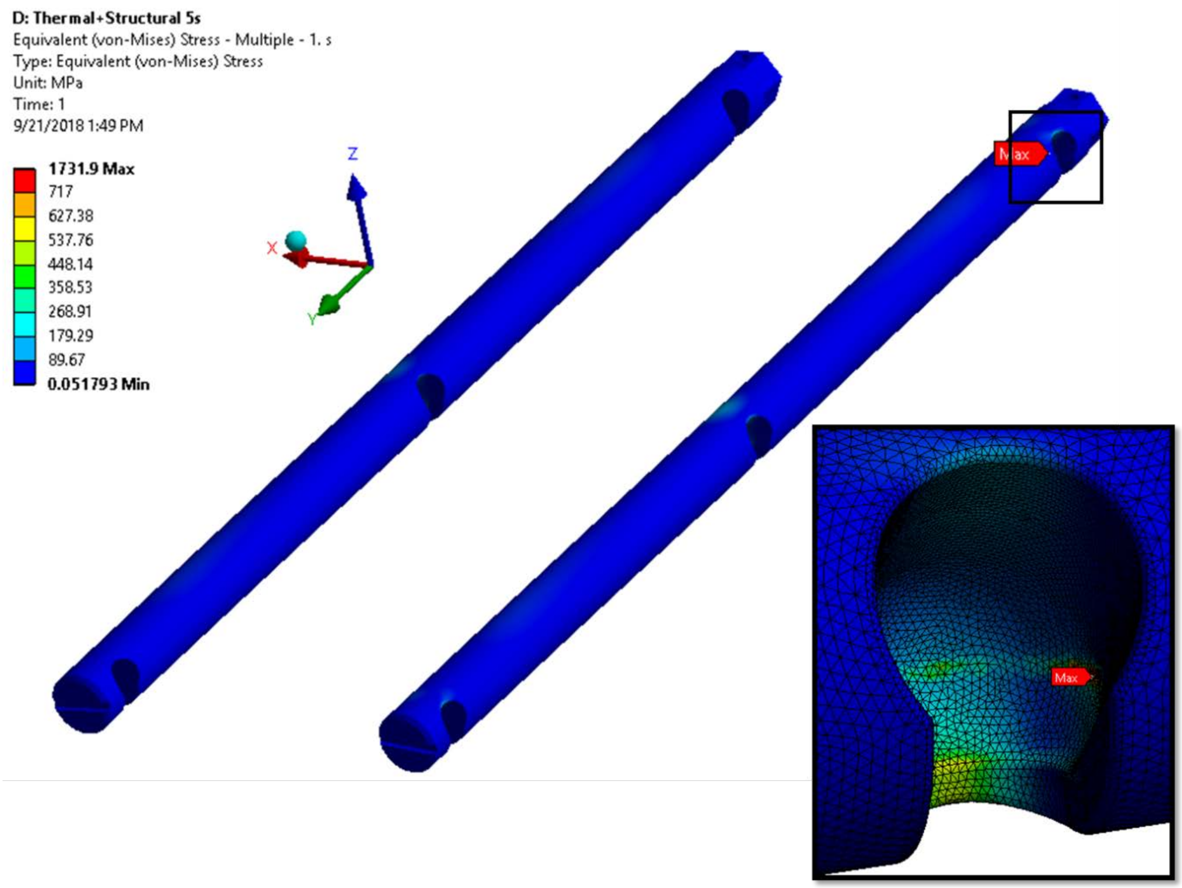

Figure 86: Equivalent stress plot of the connection rods for case 1, profile 1 at 5 seconds.

Case 1, Profile 1 at 120 seconds

The deformation contour plots in the radial, circumferential, and axial directions of the assembly as a result of the loads is shown in Figure 34, Figure 35, and Figure 36.

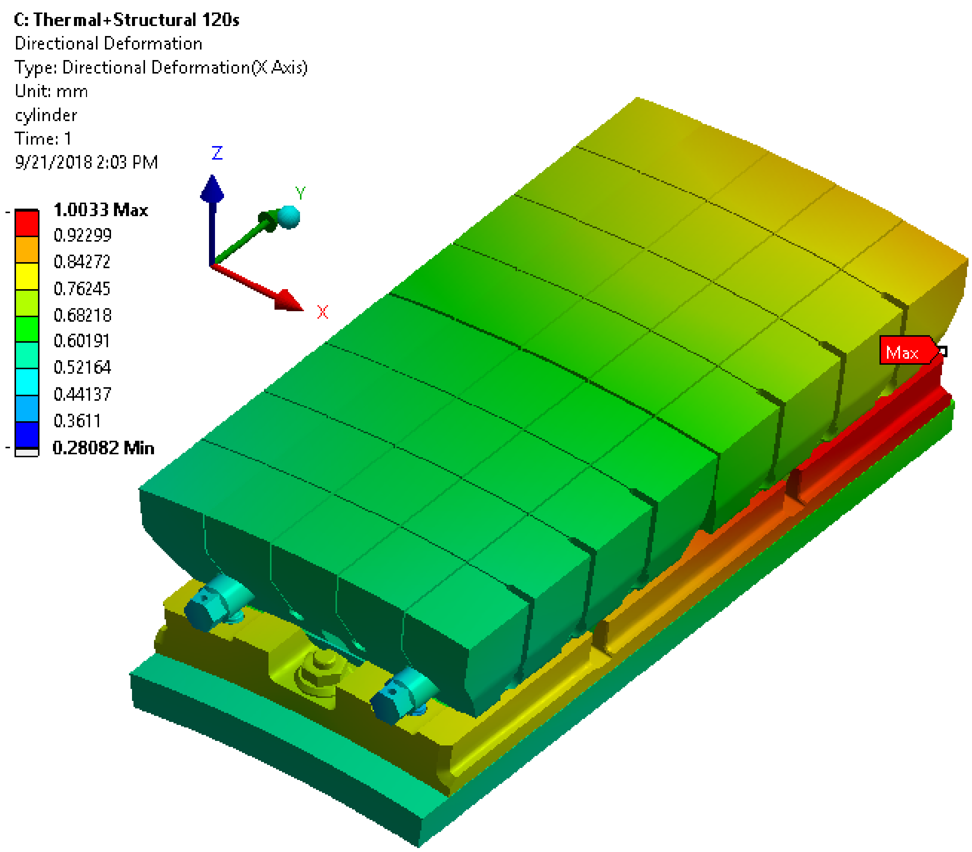

Figure 87: Radial deformation for case 1, profile 1 at 120 seconds.

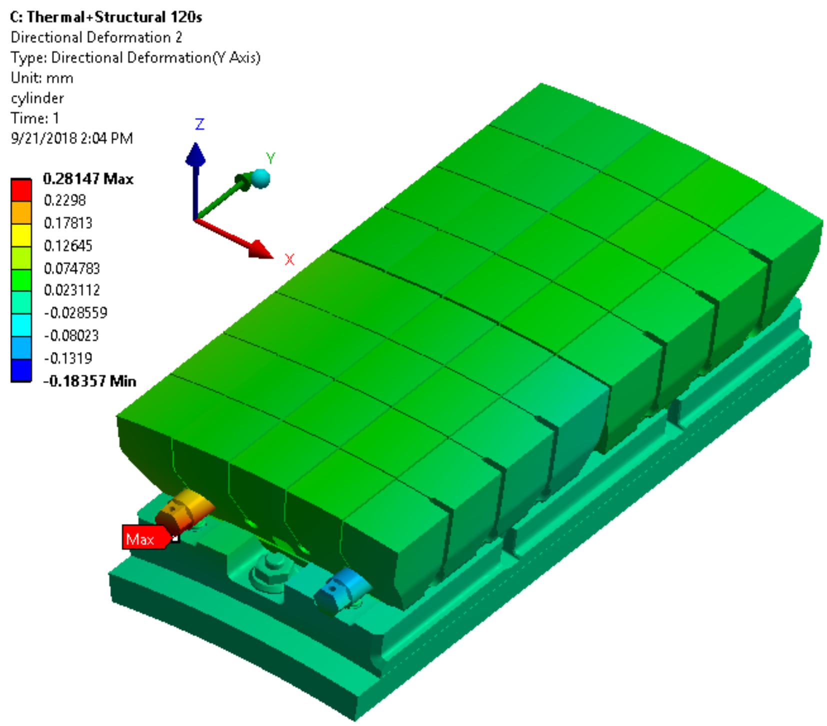

Figure 88: Circumferential deformation for case 1, profile 1 at 120 seconds.

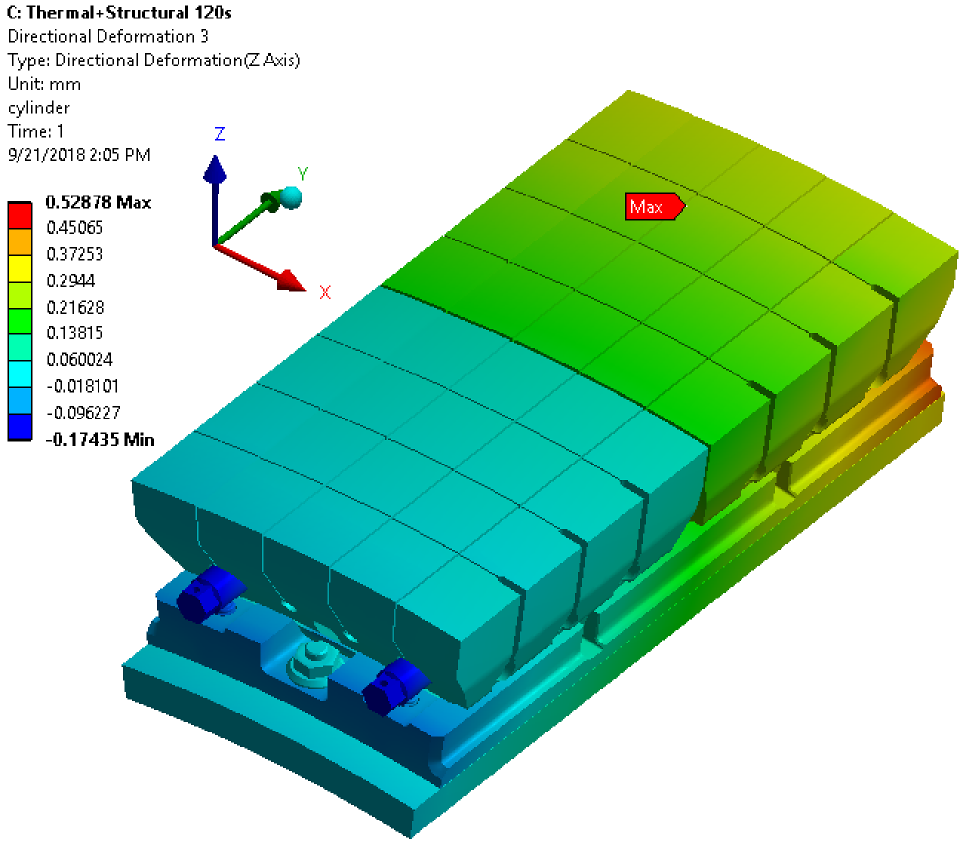

Figure 89: Axial deformation for case 1, profile 1 at 120 seconds.

All results presented in the tables below are from case 1, profile 1 at 120 second. Table 11 and Table 12 list the peak maximum and minimum principal stress and the corresponding allowable in the components made of graphite tiles and grafoil gaskets. Table 13 lists the peak equivalent stresses in the Inconel 718 components.

Table 27: Maximum Principal Stress of tiles and grafoil gaskets

Component	Peak Stress (MPa)	Allowable (MPa)	Loads
Graphite Tiles row 3	16.13	19	BPL+Halo+Eddy
Graphite Tiles row 4	16.13	19	BPL+Halo+Eddy
Grafoil Gasket	5.96	25	BPL+Halo+Eddy

Table 28: Minimum Principal Stress of tiles grafoil gaskets

Component	Peak Stress (MPa)	Allowable (MPa)	Loads
Graphite Tiles row 3	-36.71	-65	BPL+Halo+Eddy
Graphite Tiles row 4	-35.67	-65	BPL+Halo+Eddy
Grafoil Gasket	-9.42	-55	BPL+Halo+Eddy

Table 29: Equivalent Stress in Inconel 718 components

Component	Peak Stress (MPa)	Allowable (MPa)	Loads
Back Plate with integrated studs	97	717	BPL+Halo+Eddy
Vertical Tile Rail	214	717	BPL+Halo+Eddy
Connecting rods	1,739	717	BPL+Halo+Eddy
Connecting pins	1,781	717	BPL+Halo+Eddy
Nuts (150258)	97	717	BPL+Halo+Eddy

Both graphite tiles and the grafoil gaskets resulted in stresses below their allowable values. Figure 37 shows the minimum stress contour plot of the graphite tiles. Figure 38 shows the minimum stress contour plot of the grafoil gaskets.

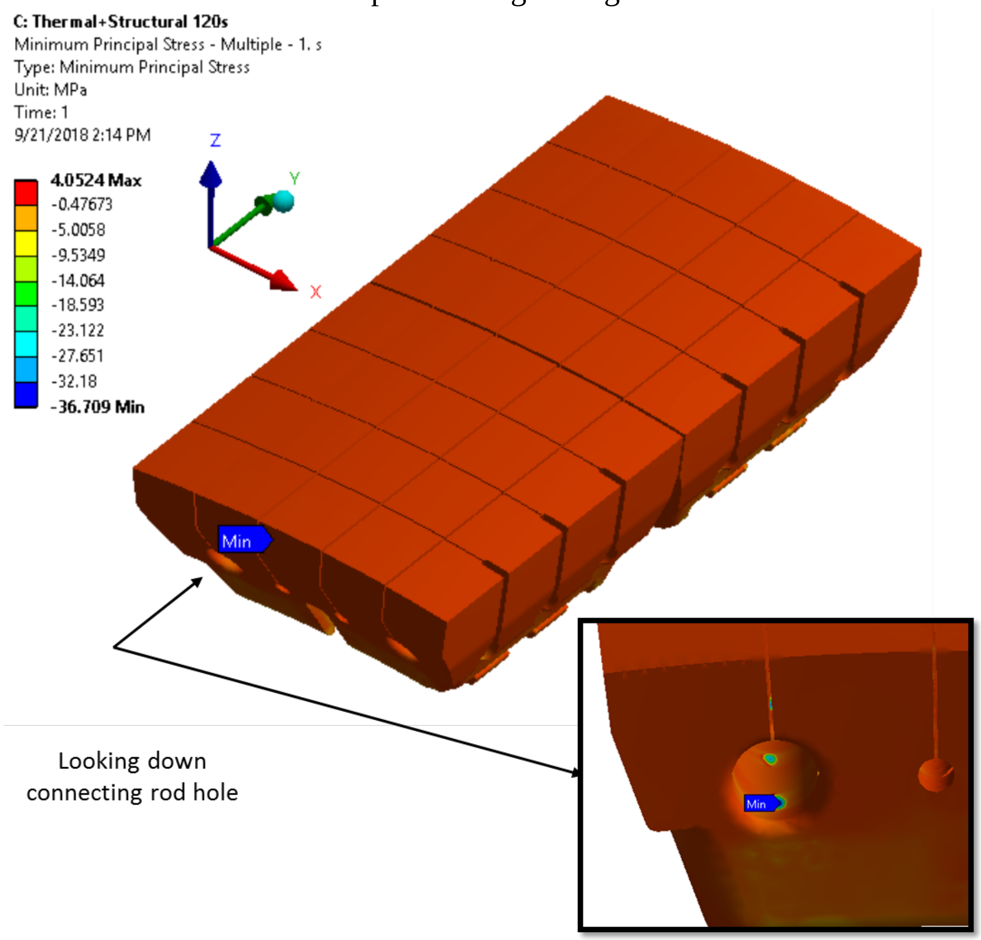

Figure 90: Minimum principal stresses in graphite tiles for case 1, profile 1 at 120 seconds.

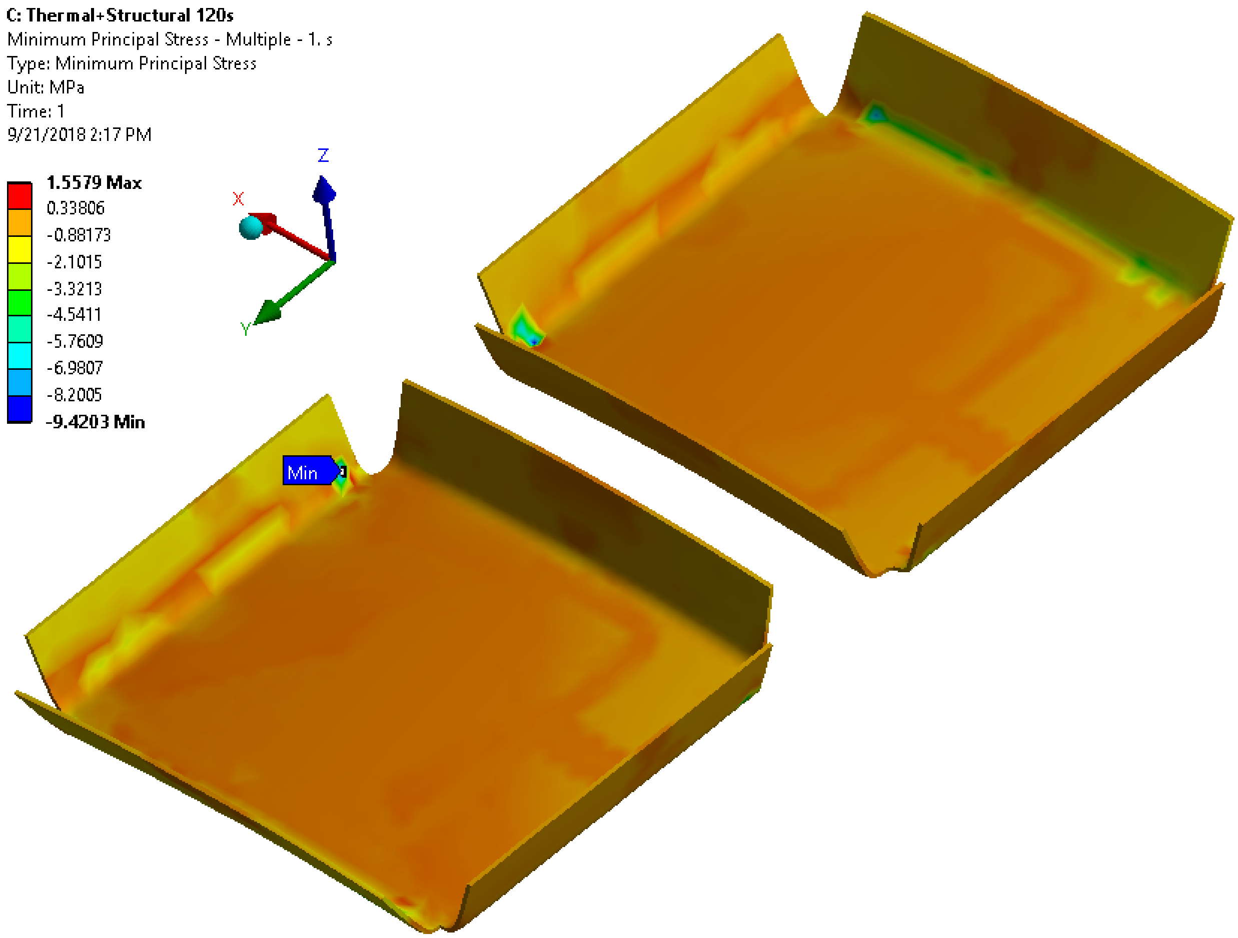

Figure 91: Minimum principal stresses in the grafoil gaskets for case 1, profile 1 at 120 seconds.

Figure 39 shows the equivalent stress contour plot of all of the Inconel 718 components. Several Inconel 718 components exceeded their allowable values. Figure 40 shows the equivalent stress contour plot of the back plate and nuts. The peak stress in these components was below the allowable. The connecting rod and pins had localized areas of high stress as shown in Figure 41. Figure 42 shows the stresses in the tile rail. Figure 43 shows the stresses in the connecting rods. A sub model of these the connecting pin and rod location was created to address these high stresses. The high stresses in the tile rail are due to thermal effects and are considered secondary stresses which are below the allowable.

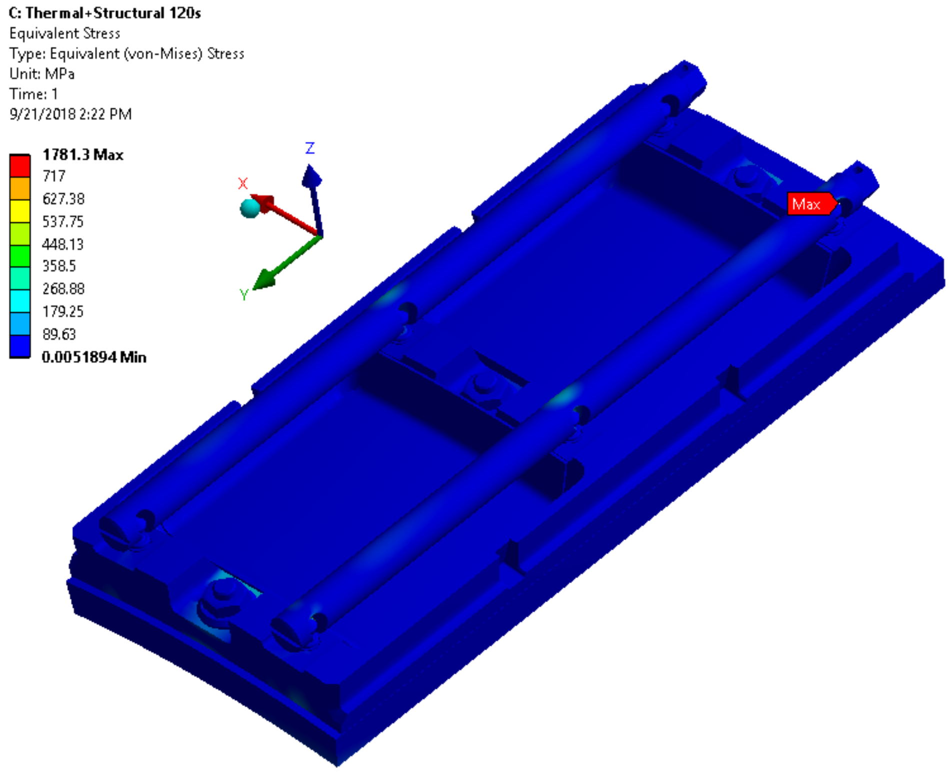

Figure 92: Equivalent stress contour plot of Inconel 718 components for case 1, profile 1 at 120 seconds.

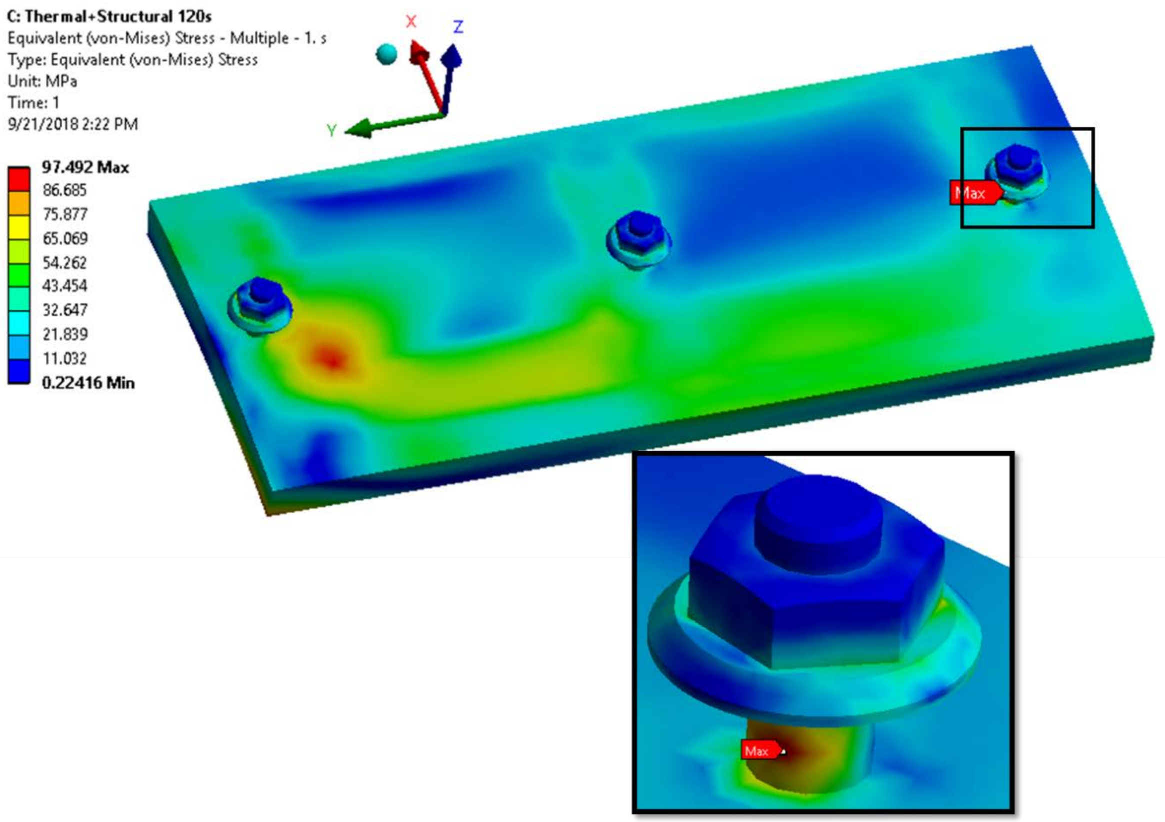

Figure 93: Back plate and nuts equivalent stress contour plot for case 1, profile 1 at 120 seconds.

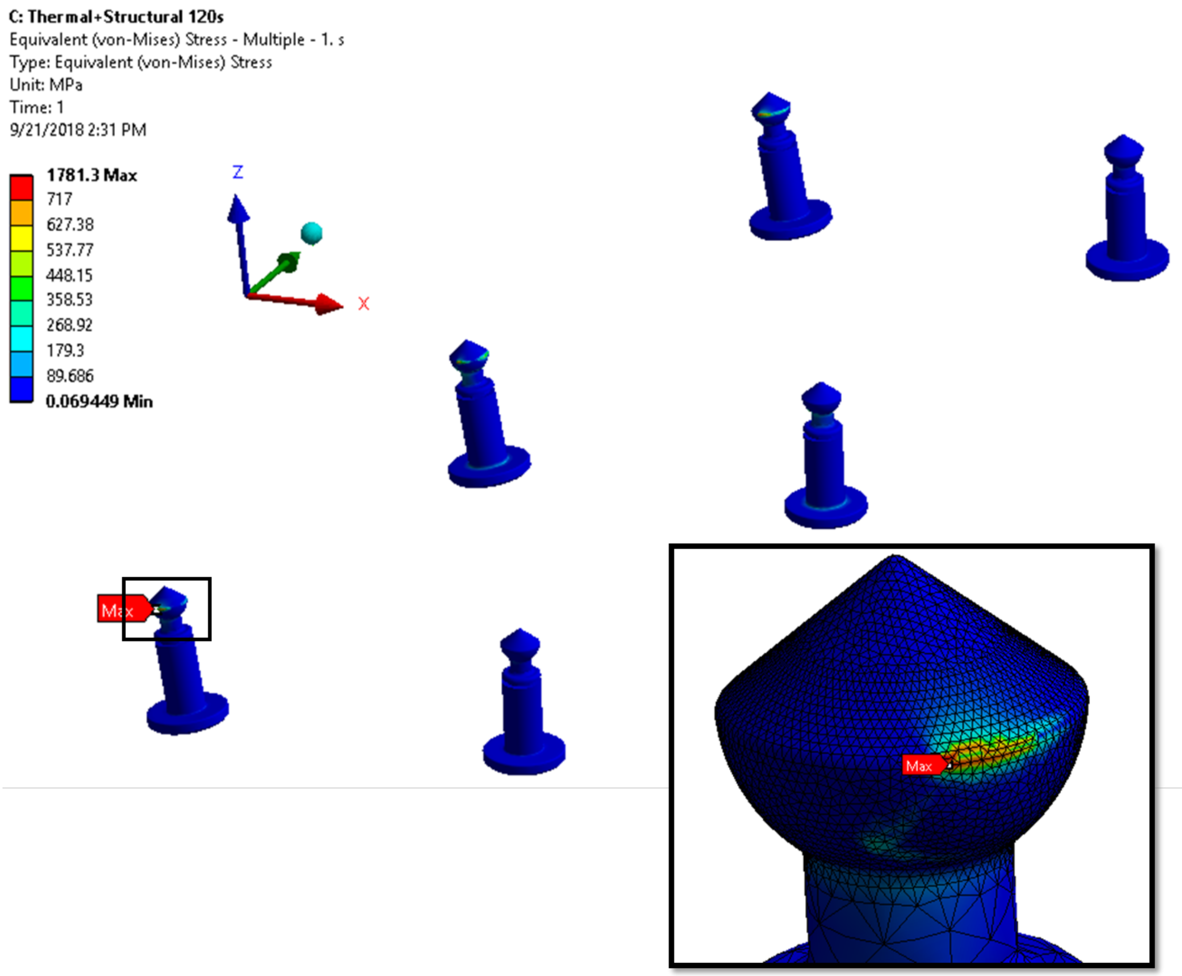

Figure 94: Connecting rod pin equivalent stress contour plot for case 1, profile 1 at 120 seconds.

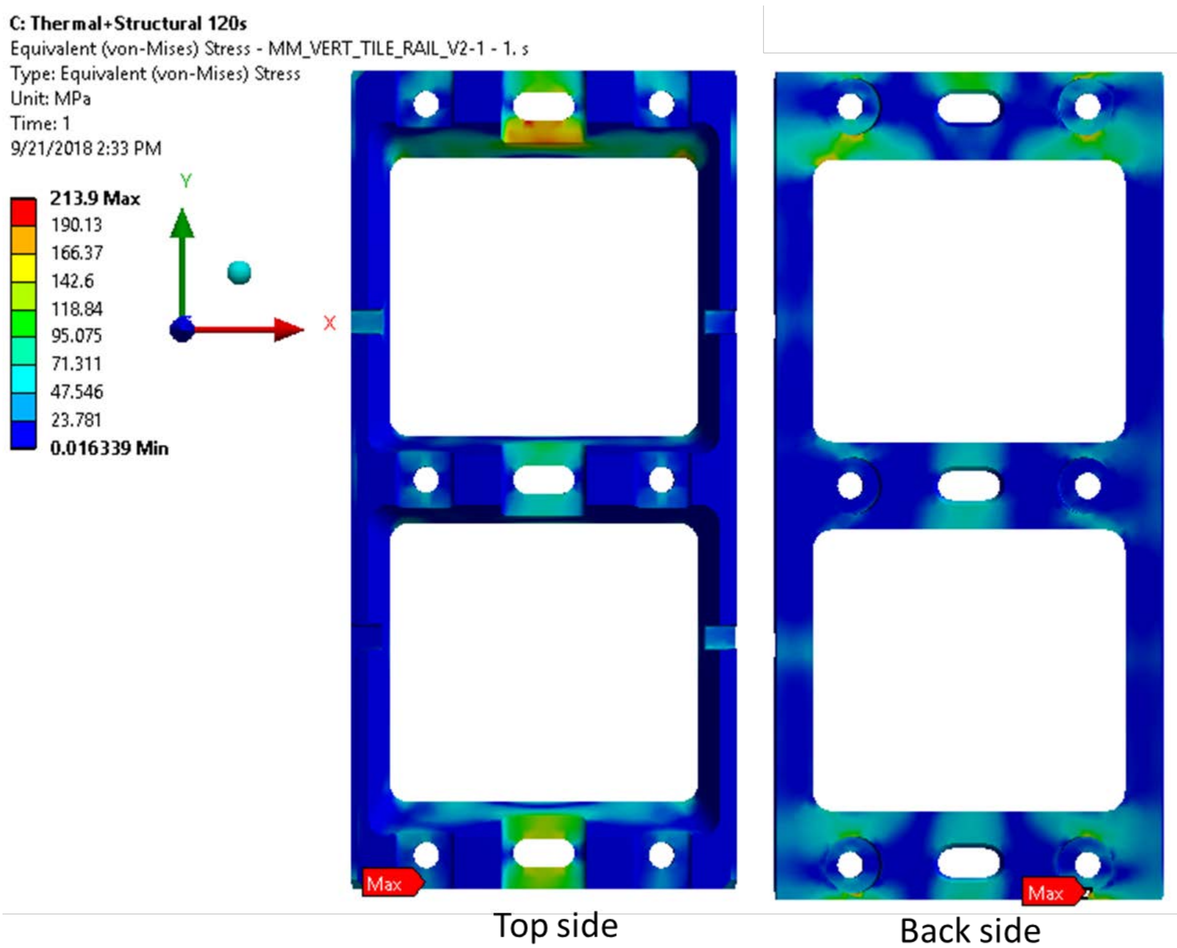

Figure 95: Tile rail equivalent stress for case 1, profile 1 at 120 seconds.

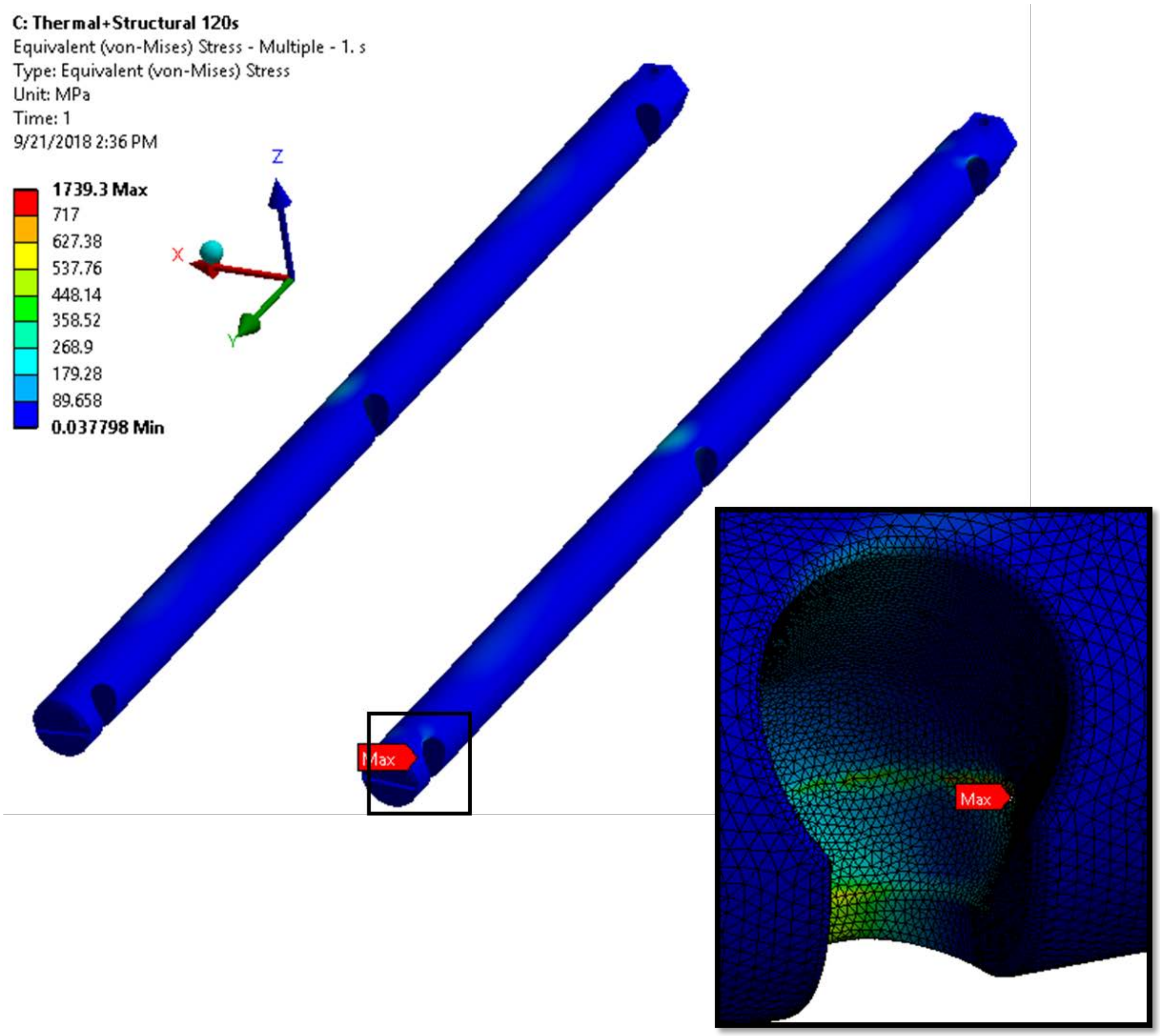

Figure 96: Equivalent stress plot of the connection rods for case 1, profile 1 at 120 seconds.

Case 3 at 1 second

The deformation contour plots in the radial, circumferential, and axial directions of the assembly as a result of the loads is shown in Figure 34, Figure 35, and Figure 36.

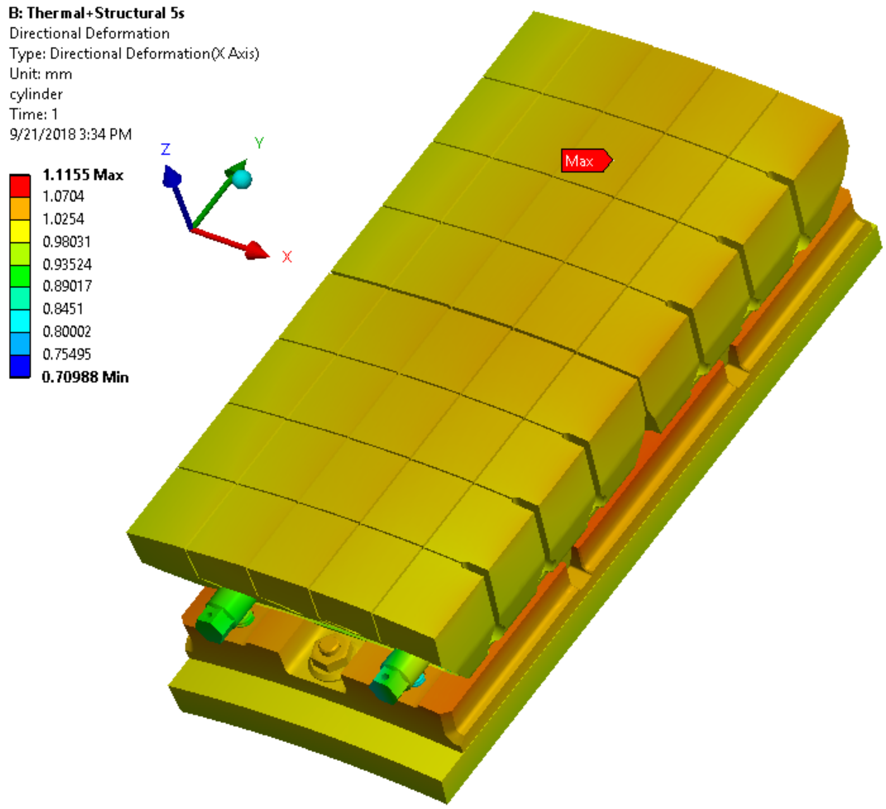

Figure 97: Radial deformation for case 3 at 1 second.

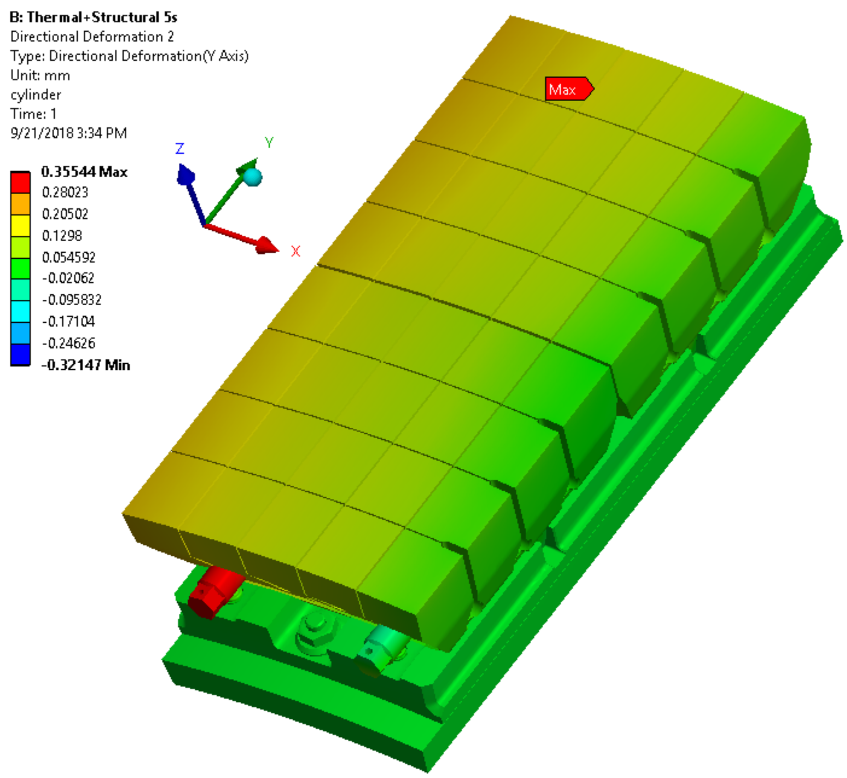

Figure 98: Circumferential deformation for case 3 at 1 second.

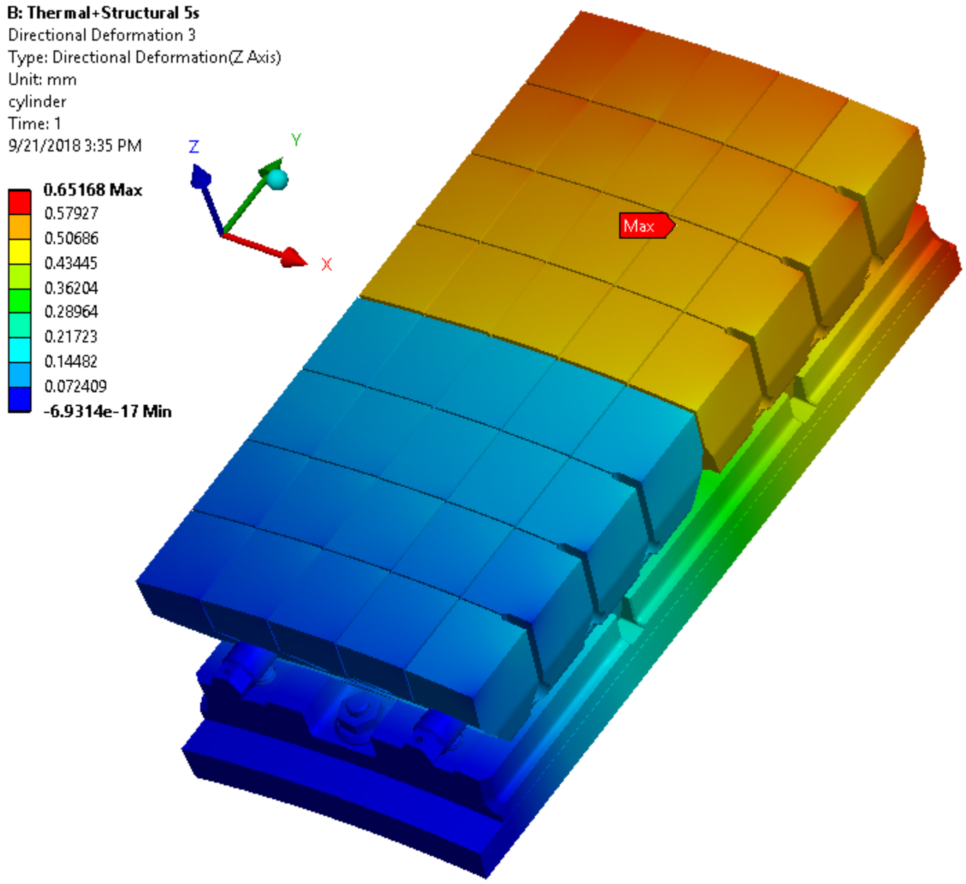

Figure 99: Axial deformation for case 3 at 1 second.

All results presented in the tables below are from case 3 at 1 second. Table 14 and Table 15 list the peak maximum and minimum principal stress and the corresponding allowable in the components made of graphite tiles and grafoil gaskets. Table 16 lists the peak equivalent stresses in the Inconel 718 components.

Table 30: Maximum Principal Stress of tiles and grafoil gaskets

Component	Peak Stress (MPa)	Allowable (MPa)	Loads
Graphite Tiles row 3	12.37	19	BPL+Halo+Eddy
Graphite Tiles row 4	12.10	19	BPL+Halo+Eddy
Grafoil Gasket	5.80	25	BPL+Halo+Eddy

Table 31: Minimum Principal Stress of tiles grafoil gaskets

Component	Peak Stress (MPa)	Allowable (MPa)	Loads
Graphite Tiles row 3	-92.31	-65	BPL+Halo+Eddy
Graphite Tiles row 4	-92.76	-65	BPL+Halo+Eddy
Grafoil Gasket	-6.74	-55	BPL+Halo+Eddy

Table 32: Equivalent Stress in Inconel 718 components

Component	Peak Stress (MPa)	Allowable (MPa)	Loads
Back Plate with integrated studs	56.48	717	BPL+Halo+Eddy
Vertical Tile Rail	63.31	717	BPL+Halo+Eddy
Connecting rods	1,733	717	BPL+Halo+Eddy
Connecting pins	1,994	717	BPL+Halo+Eddy
Nuts (150258)	56.48	717	BPL+Halo+Eddy

The grafoil gaskets resulted in stresses below their allowable values. The resulting maximum principal stresses in the tiles were below the allowable. However, the resulting minimum principal stress in the tiles exceeded the allowable. Figure 47 shows the minimum stress contour plot of the graphite tiles. Figure 48 shows the minimum stress contour plot of the grafoil gaskets.

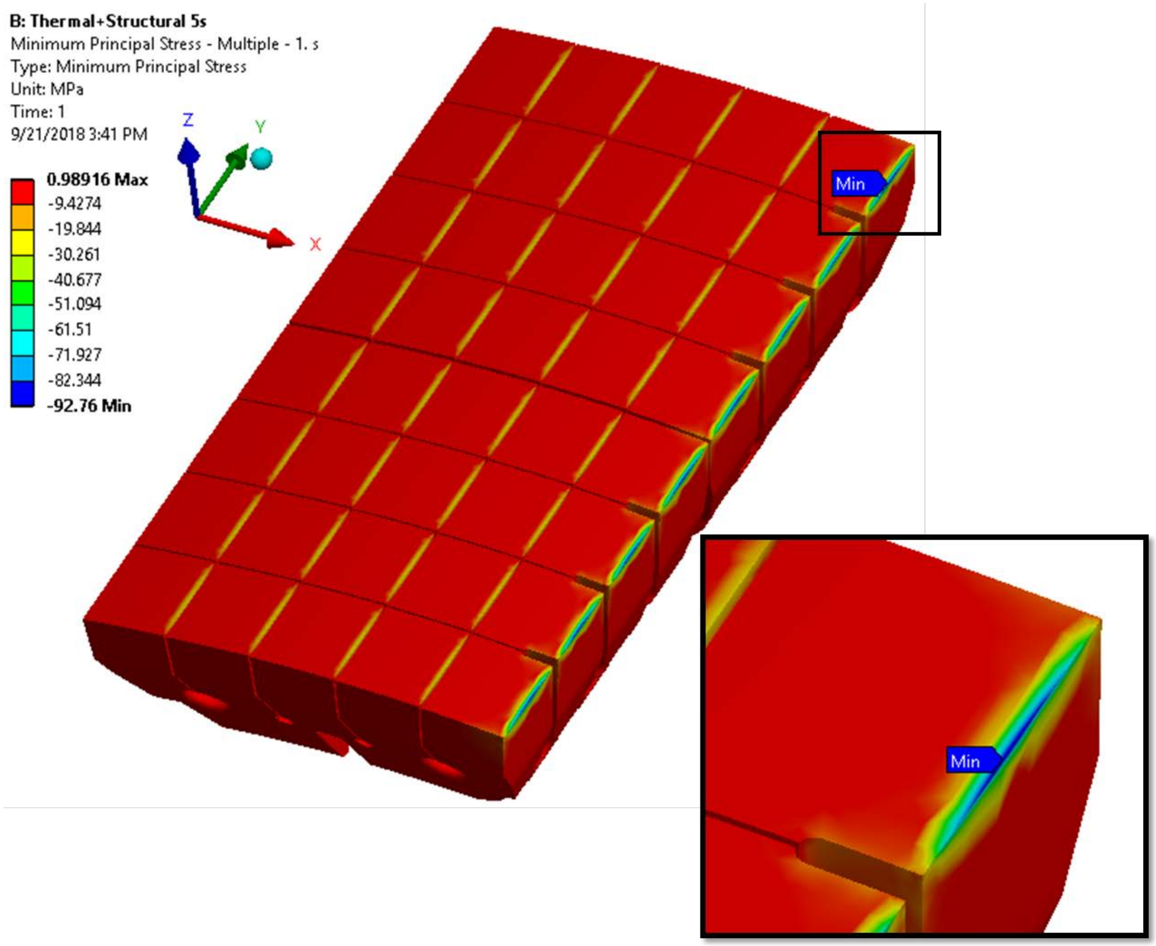

Figure 100: Minimum principal stresses in graphite tiles for case 3 at 1 second.

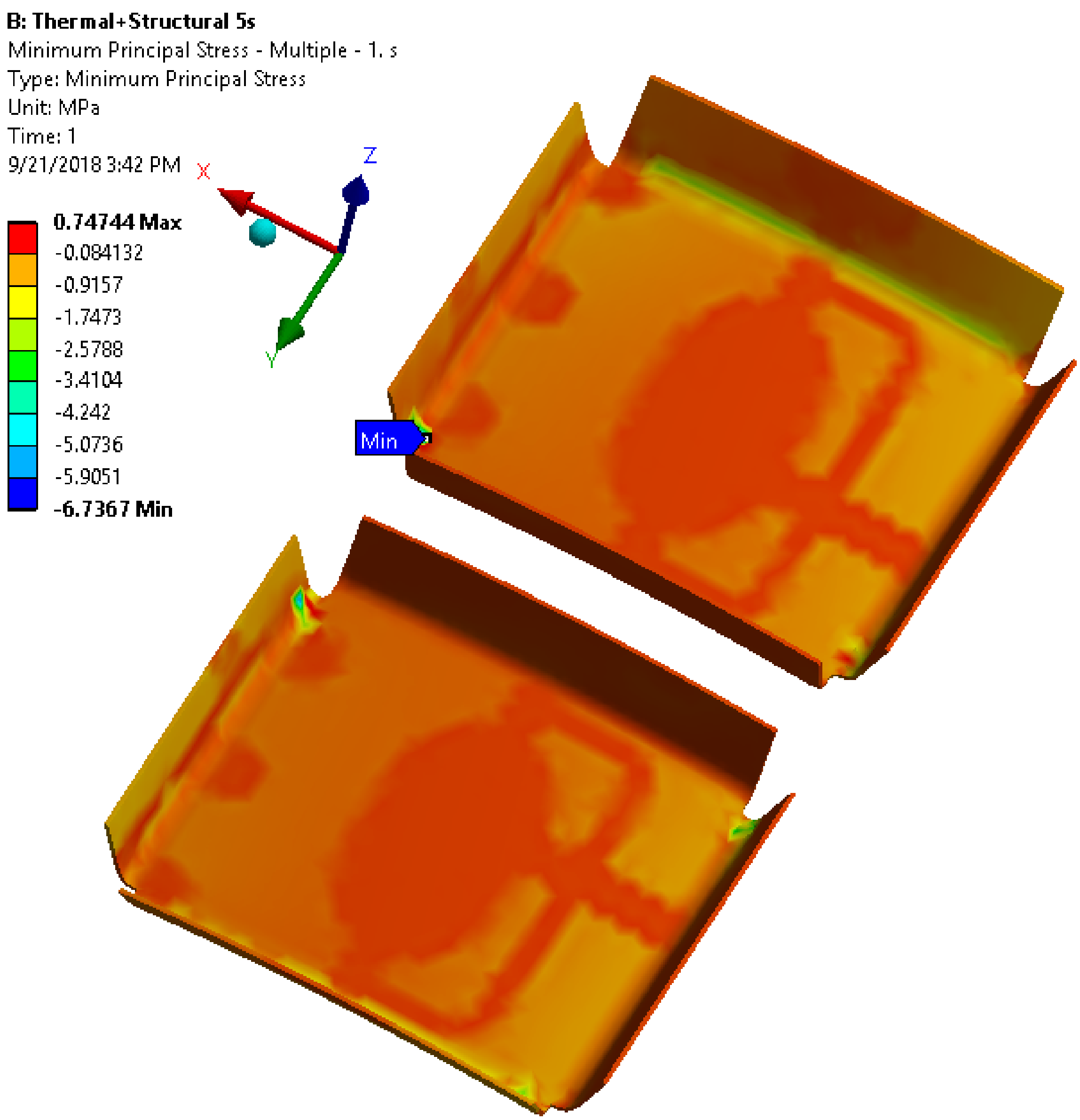

Figure 101: Minimum principal stresses in the grafoil gaskets for case 3 at 1 second.

Figure 49 shows the equivalent stress contour plot of all of the Inconel 718 components. Several Inconel 718 components exceeded their allowable values. Figure 50 shows the equivalent stress contour plot of the back plate and nuts. Figure 51 shows the equivalent stresses in the tile rail. The peak stress in these components was below the allowable. The connecting rod pins had localized areas of high stress as shown in Figure 52. Figure 53 shows the stresses in the connecting rods. These high stresses are addressed in a sub-model analysis of just the connecting pin and rod.

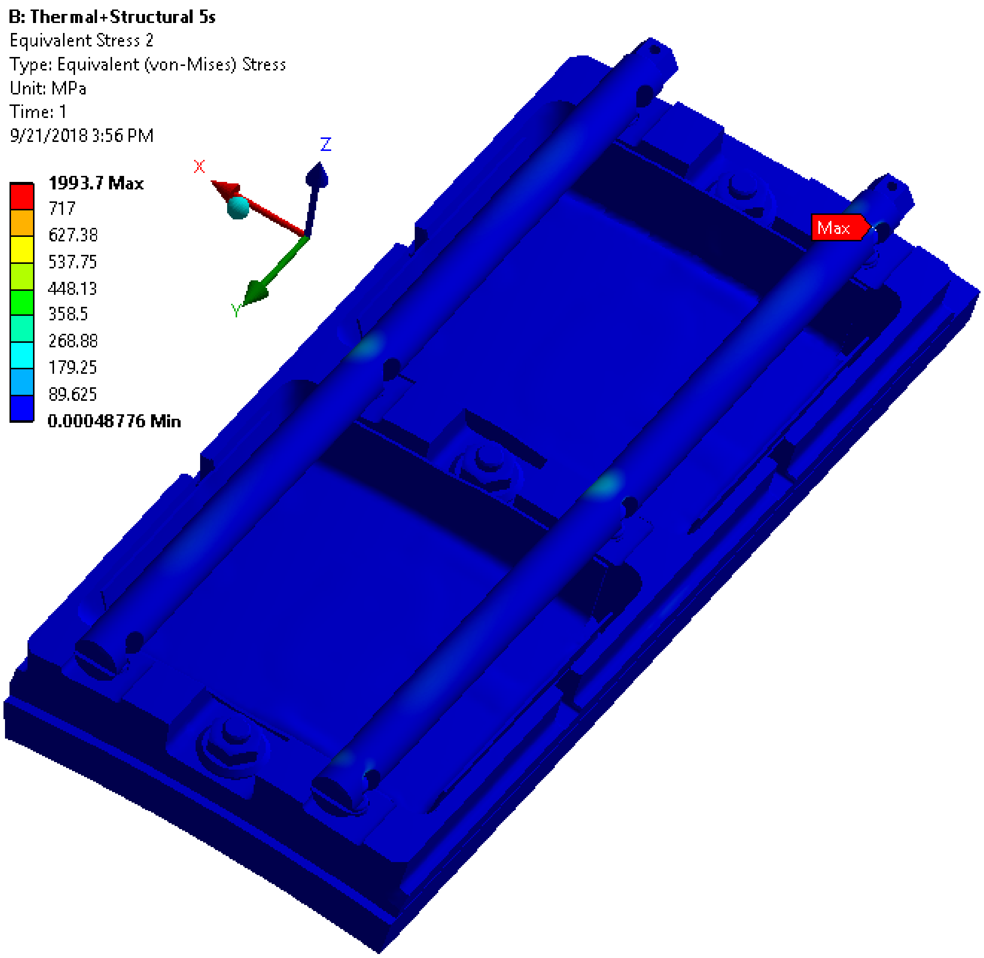

Figure 102: Equivalent stress contour plot of Inconel 718 components for case 3 at 1 second.

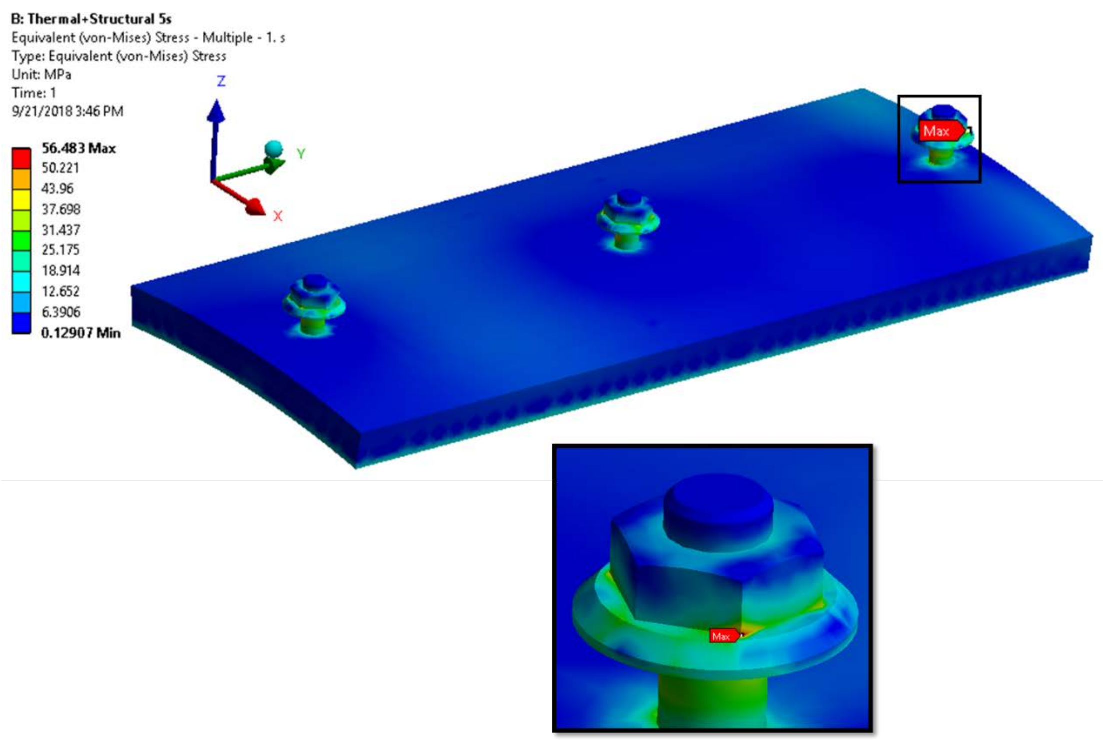

Figure 103: Back plate and nuts equivalent stress contour plot for case 3 at 1 second.

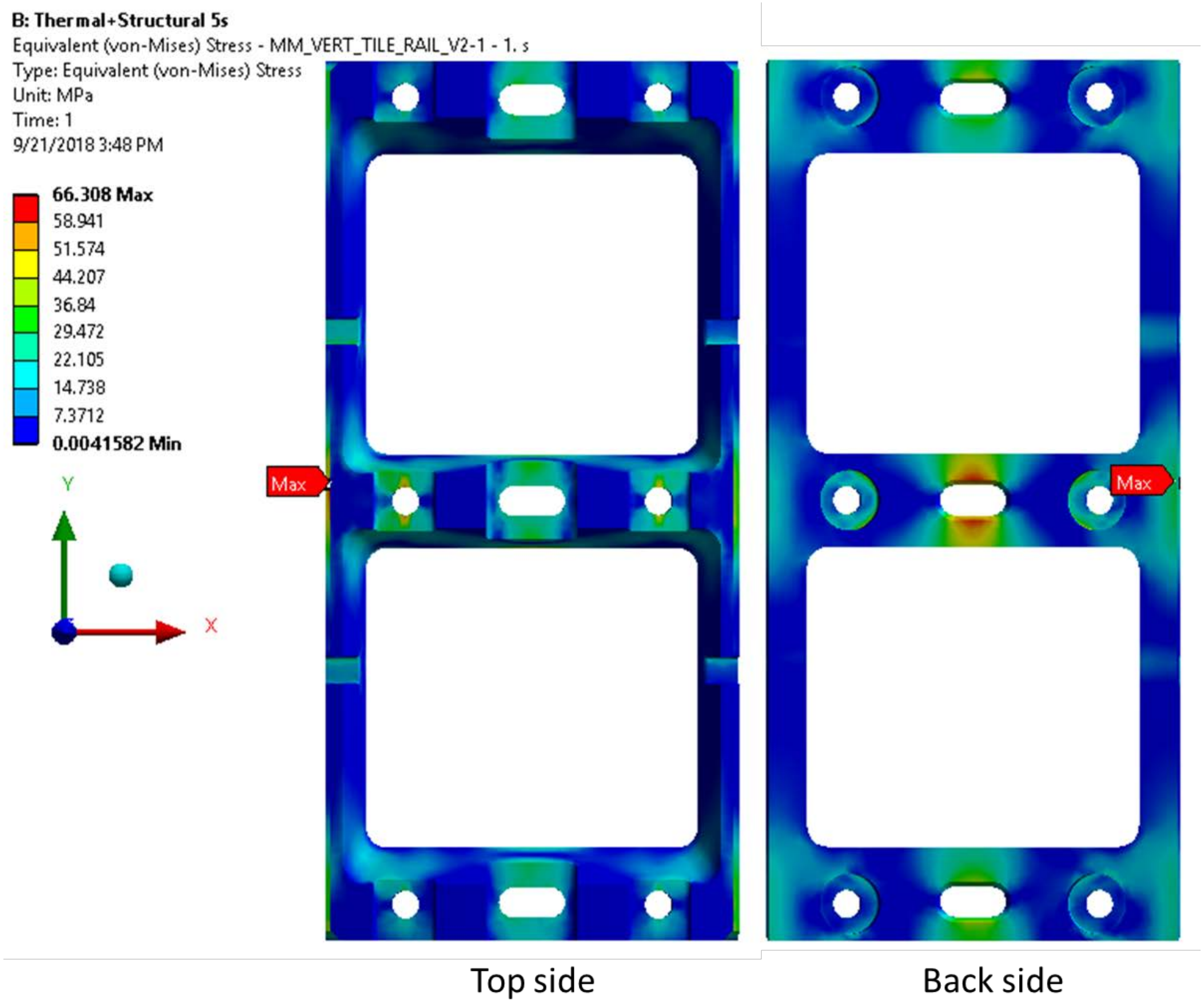

Figure 104: Tile rail equivalent stress for case 3 at 1 second.

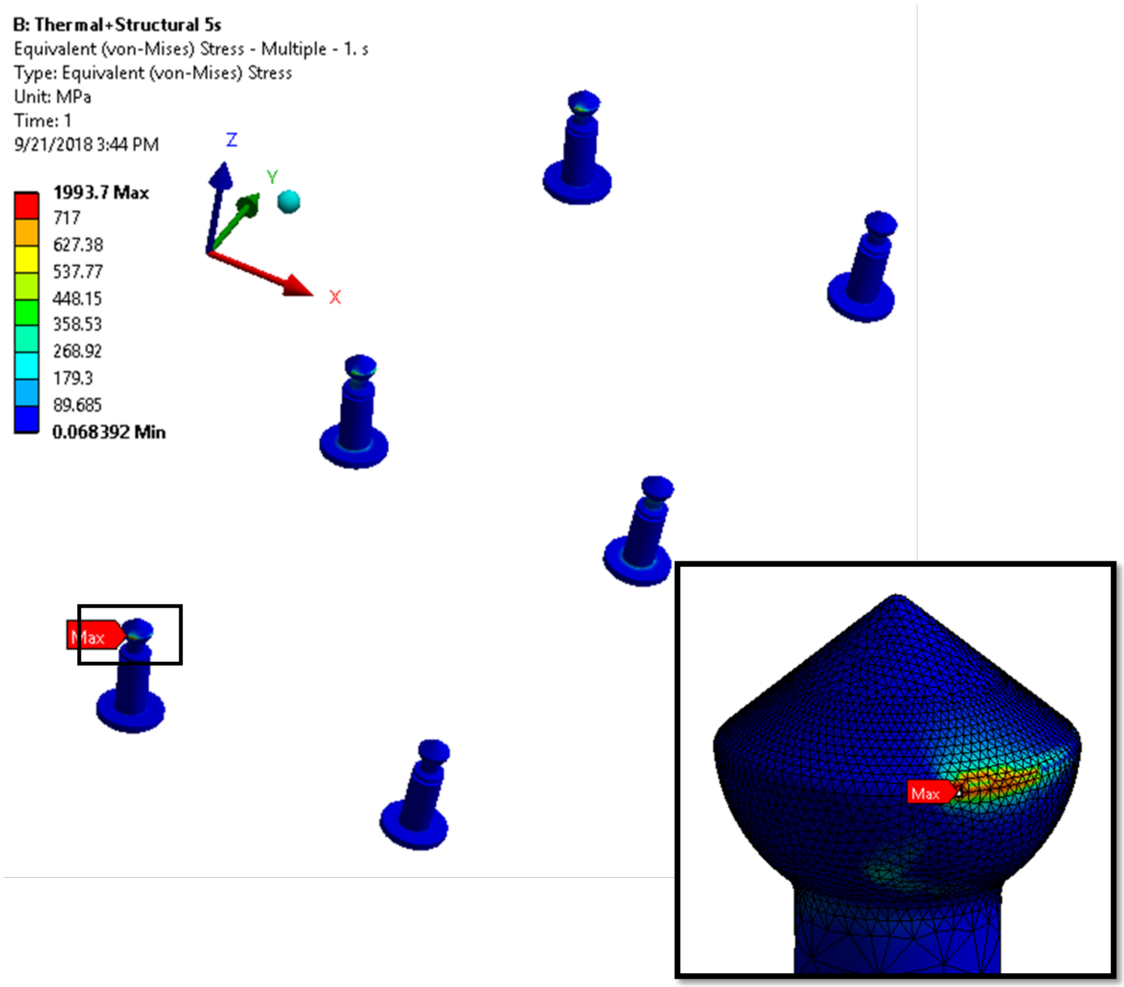

Figure 105: Connecting rod pin equivalent stress contour plot for case 3 at 1 second.

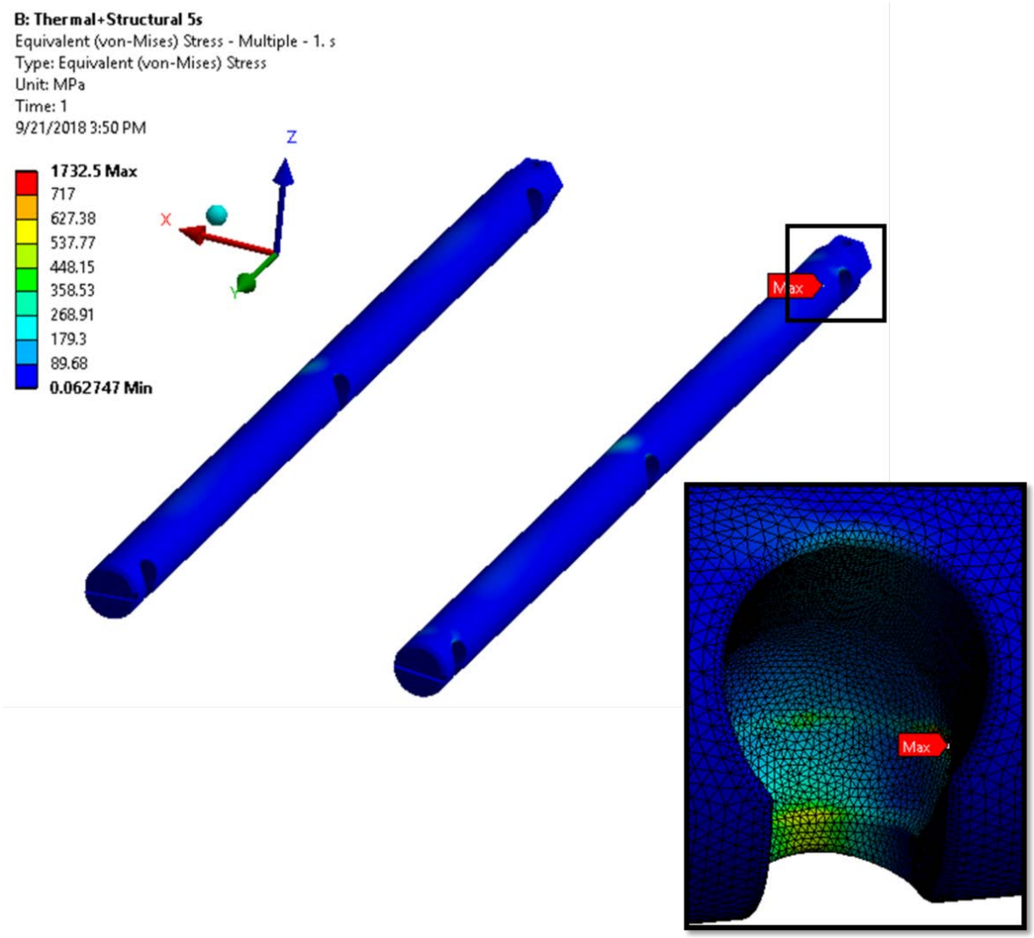

Figure 106: Equivalent stress plot of the connection rods for case 3 at 1 second.

Analysis of Inboard Diverter Vertical (IBDV) high heat flux Base tile with POCO Graphite Properties

ORNL

The ANSYS Workbench project diagram is shown in Figure 1. It included a static analysis of preload, halo, and eddy current forces without the thermal load. Two thermal loading conditions were applied to the tile. Finally, all loads were combined.

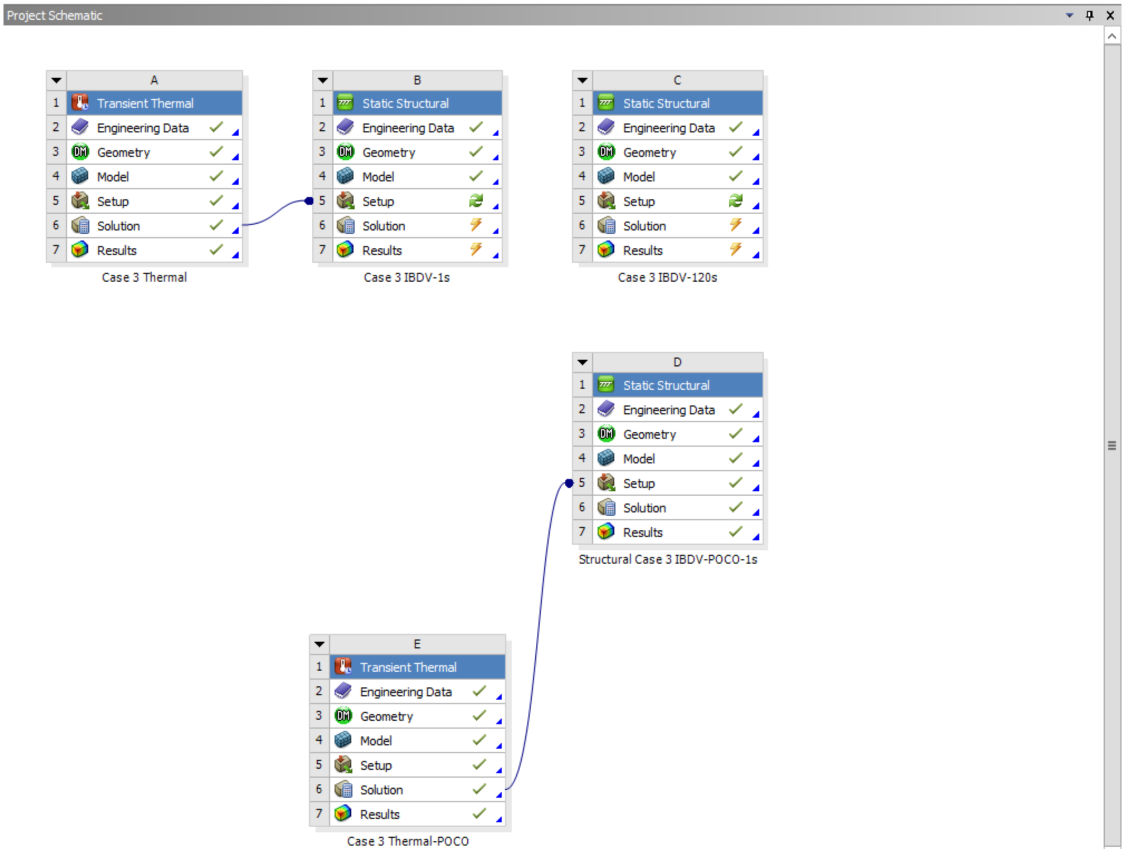

Figure 107: Workbench Schematic of IBDV Analysis.

The components considered in the analysis are listed below in Figure 2 and Figure 3.

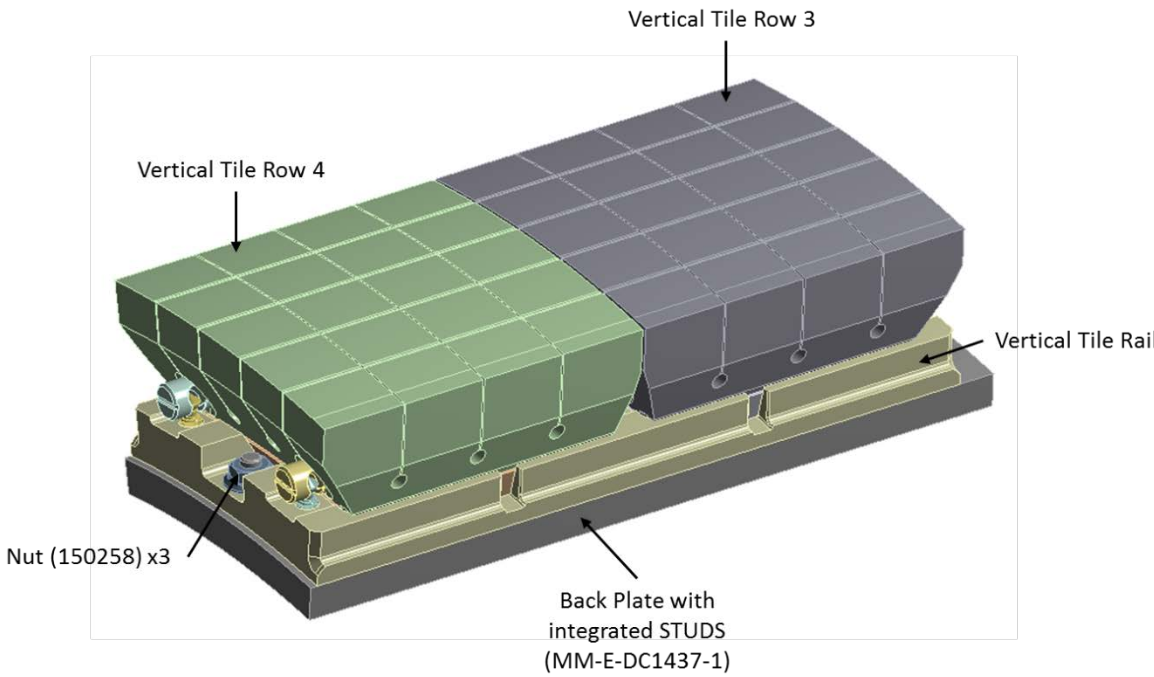

Figure 108: Inboard Diverter Vertical Tile Base Tile Assembly

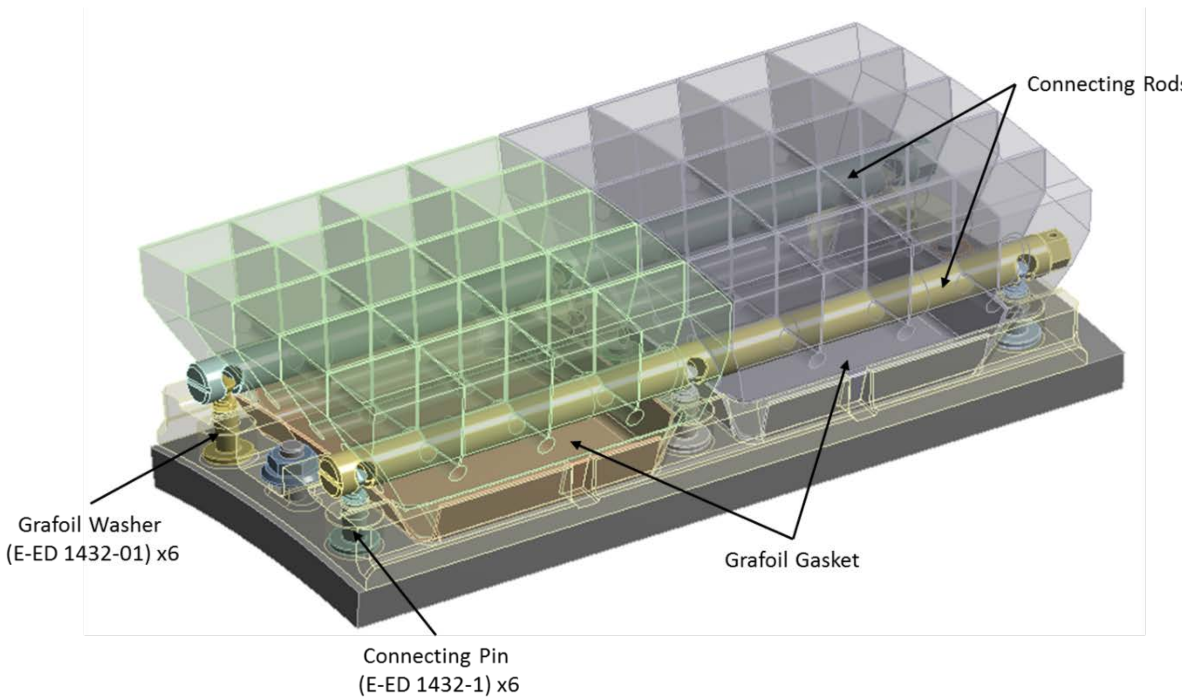

Figure 109: Inboard Diverter Vertical Tile Base Tile Assembly.

The mesh consisted of high order tetrahedrals. The total number of elements and nodes for the whole assembly is 1,494,898 and 2,470,378 respectively. The contact areas between the connecting rods and tiles had a refined mesh. The connecting pin heads also had a refined mesh where they contact the connecting rods. Figure 4 shows the mesh used in the analysis with and without the graphite tile. Figure 5 shows the refined mesh of the tile, connecting rod, and connecting pin contact areas.

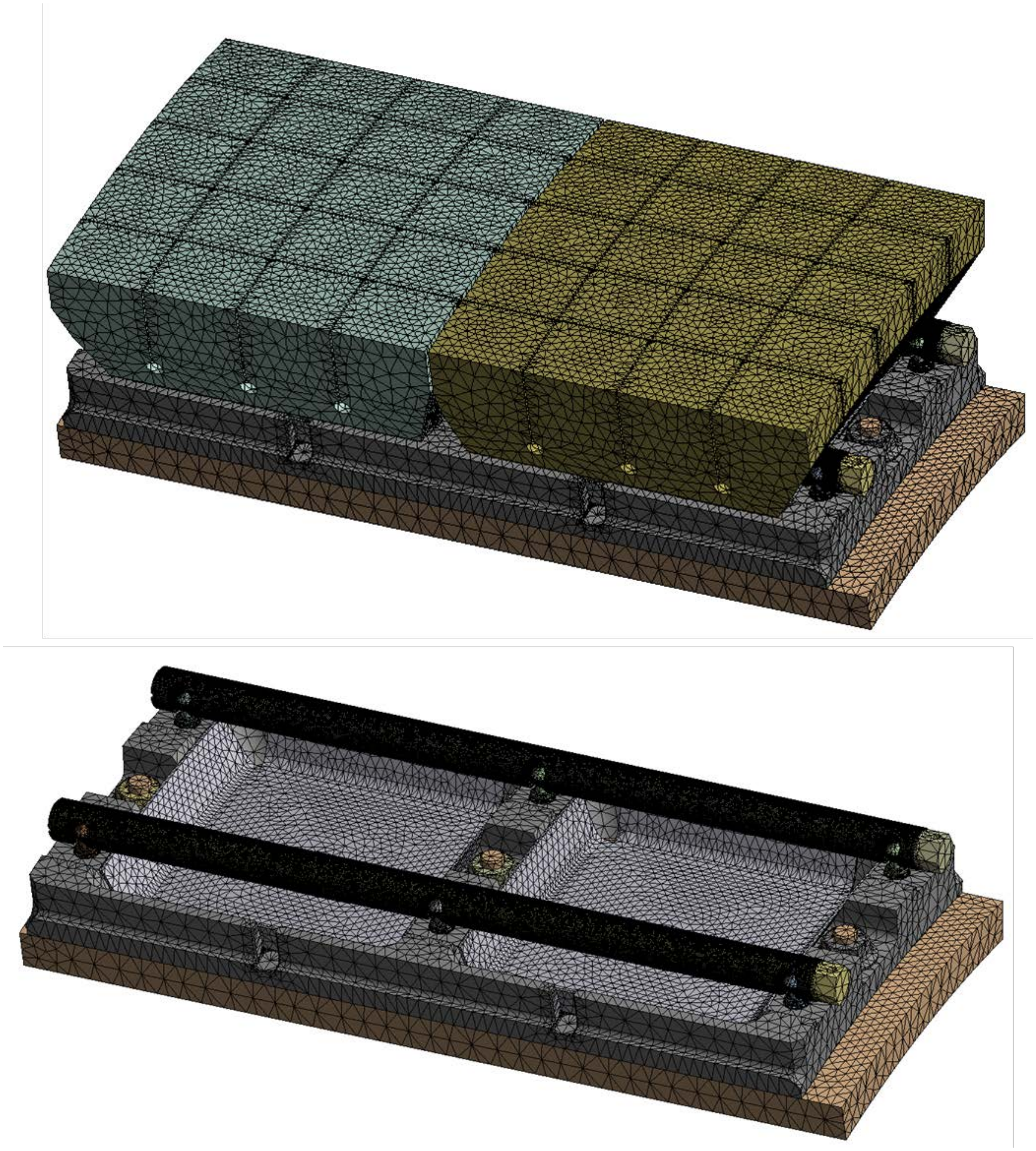

Figure 110: Mesh of the Inboard Diverter Tile Assembly with and without theTiles

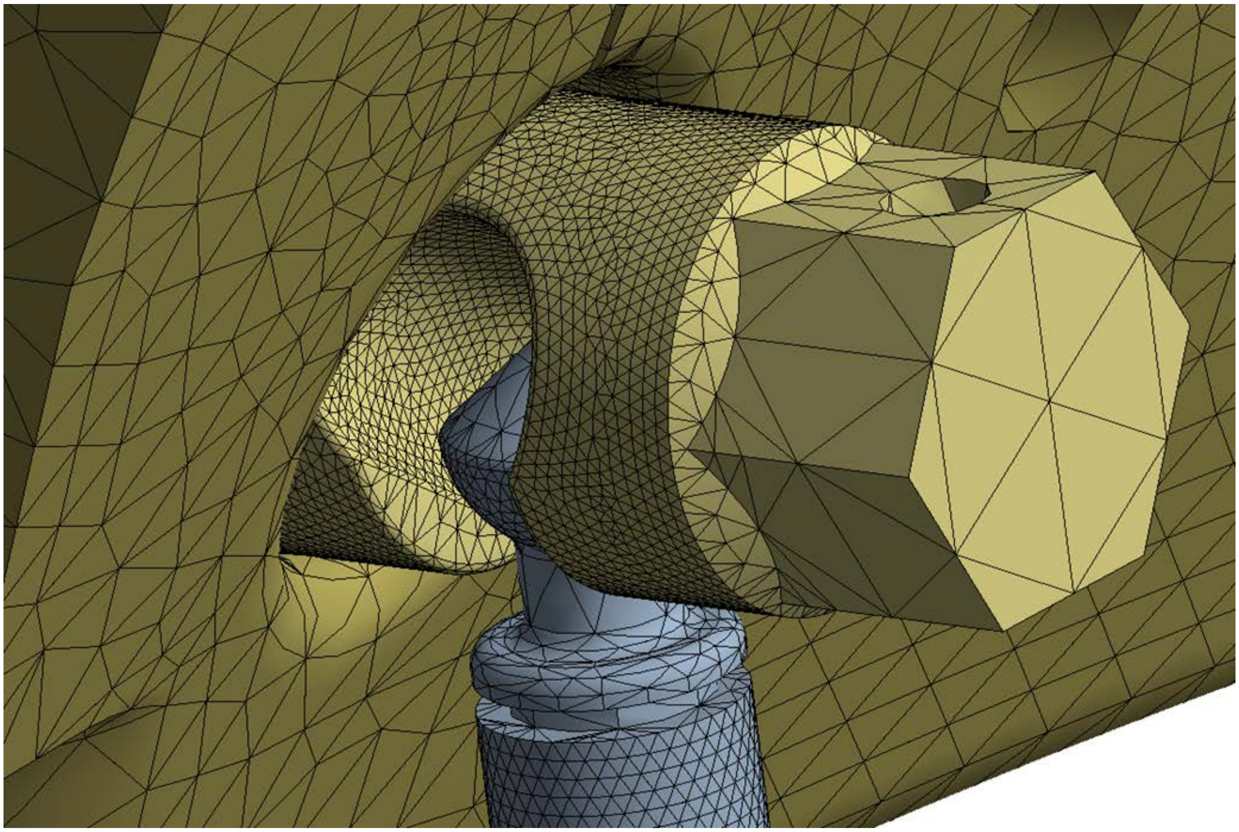

Figure 111: Refined mesh of the connecting rod, connecting pin and tile contact areas.

Table 1 lists each component of the assembly and its material.

Table 33: Components and their materials.

Component	Material
Graphite Tiles (row 3 and row 4)	POCO TM
Grafoil Gaskets and Washers	Grafoil
Back Plate with integrated studs	Inconel 718
Vertical Tile Rail	Inconel 718
Connecting rods	Inconel 718
Connecting pins	Inconel 718
Nuts (150258)	Inconel 718

Thermal Analysis

Case 3 consisted of a uniform heat flux of 57.29 MW/m^2 applied to specific areas on both tiles for 1 second followed by a 120 s cooldown. The heat flux for case 3 is only applied to a small area on the upper side of the castellations. Helium cooling using 25 C helium in the baseplate was assumed with a convective heat transfer coefficient of 300 W/m^{2}K. Radiation was included for the top tile surface only, since all other have no open view factor. The emissivity was 0.7 and the reference background temperature was 103.42 ^{o}C. The starting assembly temperature was assumed to be 192.36 ^{o}C. The heat flux profile for case 3 is shown in Figure 6. The radiation and convective surfaces are shown in Figure 7. Contact thermal conductance between all parts was 1000 W/m^2C.

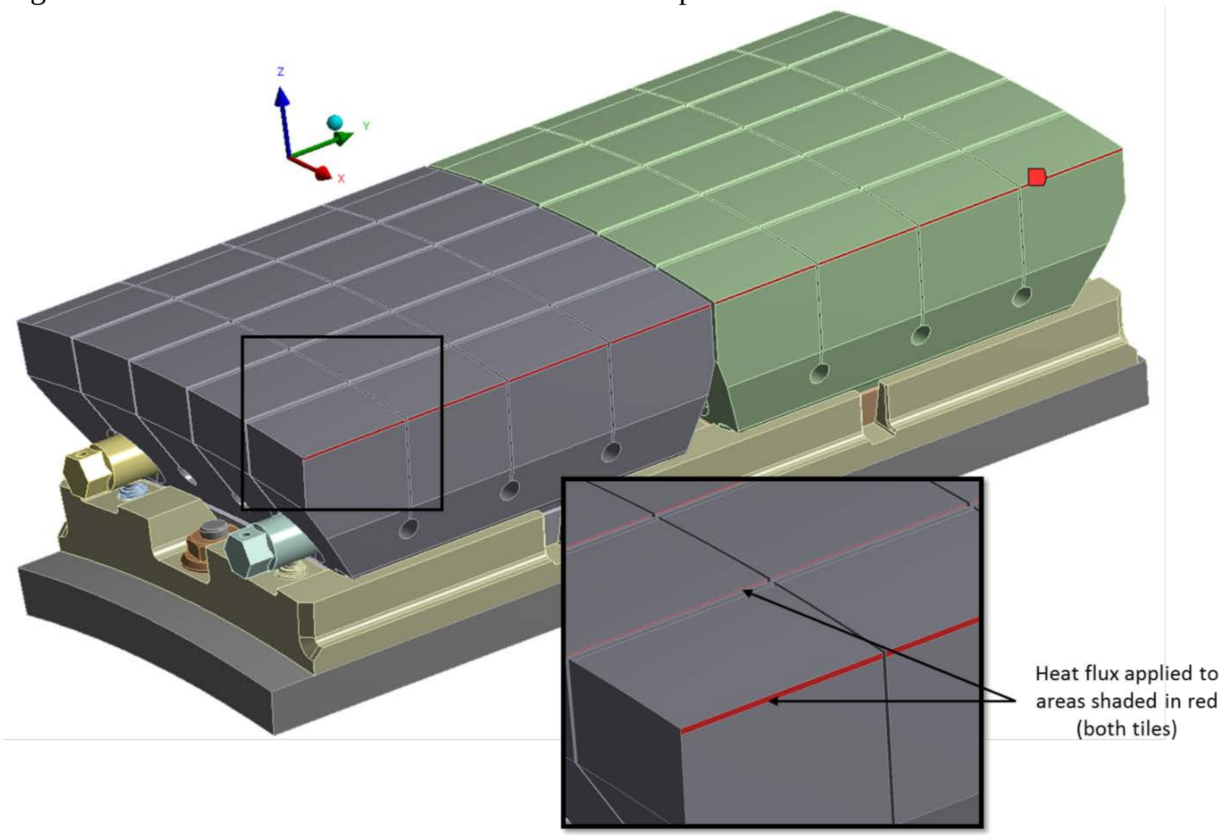

Figure 112: Case 3 heat flux profile

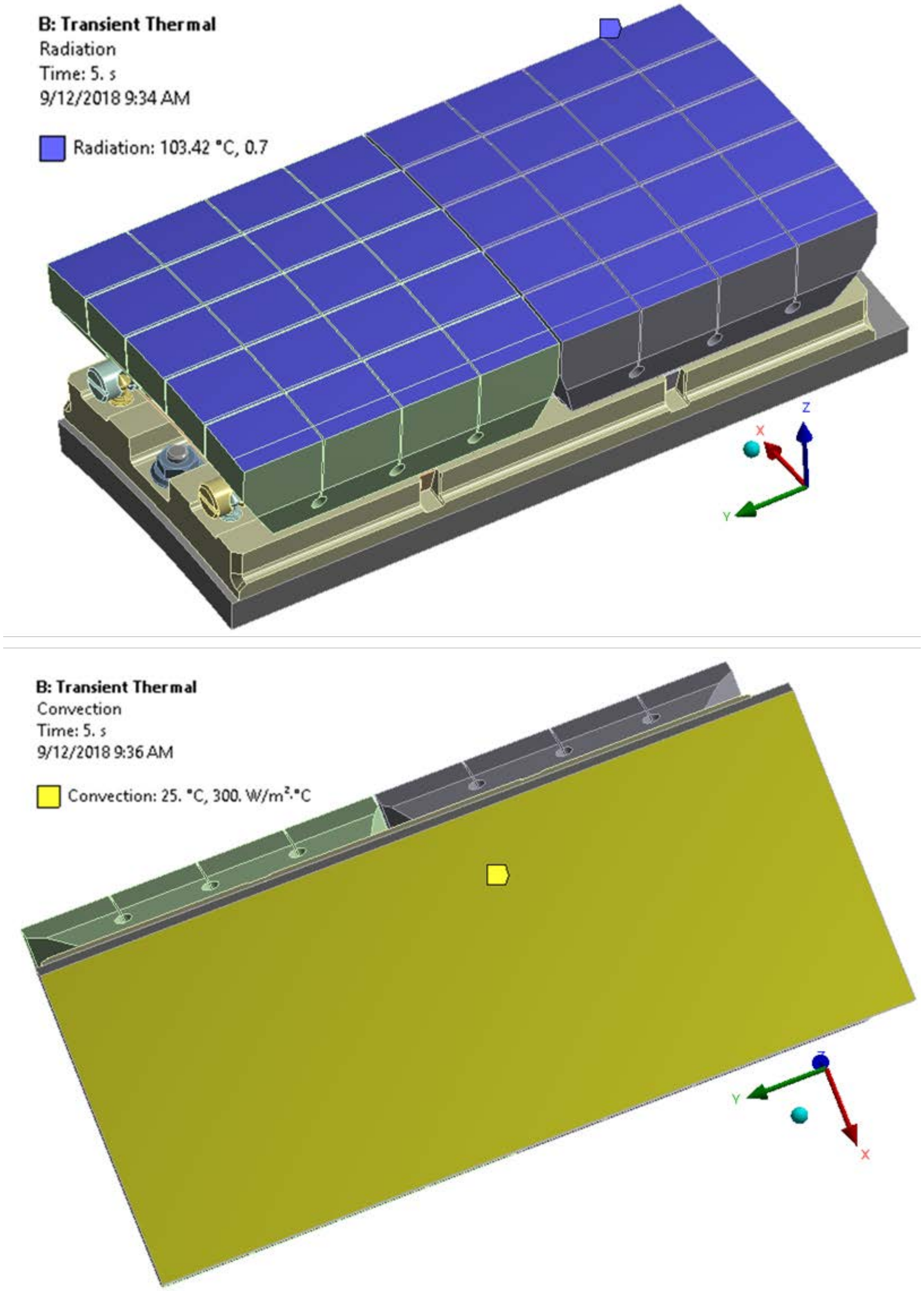

Figure 113: Radiation (top) and Convection (bottom) surfaces.

The peak temperature in the assembly was 1936 °C in the graphite tile for heat flux case 3. Figure 8 shows the temperature contour plot of the tile and substructure after 1 seconds of applied heat flux. Figure 9 shows temperature contour plot of the tiles and substructure after 120 s cooldown. Table 2 lists the peak temperature and corresponding time for each component for heat flux case 3.

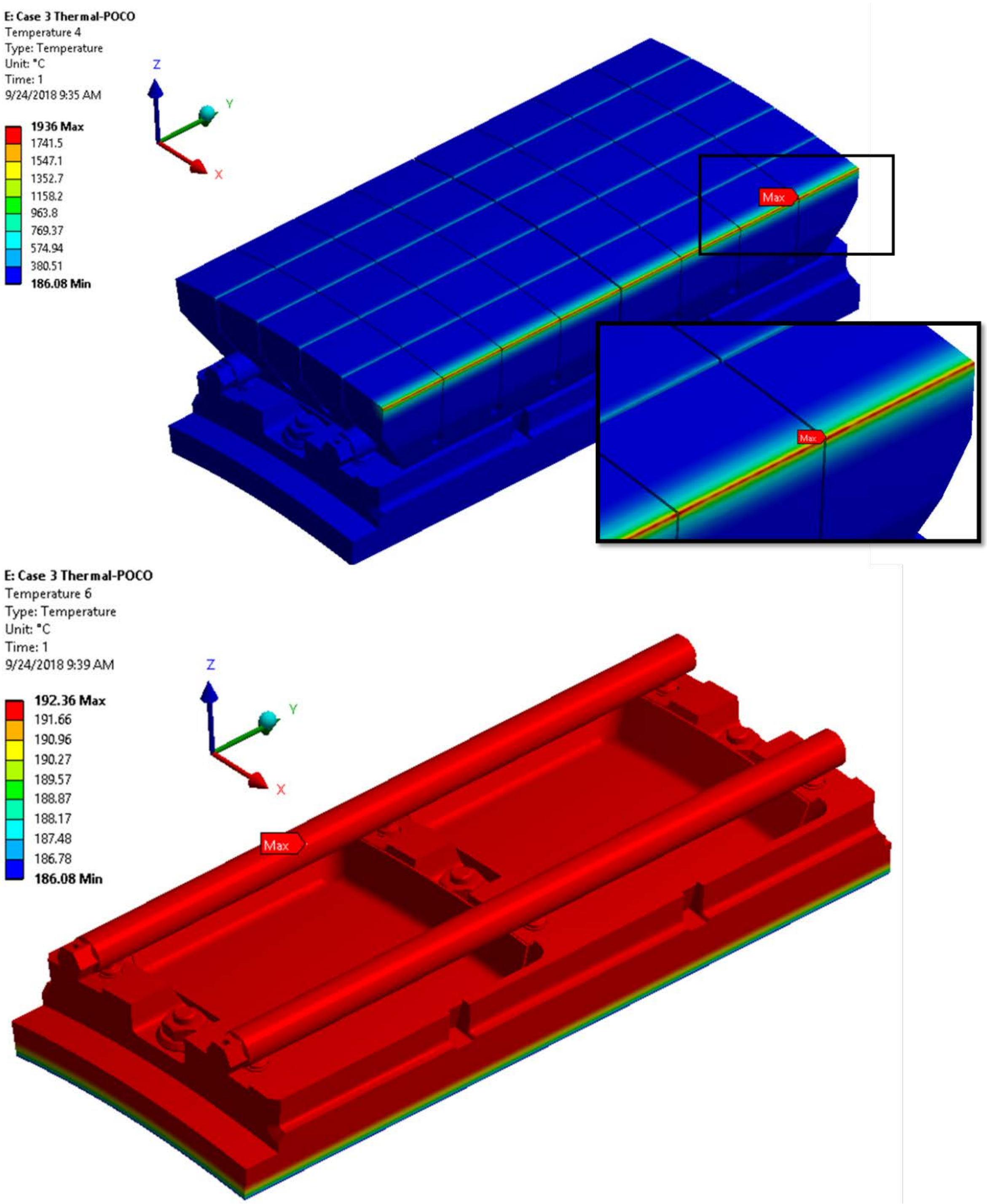

Figure 114: Temperature contour plot of the inboard diverter vertical tiles for heat flux case 3 at 1 seconds

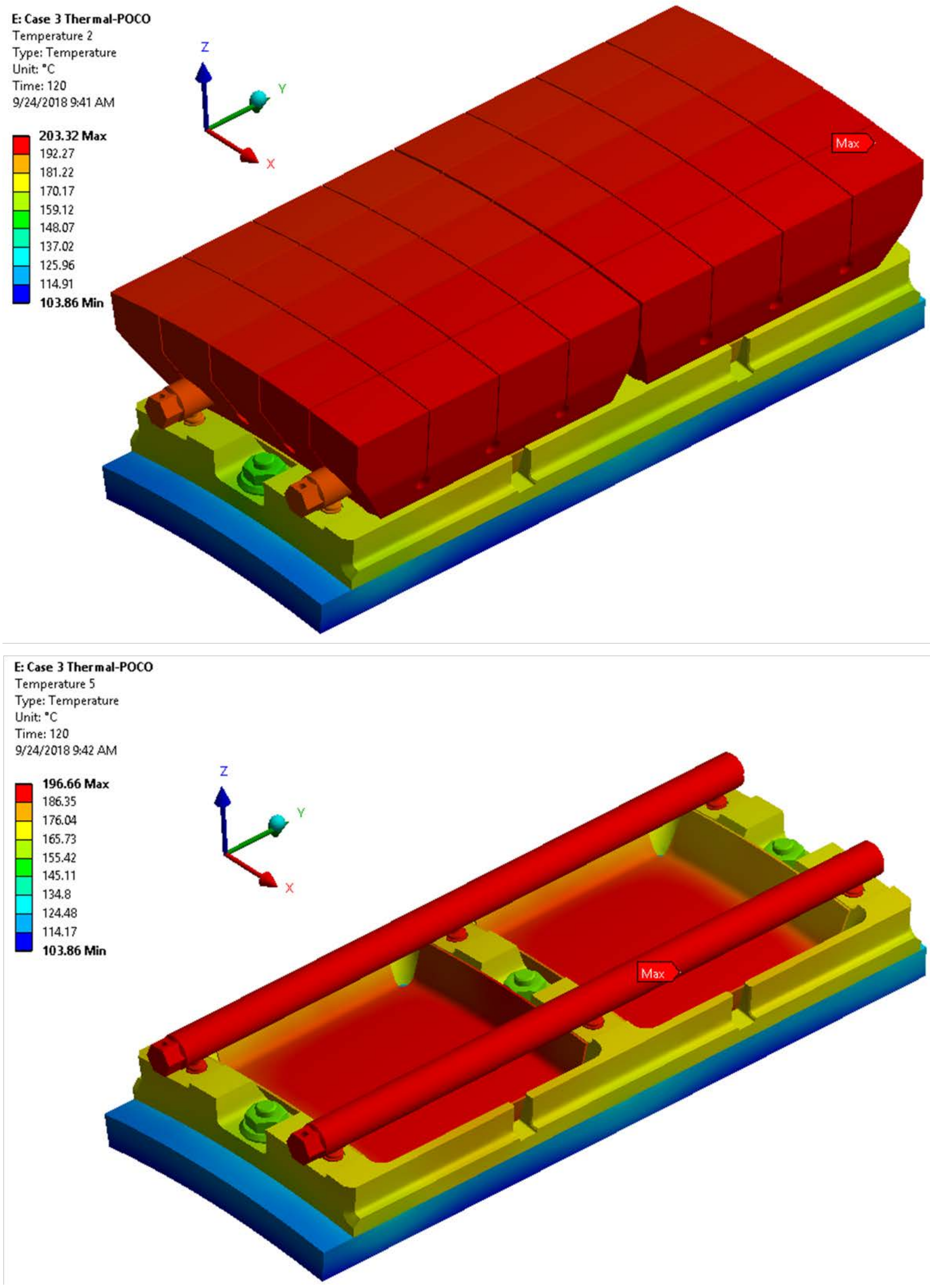

Figure 115: Temperature contour plot of the inboard diverter vertical tiles for heat flux case 3 at 120 seconds

Table 34: Peak temperatures for each component for heat flux case 3

Component	Peak Temperature (°C)	Time (sec)
Graphite Tiles (row 3 and row 4)	1936	1
Grafoil Gaskets and Washers	199	42
Back Plate with integrated studs	192	0
Vertical Tile Rail	193	18
Connecting rods	195	120
Connecting pins	192	0
Nuts (150258)	192	0

Structural-Thermal Analysis

The temperature profiles that resulted from the thermal analysis were imported into a static structure analysis that included bolt preload, eddy current forces, and halo forces. Bolt preload forces of 1000 N were applied to the tree bolts connecting the back plate to the tile rail. Equal and opposite forces were applied to the head of the pins and tile rail. 375 N of force was applied to the 4 outer pins and 750 N of force were applied to the center pins. Figure 10 shows a schematic of the bolt preload and pin loading used for the structural analysis.

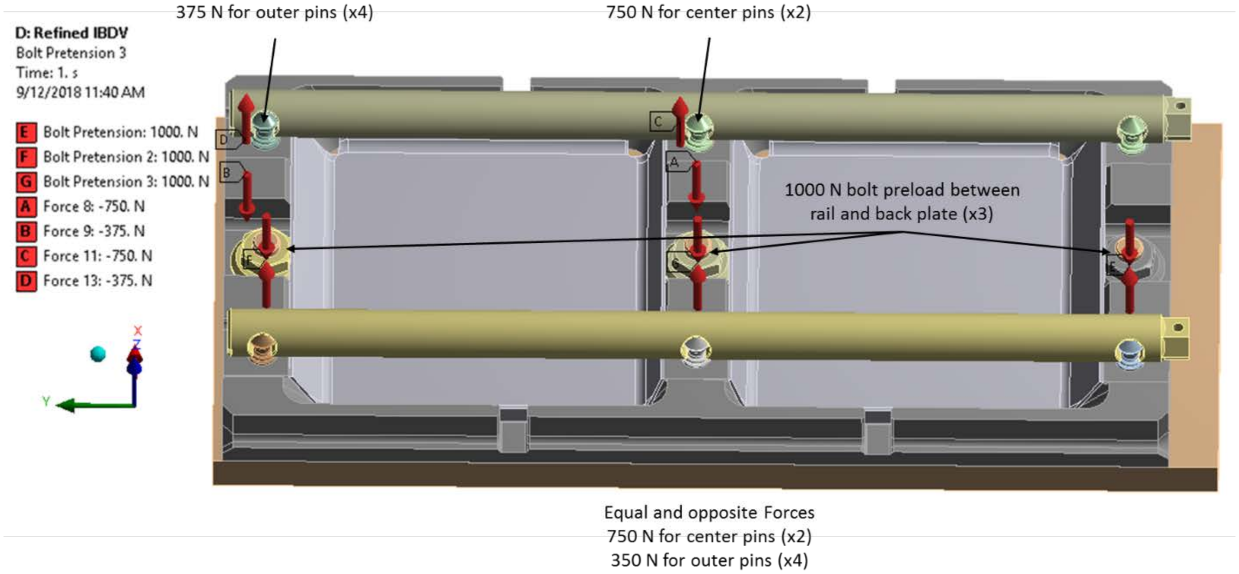

Figure 116: Bolt Preload and pin Loading.

Halo loads were applied to each tile. The row 4 tile halo load was applied in the positive axial and circumferential directions. The row 3 halo load was applied in the negative axial and positive circumferential directions. The loads were divided and applied to each node in each of the tiles. Figure 11 shows direction and magnitudes of the halo loads on the two tiles.

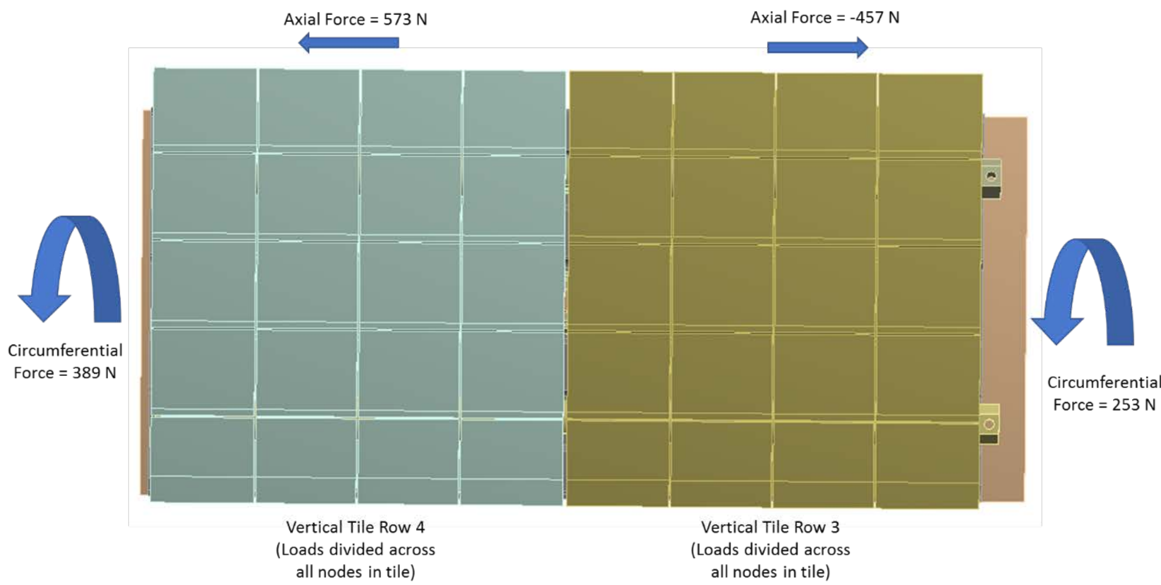

Figure 117: Halo forces applied to all nodes in each of the graphite tiles.

The eddy current loading was applied with equal and opposite loading in the radial direction on the sides of the tile creating moments. Figure 12 shows the surfaces and magnitudes of the eddy current forces applied to the tiles.

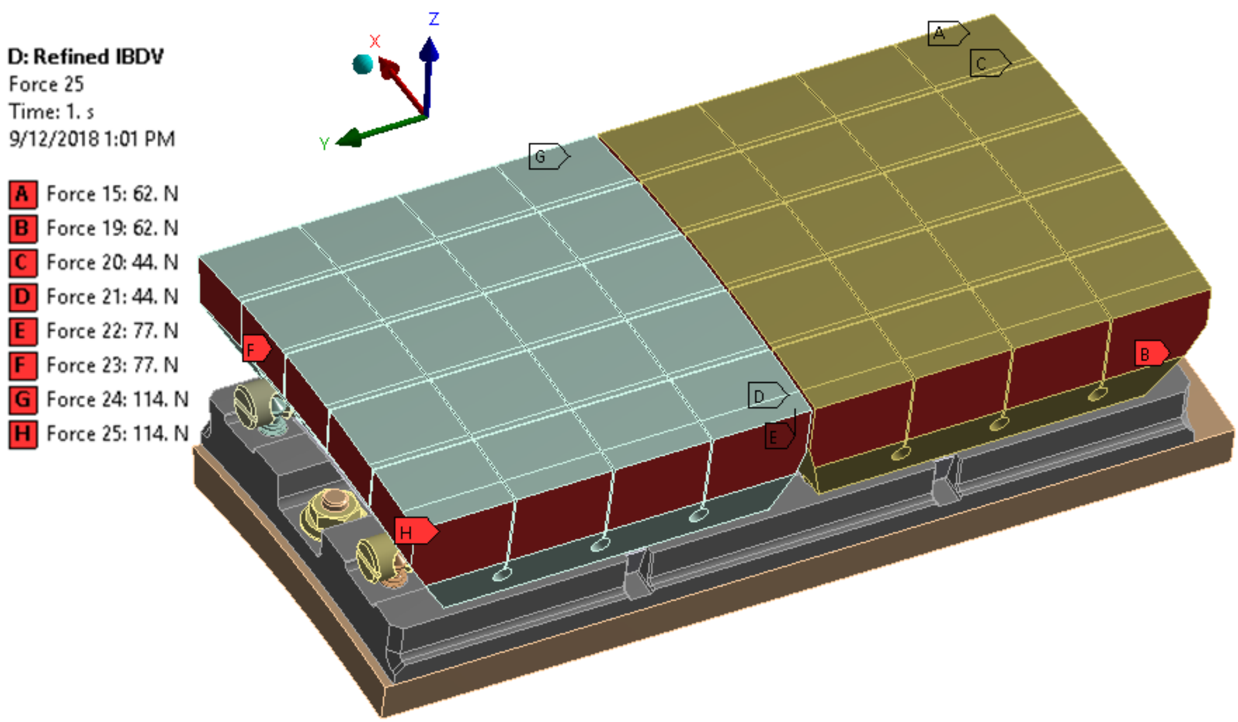

Figure 118 Eddy current loading in IBVD tiles

Fixed displacements were applied to the back plate and tile rail to constrain the model during the analysis. Circumferentially fixed displacements were placed on the sides of the back plate and tile rail. A fixed axial displacement was placed on the back plate

surface on the row 3 tile end of the assembly Figure 13 shows the location of these fixed displacements highlighted in yellow.

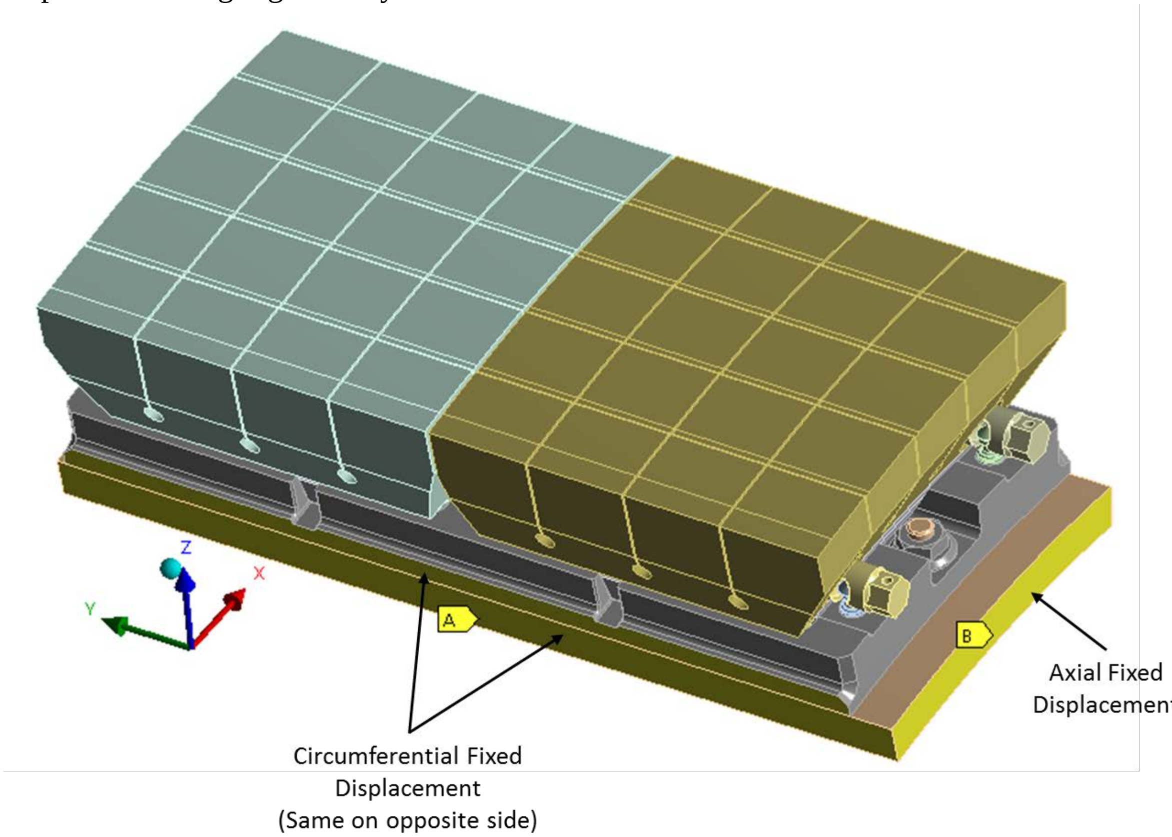

Figure 119: Fixed Displacement locations for IBDV Analysis.

The components of the assembly were connected through various forms of contact. A no separation contact was applied between the grafoil washers and the connecting rod pins as shown in Figure 14. Frictional contact with a coefficient of 0.3 was added between the nuts and tile rail connecting it to the back plate. Figure 15 shows the location of contact between the nuts and tile rail. Finally, the remaining contact between the components was assumed to be frictional with a coefficient of 0.1. This contact is between the following:

1) Tiles and gasket grafoil.
2) Tiles and connecting rods.
3) Connecting rod pins to connecting rods.
4) Tile rail and gasket grafoil.
5) Tile rail and back plate.

Figure 16 shows the locations of the remaining contact in the assembly.

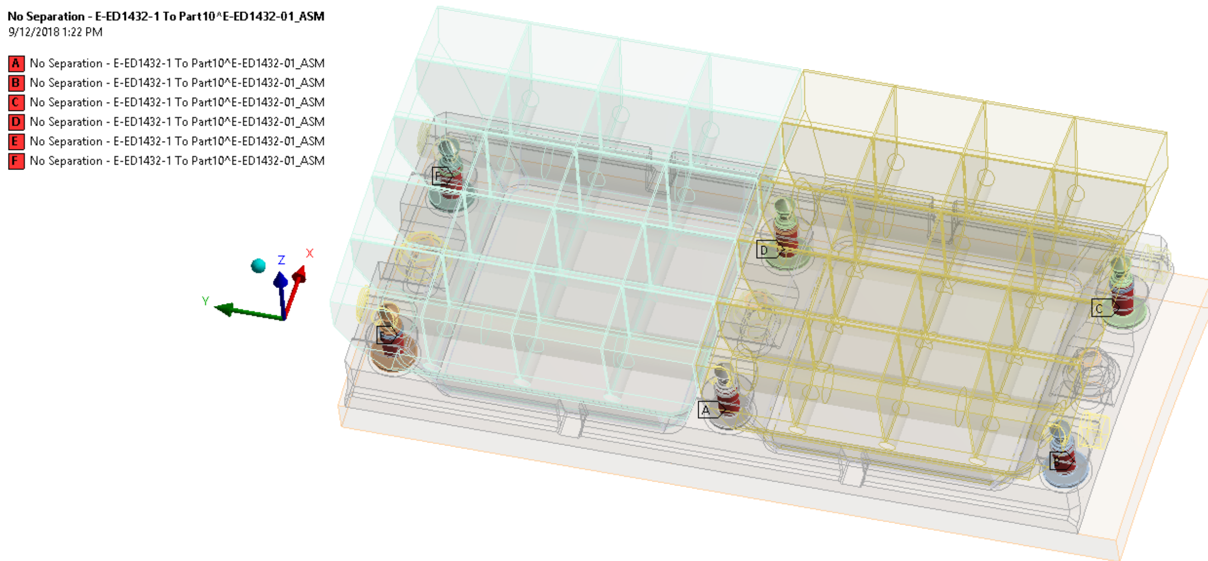

Figure 120: No separation contact between grafoil washers and connecting rod pins.

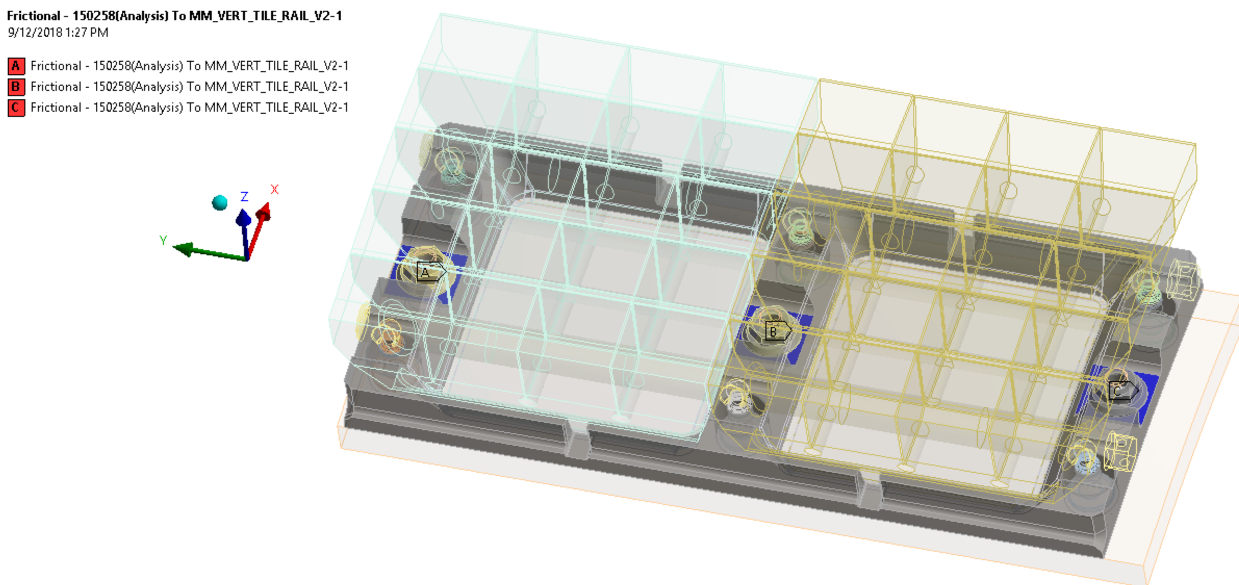

Figure 121: Frictional contact between the nuts and tile rail.

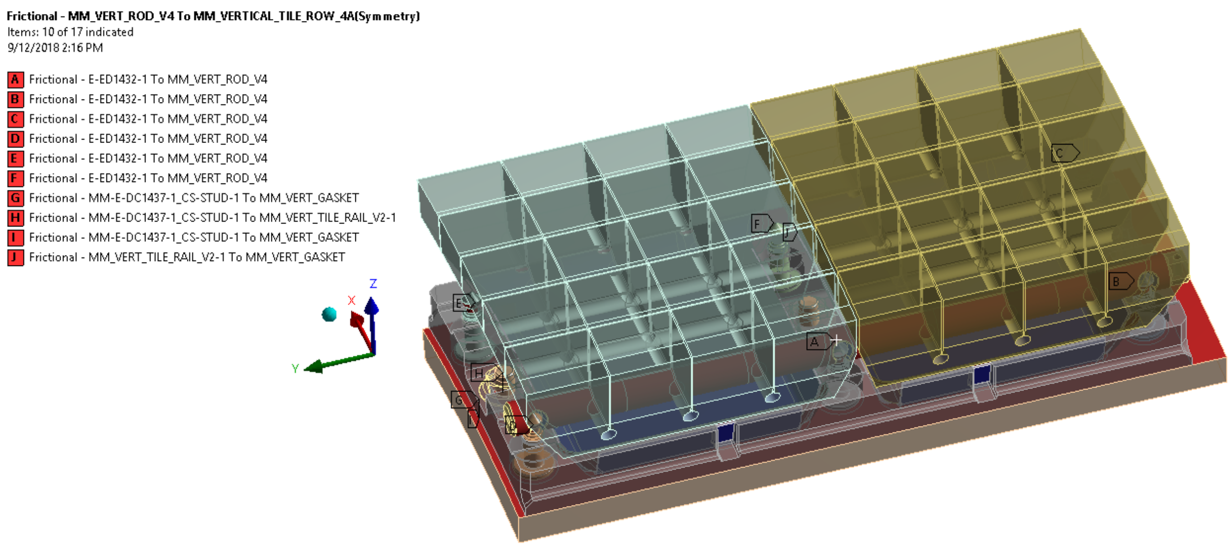

Figure 122: Frictional contact between the graphite tiles and support structure.

Results

The preload, eddy current, and halo loads were combined with the resulting temperature distribution load from the thermal analysis. Note that eddy current and halo loads will be referred to as EM loads. The temperature profile at 5 seconds for each heat flux profile in case 1 was incorporated into a static structural analysis with preload and EM loads. The temperature profile at 5 seconds for load case 3 was incorporated into a static structural model with the preload and EM loads. Finally, the temperature profile that had the highest substructure temperatures at the end of the 115 second cool down was case 1 profile 2. The temperature profile for this case was incorporated with the preload and EM loads. The results from the static analyses for all these heat flux profiles are presented below.

Case 3 at 1 second

The deformation contour plots in the radial, circumferential, and axial directions of the assembly as a result of the loads is shown in Figure 17, Figure 18, and Figure 19.

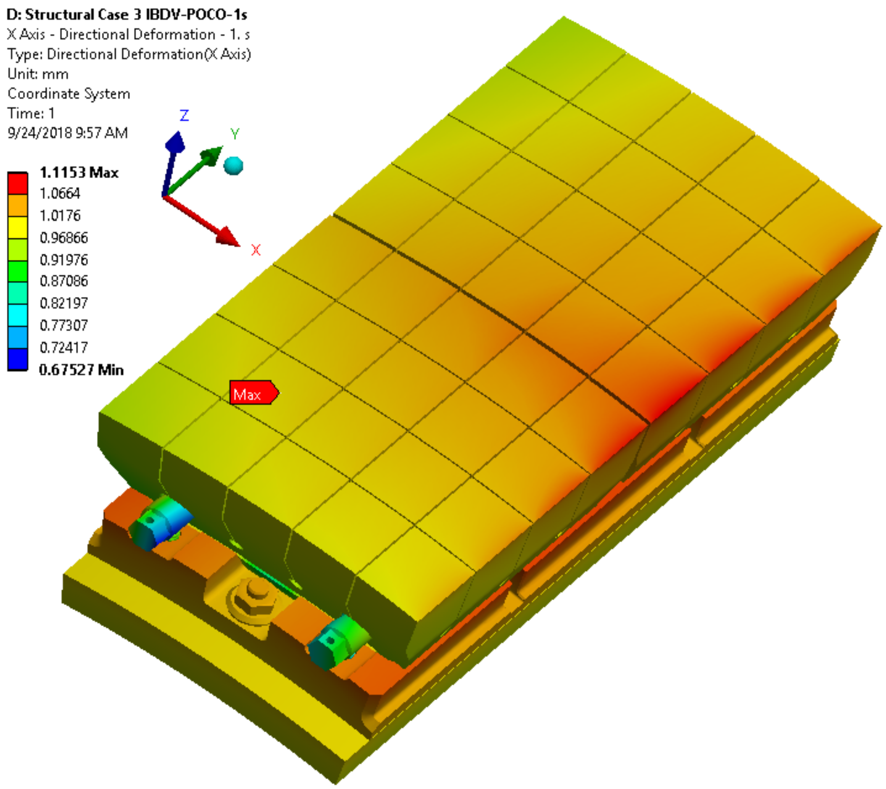

Figure 123: Radial deformation for case 3 at 1 second.

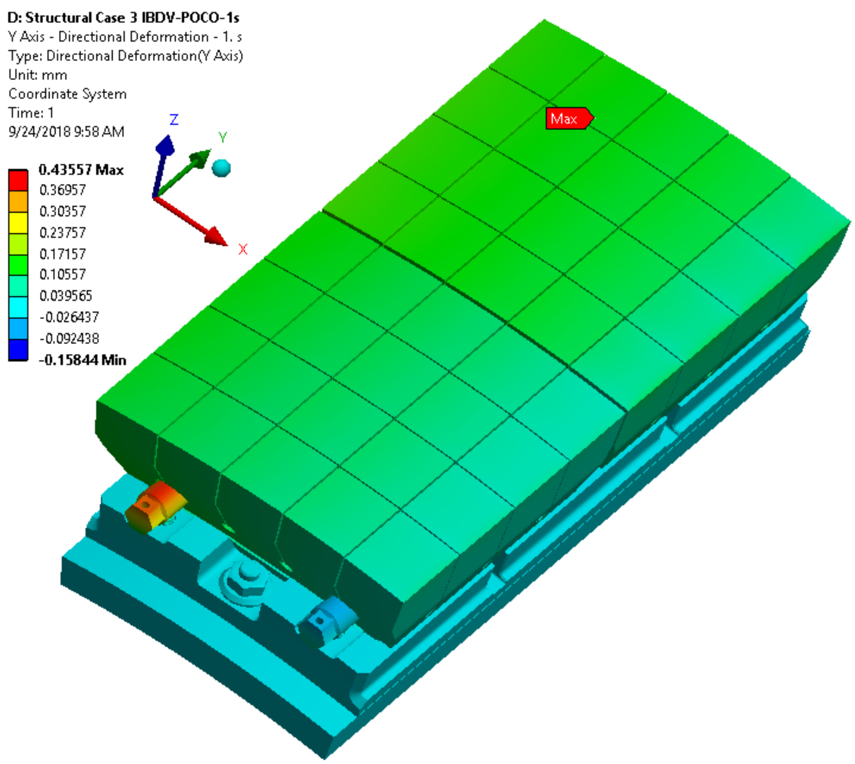

Figure 124: Circumferential deformation for case 3 at 1 second.

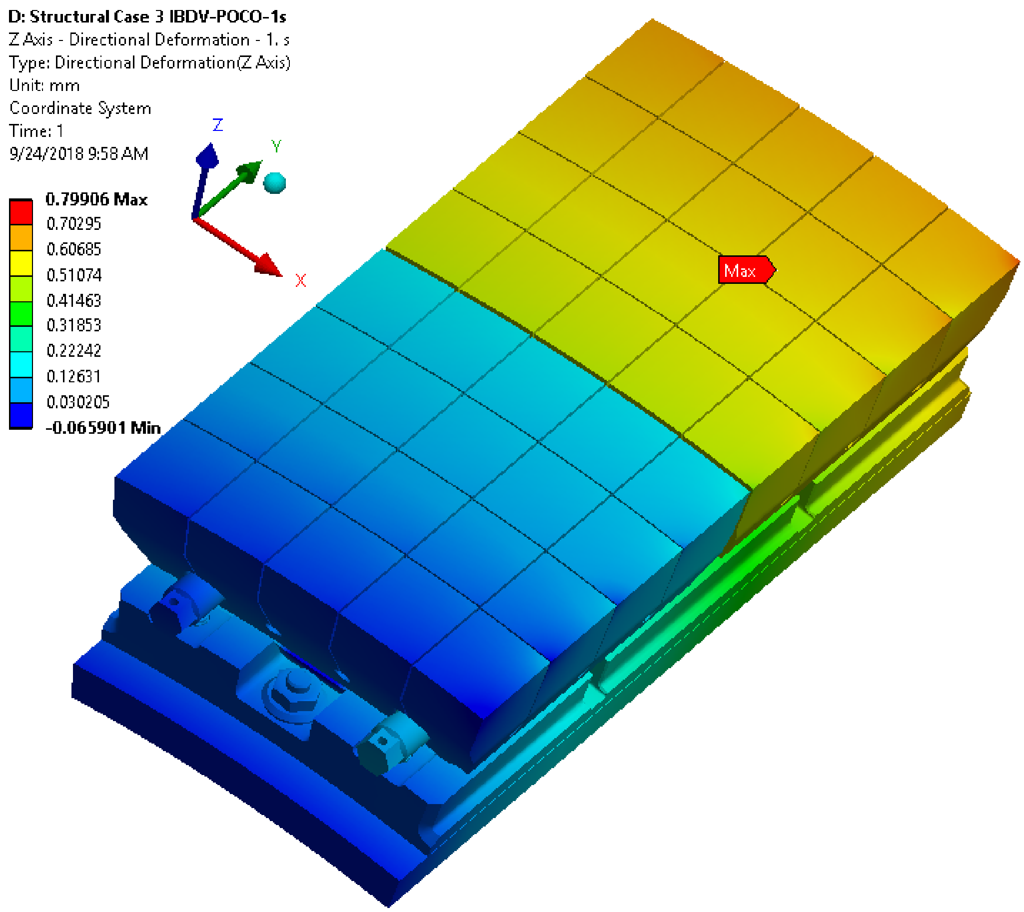

Figure 125: Axial deformation for case 3 at 1 second.

All results presented in the tables below are from case 3 at 1 second. Table 3 and Table 4 list the peak maximum and minimum principal stress and the corresponding allowable in the components made of graphite tiles and grafoil gaskets. Table 5 lists the peak equivalent stresses in the Inconel 718 components.

Table 35: Maximum Principal Stress of tiles and grafoil gaskets

Component	Peak Stress (MPa)	Allowable (MPa)	Loads
Graphite Tiles row 3	21.24	19	BPL+Halo+Eddy
Graphite Tiles row 4	19.90	19	BPL+Halo+Eddy
Grafoil Gasket	0.98	25	BPL+Halo+Eddy

Table 36: Minimum Principal Stress of tiles grafoil gaskets

Component	Peak Stress (MPa)	Allowable (MPa)	Loads
Graphite Tiles row 3	-138	-65	BPL+Halo+Eddy
Graphite Tiles row 4	-137	-65	BPL+Halo+Eddy
Grafoil Gasket	-1.96	-55	BPL+Halo+Eddy

Table 37: Equivalent Stress in Inconel 718 components

Component	Peak Stress (MPa)	Allowable (MPa)	Loads
Back Plate with integrated studs	54.05	717	BPL+Halo+Eddy
Vertical Tile Rail	64.19	717	BPL+Halo+Eddy
Connecting rods	684	717	BPL+Halo+Eddy
Connecting pins	308	717	BPL+Halo+Eddy
Nuts (150258)	54.05	717	BPL+Halo+Eddy

The grafoil gaskets resulted in stresses below their allowable values. The resulting maximum principal stresses in the tiles were below the allowable. However, the resulting minimum principal stress in the tiles exceeded the allowable. Figure 20 shows the minimum stress contour plot of the graphite tiles. Figure 21 shows the minimum stress contour plot of the grafoil gaskets.

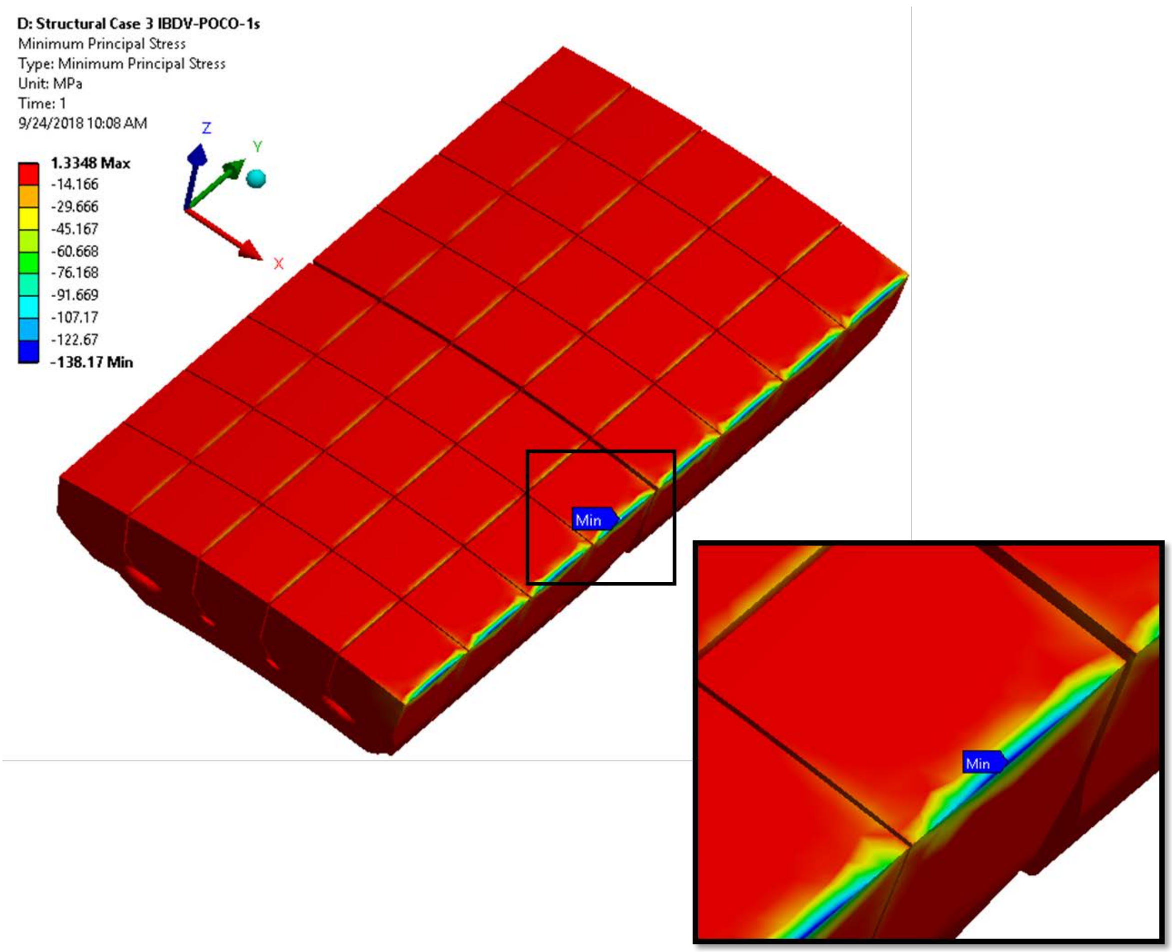

Figure 126: Minimum principal stresses in graphite tiles for case 3 at 1 second.

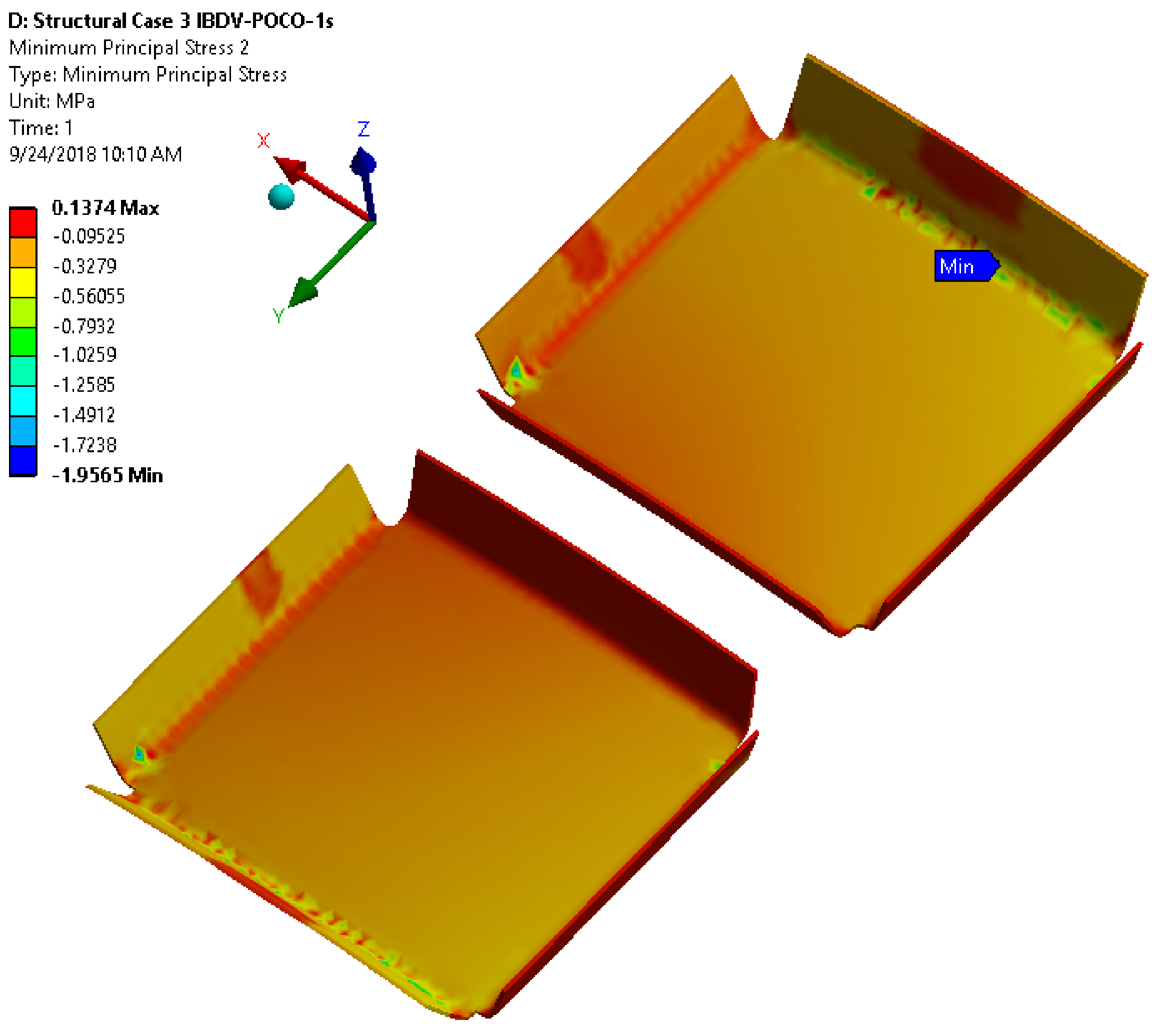

Figure 127: Minimum principal stresses in the grafoil gaskets for case 3 at 1 second.

Figure 22 shows the equivalent stress contour plot of all of the Inconel 718 components. Several Inconel 718 components exceeded their allowable values. Figure 23 shows the equivalent stress contour plot of the back plate and nuts. Figure 24 shows the equivalent stresses in the tile rail. The peak stress in these components was below the allowable. The connecting rod pins had localized areas of high stress as shown in Figure 25. These components are likely okay. However, the high stresses in the connecting rods may be cause for concern. Not only are they high, but the high stress extends across several elements. Figure 26 shows the stresses in the connecting rods. It may be possible to reduce the stress in the connecting rods by reducing the preload in the center pins from 750 N to 375 N.

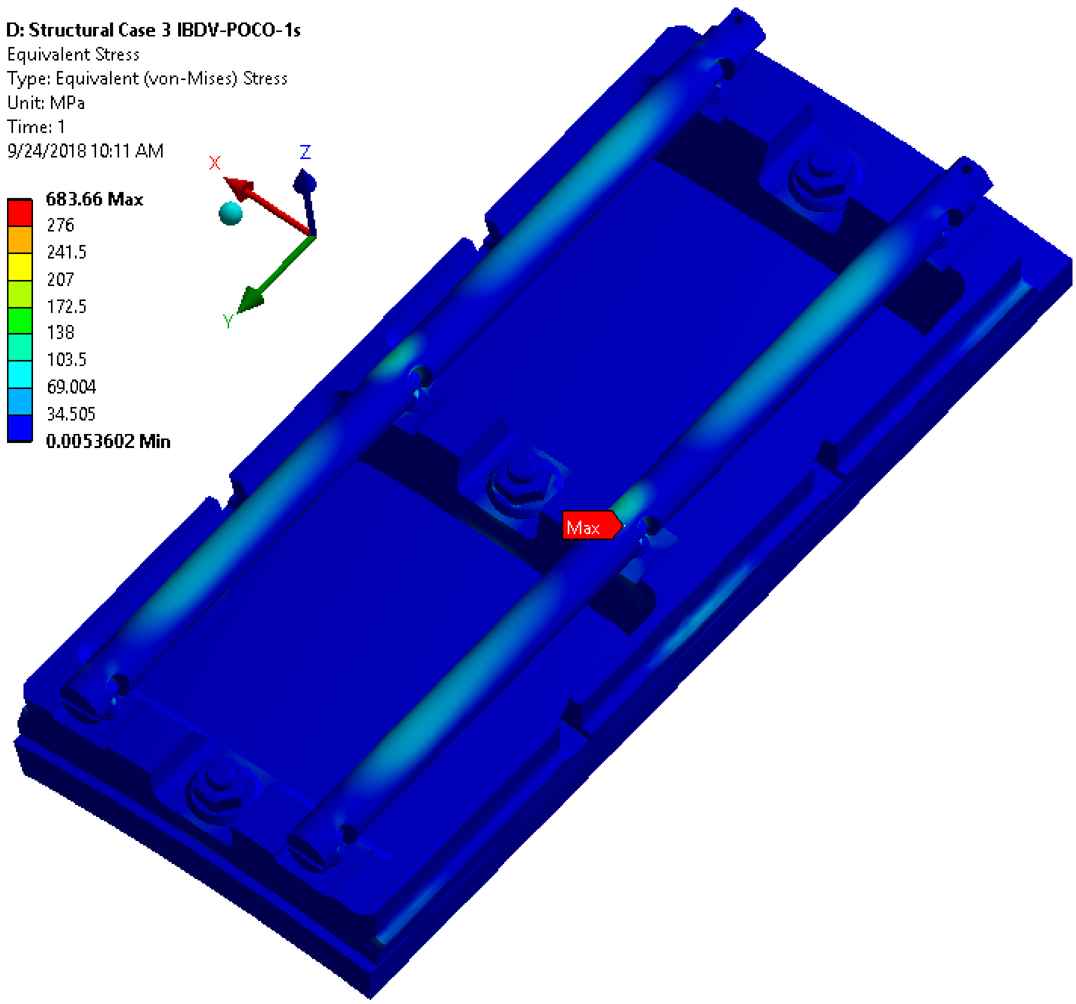

Figure 128: Equivalent stress contour plot of Inconel 718 components for case 3 at 1 second.

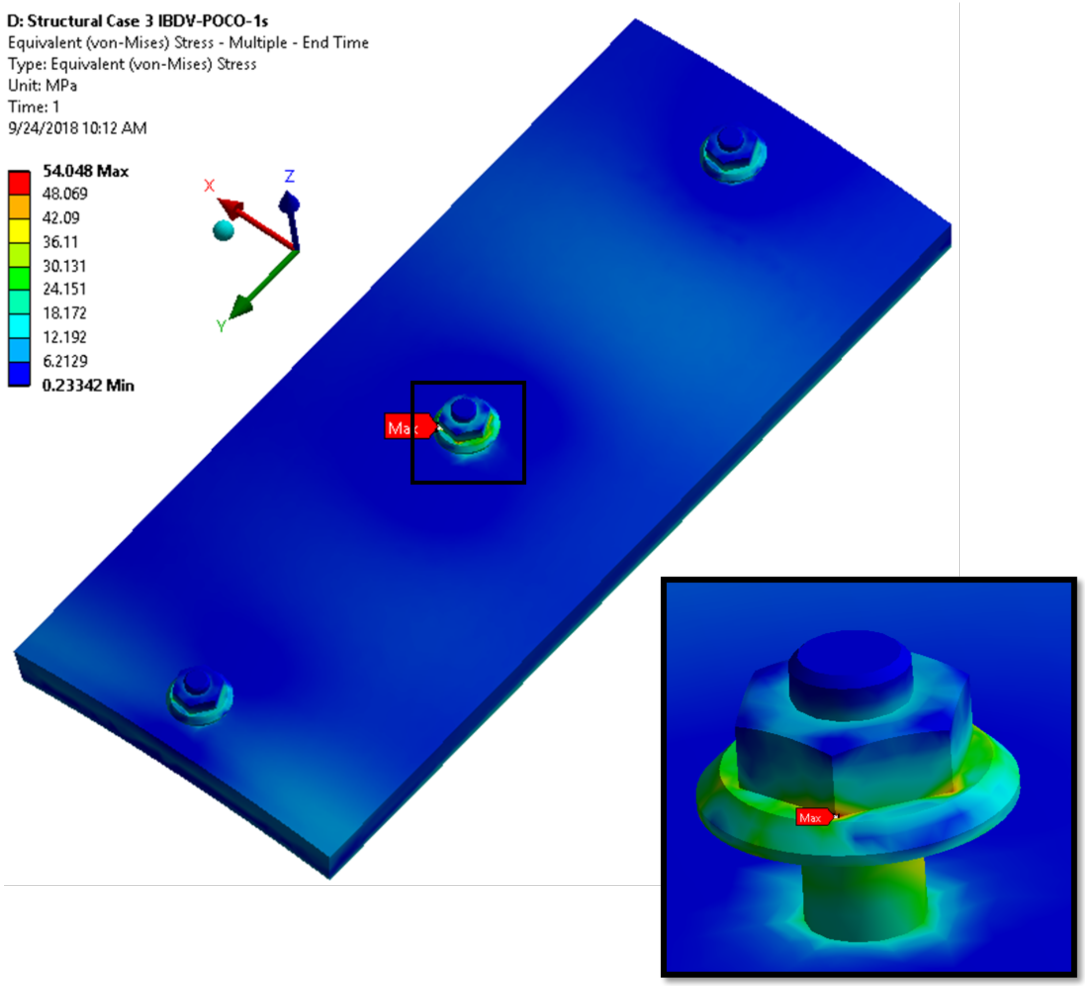

Figure 129: Back plate and nuts equivalent stress contour plot for case 3 at 1 second.

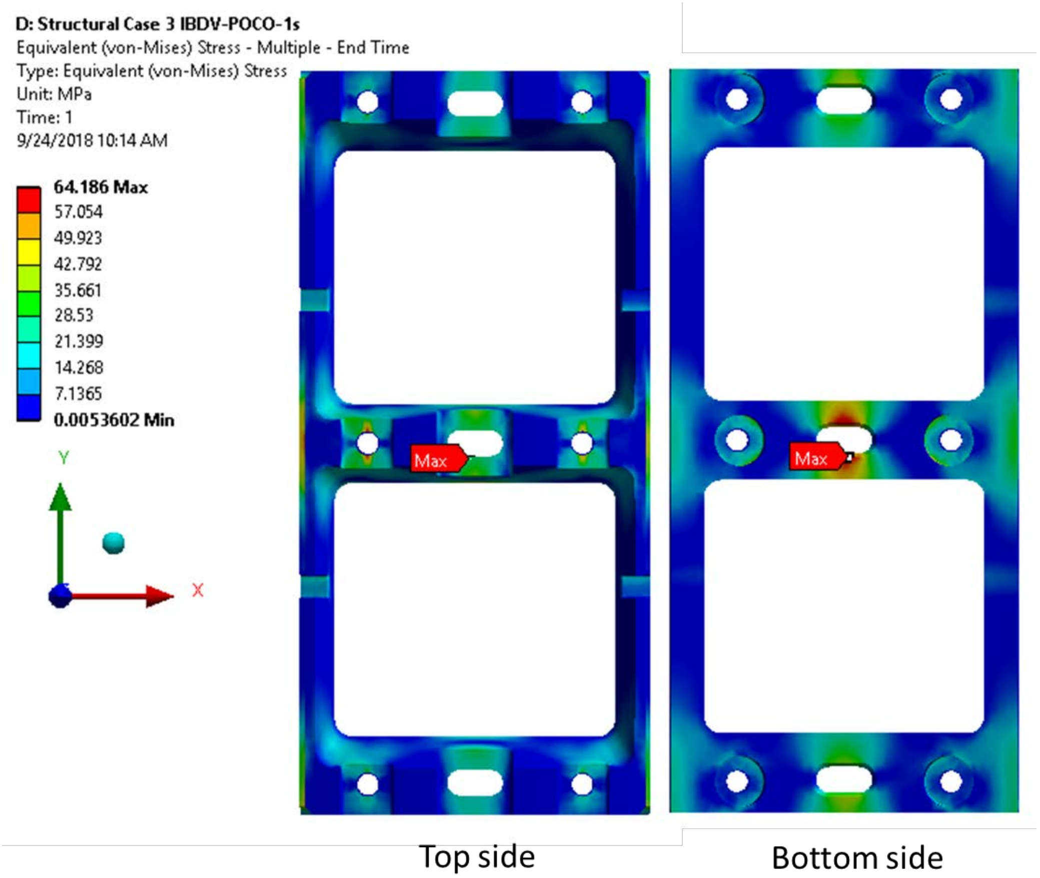

Figure 130: Tile rail equivalent stress for case 3 at 1 second.

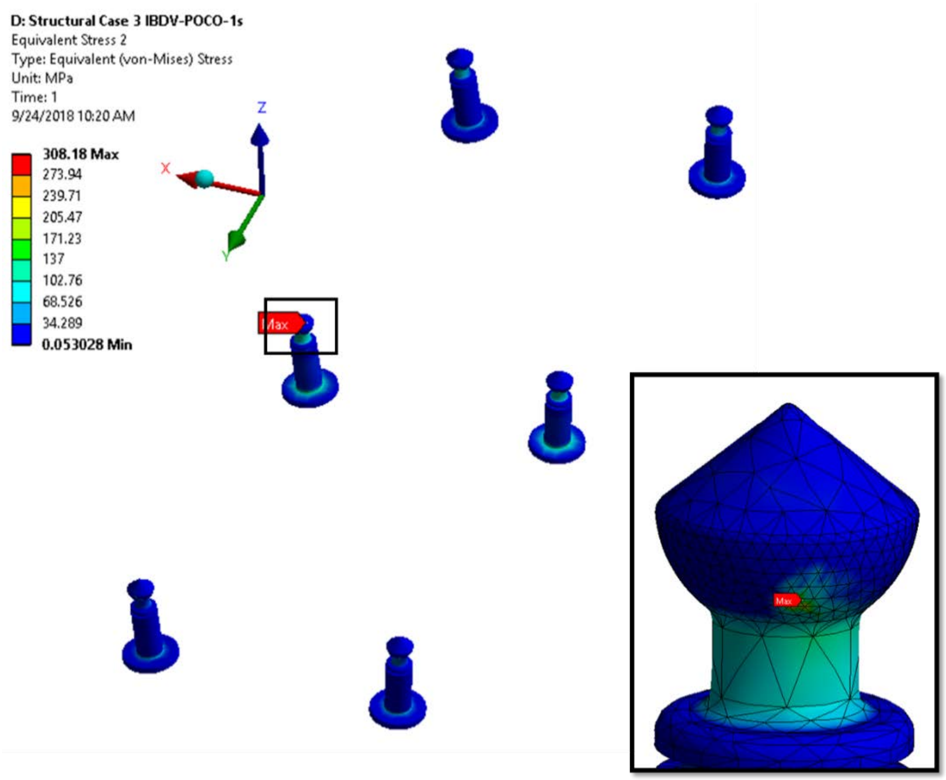

Figure 131: Connecting rod pin equivalent stress contour plot for case 3 at 1 second.

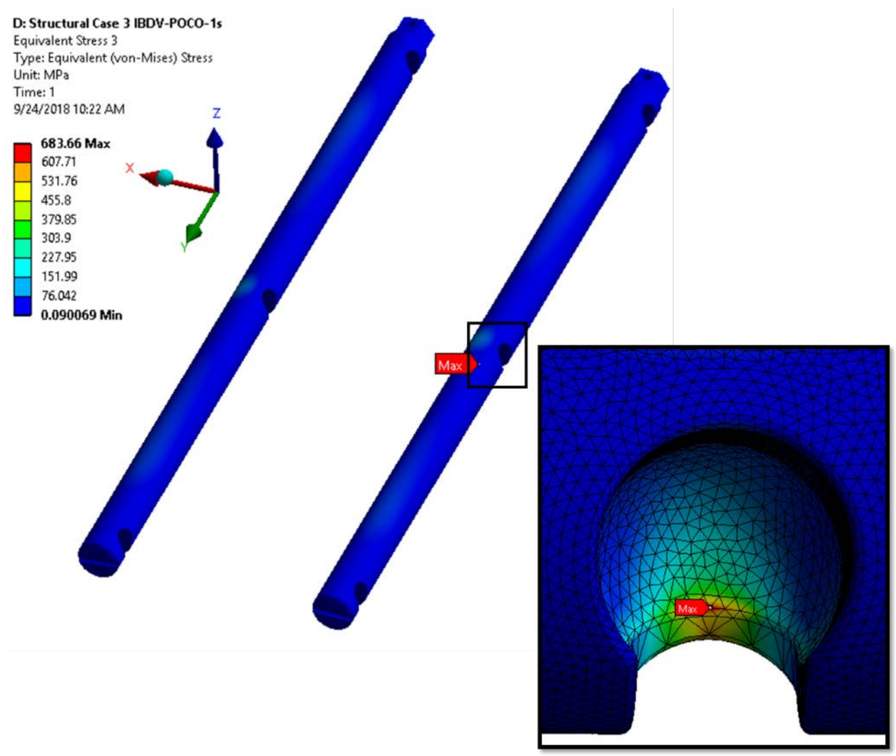

Figure 132: Equivalent stress plot of the connection rods for case 3 at 1 second.

Summary

The results show the tile temperatures are within the allowables but is has identified several areas where high stresses exist. The spherical connection of the pins to the rods show high contact stresses though hand calculations suggest it should be acceptable. It is recommended that the connection be tested to demonstrate acceptable life. Also, the reverse helicity case results in high surface compression for the prescribed 1 MW/m2 for 1 sec. The recommendation is to relax these requirements if possible. Finally, the diagnostic tile with cutouts for the Langmuir Probes show high stresses at the one location where it is in the middle of a castellation whereas the other 4 locations between castellations are acceptable

The graphite tiles resulted in minimum principal stresses that exceeded their allowable for case 3 with POCO TM graphite material properties. The minimum stress was -138 MPa with POCO TM properties compared with 93 MPa with SGL R6510 properties. This was a result of the larger coefficient of thermal expansion (CTE) for the POCO TM material. Figure 27 shows a comparison of the CTE for the two graphite materials. The higher the CTE the more the tile grows with temperature which results in higher stresses.

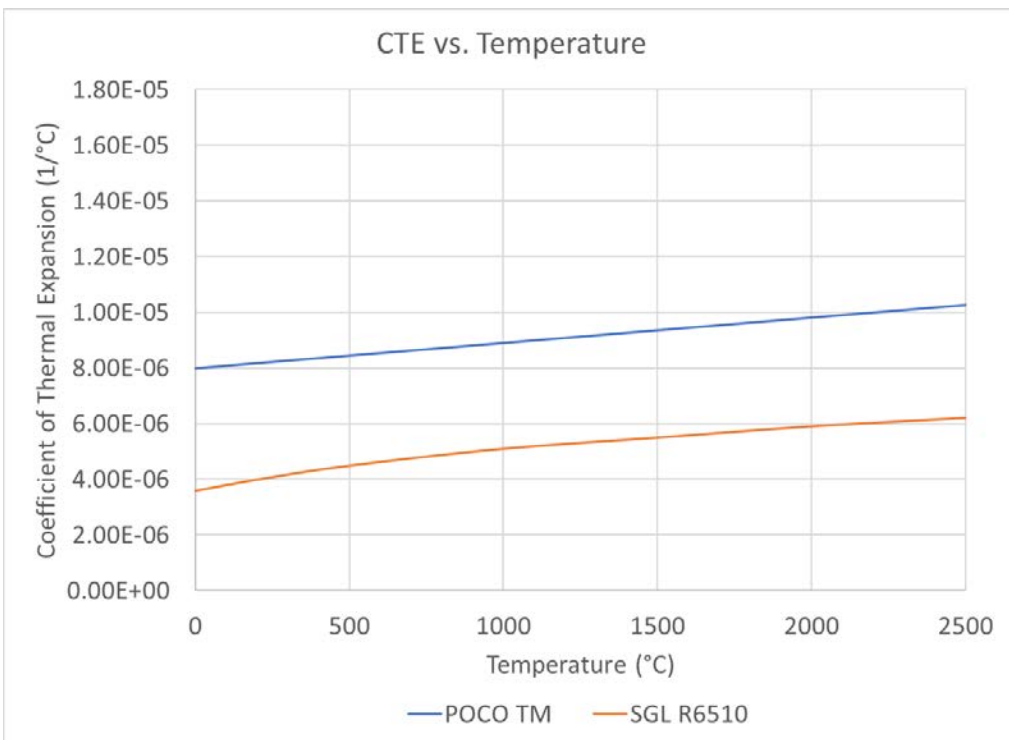

Figure 133: CTE versus temperature for POCO TM and SGL R6510

References

1) GENERAL REQUIREMENTS DOCUMENT NSTX-U-RQMT-GRD-001-02
2) NSTX-U SYSTEM REQUIREMENTS DOCUMENT Plasma Facing Components NSTX-U-RQMT-SRD-003-01 July 14, 2018
3) NSTX-U Disruption Analysis Requirements NSTX-U-RQMT-RD-003-02 7/23/18
4) NSTXU Recovery Global Heat Balance Calculations, NSTXU-CALC-10-06-00, by H Zhang